involve

a journal of mathematics

msp

involve

msp.org/involve

INVOLVE YOUR STUDENTS IN RESEARCH

Involve showcases and encourages high-quality mathematical research involving students from all academic levels. The editorial board consists of mathematical scientists committed to nurturing student participation in research. Bridging the gap between the extremes of purely undergraduate research journals and mainstream research journals, *Involve* provides a venue to mathematicians wishing to encourage the creative involvement of students.

MANAGING EDITOR

Kenneth S. Berenhaut   Wake Forest University, USA

BOARD OF EDITORS

PRODUCTION

Silvio Levy, Scientific Editor

Cover: Alex Scorpan

PUBLISHED BY

mathematical sciences publishers

nonprofit scientific publishing

http://msp.org/

Dynamics of vertical real rhombic Weierstrass elliptic functions

Lorelei Koss and Katie Roy

(Communicated by Michael E. Zieve)

In this paper, we investigate the dynamics of iterating the Weierstrass elliptic functions on vertical real rhombic lattices. The main result of this paper is to show that these functions can have at most one real attracting or parabolic cycle. If there is no real attracting or parabolic cycle, we prove that the real and imaginary axes, as well as translations of these lines by the lattice, lie in the Julia set. Further, we prove that if there exists a real attracting fixed point, then the intersection of the Julia set with the real axis is a Cantor set. Finally, we apply the theorem to find parameters in every real rhombic shape equivalence class for which the Julia set is the entire sphere.

1. Introduction

There is a rich literature investigating the dynamics of iterating Weierstrass elliptic functions [Hawkins 2006; 2010; 2013; Hawkins and Koss 2002; 2004; 2005; Clemons 2012; Hawkins and McClure 2011; Koss 2014]. Both the lattice shape and its orientation in the plane can affect the dynamical behavior of these functions. Outside of specialized lattice shapes, such as triangular or rhombic square lattices, few results have appeared on the dynamics of elliptic functions on rhombic lattices.

On any lattice, the Weierstrass elliptic function has three distinct critical values. Standard results in the dynamics of meromorphic functions imply that there are at most three different types of periodic Fatou components. Here, we focus on a large subset of real rhombic lattices and show that these lattice shapes force restrictions on the types of periodic Fatou components possible for the Weierstrass elliptic function.

In Section 2, we give background on the Weierstrass elliptic function and describe some results on iterating these functions. In Section 3, we focus on the dynamics of the Weierstrass elliptic function restricted to the real line. In particular, we use the Schwarzian derivative to extend results from [Hawkins 2010; Koss 2014] and show

that there can be at most one real attracting or parabolic periodic cycle. We use this result in Section 4 to investigate the Weierstrass elliptic function in the complex plane and find examples that satisfy certain interesting dynamical properties. First, we construct examples in Section 4A for which the real and imaginary axes lie in the Julia set. Second, we develop criteria in Section 4B that guarantee that the intersection of the real and imaginary axes with the Julia set is a Cantor set. Finally, we find parameters in every real rhombic shape equivalence class for which the Julia set is the entire sphere in Section 4C.

2. Background

We begin by fixing a lattice Λ defined by

$$\Lambda = [\lambda_1, \lambda_2] = \{m\lambda_1 + n\lambda_2 \mid m, n \in \mathbb{Z}, \ \lambda_1, \lambda_2 \in \mathbb{C} \setminus \{0\}, \ \lambda_2/\lambda_1 \notin \mathbb{R}\}.$$

We define the Weierstrass elliptic function by

$$\wp_\Lambda(z) = \frac{1}{z^2} + \sum_{w \in \Lambda \setminus \{0\}} \left(\frac{1}{(z-w)^2} - \frac{1}{w^2} \right).$$

The Weierstrass elliptic function is an even, meromorphic function that is periodic with respect to the lattice Λ. In the following, we distinguish between iteration and products by using the notation $\wp_\Lambda^n$ or $\wp_\Lambda^n(z)$ to denote iteration and $(\wp_\Lambda)^n$ or $(\wp_\Lambda(z))^n$ to denote products.

The Weierstrass elliptic function can also be defined by the differential equation

$$(\wp'_\Lambda(z))^2 = 4(\wp_\Lambda(z))^3 - g_2\wp_\Lambda(z) - g_3, \tag{1}$$

where $g_2(\Lambda) = 60 \sum_{w \in \Lambda \setminus \{0\}} w^{-4}$ and $g_3(\Lambda) = 140 \sum_{w \in \Lambda \setminus \{0\}} w^{-6}$. Each pair of complex numbers (g_2, g_3) with $g_2^3 - 27g_3^2 \neq 0$ determines a unique equivalence class of lattices and vice versa, where equivalence means that they generate the same subgroup [Du Val 1973]. We call a lattice Λ with invariants $g_2(\Lambda)$ and $g_3(\Lambda)$ a (g_2, g_3)-*lattice*.

The critical points of $\wp_\Lambda$ are the half-lattice points $\frac{1}{2}\lambda_1 + \Lambda$, $\frac{1}{2}\lambda_2 + \Lambda$ and $\frac{1}{2}\lambda_3 = \frac{1}{2}\lambda_1 + \frac{1}{2}\lambda_2 + \Lambda$. By the periodicity of the Weierstrass elliptic function, $\wp_\Lambda$ has exactly three distinct critical values denoted by

$$e_1 = \wp_\Lambda\left(\tfrac{1}{2}\lambda_1\right), \quad e_2 = \wp_\Lambda\left(\tfrac{1}{2}\lambda_2\right), \quad e_3 = \wp_\Lambda\left(\tfrac{1}{2}\lambda_3\right). \tag{2}$$

The critical values of $\wp_\Lambda$ satisfy the equations

$$e_1 + e_2 + e_3 = 0, \quad e_1e_3 + e_2e_3 + e_1e_2 = -\tfrac{1}{4}g_2, \quad e_1e_2e_3 = \tfrac{1}{4}g_3. \tag{3}$$

The second derivative of the Weierstrass elliptic function satisfies the equation

$$\wp''_\Lambda(z) = 6(\wp_\Lambda(z))^2 - \tfrac{1}{2}g_2(\Lambda). \tag{4}$$

If $\Lambda = [\lambda_1, \lambda_2]$, and $k \neq 0$ is any complex number, then $k\Lambda$ is the lattice defined by taking $k\lambda$ for each $\lambda \in \Lambda$, and $k\Lambda$ is said to be *similar* to Λ. Similarity is an equivalence relation between lattices, and an equivalence class of lattices is called a *shape*. Similar lattices give rise to homogeneity properties of the Weierstrass elliptic functions and their invariants:

Lemma 2.1 [Du Val 1973]. *For lattices Λ and Λ' and for $k \in \mathbb{C} \backslash \{0\}$:*

(1) *If $\Lambda' = k\Lambda$ then $g_2(\Lambda') = k^{-4}g_2(\Lambda)$ and $g_3(\Lambda') = k^{-6}g_3(\Lambda)$.*

(2) *If $\Lambda' = k\Lambda$ then $\wp_{\Lambda'}(ku) = k^{-2}\wp_{\Lambda}(u)$ for all $u \in \mathbb{C}$.*

The Weierstrass elliptic function satisfies a number of algebraic identities. If z is neither a lattice point nor a half-lattice point, then

$$\frac{1}{4}\left(\frac{\wp_{\Lambda}''(z)}{\wp_{\Lambda}'(z)}\right)^2 = \wp_{\Lambda}(2z) + 2\wp_{\Lambda}(z). \tag{5}$$

A lattice Λ is *real* if $\overline{\Lambda} = \Lambda$. We say $\wp_{\Lambda}$ is *real* if $z \in \mathbb{R}$ implies $\wp_{\Lambda}(z) \in \mathbb{R} \cup \{\infty\}$. Real lattices are associated with real lattice invariants.

Theorem 2.2 [Jones and Singerman 1987]. *The following are equivalent*:

(1) $\wp_{\Lambda}$ *is real.*

(2) Λ *is a real lattice.*

(3) $g_2, g_3 \in \mathbb{R}$.

By Theorem 2.2, we can identify a real lattice Λ with a point (g_2, g_3) in $\mathbb{R}^2$. Further, any point (g_2, g_3) in $\mathbb{R}^2$ with $g_2^3 - 27g_3^2 \neq 0$ gives rise to a real lattice [Du Val 1973].

The following lemma appeared in [Hawkins and Koss 2002] and gives information about $\wp_{\Lambda}$ on the real line in the case when Λ is real.

Lemma 2.3 [Hawkins and Koss 2002]. *If $\wp_{\Lambda}$ is real, then it is periodic as a map on $\mathbb{R}$ and has infinitely many real critical points and at least one real critical value. The image of the real critical point is the minimum of $\wp_{\Lambda}$ on $\mathbb{R}$. In particular, if e_1 denotes the critical value of the real critical points, then $\wp_{\Lambda}|_{\mathbb{R}} : \mathbb{R} \to [e_1, \infty]$ is piecewise monotonic and onto.*

2A. *Properties of lattice shapes.* The real lattices have distinctive shapes for their period parallelograms. We say $\Lambda = [\lambda_1, \lambda_2]$ is *real rectangular* if there exist generators such that λ_1 is real and λ_2 is purely imaginary. We say $\Lambda = [\lambda_1, \lambda_2]$ is *real rhombic* if there exist generators such that $\lambda_2 = \bar{\lambda}_1$. In each case, the period parallelogram with vertices 0, λ_1, λ_2, and $\lambda_1 + \lambda_2$ is rectangular or rhombic, respectively.

Real rhombic and real rectangular lattices lie in regions of the (g_2, g_3)-plane described in the following proposition.
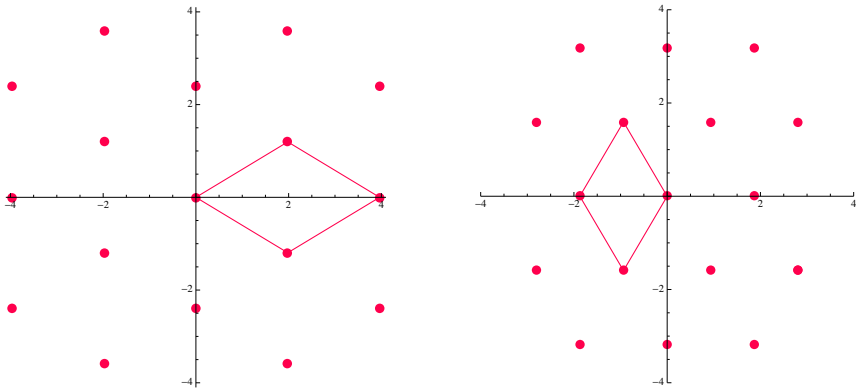
Figure 1. Horizontal (left) and vertical (right) lattices with period parallelograms.

Proposition 2.4 [Du Val 1973]. (1) Λ *is real rhombic if and only if* $g_2^3 - 27g_3^2 < 0$.
(2) Λ *is real rectangular if and only if* $g_2^3 - 27g_3^2 > 0$.

In this paper, we focus primarily on real rhombic lattices Λ, those which have generators of the form $\Lambda = [\lambda, \bar{\lambda}]$. Without loss of generality, we assume that λ lies in quadrant one. Real rhombic lattices always have a real lattice point, which we denote by $\lambda_1 = \lambda + \bar{\lambda} \in \mathbb{R}^+$. Given a real rhombic lattice $\Lambda = [\lambda, \bar{\lambda}]$ with $\lambda = a + ib$, we say Λ is *vertical* if $|b| > |a|$ and *horizontal* if $|b| < |a|$. If $|a| = |b|$, then the lattice is called rhombic square. Figure 1 (left) shows a horizontal lattice and the boundary of one period parallelogram, and Figure 1 (right) shows a vertical lattice and the boundary of one period parallelogram.

Vertical real rhombic lattices have $g_3 > 0$, and horizontal real rhombic lattices have $g_3 < 0$ [Du Val 1973]. Figure 2 shows the location of vertical and horizontal real rhombic lattices in the (g_2, g_3)-plane. The light gray region represents the location of vertical real rhombic lattices, the dark gray region represents horizontal real rhombic lattices, and the white region represents rectangular lattices.

We can use Lemma 2.1 to find all real lattices that are similar to a given real lattice. If Λ is the real lattice corresponding to the invariants (a, b) in the (g_2, g_3)-plane, then parameters that lie on the planar curve $g_3^2 = b^2 g_2^3 / a^3$ represent real lattices similar to Λ. In Figure 2, the orange curve represents the invariants of real lattices that are similar to the lattice Λ with invariants $(g_2, g_3) = (-5, -1)$. In this case, the portion of the curve lying in the upper half-plane represents a vertical real rhombic lattice similarity class, and the portion of the curve lying in the lower half-plane represents horizontal real rhombic lattices in the similarity class.

This paper primarily focuses on real rhombic lattices in the vertical position. The following properties hold true for any such lattice.
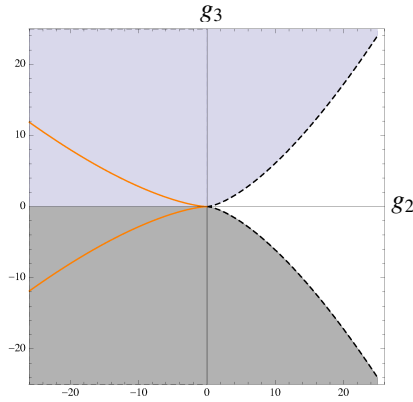
Figure 2. Real rhombic lattices are located in the shaded region of the (g_2, g_3)-plane. Light gray shading shows the location of vertical real rhombic lattices, and dark gray shading shows the location of horizontal real rhombic lattices. Rectangular lattices lie in the white region. All points colored orange represent real lattices similar to the $(-5, -1)$-lattice.

Proposition 2.5 [Hawkins and Koss 2004; 2005; Du Val 1973]. *If Λ is a vertical real rhombic lattice, then all of the following properties hold true*:

(1) $g_3 > 0$.

(2) $e_1 > 0$, *where e_1 is the image of the real critical point.*

(3) $e_2 = \bar{e}_3$.

(4) $\mathrm{Re}(e_2) = \mathrm{Re}(e_3) = -\frac{1}{2}e_1$.

(5) *If z lies on a vertical line passing through any real lattice point or any real half-lattice point, then $\wp_\Lambda(z) \in [-\infty, e_1)$.*

Although our focus in this paper is rhombic lattices, the following proposition about rectangular lattices will be used in Section 4A.

Proposition 2.6 [Hawkins and Koss 2004; 2005; Du Val 1973]. *If Λ is a real rectangular lattice, then all of the following properties hold true*:

(1) $e_1, e_2, e_3 \in \mathbb{R}$.

(2) *If $g_3 > 0$, then $e_2 < e_3 < 0 < e_1$.*

(3) *If $g_3 < 0$, then $e_2 < 0 < e_3 < e_1$.*

(4) $\wp_\Lambda$ *maps the imaginary axis to $[-\infty, e_2)$.*

It will be helpful to identify a specified lattice within each shape equivalence class. We define the *standard lattice* within any real (rhombic or rectangular) equivalence
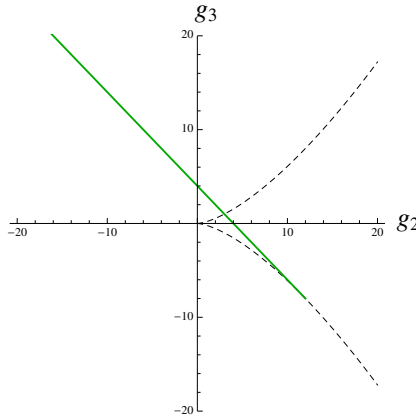
Figure 3. Standard lattices are shown in green.

class as the lattice Γ for which the real half-lattice point $\frac{1}{2}\gamma_1$ satisfies $\wp_\Gamma\left(\frac{1}{2}\gamma_1\right) = 1$. Using the equations appearing in (3) with $e_1 = 1$, we obtain

$$1 + e_2 + e_3 = 0, \quad e_2 + e_3 + e_2 e_3 = -\tfrac{1}{4}g_2, \quad e_2 e_3 = \tfrac{1}{4}g_3.$$

All real rhombic standard lattices lie on the line segment $g_3 = -g_2 + 4$ with $g_2 < 3$ in real lattice space. All real rectangular standard lattices lie on the line segment $g_3 = -g_2 + 4$ with $3 < g_2 < 12$ in real lattice space. (The ray when $g_2 > 12$ represents real rectangular lattices for which one of the nonreal critical points gives rise to the critical value of 1.) Figure 3 shows the location of real standard lattices in the (g_2, g_3)-plane in green.

Given any standard lattice, we can use the homogeneity property to find infinitely many similar lattices for which the real critical points land on a pole in one iteration. The following lemma is a result of the homogeneity property in Lemma 2.1.

Lemma 2.7 [Hawkins and Koss 2004]. *Let Γ be a standard real lattice, where γ_1 is chosen to be the smallest real positive lattice point. If m is any positive integer and $k = \sqrt[3]{1/(m\gamma_1)}$, then the lattice $\Lambda = k\Gamma$ has $\wp_\Lambda\left(\frac{1}{2}\lambda_1\right) = m\lambda_1$, and thus $\wp_\Lambda\left(\frac{1}{2}\lambda_1\right)$ is a pole.*

2B. *Iterating elliptic functions.* We give a brief overview of the dynamics of meromorphic functions; more details can be found in [Baker et al. 1992; Bergweiler 1993; Rippon and Stallard 1999]. Let $f : \mathbb{C} \to \mathbb{C}_\infty$ be a meromorphic function. The *Fatou set* $F(f)$ is the set of points $z \in \mathbb{C}_\infty$ such that $\{f^n \mid n \in \mathbb{N}\}$ is defined and normal in some neighborhood of z. The *Julia set* is the complement of the Fatou set on the sphere, $J(f) = \mathbb{C}_\infty \backslash F(f)$. A point z_0 is *periodic* of period p if there exists a $p \geq 1$ such that $f^p(z_0) = z_0$. We also call the set $\{z_0, f(z_0), \ldots, f^{p-1}(z_0)\}$ a *p-cycle*. The *multiplier* of a point z_0 of period p is the derivative $(f^p)'(z_0)$. A periodic point z_0 is classified as *attracting, repelling,* or *neutral* if $|(f^p)'(z_0)|$ is

less than, greater than, or equal to 1 respectively. If $|(f^p)'(z_0)| = 0$ then z_0 is called a *superattracting* periodic point.

Suppose U is a connected component of the Fatou set. We say U is *preperiodic* if there exists $n > m \geq 0$ such that $f^n(U) = f^m(U)$, and the minimum of $n - m = p$ for all such n, m is the *period* of the cycle. Elliptic functions have a finite number of critical values, and thus it turns out that the classification of periodic components of the Fatou set is no more complicated than that of rational maps of the sphere. Periodic components of the Fatou set of elliptic functions may be attracting domains, parabolic domains, Siegel disks, or Herman rings. In particular, elliptic functions have no wandering domains or Baker domains [Baker et al. 1992; Hawkins and Koss 2002; Rippon and Stallard 1999].

Let $C = \{U_0, U_1, \ldots, U_{p-1}\}$ be a periodic cycle of components of $F(f)$. If C is a cycle of immediate attractive basins or parabolic domains, then $U_j \cap \mathrm{Crit}(f) \neq \varnothing$ for some $0 \leq j \leq p - 1$. If C is a cycle of Siegel disks or Herman rings, then $\partial U_j \subset \bigcup_{n \geq 0} f^n(\mathrm{Crit}(f))$ for all $0 \leq j \leq p-1$. In particular, any periodic component of an elliptic function has an associated critical point.

Although the Weierstrass elliptic function can have three distinct postcritical orbits, there are restrictions on the possible types of distinct Fatou cycles. Rectangular lattices have been investigated in [Hawkins and Koss 2002; 2004; 2005; Koss 2014]. The following proposition, proved in [Hawkins and Koss 2005], describes the possible postcritical behavior of the Weierstrass elliptic function on real rhombic lattices.

Proposition 2.8 [Hawkins and Koss 2005]. *For any real rhombic lattice Λ one of the following must occur*:

(1) $J(\wp_\Lambda) = \mathbb{C}_\infty$.

(2) *There exist one real postcritical orbit and two conjugate postcritical orbits; therefore, there are at most two different types of periodic Fatou components. If the nonreal critical values lie in the Fatou set, then they are associated with cycles with the same period and multiplier.*

The periodicity of $\wp_\Lambda$ on any real lattice Λ gives rise to many forms of symmetry in the Fatou and Julia sets, as well as restrictions on possible Fatou behavior.

Proposition 2.9 [Hawkins and Koss 2002; 2004]. *For any real lattice Λ*:

(1) $J(\wp_\Lambda) + \Lambda = J(\wp_\Lambda)$ *and* $F(\wp_\Lambda) + \Lambda = F(\wp_\Lambda)$.

(2) $(-1)J(\wp_\Lambda) = J(\wp_\Lambda)$ *and* $(-1)F(\wp_\Lambda) = F(\wp_\Lambda)$.

(3) $\overline{J(\wp_\Lambda)} = J(\wp_\Lambda)$ *and* $\overline{F(\wp_\Lambda)} = F(\wp_\Lambda)$.

(4) $J(\wp_\Lambda)$ *and* $F(\wp_\Lambda)$ *are symmetric with respect to any critical point. That is, if c is any critical point of $\wp_\Lambda$, then $c + z \in F(\wp_\Lambda)$ if and only if $c - z \in F(\wp_\Lambda)$.*

(5) $\wp_\Lambda$ *has no cycle of Herman rings.*

3. Dynamics on the real line

In this section, we focus on the dynamics of $\wp_\Lambda$ restricted to the real line. When $g_3 = 0$ and $g_2 < 0$, Hawkins [2010] showed that $\wp_\Lambda$ has a Julia set that is equal to the entire sphere. The proof of this result involved showing that $\wp_\Lambda$ has no attracting or parabolic cycles because the Schwarzian derivative of $\wp_\Lambda$ was negative, extending work of Singer [1978] on interval maps to the case of elliptic functions. Koss [2014] showed that when Λ is real rectangular, the Schwarzian of $\wp_\Lambda$ is negative, so there can be at most one attracting fixed point. The techniques used in these proofs relied on special properties of the critical values for these lattices: for real rhombic square lattices, the critical values lie on the imaginary axis, and for real rectangular lattices, the critical values are all real. As such, these methods cannot be applied in the case of real rhombic lattices because the critical values are located elsewhere in the plane. In this section, we present a different proof that when Λ is a vertical real rhombic lattice, the Schwarzian is negative.

We begin with the definition of the Schwarzian derivative.

Definition 3.1. If x is not a critical point or pole of a meromorphic function F, the *Schwarzian derivative* is defined to be

$$S_F(x) = \frac{F'''(x)}{F'(x)} - \frac{3}{2}\left(\frac{F''(x)}{F'(x)}\right)^2.$$

When $F = \wp_\Lambda$, we have $S_{\wp_\Lambda}$ restricted to $\mathbb{R}$ is a real-valued, even elliptic function with poles at lattice points and half-lattice points [Hawkins 2010].

Using Lemma 2.3, we know $\wp_\Lambda(\mathbb{R}) \subset \mathbb{R} \cup \{\infty\}$. For any p-cycle

$$S = \{x_0, \wp_\Lambda(x_0), \ldots, \wp_\Lambda^{p-1}(x_0)\} \subset \mathbb{R},$$

we associate to it a set

$$B(S) = \{x \in \mathbb{R} \mid \wp_\Lambda^k(x) \to S \text{ as } k \to \infty\}.$$

The set S is *topologically attracting* if $B(S)$ contains an open interval, and in this case we call $B(S)$ the *real attracting basin* of S. The *real immediate attracting basin* of S is the union of components of $B(S)$ in $\mathbb{R}$ that contain points from S, and we denote this set by $B_0(S)$. Using Lemma 2.3, if $|(\wp_\Lambda^p)'(z_0)| < 1$, then $S \subset [e_1, \infty)$ and $B(S) \neq \varnothing$, so S is topologically attracting.

Hawkins [2010] proved that when $g_3 = 0$ and $g_2 < 0$, the Weierstrass elliptic function satisfied a minimum principle. The proof relied on special properties of the lattice shape, but the result was extended to all real rectangular lattices in [Koss 2014]. The proof in [Koss 2014] carries over identically for real rhombic lattices, and we state the result here without proof.

Lemma 3.2 (minimum principle). *Assume that Λ is a real lattice. Suppose we have a closed interval $I \subset \mathbb{R}$ with endpoints $l < r$, not containing any poles or critical points of $f_{n,\Lambda,b}$. Then*

$$|f'_{n,\Lambda,b}(x)| > \min\{|f'_{n,\Lambda,b}(l)|, |f'_{n,\Lambda,b}(r)|\} \quad \forall x \in (l, r).$$

In [Hawkins 2010], the minimum principle was used to extend Singer's theorem on interval maps to the setting of the Weierstrass elliptic function on a real square lattice. The extension of Singer's theorem given in [Hawkins 2010] relied only on the minimum principle and generic properties of elliptic functions on real lattices; the proof for our setting follows identically, so we do not provide it.

Theorem 3.3. *If Λ is a real rhombic lattice and $S_{\wp_\Lambda} < 0$, then:*

(1) *The real immediate basin of attraction of a topologically attracting periodic orbit of $\wp_\Lambda$ contains a real critical point.*

(2) *If $y \in \mathbb{R}$ is in a rationally neutral p-cycle for $\wp_\Lambda$, then it is topologically attracting; i.e., there exists an open interval I such that for every $x \in I$, $\lim_{k\to\infty} \wp_\Lambda^{kp}(x) = y$.*

Next, we show that the Schwarzian of $\wp_\Lambda$ is negative on any vertical real rhombic lattice.

Theorem 3.4. *If Λ is a vertical real rhombic lattice, then $S_{\wp_\Lambda} < 0$.*

Proof. Suppose $g_3 > 0$ and $g_2^3 - 27g_3^2 \neq 0$. From Lemma 2.3, $g_3 > 0$ implies that the critical value e_1 is also positive. Further, e_1 is the absolute minimum of $\wp_\Lambda$ by Lemma 2.3, so it follows that $\wp_\Lambda(x) > 0$ for all x except lattice points when $g_3 > 0$. Rearranging (5) to

$$\left(\frac{\wp_\Lambda''(x)}{\wp_\Lambda'(x)}\right)^2 = \wp_\Lambda(2x) + 2\wp_\Lambda(x),$$

we find that

$$S_{\wp_\Lambda}(x) = \frac{\wp_\Lambda'''(x)}{\wp_\Lambda'(x)} - 6\wp_\Lambda(2x) - 12\wp_\Lambda(x). \tag{6}$$

Twice differentiating (1) yields $\wp_\Lambda''' = 12\wp_\Lambda\wp_\Lambda'$, and substituting into (6), we find

$$S_{\wp_\Lambda}(x) = -6\wp_\Lambda(2x).$$

Because $\wp_\Lambda(x) > 0$, we have $S_{\wp_\Lambda}(x) = -6\wp_\Lambda(2x) < 0$. $\qquad\square$

We show graphs of $\wp_\Lambda$ and $S_{\wp_\Lambda}$ on the lattice with invariants $g_2(\Lambda) = 4$ and $g_3(\Lambda) = 2$ in Figure 4. Note that the proof of Theorem 3.4 did not rely on our assumption that the lattice was rhombic but instead relied on the critical value being positive. Thus it provides a new and much simpler proof that the Schwarzian is negative for real rectangular lattices when $g_3 > 0$.
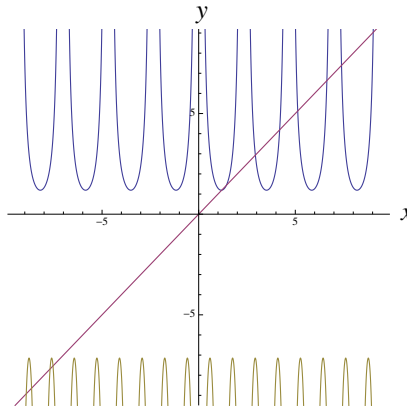
Figure 4. Graph of $\wp_\Lambda$ shown in blue and $S_{\wp_\Lambda}$ shown in yellow for $g_2 = 4$ and $g_3 = 2$. The line $y = x$ is shown in red.

The corollary below follows immediately from Theorems 3.3 and 3.4.

Corollary 3.5. *If Λ is a vertical real rhombic lattice, then $\wp$ has either 0 or 1 real attracting or parabolic cycles. If there exists a real nonrepelling cycle, then a real critical point is contained in the cycle of Fatou components.*

The assumption that Λ is a vertical real rhombic lattice is far from trivial. In fact, it seems to be necessary because the next example, found experimentally, shows that horizontal lattices might violate Corollary 3.5.

Example 3.6. Consider $\wp_\Lambda(x)$ with $g_2 = 27$ and $g_3 = -27.07$, shown in Figure 5. In this case, Λ is a horizontal real lattice since $g_3 < 0$. This function has only one
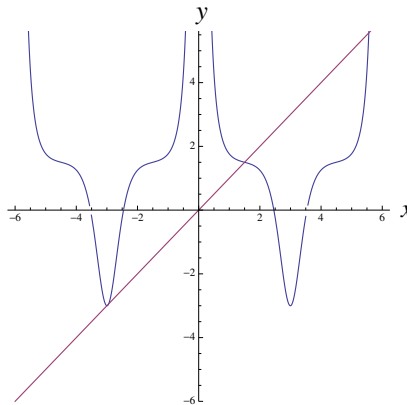
Figure 5. The graph of $\wp_\Lambda$ as described in Example 3.6, which has a real attracting fixed point that does not attract a real critical point. The function $\wp_\Lambda$ is shown in blue, and the line $y = x$ is shown in red.

real critical value, but it has two real attracting fixed points. The critical value at $x \approx -2.997$ is attracted to the attracting fixed point at $x \approx -3.0006$. There is an additional attracting fixed point at $x \approx 1.50037$ that does not attract any real critical points.

4. Dynamics on the complex plane

Connectivity properties of Julia sets of Weierstrass elliptic functions are not well understood except for the most regular cases where the lattice is square or triangular [Clemons 2012; Hawkins 2006; 2010; Hawkins and Look 2006; Hawkins and Koss 2002; 2004; 2005]. It is not clear whether the Julia set of an arbitrary real rhombic lattice or real rectangular lattice is connected, Cantor, or infinitely disconnected but not Cantor.

In this section, we examine what the results of Section 3 imply for the complex function $\wp_\Lambda$. In Sections 4A and 4B, we prove some results about the Julia set restricted to the real axis. In Section 4C, we find invariants for which the Julia set is the entire sphere.

4A. *The real axis lies in the Julia set.* Here, we present conditions under which the entire real axis must lie in the Julia set. We begin with a theorem, proved in [Hawkins and Koss 2005]. It required knowing that the real critical value belonged to the Julia set, as well as information about the orbits of the complex critical points.

Theorem 4.1 [Hawkins and Koss 2005]. *If Λ is a real rhombic lattice such that the complex critical values are associated with nonrepelling complex cycles and the real critical value is in $J(\wp_\Lambda)$, then the real and imaginary axes are contained in $J(\wp_\Lambda)$.*

The hypotheses about the orbits of the complex critical values are necessary because of behavior such as that which occurs in Example 3.6: it may be possible that the real critical value lies in $J(\wp_\Lambda)$ but there is a real attracting cycle that attracts the complex critical values. However, the results in Section 3 enable us to remove the hypotheses relating to the orbits of the complex critical values for $\wp_\Lambda$ on a vertical real rhombic lattice.

Theorem 4.2. *If Λ is a vertical real rhombic lattice and the real critical value is in $J(\wp_\Lambda)$, then the real and imaginary axes are contained in $J(\wp_\Lambda)$.*

Proof. By Proposition 2.9(5), $\wp_\Lambda$ has no Herman rings. By Theorem 2.2, $\wp_\Lambda$ is real. No interval in $\mathbb{R}$ can lie within a Siegel disk component because $\wp_\Lambda : \mathbb{R} \to \mathbb{R}$, which would contradict that $\wp_\Lambda^n$ is conjugate to an irrational rotation of the unit disk. Since the real critical value lies in $J(\wp_\Lambda)$, Corollary 3.5 implies that there are no attracting or parabolic cycles on the real axis. Therefore, the entire real axis must lie in $J(\wp_\Lambda)$. Proposition 2.5(5) implies that the imaginary axis maps to the
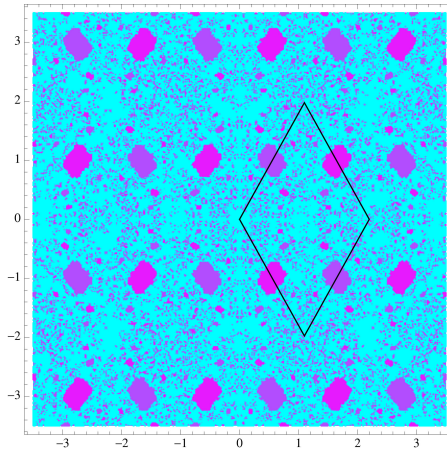
Figure 6. The function $\wp_\Lambda$ for $g_2 = 1$ and $g_3 = 6.5$ has the real and imaginary axes lying in the Julia set.

real axis, and thus the imaginary axis must lie in $J(\wp_\Lambda)$ by the invariance of the Julia set. □

Figure 6 illustrates an example, found experimentally, of a function $\wp_\Lambda$ for which the real axis lies in the Julia set. The lattice Λ in this example has invariants $g_2 = 1$ and $g_3 = 6.5$. The function has two attracting fixed points at $-0.607 \pm 0.942i$, each of which attracts a complex critical value. All points colored pink iterate to $-0.607 + 0.942i$, and all points colored purple iterate to $-0.607 - 0.942i$. Points colored blue lie in the Julia set.

4B. *The Julia set restricted to the real axis is Cantor.* Next, we move to a discussion about conditions which imply that the Julia set restricted to the real axis is Cantor. In [Hawkins and Koss 2005], any real rectangular square lattice or real triangular lattice with an attracting fixed point was shown to have a Cantor Julia set on the real axis. Here we extend the result to all real rectangular and all vertical real rhombic lattices.

The following proposition is an amalgamation of results from [Hawkins and Koss 2002; 2005].

Proposition 4.3. *Assume that Λ is a real rectangular or vertical real rhombic lattice with real period λ_1 such that $\wp_\Lambda$ has an attracting fixed point. If $\Lambda_{n_0} = [n_0\lambda_1, (n_0 + 1)\lambda_1]$ is the interval containing e_1, then the attracting fixed point t_{n_0} is in Λ_{n_0}. Further, there is a repelling fixed point $P_{n_0} \in \Lambda_{n_0}$ where $P_{n_0} = c_{n_0} + q$ for the critical point $c_{n_0} \in \Lambda_{n_0}$ and $0 < q < \frac{1}{2}\lambda_1$. Then $B = (P'_{n_0}, P_{n_0})$ is the immediate basin of attraction for t_{n_0}, where $P'_{n_0} = c_{n_0} - q$.*

In addition, we need the following lemma in the proof.

Lemma 4.4. *If Λ is a real rectangular or vertical real rhombic lattice then $\wp'_\Lambda(x)$ is monotone increasing.*

Proof. We begin with (4),

$$\wp''_\Lambda(x) = (6\wp_\Lambda(x))^2 - \tfrac{1}{2}g_2.$$

If $g_2 < 0$, then $\wp''_\Lambda(x) > 0$ at all x except lattice points.

Next, suppose $g_2 > 0$ and $g_3 > 0$. Using Lemma 2.3, e_1 is the minimum of $\wp_\Lambda$ on the real axis, so

$$\wp''_\Lambda(x) = (6\wp_\Lambda(x))^2 - \tfrac{1}{2}g_2 \geq 6e_1^2 - \tfrac{1}{2}g_2. \tag{7}$$

Using the second property from (3),

$$6e_1^2 - \tfrac{1}{2}g_2 = 6e_1^2 + 2(e_1e_3 + e_2e_3 + e_1e_2) = 6e_1^2 + 2e_1(e_2 + e_3) + 2e_2e_3.$$

Using the first property from (3),

$$6e_1^2 + 2e_1(e_2 + e_3) + 2e_2e_3 = 6e_1^2 - 2e_1^2 + 2e_2e_3 = 4e_1^2 + 2e_2e_3. \tag{8}$$

Finally, we apply the third property from (3) to obtain

$$4e_1^2 + 2e_2e_3 = 4e_1^2 + \frac{g_3}{2e_1}.$$

Since $g_3 > 0$ and $e_1 > 0$ by Propositions 2.5(2) and 2.6(2), we have $\wp''_\Lambda(x) > 0$.

Finally, if $g_3 < 0$ and Λ is real rectangular, Proposition 2.6(3) implies that $e_2 < 0 < e_3 < e_1$, and e_1 is the minimum of $\wp_\Lambda$ on the real axis. Using the argument from (7) to (8) in the previous paragraph, we have

$$\wp''_\Lambda(x) > 4e_1^2 + 2e_2e_3.$$

Using the first property from (3),

$$4e_1^2 + 2e_2e_3 = 4e_1^2 + 2e_3(-e_1 - e_3)$$
$$= 2(e_1^2 - e_1e_3) + 2(e_1^2 - e_3^2).$$

Since $0 < e_3 < e_1$, both terms are positive, so $\wp''_\Lambda(x) > 0$.

Thus, $\wp'_\Lambda(x)$ is monotone increasing over the intervals on which it is defined. $\square$

The concavity can be observed in Figure 4. We are now ready to prove the main result of this section.

Proposition 4.5. *If Λ is a real rectangular or vertical real rhombic lattice for which $\wp_\Lambda$ has a real attracting fixed point, we have the following for any $\lambda \in \Lambda$:*

(1) $J(\wp_\Lambda) \cap (\mathbb{R} + \lambda)$ *is a Cantor set.*

(2) $J(\wp_\Lambda) \cap (\{z \mid z = iy, y \in \mathbb{R}\} + \lambda)$ *is a Cantor set.*

Proof. Using the notation of Proposition 4.3, let $B = (P'_{n_0}, P_{n_0})$ be the immediate basin of attraction for the attracting fixed point t_{n_0} lying in the interval Λ_{n_0}. By Lemma 2.3 and Proposition 2.9, if $\Lambda_j = [j\lambda_1, (j+1)\lambda_1]$, then $\wp_\Lambda(\Lambda_j) = [e_1, \infty]$ for all j. Further, $\wp_\Lambda^{-1}(B)$ consists of infinitely many disjoint open intervals, one in each Λ_j, each of which is a translation of B by a real lattice point. We label those intervals $B_j \subset \Lambda_j$. We label the intervals complementary to the B_j using C_j such that C_o contains the pole at the origin; then C_{n_0+1} contains the repelling fixed point P_{n_0}.

Let $s = |\wp'_\Lambda(P_{n_0})| > 1$ and $\alpha = \frac{1}{2}(1+s)$. Since $\wp'_\Lambda$ is strictly monotonic by Lemma 4.4,

$$\wp_\Lambda : C_j \to [e_1, \infty] \setminus (B \cap [e_1, \infty])$$

for each j, and $|\wp'_\Lambda(x)| > \alpha > 1$ for each $x \in C_j$.

Defining

$$JR = \left\{ x \in \mathbb{R} \mid \wp_\Lambda^m(x) \in \bigcup_{j \geq n_0} C_j \text{ for all } m \text{ for which } \wp_\Lambda^m \text{ is analytic} \right\},$$

we have

$$z \in JR \iff z \in J(\wp_\Lambda) \cap \mathbb{R}.$$

Since $|\wp'_\Lambda(z)| > \alpha > 1$ for all $z \in C_j$, we know $\mathrm{diam}(\wp_\Lambda^{-m} C_j) \to 0$ as $m \to \infty$. Standard arguments imply that JR is a Cantor set (see [Devaney and Keen 1988]).

To show that the intersection of the Julia set with the imaginary axis is Cantor, we need to investigate rectangular lattices and vertical real rhombic lattices separately. First, if Λ is vertical real rhombic, then by Proposition 2.5(5) and the evenness of $\wp_\Lambda$, every point $x \in (-\infty, e_1)$ has infinitely many pairs of preimages of the form $\pm ia$, $a \in \mathbb{R}$, that lie on the imaginary axis. More precisely, let $\lambda' = \lambda - \bar{\lambda}$ denote the period of $\wp_\Lambda$ along the imaginary axis, and set

$$\Lambda'_j = \left\{ z \in \mathbb{C} \mid \mathrm{Re}(z) = 0 \text{ and } j\lambda' < \mathrm{Im}(z) < (j+1)\lambda' \right\};$$

we can think of Λ'_j as a set of line segments along the imaginary axis on which $\wp_\Lambda$ is periodic. Then in each Λ'_j, $j \in \mathbb{Z}$, there are exactly two preimages of every point $x \in (-\infty, e_1)$. Therefore, for each j, the set

$$\wp_\Lambda^{-1}(JR) \cap \Lambda'_j = J(\wp_\Lambda) \cap \Lambda'_j$$

is a homeomorphic image of JR and hence a Cantor set. If we denote by JR_i the set $J(\wp_\Lambda) \cap \{z = iy\}$, then we have shown that JR_i is a Cantor set.

Finally, if Λ is real rectangular, then by Proposition 2.6(4) and the evenness of $\wp_\Lambda$, every point $x \in (-\infty, e_2)$ again has infinitely many pairs of preimages of the form $\pm ia$, $a \in \mathbb{R}$, that lie on the imaginary axis. If $\Lambda = [\lambda_1, \lambda_2]$, where λ_2 is pure imaginary, then let

$$\Lambda'_j = \left\{ z \in \mathbb{C} \mid \mathrm{Re}(z) = 0 \text{ and } j\lambda_2 < \mathrm{Im}(z) < (j+1)\lambda_2 \right\}.$$

Proceeding as in the vertical real rhombic case, JR_i is Cantor. $\qquad\square$
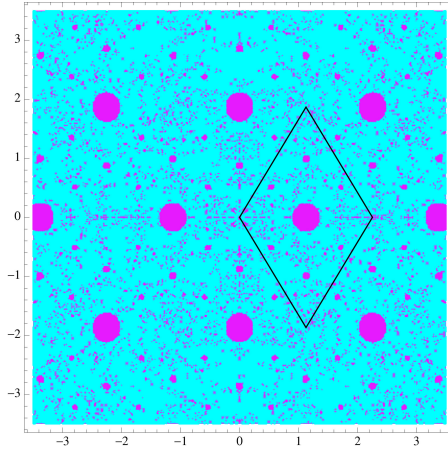
Figure 7. An example where the Julia set restricted to the real axis is Cantor.

We note that finding examples that satisfy the hypothesis of Proposition 4.5 is straightforward using the homogeneity property.

Corollary 4.6. *Let* Γ *be a standard real rectangular or a standard real vertical rhombic lattice, where* γ_1 *is chosen to be the smallest positive real lattice point. If m is any positive odd integer,* $k = \sqrt[3]{2/(m\gamma_1)}$, *and* $\Lambda = k\Gamma$, *then*

(1) $J(\wp_\Lambda) \cap (\mathbb{R} + \lambda)$ *is a Cantor set,*

(2) $J(\wp_\Lambda) \cap \big(\{z \mid z = iy,\, y \in \mathbb{R}\} + \lambda\big)$ *is a Cantor set*

for any $\lambda \in \Lambda$.

Proof. Let Γ be a standard real rectangular or a standard real vertical rhombic lattice, where γ_1 is chosen to be the smallest positive real lattice point, m a positive odd integer, $k = \sqrt[3]{2/(m\gamma_1)}$, and $\Lambda = k\Gamma$. Lemma 2.1(2) implies

$$\wp_\Lambda\big(\tfrac{1}{2}\lambda_1\big) = \wp_{k\Gamma}\big(\tfrac{1}{2}k\gamma_1\big) = \frac{1}{k^2}\wp_\Gamma\big(\tfrac{1}{2}\gamma_1\big) = \tfrac{1}{2}m\lambda_1.$$

Thus $\tfrac{1}{2}m\lambda_1$ is a superattracting fixed point by the periodicity of $\wp_\Lambda$. Proposition 4.5 gives the result. □

Figure 7 illustrates an example constructed through Corollary 4.6 of a function $\wp_\Lambda$ for which the intersection of the real axis and the Julia set is Cantor. We begin with the standard real vertical rhombic lattice Γ with invariants $g_2(\Gamma) = -1$ and $g_3(\Gamma) = 5$ and obtain the lattice Λ with invariants $g_2(\Lambda) \approx -1.269$ and $g_3(\Lambda) \approx 7.148$. The function $\wp_\Lambda$ has a superattracting fixed point at approximately 1.126. Points colored pink in Figure 7 iterate to the superattracting fixed point, and points colored blue lie in the Julia set.

4C. *Invariants for which the Julia set is everything.* Lemma 2.7 was used in [Hawkins and Koss 2002; 2004] to find isolated examples for which the Julia set of $\wp_\Lambda$ is the entire sphere by constructing real lattices for which all three critical values were prepoles. These results were broadened to $\wp_\Lambda$ for every real rhombic square lattice Λ in [Hawkins 2010] and a countable number of real rectangular lattices Λ in every similarity class in [Koss 2014]. For real rhombic square or real rectangular lattices, the entire postcritical orbit of $\wp_\Lambda$ is real, except for at most two points. The Schwarzian derivative was used to show that the functions examined in these papers have no Fatou components.

For real rhombic lattices, the postcritical set is not real. However, we can use the results of Section 3 to find parameters in each real rhombic shape equivalence class for which the Fatou set is empty.

Theorem 4.7. *Let Γ be a standard real vertical rhombic lattice, where γ_1 is chosen to be the smallest positive real lattice point. If m is any positive integer and $k = \sqrt[3]{1/(m\gamma_1)}$, then $\wp_\Lambda$ on the lattice $\Lambda = k\Gamma$ has $J(\wp_\Lambda) = \mathbb{C}_\infty$.*

Proof. Let Γ, m, k, and Λ be defined as in the hypothesis. Since m is a positive integer, $k > 0$ and Λ is a real vertical rhombic lattice. By Proposition 2.9(5), $\wp_\Lambda$ has no Herman rings. By Lemma 2.7, $\wp_\Lambda\left(\frac{1}{2}\lambda_1\right) = m\lambda_1 = e_1$ is a pole. By Proposition 2.5(4), $\text{Re}(e_2) = \text{Re}(e_3) = -\frac{1}{2}m\lambda_1$, so e_2 and e_3 lie on a vertical line passing through a real lattice point or a real half-lattice point. Proposition 2.5(5) implies

$$\wp_\Lambda(e_2) = \wp_\Lambda(e_3) \in \mathbb{R} \cup \{\infty\}.$$

Using Theorem 2.2, the postcritical set is a subset of $\mathbb{R} \cup \{e_1, e_2, \infty\}$. No interval in $\mathbb{R}$ can lie within a Siegel disk component because $\wp_\Lambda : \mathbb{R} \to \mathbb{R}$, which would contradict that $\wp_\Lambda^n$ is conjugate to an irrational rotation of the unit disk. No subset of $\mathbb{R}$ can form the boundary of a Siegel disk since $\wp_\Lambda$ is periodic with respect to Λ. Theorem 3.3 implies that if there were an attracting or parabolic cycle of Fatou components, then the cycle must lie on the real axis and contain a real critical point, a contradiction to the assumption that all real critical points are prepoles. Thus there can be no Fatou components, and $J(\wp_\Lambda) = \mathbb{C}_\infty$. □

We can use Theorem 4.7 and previous results from [Hawkins 2010; Koss 2014] to illustrate parameters in the (g_2, g_3)-plane for which $J(\wp_\Lambda) = \mathbb{C}_\infty$. We show an approximation of the locus of parameters for the cases $m = 1, 2, 3$, and 4 from Theorem 4.7 in this paper and the corresponding Theorem 4.3 in [Koss 2014] in increasingly darker shades in Figure 8: light blue corresponds to $m = 1$, medium blue corresponds to $m = 2$, dark blue corresponds to $m = 3$, black corresponds to $m = 4$. If Λ is a real rhombic square lattice, then $J(\wp_\Lambda) = \mathbb{C}_\infty$ [Hawkins 2010]; these lattices appear in gray in Figure 8 as the negative real axis.
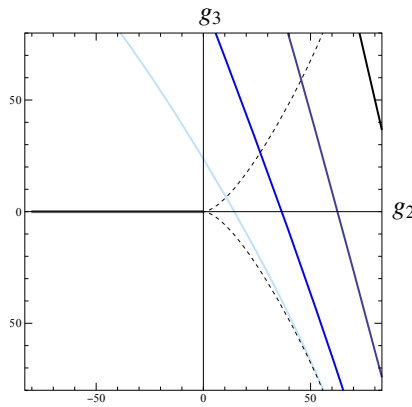
Figure 8. The locus of parameters for which $J(\wp_\Lambda) = \mathbb{C}_\infty$.

Acknowledgement

The authors would like to express their sincere appreciation to the referee, whose comments and suggestions significantly improved the paper.

References

[Baker et al. 1992] I. N. Baker, J. Kotus, and L. Yinian, "Iterates of meromorphic functions, IV: Critically finite functions", *Results Math.* **22**:3–4 (1992), 651–656. MR Zbl

[Bergweiler 1993] W. Bergweiler, "Iteration of meromorphic functions", *Bull. Amer. Math. Soc. (N.S.)* **29**:2 (1993), 151–188. MR Zbl

[Clemons 2012] J. J. Clemons, "Connectivity of Julia sets for Weierstrass elliptic functions on square lattices", *Proc. Amer. Math. Soc.* **140**:6 (2012), 1963–1972. MR Zbl

[Devaney and Keen 1988] R. L. Devaney and L. Keen, "Dynamics of tangent", pp. 105–111 in *Dynamical systems* (College Park, MD, 1986–87), Lecture Notes in Math. **1342**, Springer, 1988. MR Zbl

[Du Val 1973] P. Du Val, *Elliptic functions and elliptic curves*, London Mathematical Society Lecture Note Series **9**, Cambridge University Press, 1973. MR Zbl

[Hawkins 2006] J. Hawkins, "Smooth Julia sets of elliptic functions for square rhombic lattices", *Topology Proc.* **30**:1 (2006), 265–278. MR Zbl

[Hawkins 2010] J. Hawkins, "A family of elliptic functions with Julia set the whole sphere", *J. Difference Equ. Appl.* **16**:5–6 (2010), 597–612. MR Zbl

[Hawkins 2013] J. M. Hawkins, "Proof of a folklore Julia set connectedness theorem and connections with elliptic functions", *Conform. Geom. Dyn.* **17** (2013), 26–38. MR Zbl

[Hawkins and Koss 2002] J. Hawkins and L. Koss, "Ergodic properties and Julia sets of Weierstrass elliptic functions", *Monatsh. Math.* **137**:4 (2002), 273–300. MR Zbl

[Hawkins and Koss 2004] J. Hawkins and L. Koss, "Parametrized dynamics of the Weierstrass elliptic function", *Conform. Geom. Dyn.* **8** (2004), 1–35. MR Zbl

[Hawkins and Koss 2005] J. Hawkins and L. Koss, "Connectivity properties of Julia sets of Weierstrass elliptic functions", *Topology Appl.* **152**:1–2 (2005), 107–137. MR Zbl

[Hawkins and Look 2006] J. M. Hawkins and D. M. Look, "Locally Sierpinski Julia sets of Weierstrass elliptic $\wp$ functions", *Internat. J. Bifur. Chaos Appl. Sci. Engrg.* **16**:5 (2006), 1505–1520. MR Zbl

[Hawkins and McClure 2011] J. Hawkins and M. McClure, "Parameterized dynamics for the Weierstrass elliptic function over square period lattices", *Internat. J. Bifur. Chaos Appl. Sci. Engrg.* **21**:1 (2011), 125–135. MR Zbl

[Jones and Singerman 1987] G. A. Jones and D. Singerman, *Complex functions: an algebraic and geometric viewpoint*, Cambridge University Press, 1987. MR Zbl

[Koss 2014] L. Koss, "Examples of parametrized families of elliptic functions with empty Fatou sets", *New York J. Math.* **20** (2014), 607–625. MR Zbl

[Rippon and Stallard 1999] P. J. Rippon and G. M. Stallard, "Iteration of a class of hyperbolic meromorphic functions", *Proc. Amer. Math. Soc.* **127**:11 (1999), 3251–3258. MR Zbl

[Singer 1978] D. Singer, "Stable orbits and bifurcation of maps of the interval", *SIAM J. Appl. Math.* **35**:2 (1978), 260–267. MR Zbl

koss@dickinson.edu   Department of Mathematics and Computer Science, Dickinson College, P.O. Box 1773, Carlisle, PA 17013, United States

roy.katie.a@gmail.com   Department of Mathematics and Computer Science, Dickinson College, P.O. Box 1773, Carlisle, PA 17013, United States

Pattern avoidance in double lists

Charles Cratty, Samuel Erickson, Frehiwet Negassi and Lara Pudwell

(Communicated by Anant Godbole)

We consider pattern avoidance in a subset of words on $\{1, 1, 2, 2, \ldots, n, n\}$ called double lists. We enumerate double lists avoiding any permutation pattern of length at most 4 and completely determine the corresponding Wilf classes.

1. Introduction

Let $\mathcal{S}_n$ be the set of all permutations on $\{1, 2, \ldots, n\}$. Given $\pi \in \mathcal{S}_n$ and $\rho \in \mathcal{S}_m$, we say that π *contains* ρ as a pattern if there exists $1 \leq i_1 < i_2 < \cdots < i_m \leq n$ such that $\pi_{i_a} \leq \pi_{i_b}$ if and only if $\rho_a \leq \rho_b$. In this case we say that $\pi_{i_1} \cdots \pi_{i_m}$ is *order-isomorphic* to ρ, and that $\pi_{i_1} \cdots \pi_{i_m}$ is an *occurrence* of ρ in π. If π does not contain ρ, then we say that π *avoids* ρ. An *inversion* is an occurrence of the pattern 21, and a *coinversion* is an occurrence of the pattern 12. Pattern-avoiding permutations have been well-studied with applications to algebraic geometry, theoretical computer science, and more. Of particular interest are the sets $\mathcal{S}_n(\rho) = \{\pi \in \mathcal{S}_n \mid \pi \text{ avoids } \rho\}$. Let $s_n(\rho) = |\mathcal{S}_n(\rho)|$. It is well known that $s_n(\rho) = \binom{2n}{n}/(n+1)$ for $\rho \in \mathcal{S}_3$ [Knuth 1968]. For $\rho \in \mathcal{S}_4$, three different sequences are possible for $\{s_n(\rho)\}_{n \geq 1}$. Two of these sequences are well-understood, but the computation of $s_n(1324)$ remains open for $n \geq 37$ [Conway and Guttmann 2014].

Pattern avoidance has been studied for a number of combinatorial objects other than permutations. The definition above extends naturally for patterns in words (i.e., permutations of multisets) and there have been several algorithmic approaches to determining the number of words avoiding various patterns [Brändén and Mansour 2005; Burstein 1998; Jelínek and Mansour 2009; Pudwell 2010].

In another direction, a permutation may be viewed as a bijection on $[n] = \{1, \ldots, n\}$. When we graph the points (i, π_i) in the Cartesian plane, all points lie in the square $[0, n+1] \times [0, n+1]$, and thus we may apply various symmetries of the square to obtain involutions on the set $\mathcal{S}_n$. For $\pi \in \mathcal{S}_n$, let $\pi^r = \pi_n \cdots \pi_1$ be the reverse of π and let $\pi^c = (n+1-\pi_1) \cdots (n+1-\pi_n)$ be the complement of π.
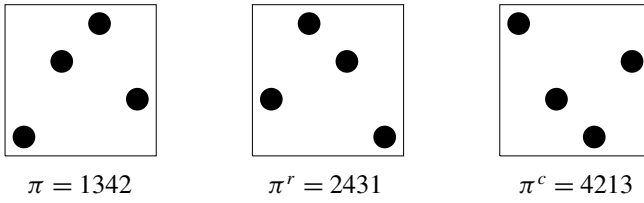
$$\pi = 1342 \qquad\qquad \pi^r = 2431 \qquad\qquad \pi^c = 4213$$

Figure 1. The graphs of $\pi = 1342$, $\pi^r = 2431$, and $\pi^c = 4213$.

For example, the graphs of $\pi = 1342$, $\pi^r = 2431$, and $\pi^c = 4213$ are shown in Figure 1. Pattern avoidance in centrosymmetric permutations, i.e., permutations π such that $\pi^{rc} = \pi$, has been studied by Egge [2010] and by Barnabei, Bonetti and Silimbani [Barnabei et al. 2010]. Ferrari [2011] generalized this idea to pattern avoidance in centrosymmetric words. In all of these cases, knowing the first half of the word or permutation uniquely determines the second half.

A final variation involves circular permutations. In a circular permutation $\pi_1 \cdots \pi_n$, we consider the last digit in the permutation to be adjacent to the first and two permutations are considered the same if they differ by only a rotation. For example, 1234, 2341, 3412, and 4123 are all the same circular permutation. A circular permutation π is said to contain ρ as a pattern if there exists a rotation of π that contains ρ. Circular permutations avoiding permutation patterns were studied by Callan [2002] and Vella [2002/03], who obtained a number of interesting enumeration sequences.

In this paper we consider a specific type of word that borrows ideas from centrosymmetric and circular permutations. In particular, we define the set of *double lists* on n letters to be

$$\mathcal{D}_n = \{\pi\pi \mid \pi \in \mathcal{S}_n\}.$$

In other words, a double list is a permutation of $\{1, \ldots, n\}$ concatenated with itself. We see immediately that $|\mathcal{D}_n| = n!$. As with centrosymmetric objects, knowing the first half of a double list determines the second half. As with circular permutations, we have taken a permutation and appended the end to the beginning. Yet, double lists are a new combinatorial object of interest in their own right. Consider

$$\mathcal{D}_n(\rho) = \{\sigma \in \mathcal{D}_n \mid \sigma \text{ avoids } \rho\},$$

and let $d_n(\rho) = |\mathcal{D}_n(\rho)|$. We obtain a number of interesting enumeration sequences for $\{d_n(\rho)\}_{n \geq 1}$ with connections to other combinatorial objects. The goal of this paper is to completely determine $d_n(\rho)$ for $\rho \in \mathcal{S}_1 \cup \mathcal{S}_2 \cup \mathcal{S}_3 \cup \mathcal{S}_4$.

2. Avoiding patterns of length 1, 2, or 3

The main focus of this paper is avoidance of length-4 patterns, but for completeness we first consider shorter patterns. First, notice that the graph of a double list $\sigma \in \mathcal{D}_n$

is a set of points on the rectangle $[0, 2n+1] \times [0, n+1]$. Using the reverse and complement involutions described in Section 1, we see that

$$\sigma \in \mathcal{D}_n(\rho) \iff \sigma^r \in \mathcal{D}_n(\rho^r) \iff \sigma^c \in \mathcal{D}_n(\rho^c).$$

We will partition the set of permutation patterns of length m into equivalence classes, where $\rho \sim \tau$ means that $d_n(\rho) = d_n(\tau)$ for $n \geq 1$. In this case ρ and τ are said to be *Wilf equivalent*. When this equivalence holds because of one of the symmetries of the rectangle, we say that ρ and τ are *trivially Wilf equivalent*. Using trivial Wilf equivalence, we have $12 \sim 21$, $123 \sim 321$ and $132 \sim 213 \sim 231 \sim 312$, so we need only consider four patterns in this section: 1, 12, 123, and 132.

Avoiding a pattern of length 1 or length 2 is trivial. It is straightforward to check that for $n \geq 1$, we have $d_n(1) = 0$, and similarly

$$d_n(12) = d_n(21) = \begin{cases} 1 & \text{if } n = 1, \\ 0 & \text{if } n \geq 2. \end{cases}$$

With pattern-avoiding permutations, avoiding a pattern of length 3 is the first nontrivial enumeration, and for any pattern ρ of length 3, we have that $s_n(\rho)$ is the n-th Catalan number. Double lists are more restrictive, so we obtain simpler sequences for $d_n(\rho)$. More strikingly, although $s_n(123) = s_n(132)$ for $n \geq 1$, we obtain two distinct sequences in this new context.

Proposition. $\qquad\qquad d_n(123) = d_n(321) = \begin{cases} n! & \text{if } n \leq 2, \\ 1 & \text{if } n \geq 3. \end{cases}$

Proof. For $n \leq 2$, all double lists avoid permutation patterns of length 3. However, for $n \geq 3$, the unique double list avoiding 123 is $n \cdots 1n \cdots 1$. We verify this directly for the six members of $\mathcal{D}_3$, with a copy of 123 underlined in each of the other five double lists: $\underline{123}123$, $\underline{13}2\underline{13}2$, $2\underline{13}2\underline{13}$, $231\underline{231}$, $3\underline{123}12$. Now, assume $\mathcal{D}_n(123) = \{n \cdots 1n \cdots 1\}$ and consider $\mathcal{D}_{n+1}(123)$. Given $\sigma \in \mathcal{D}_{n+1}(123)$, let σ' be the double list obtained by deleting both copies of $n+1$ in σ. Since $\sigma \in \mathcal{D}_{n+1}(123)$, we know $\sigma' \in \mathcal{D}_n(123)$. By assumption, $\sigma' = n \cdots 1n \cdots 1$. To construct σ, we must only reinsert the two copies of $n+1$ so that σ avoids 123. If $n+1$ is inserted after the initial n, then we have $1n(n+1)$ as a copy of 123 in σ, where the 1 is in the first half of σ, and $n(n+1)$ is in the second half of σ. Therefore, $n+1$ must be inserted before the initial n, and $\mathcal{D}_{n+1}(123) = \{(n+1)n \cdots 1(n+1)n \cdots 1\}$. $\qquad \square$

Finally, we consider double lists avoiding 132.

Proposition. $\quad d_n(132) = d_n(213) = d_n(231) = d_n(312) = \begin{cases} n! & \text{if } n \leq 2, \\ 1 & \text{if } n = 3, \\ 0 & \text{if } n = 4. \end{cases}$

Proof. For $n \leq 2$, all double lists avoid permutation patterns of length 3. However, for $n = 3$, the unique double list avoiding 132 is 231231. Indeed for the other

five double lists in $\mathcal{D}_3$, we have 1̲2̲3̲1̲2̲3, 1̲3̲2̲1̲3̲2, 2̲1̲3̲2̲1̲3, 3̲1̲2̲3̲1̲2, 3̲2̲1̲3̲2̲1. Now, consider the four ways to insert 4 into 231231: 42̲3̲1̲4231, 24̲3̲1̲2̲4̲31, 23̲4̲1̲2̲341, 23̲1̲4̲2̲314. We see (via the underlined occurrences) that each of these double lists contains a 132 pattern. If there are no 132-avoiding double lists of length n, then there are no 132-avoiding double lists of length $n+1$, since deleting both occurrences of $n+1$ in such a list should produce another 132-avoiding double list.   □

At this point, we have completely characterized double lists avoiding a single pattern of length 1, 2, or 3. Although we obtained only trivial sequences, the fact that we obtained two distinct Wilf classes for avoiding patterns of length 3 is a noteworthy difference between avoidance in double lists and avoidance in permutations.

3. Avoiding patterns of length 4

The remainder of this paper is concerned with double lists avoiding a single pattern of length 4. Using the symmetries of the rectangle, we can partition the 24 patterns of length 4 into eight trivial Wilf classes, as shown in Table 1. Notably, the trivial Wilf equivalences are the *only* Wilf equivalences for patterns of length 4. This is in contrast to the case for pattern-avoiding permutations. In that context, we have an additional trivial Wilf equivalence since $s_n(\rho) = s_n(\rho^{-1})$ for $n \geq 1$, so $s_n(1342) = s_n(1423)$. As it turns out, there are a number of nontrivial Wilf equivalences for pattern-avoiding permutations so that every length-4 pattern is equivalent to one of 1342, 1234, or 1324. For large n, we have

$$s_n(1342^\bullet) < s_n(1234^\dagger) < s_n(1324^\circ).$$

In Table 1 each pattern is marked according to its Wilf equivalence class for permutations; patterns equivalent to 1342 are marked with •, those equivalent to 1234 are marked with †, and those equivalent to 1324 are marked with ○. A closer look at the table reveals a couple more subtleties of the pattern-avoiding double

pattern ρ	$\{d_n(\rho)\}_{n=1}^{10}$
$1342^\bullet \sim 2431^\bullet \sim 3124^\bullet \sim 4213^\bullet$	1, 2, 6, 12, 15, 15, 15, 15, 15, 15
$2143^\dagger \sim 3412^\dagger$	1, 2, 6, 12, 13, 14, 16, 18, 20, 22
$1423^\bullet \sim 2314^\bullet \sim 3241^\bullet \sim 4132^\bullet$	1, 2, 6, 12, 17, 23, 27, 30, 33, 36
$1432^\dagger \sim 2341^\dagger \sim 3214^\dagger \sim 4123^\dagger$	1, 2, 6, 12, 17, 23, 31, 40, 50, 61
$1243^\dagger \sim 2134^\dagger \sim 3421^\dagger \sim 4312^\dagger$	1, 2, 6, 12, 19, 25, 34, 44, 55, 67
$2413^\bullet \sim 3142^\bullet$	1, 2, 6, 12, 18, 29, 47, 76, 123, 199
$1324^\circ \sim 4231^\circ$	1, 2, 6, 12, 21, 38, 69, 126, 232, 427
$1234^\dagger \sim 4321^\dagger$	1, 2, 6, 12, 27, 58, 121, 248, 503, 1014

Table 1. Enumeration of double lists avoiding a pattern of length 4.

lists problem. For permutations, the monotone pattern 1234 is neither the hardest nor the easiest pattern to avoid; for double lists, it is the easiest pattern to avoid. Similarly, one might expect that all patterns equivalent to 1324 may produce smaller sequences than those avoiding 1234, which produce smaller sequences than those avoiding 1324, but this is also not the case. Other than the trivial equivalences of reverse and complement, Wilf equivalence in the context of double lists appears to be a very different phenomenon than equivalence in the context of permutations. We now consider each of these patterns in turn.

3.1. *The pattern 1342.* The pattern 1342 is the hardest permutation of length 4 to avoid, and, from initial data, is the easiest pattern for which to conjecture a general enumeration formula.

Theorem 1.
$$d_n(1342) = \begin{cases} n! & \text{if } n \leq 3, \\ 12 & \text{if } n = 4, \\ 15 & \text{if } n \geq 5. \end{cases}$$

Proof. For $n \leq 3$, all double lists avoid 1342, and for $n = 4$, a check of the 24 members of $\mathcal{D}_n$ yields exactly 12 that avoid 1342. They are 12431243, 21342134, 23142314, 23412341, 24132413, 24312431, 31243124, 32143214, 32413241, 42314231, 43124312, 43214321.

We now consider $\mathcal{D}_n(1342)$ for $n \geq 5$ and make three key structural observations. Let $\sigma = \pi\pi \in \mathcal{D}_n(1342)$ and let $\sigma' = \pi'\pi' \in \mathcal{D}_{n-2}(1342)$ be the double list obtained by deleting both copies of n and both copies of $n-1$ from σ. Then:

(1) π' avoids 123.

(2) π' contains at most one coinversion.

(3) If π' contains a coinversion, then the coinversion is composed of the digits 1 and 2 or the digits 2 and 3.

For the first observation, suppose to the contrary that π' contains 123 and the occurrence of 123 is formed by the digits $\pi'_a < \pi'_b < \pi'_c$. If n (resp. $n-1$) appears before π'_b or after π'_c in π, then $\pi'_a\pi'_c n\pi'_b$ (resp. $\pi'_a\pi'_c(n-1)\pi'_b$) is a copy of 1342 in $\sigma = \pi\pi$. Therefore, n and $n-1$ must both appear between π'_b and π'_c in π. If they are in increasing order, then $\pi'_a(n-1)n\pi'_c$ is a copy of 1342 in π, and thus in σ. If they are in decreasing order, then $\pi'_a(n-1)n\pi'_c$ is a copy of 1342 in σ. Since we have exhausted all possible options, it must be the case that π' avoids 123.

For the second observation, we know π' avoids 123, so if π' contains two coinversions, either (a) π' contains the pattern 132, (b) π' contains the pattern 213, or (c) π' contains the pattern 3412. It can be shown that cases (a) and (b) are impossible by an analysis similar to the previous paragraph, conditioning on various possible positions of n and $n-1$. Case (c) is even more readily discounted, since 34123412 already contains a copy of 1342.

Finally, if π' contains a coinversion, we show that it must use two consecutive digits and they must include the digit 2. Suppose on the contrary that we have the coinversion $\pi_i' < \pi_j'$, where $|\pi_j' - \pi_i'| > 1$. Then no matter the location of $\pi_i' + 1$, it forms a coinversion with either π_i' or π_j'. This contradicts our previous observation that π' contains at most one coinversion. Therefore, the coinversion must use consecutive digits. Now suppose the coinversion uses digits π_i' and $\pi_i' + 1$, where $\pi_i' \geq 3$. To avoid other coinversions, it must be the case that

$$\pi' = (n-2)(n-3)(n-4)\cdots(\pi_i'+3)(\pi_i'+2)\pi_i'(\pi_i'+1)(\pi_i'-1)(\pi_i'-2)\cdots 21.$$

However, in this case, $1\pi_i'(\pi_i'+1)2$ is a copy of 1342 in σ. Therefore, any coinversion must either use the digits 1 and 2 or the digits 2 and 3.

Using these three observations, we see that there are only three possible forms for π'. They are $(n-2)\cdots 1$ (the decreasing permutation), $(n-2)\cdots 4231$, and $(n-2)\cdots 312$. Now, we consider ways to reinsert n and $n-1$ into π' to form π so that $\sigma = \pi\pi$ is a member of $\mathcal{D}_n(1342)$. There are six ways to insert them into the decreasing permutation; namely,

$$n\cdots 1, \qquad (n-1)\cdots 1n, \qquad (n-1)\cdots 2n1,$$
$$(n-2)\cdots 1n(n-1), \quad (n-2)\cdots 2n1(n-1), \quad (n-2)\cdots 2n(n-1)1.$$

There are also six ways to insert them into $(n-2)\cdots 4231$; namely,

$$n\cdots 4231, \qquad (n-1)\cdots 4231n,$$
$$(n-1)\cdots 423n1, \qquad (n-2)\cdots 4231n(n-1),$$
$$(n-2)\cdots 423n1(n-1), \quad (n-2)\cdots 423n(n-1)1.$$

Finally, there are only three ways to insert them into $(n-2)\cdots 312$; namely,

$$n\cdots 312, \quad (n-1)\cdots 312n, \quad (n-2)\cdots 312n(n-1).$$

These 15 permutations π uniquely describe all possible members $\sigma = \pi\pi \in \mathcal{D}_n(1342)$ for $n \geq 5$. $\qquad\square$

To illustrate, the 15 members of $\mathcal{D}_6(1342)$ are shown in Figure 2. While an eventually constant sequence is expected for smaller patterns, the constant sequence 15 is perhaps a bit more surprising in this context. Nonetheless the structural argument in this proof sets the stage for several of the proofs in the following subsections.

3.2. The patterns 2143 and 1423. Two of our patterns yield avoidance sequences that grow linearly.

Theorem 2.
$$d_n(2143) = \begin{cases} n! & \text{if } n \leq 3, \\ 12 & \text{if } n = 4, \\ 13 & \text{if } n = 5, \\ 2(n+1) & \text{if } n \geq 6. \end{cases}$$
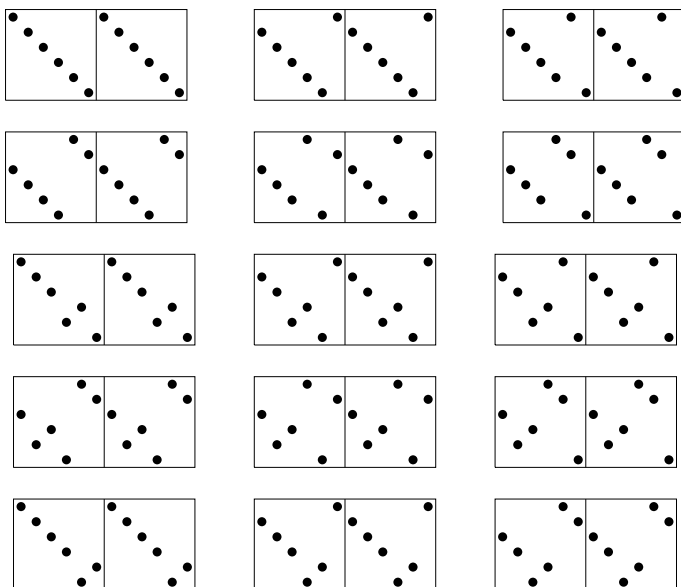
Figure 2. The members of $\mathcal{D}_6(1342)$.

Proof. The cases for $n \leq 5$ are easily verified by brute force methods, so we focus on the case where $n \geq 6$. Intuitively there are an even number of double lists avoiding 2143 for a geometric reason. We have $2143^{rc} = 2143$, so ρ avoids 2143 if and only if ρ^{rc} avoids 2143. For $n \geq 6$, there are exactly two members $\sigma = \pi\pi$ of $\mathcal{D}_n(2143)$ that are reverse-complement invariant. If n is even, they are

$$\pi = 12 \cdots n \quad \text{and} \quad \pi = \frac{n+2}{2} \cdots n 1 \cdots \frac{n}{2}.$$

If n is odd, they are

$$\pi = 12 \cdots n \quad \text{and} \quad \pi = \frac{n+3}{2} \cdots n \frac{n+1}{2} 1 \cdots \frac{n-1}{2}.$$

All other 2143-avoiders come in pairs ρ and ρ^{rc}. However, it turns out that it is easier to characterize the members of $\mathcal{D}_n(2143)$ using other distinguishing features.

Notice that there are no inversions among elements after 1 and larger than 2 in π. Suppose to the contrary that $i < j < k$, where $\pi_i = 1$ and $\pi_j > \pi_k > 2$. Then $21\pi_j\pi_k$ forms an occurrence of 2143 in σ. Similarly, all elements before n and other than $n-1$ must appear in increasing order. Therefore, there are only three possible double lists $\sigma = \pi\pi$ where 1 precedes n: $\pi = 12 \cdots n$, $\pi = 13 \cdots n2$, and $\pi = (n-1)12 \cdots (n-2)n$. So far, we have described three members of $\mathcal{D}_n(2143)$, as shown in . It remains to consider when n precedes 1 in π.
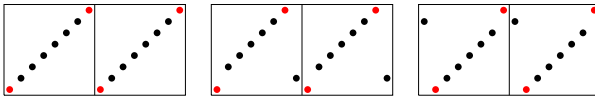
Figure 3. 2143-avoiding lists where 1 precedes n.
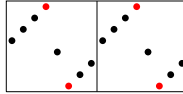
Figure 4. 2143-avoiders where n is two positions before 1.
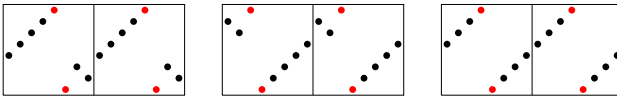
Figure 5. 2143-avoiders where n immediately precedes 1.

If n precedes 1, then there is at most one element between n and 1. Suppose to the contrary that there are two elements $\pi_a > \pi_b$ that appear between n and 1 in π. Then $\pi_b 1 n \pi_a$ forms a 2143 pattern in σ, taking $\pi_b 1$ from the first copy of π and $n \pi_a$ from the second copy. We have two subcases: either $\pi_{j-1} = n$ and $\pi_{j+1} = 1$ or $\pi_{j-1} = n$ and $\pi_j = 1$.

In the case where $\pi_{j-1} = n$ and $\pi_{j+1} = 1$, let $i = \pi_j$. Consider elements π_a and π_b, such that $a < j - 1$ and $b > j + 1$. It must be the case that $\pi_a > \pi_j > \pi_b$; otherwise, a case analysis shows that σ contains a 2143 pattern. Next, an inversion $\pi_a > \pi_b$ after π_{j+1} creates the 2143 occurrence $\pi_a \pi_b n i$ in σ, while an inversion $\pi_a > \pi_b$ before π_{j-1} creates the 2143 occurrence $i 1 \pi_a \pi_b$ in σ. Therefore, the only 2143-avoiders in this case are the $n - 2$ lists where $\pi = (i + 1) \cdots n i 1 \cdots (i - 1)$ $(2 \le i \le n - 1)$, as shown in Figure 4.

On the other hand, if $\pi_{j-1} = n$ and $\pi_j = 1$, if there is an inversion in $\pi_1 \cdots \pi_{j-2}$ or in $\pi_{j+1} \cdots \pi_n$, there is a 2143 pattern with two exceptions. The double lists where $\pi = 4 \cdots n 1 3 2$ or $\pi = (n - 1)(n - 2) n 1 \cdots (n - 3)$ are 2143-avoiding. In addition, we obtain $n - 1$ lists where $\pi = i \cdots n 1 \cdots i - 1$ $(2 \le i \le n)$. There are $2 + (n - 1) = n + 1$ members of $\mathcal{D}_n(2143)$ where n immediately precedes 1, as shown in Figure 5.

We have now accounted for $(n - 2) + (n + 1) = 2n - 1$ additional permutations π such that $\pi \pi \in \mathcal{D}_n(2143)$. Together with the original three lists we have $2n - 1 + 3 = 2(n + 1)$ double lists avoiding 2143. $\qquad \square$

The number of 1423-avoiding double lists also grows linearly but for a different reason.

Theorem 3.
$$d_n(1423) = \begin{cases} n! & \text{if } n \le 3, \\ 12 & \text{if } n = 4, \\ 17 & \text{if } n = 5, \\ 23 & \text{if } n = 6, \\ 3(n+2) & \text{if } n \ge 7. \end{cases}$$

Proof. Again, the cases for $n \le 6$ are easily verified by brute force methods, so we focus on the case where $n \ge 7$. Now, we condition on which of the letters 1 and n comes first in $\sigma = \pi\pi \in \mathcal{D}_n(1423)$.

If 1 precedes n, then all other digits must appear in decreasing order in π; otherwise, $1n$ in the first copy of π and any increasing pair in the second copy of π form a 1423 pattern in $\sigma = \pi\pi$. Further, n must be the last element of π. Since all other digits appear in decreasing order, if n is not the last digit of π, then $\pi_n = 2$, and $1n23$ is a 1423 pattern in σ. Since n is last, then either $\pi_{n-1} = 1$, $\pi_{n-2} = 1$, or $\pi_{n-3} = 1$. Otherwise, $\pi_{n-3} > \pi_{n-2} > \pi_{n-1}$ and $1\pi_{n-3}\pi_{n-1}\pi_{n-2}$ is a copy of 1423 in σ, taking the first three digits from the first copy of π and the remaining digit from the second copy. There are exactly three double lists in $\mathcal{D}_n(1423)$ where 1 precedes n; namely, $\pi = (n-1)\cdots 4132n$, $\pi = (n-1)\cdots 312n$ and $\pi = (n-1)\cdots 1n$.

Now, suppose n precedes 1. We quickly see that the digits after 1 in π must appear in decreasing order; otherwise, 1 from the first copy of π and n and the increasing pair from the second copy form a 1423 pattern. This implies there are at most two digits after 1 in π; otherwise, we can form a 1423 pattern using $1\pi_{n-2}\pi_n$ from the first copy of π and π_{n-1} from the second copy of π. Similarly, all digits after n and larger than 1 in π must appear in decreasing order.

What can be said about the digits that appear before n? Two things: (a) either the only digit before n is $n-2$, or all digits before n are larger than all digits after n, and (b) if there are at least four digits before n, then they appear in decreasing order. For observation (a), if $\pi_1 = i$ and $\pi_2 = n$, where $i < n-2$, then $in(n-2)(n-1)$ forms a 1423 pattern in σ, where the first three digits come from the first copy of π. Further, if there is more than one digit before n in π, let the first two digits of π be a and b, where $a < b$. By assumption there exists a digit c that appears after n in π, where $a < c$. We have either *anbc* or *ancb* is a 1423 pattern in σ, where in the first case, *an* comes from the first copy of π and in the second case, *anc* comes from the first copy of π. Therefore, observation (a) holds. A similar analysis supports observation (b). If there are two digits before n in π, they may appear in either order, and if there are three digits before n they may form either a 132 pattern or a 321 pattern as all other patterns lead to a 1423 pattern in σ.

Here, then, is the final enumeration. We have seen three double lists where $\pi_n = n$. We have also seen that if n precedes 1, we may choose the position of n, the

arrangement of the digits before n, and the position of 1 (one of the last three digits), and then the rest of the double list is decreasing. Therefore, there are three double lists beginning with n, three beginning with $(n-1)n$, three beginning with $(n-2)n$, three beginning with $(n-2)(n-1)n$, three beginning with $(n-1)(n-2)n$, three beginning with $(n-3)(n-1)(n-2)n$, three beginning with $(n-1)(n-2)(n-3)n$, and three where $\pi_i = n$ for $5 \le i \le n-3$. Finally there are two lists where $\pi_{n-2} = n$ (since there are only two positions to place 1 following n), and one list where $\pi_{n-1} = n$. Adding these together, we have $3 \cdot 8 + 3 \cdot (n-7) + 3 = 3(n+2)$ double lists avoiding 1423.   □

3.3. *The patterns 1432 and 1243.* The avoidance sequences for two patterns grow quadratically.

Theorem 4.
$$d_n(1432) = \begin{cases} n! & \text{if } n \le 3, \\ 12 & \text{if } n = 4, \\ 17 & \text{if } n = 5, \\ \frac{1}{2}n^2 + \frac{3}{2}n - 4 & \text{if } n \ge 6. \end{cases}$$

Proof. Again, the base cases are easily checked by brute force techniques, so we focus on the case where $n \ge 7$.

First, consider $\sigma' = \pi'\pi' \in \mathcal{D}_{n-1}(1432)$. Notice that all digits after $n-1$ in π' and larger than 1 must appear in increasing order; otherwise, the 1 from the first copy of π' followed by $n-1$ and a decreasing pair from the second copy of π' form a 1432 pattern.

Now, we claim that if $\sigma' = \pi'\pi' \in \mathcal{D}_{n-1}(1432)$, then inserting n immediately after $n-1$ produces a member $\sigma = \pi\pi$ of $\mathcal{D}_n(1432)$. Suppose to the contrary that inserting n immediately after $n-1$ creates a 1432 pattern. Then n must play the role of "4" in this new occurrence. If $n-1$ does not play the role of "3", then using $n-1$ instead of n would be a 1432 pattern in σ'. Therefore, the new forbidden pattern must involve the n from the first copy of π and the $n-1$ from the second copy of π with two numbers a and b playing the roles of "1" and "2" respectively. Next, if $b < n-2$, we know that one copy of $n-2$ must occur somewhere between the two copies of $n-1$ in σ', so $a(n-1)(n-2)b$ would be a forbidden pattern in σ'. Thus, $b = n-2$. If $a < n-3$, then one copy of $n-3$ must appear somewhere between the two copies of $n-2$ in σ', so $a(n-1)(n-2)(n-3)$ would be a forbidden pattern in σ'. Thus, $a = n-3$. We now know that in π', the largest four digits appear in the order $(n-3)(n-1)n(n-2)$. We also assume $n \ge 7$, so there are at least three smaller digits in π'. If any of these smaller digits d appears before $n-1$ in π', then $d(n-1)(n-2)(n-3)$ would be a forbidden pattern in σ', so it must be the case that all digits smaller than $n-3$ appear after $n-1$ in π'. From the previous paragraph, we know that the digits $2, 3, \ldots, n-4$ must appear in increasing order before $n-2$. Now, $1(n-2)$ from the first copy of π', followed by $(n-3)(n-4)$ from the second copy of π' form

a forbidden pattern in σ'. In every case, we have shown that if σ' avoids 1432, then the insertion of n immediately after $n - 1$ results in σ avoiding 1432 as well.

Further, there is at most one digit after $n - 1$ in π'. Suppose to the contrary that both digits b and c (with $b < c$) appear after $n - 1$ in π'. Then $a(n-1)cb$ is a 1432 pattern in σ', where the first three digits come from the first copy of π'. Also, since we assumed $n \geq 7$, there are at least two digits that appear before $n - 1$ in π'. Pick one such digit d, where $d \neq a$. If $d < a$, then $d(n-1)ba$ is a forbidden pattern. If $d > a$, then $a(n-1)bd$ or $a(n-1)db$ is a forbidden pattern. In any case, we have shown that σ contains a forbidden pattern not including n, so $\sigma' \notin \mathcal{D}_{n-1}(1432)$, which is a contradiction.

Now, we must account for members $\sigma = \pi\pi$ of $\mathcal{D}_n(1432)$ where n does not immediately follow $n-1$ in π. We consider two cases: n follows $n-1$ and n precedes $n-1$.

If n follows $n - 1$, but not immediately, there can be at most one digit between them; otherwise, if $a < b$ are two digits between them in π, then $an(n-1)b$ forms a 1432 pattern in σ. Further, that one digit between n and $n - 1$ must be smaller than all digits before $n - 1$ and larger than all digits after n. Otherwise, suppose $a < b$ or $b < c$, where a is before $n - 1$, b is between $n - 1$ and n, and c is after n. If $a < b$, then $an(n-1)b$ forms a forbidden pattern. If $b < c$, then $bn(n-1)c$ forms a forbidden pattern. Next, all digits before $n - 1$ in π must appear in increasing order; otherwise, bn from the first copy of π followed by the descent is a forbidden pattern. Finally, the only digit that can appear after n is 1. We already have seen that all digits after $n - 1$ and smaller than $n - 1$ and larger than 1 must appear in increasing order. A digit cannot be smaller than b and in increasing order with b at the same time. The only two lists of this form are when $\pi = 2 \cdots (n-1)1n$ or $\pi = 3 \cdots (n-1)2n1$.

If n precedes $n - 1$, we have a different situation. We know everything after n and larger than 1 appears in increasing order; otherwise, 1 from the first copy of π followed by n and the decreasing pair form a 1432 pattern. Finally we show that in this case, n must be the first digit of π. Suppose n is preceded by two digits $a < b$. Then $an(n-1)b$ is a forbidden pattern in σ, where $an(n-1)$ comes from the first copy of π and b comes from the second copy. Therefore, n must be the first or second digit in π. Suppose n is preceded by a digit a. If $a < n - 2$ then $an(n-1)(n-2)$ is a forbidden pattern in σ. If $a = n - 2$, recall all digits after n other than 1 must be in increasing order and $n \geq 6$ so $(n-4)(n-1)(n-2)(n-3)$ is a forbidden pattern. Thus if n precedes $n - 1$, then n is the first digit of π, and after choosing the position of 1, the rest of π is uniquely determined. There are $n - 1$ choices for the position of 1, so we get $n - 1$ double lists in this case.

In summary, we have shown that

$$\mathrm{d}_n(1432) = \mathrm{d}_{n-1}(1432) + 2 + (n - 1) = \mathrm{d}_{n-1}(1432) + n + 1,$$

and combining this with $\mathrm{d}_6(1432) = 23$ yields the quadratic formula above. $\qquad \square$

Theorem 5. $d_n(1243) = \begin{cases} n! & \text{if } n \leq 3, \\ 12 & \text{if } n = 4, \\ 19 & \text{if } n = 5, \\ \frac{1}{2}n^2 + \frac{5}{2}n - 8 & \text{if } n \geq 6. \end{cases}$

Proof. Again, the base cases are easily checked by brute force techniques, so we focus on the case where $n \geq 7$.

We claim that if $\sigma' = \pi'\pi' \in \mathcal{D}_{n-1}(1243)$, then appending 1 to the end of π' and increasing all other digits by 1 produces a member $\sigma = \pi\pi$ of $\mathcal{D}_n(1243)$. Suppose to the contrary that σ contains a 1243 pattern but σ' does not. Then the 1 at the end of the first copy of π must play the role of "1" and π' contains a 132 pattern. Further, the digit 2 in the second copy of π must play the role of "1" in this 132 pattern; otherwise, taking 2 from the first copy of π followed by the 132 pattern in the second copy of π implies there is a 1243 pattern in σ'. Therefore the 1243 pattern in σ uses 1 from the first copy of π, 2 from the second copy of π, and digits a and b playing the roles of "4" and "3" respectively.

Further, there are at most two digits between the 2 and the 1 in π. If the digits between 2 and 1 contain a 132 occurrence then 2 followed by this occurrence is a forbidden 1243 occurrence. We know that the only double list of length 3 or more that avoids 132 is 231231. If the digits between 2 and 1 contain the pattern 231231, then a sublist of σ is 2453124531, which contains the 1243 occurrence 1253. Now, since $n \geq 7$, there are at least three digits appearing before 2. If at least one of them, c, is less than b, then $2cab$ is a forbidden pattern in σ. If at least one of them, d, is greater than a, then $2bda$ is a forbidden pattern. If all three digits are greater than b and less than a and there is a decreasing pair $e > f$, then $2bef$ is a forbidden pattern, so we may assume the three digits before 2 appear in increasing order with $e < f < g$ and are all between a and b in value. However, in this case $efag$ is a forbidden pattern. In all cases we have found a copy of 1243 in σ', so it must be the case that inserting a 1 at the end of π' and incrementing all other digits produces another 1243-avoiding double list.

Now, we consider members $\sigma = \pi\pi$ of $\mathcal{D}_n(1243)$ that do not end in 1. Notice that 1 must be one of the last three digits of π. If there were three digits after 1 with $a < b < c$, then in order for the digits $1, a, b, c$ to avoid 1243, we must have $1bca1bca$. Now consider d and e as digits before 1. If $d < a$ then $1dba$ is a forbidden pattern. If $d > b$ then $1adb$ is a forbidden pattern so we may assume d and e are both between a and b in value. If $d > e$ appear in decreasing order, then $1ade$ is a forbidden pattern. If $d > e$ appear in increasing order, then $edcb$ is a forbidden pattern. Thus, it must be the case that there are at most two digits after 1.

Suppose then that 1 is followed by two digits in π. Let $a < b$ be those two digits. If $b < n$, then $1anb$ forms a forbidden pattern, so $b = n$. Further, we know

that all digits larger than a must appear in increasing order in π, lest we create
a 1243 pattern using 1 and a as "1" and "2". Thus, the last three digits of π are
$1ab = 1an$. If there are at least four digits $c < d < e < f$ larger than a, then $cdfe$ is
a 1243 pattern in σ. So, it must be the case that $a \geq n - 3$. If $a = n - 3$ or $a = n - 2$,
then $1an(n-1)$ is a forbidden pattern, so the only option is to end in $1(n-1)n$.
The digits before 1 must appear in decreasing order; otherwise, the increasing pair
followed by $n(n-1)$ is a forbidden pattern. In this case, we get one double list
where $\pi = (n-2) \cdots 1(n-1)n$.

Suppose 1 is followed by exactly one digit in π. If π ends in $1i$, where
$i \leq n - 4$, then all numbers larger than i must be in increasing order in π and
$(n-3)(n-2)n(n-1)$ is a forbidden pattern in σ. If 1 is followed by n, then we
have $n - 2$ choices for the location of $n - 1$ and the rest of the digits must appear
in decreasing order, lest we have a 1243 pattern. If 1 is followed by i, where
$n - 2 \leq i \leq n - 1$, then n appears in position $n - i$ and the rest of the digits are
decreasing. If 1 is followed by $n-3$, we have $\pi = (n-2)(n-1)n(n-4) \cdots 1(n-3)$.
There are $1 + (n - 2) + 3 = n + 2$ possible double lists that do not end in 1.

In summary, $d_n(1243) = d_{n-1}(1243) + n + 2$, and putting this together with the
base cases above, we achieve the desired enumeration.   □

3.4. *The patterns 1234, 2413, and 1324.* The results of the previous sections make
a stark contrast with pattern-avoiding permutations, where most avoidance sequences
grow exponentially. However, pattern avoidance in double lists is more restrictive,
so it should not be surprising that we achieve such a variety of behaviors. We
conclude by examining the three final patterns of length 4, each of whose avoidance
sequences exhibits exponential growth.

We begin with the monotone pattern. In the context of permutations, 1234 is
neither the hardest nor the easiest pattern to avoid, but for double lists it turns out
that it is the easiest to avoid.

Theorem 6.
$$d_n(1234) = \begin{cases} n! & \text{if } n \leq 3, \\ 12 & \text{if } n = 4, \\ 2^n - n & \text{if } n \geq 5. \end{cases}$$

Proof. If $\sigma = \pi\pi \in \mathcal{D}_n(1234)$, where $n \geq 5$, the digits of π may be partitioned
into two subsequences: for some i, where $0 \leq i \leq n$, the largest i digits appear in
decreasing order in π, the smallest $n - i$ digits appear in decreasing order in π,
and these two subsequences may be interleaved in any way. In either case, the
permutation π may be encoded by a list of ℓ's and s's for whether a digit belongs
to the decreasing subsequence of larger digits or the decreasing subsequence of
smaller digits. There are 2^n such encodings of a sequence of n ℓ's and s's; however,
$n + 1$ of them (those of the form $\ell^i s^{n-i}$) encode the decreasing permutation, so we
have overcounted by n. There are $2^n - n$ double lists avoiding the pattern 1234. □

The remaining two patterns also produce nice sequences that are characterized by linear recurrences with constant coefficients. Double lists avoiding 2413 are counted by the Lucas numbers L_n, where $L_0 = 2$, $L_1 = 1$, and $L_n = L_{n-1} + L_{n-2}$ for $n \geq 2$.

Theorem 7.
$$d_n(2413) = \begin{cases} n! & \text{if } n \leq 3, \\ 12 & \text{if } n = 4, \\ L_{n+1} & \text{if } n \geq 5. \end{cases}$$

Proof. As usual, it is straightforward to confirm the theorem via brute force techniques for specific small n. We show that $d_n(2413) = d_{n-1}(2413) + d_{n-2}(2413)$ for $n \geq 7$.

We actually prove a more specific result. Let
$$\mathcal{D}_n^i = \{\sigma \in \mathcal{D}_n(2413) \mid \sigma_1 = i\}$$

and $d_n^i(2413) = |\mathcal{D}_n^i(2413)|$. It turns out that $d_n^i(2413) = 0$ if $i \notin \{1, n-2, n-1, n\}$, and for $n \geq 7$,
$$d_n^1(2413) = d_{n-1}^1(2413) + d_{n-2}^1(2413),$$
$$d_n^{n-2}(2413) = d_{n-1}^{n-2}(2413) + d_{n-2}^{n-2}(2413),$$
$$d_n^{n-1}(2413) = d_{n-1}^{n-1}(2413) + d_{n-2}^{n-1}(2413),$$
$$d_n^n(2413) = d_{n-1}^n(2413) + d_{n-2}^n(2413).$$

First, consider $\sigma = \pi\pi \in \mathcal{D}_n^i(2413)$ for $i \notin \{1, n-2, n-1, n\}$. If $n-2$ precedes n in π then $(n-2)ni(n-1)$ forms a forbidden pattern in σ, where the first two digits come from the first copy of π and the last two digits come from the second copy. Therefore, $n-2$ comes after n. Now, $in1(n-2)$ forms a forbidden pattern, where in comes from the first copy of π, 1 comes from somewhere between the two copies of n, and $n-2$ comes from the second copy of π. In every event, it is impossible to avoid 2413, so $d_n^i(2413) = 0$ for $i \notin \{1, n-2, n-1, n\}$.

Next, consider $\sigma = \pi\pi \in \mathcal{D}_n^1(2413)$. Any coinversion in π that does not include the digit 1 must consist of a pair of consecutive digits and therefore must appear in consecutive positions. Suppose to the contrary there is a coinversion with $a < b$ such that $b \neq a+1$. Then $ab1(a+1)$ forms a forbidden pattern, where the first two digits come from the first copy of π. If $a(a+1)$ is a coinversion in nonconsecutive positions, we have the subsequence $ab(a+1)$ in π. If $b < a$ then $b(a+1)$ is another coinversion with nonconsecutive digits, which is not allowed. If $b > a + 1$ then ab is another coinversion with nonconsecutive digits, which is still not allowed. We may only preserve these properties of coinversions by inserting $(n-1)n$ after 1 in any member of $\mathcal{D}_{n-2}^1(2413)$ or inserting n after 1 in any member of $\mathcal{D}_{n-1}^1(2413)$ to obtain σ.

Next, consider $\sigma = \pi\pi \in \mathcal{D}_n^{n-2}(2413)$. If $\pi_1 = n-2$, we claim that $\pi_2 = n-1$ and $\pi_n = n$. Suppose to the contrary that n precedes $n-1$. Then $(n-2)n1(n-1)$ is a

forbidden pattern in σ. Now suppose $\pi_2 = i < n-2$. Then $(n-2)ni(n-1)$ is a forbidden pattern, so $\pi_2 = n-1$. Finally, suppose $\pi_n = i < n-2$. Then $(n-2)ni(n-1)$ is a forbidden pattern, so we know $\pi_1 = n-2$, $\pi_2 = n-1$, and $\pi_n = n$. Now, the digits $n-2$, $n-1$, and n can only play the role of "4" in a 2413 pattern so any coinversions amongst the digits $1, \ldots, n-3$ in π must appear between consecutive digits in consecutive positions as in the previous case. Given a member of $\mathcal{D}_{n-2}^{n-4}(2413)$, we may increment $n-4$, $n-3$, and $n-2$ by 2 and insert $(n-4)(n-3)$ in the third and fourth positions to obtain a member of $\mathcal{D}_n^{n-2}(2413)$. For example, $34215 \in \mathcal{D}_5^3(2413)$ produces $5634217 \in \mathcal{D}_7^5(2413)$. Given a member of $\mathcal{D}_{n-1}^{n-3}(2413)$, we may increment $n-3$, $n-2$, and $n-1$ by 1 and insert $n-3$ in the third position to obtain a member of $\mathcal{D}_n^{n-2}(2413)$. For example, $452316 \in \mathcal{D}_6^4(2413)$ produces $5642317 \in \mathcal{D}_7^5(2413)$.

Next, consider $\sigma = \pi\pi \in \mathcal{D}_n^{n-1}(2413)$. Then either $\pi_2 = n$ or $\pi_n = n$. Suppose to the contrary that $\pi_i = n$, where $3 \le i \le n-1$. First, all digits between $n-1$ and n in π must be smaller than all digits after n in π; otherwise, we have a 2413 pattern in σ. Since we assume $n \ge 7$, either there are at least two digits between $n-1$ and n in π or there are at least two digits after n in π. In the first case, suppose the digits between $n-1$ and n include $a < b$ and c is a digit after n in π. Then $bnac$ is a 2413 pattern in σ. If the digits after n in π include $a < b$ and c is a digit between $n-1$ and n then $a(n-1)cb$ is a forbidden pattern in σ. Therefore n is either the second or the last digit in π. In the first case, given $\sigma = \pi\pi \in \mathcal{D}_{n-2}^{n-3}(2413)$, where $\pi_2 = n-2$, we may prepend $(n-1)n$ to the front of π to obtain a 2413-avoiding member of $\mathcal{D}_n^{n-1}(2413)$. If $\sigma = \pi\pi \in \mathcal{D}_{n-1}^{n-2}(2413)$, where $\pi_2 = n-1$, then increment π_1 and π_2 and insert $n-2$ into the third position. For example, $563412 \in \mathcal{D}_6^5(2413)$ becomes $6753412 \in \mathcal{D}_7^6(2413)$. Now, if $\pi_n = n$, we approach the situation differently. If $\sigma' = \pi'\pi' \in \mathcal{D}_{n-2}^{n-3}(2413)$ with $\pi'_{n-2} = n-2$, then remove π'_1 and π'_{n-2} to obtain a permutation on $\{1, \ldots, n-4\}$ then create the new permutation

$$\pi = (n-1)(n-3)(n-2)\pi'_2 \cdots \pi'_{n-3}n.$$

By inspection, $\pi\pi \in \mathcal{D}_n^{n-1}(2413)$. If $\sigma' = \pi'\pi' \in \mathcal{D}_{n-1}^{n-2}(2413)$ with $\pi'_{n-1} = n-1$, then remove π'_1 and π'_{n-1} to obtain a permutation on $\{1, \ldots, n-3\}$; then create the new permutation

$$\pi = (n-1)(n-2)\pi'_2 \cdots \pi'_{n-2}n,$$

where again, by inspection, $\pi\pi \in \mathcal{D}_n^{n-1}(2413)$.

Finally, consider $\sigma = \pi\pi \in \mathcal{D}_n^n(2413)$. Given $\sigma' = \pi'\pi' \in \mathcal{D}_{n-2}^{n-2}(2413)$, delete π'_1 and create

$$n(n-2)(n-1)\pi'_2 \cdots \pi'_{n-2}n(n-2)(n-1)\pi'_2 \cdots \pi'_{n-2} \in \mathcal{D}_n^n(2413).$$

If $\sigma' = \pi'\pi' \in \mathcal{D}_{n-1}^{n-1}(2413)$, prepend n to the front of π' to obtain a member σ of $\mathcal{D}_n^n(2413)$. $\qquad\square$

The final sequence is perhaps the most surprising result. The task of enumerating 1324-avoiders in other contexts has proven especially challenging. For double lists, however, structure is evident beginning with the $n = 7$ term. It turns out these double lists satisfy a tribonacci recurrence.

Theorem 8. $d_n(1324) = \begin{cases} n! & \text{if } n \leq 3, \\ 12 & \text{if } n = 4, \\ 21 & \text{if } n = 5, \\ 38 & \text{if } n = 6, \\ 69 & \text{if } n = 7, \\ 126 & \text{if } n = 8, \\ 232 & \text{if } n = 9, \\ d_{n-1}(1324) + d_{n-2}(1324) + d_{n-3}(1324) & \text{if } n \geq 10. \end{cases}$

Proof. As before, we focus on the $n \geq 10$ case, and leave the $n \leq 9$ cases to brute force verification.

First, given $\sigma = \pi\pi \in \mathcal{D}_n(1324)$, it is impossible for 1 to precede n if $n \geq 7$. Suppose to the contrary that 1 precedes n. All digits in $\{2, \ldots, n-1\}$ appear between the first 1 and the last n and must appear in increasing order to avoid 1324. Suppose two digits $a < b$ appear between 1 and n in π. Then $1ban$ is a 1324 pattern in σ. Suppose there is just one digit i between 1 and n in π. If $i > 2$, the $1i2n$ is a forbidden pattern, and if $i = 2$, then $132n$ is a forbidden pattern. Therefore if 1 appears before n, it must be immediately before n and the digits $2, \ldots, n-1$ appear in increasing order between the first occurrence of $1n$ and the second occurrence of $1n$ in σ. Since $n \geq 7$, there are either three digits $a < b < c$ before the first 1 (in which case $acbn$ is a forbidden pattern) or there are three digits $a < b < c$ in π after the first n (in which case $1bac$ is a forbidden pattern). In every event we have forced the occurrence of a 1324 pattern, so it is impossible for 1 to precede n if $n \geq 7$.

Now, if n precedes 1, then n must appear as one of the first three digits of π. Suppose n appears in position $i \geq 4$. Then $\pi_1 \cdots \pi_{i-1}\pi_1 \cdots \pi_{i-1}$ must avoid 132. We have seen that this is impossible for $i - 1 \geq 4$, and the only way to do this if $i - 1 = 3$ is for $\pi_1\pi_2\pi_3$ to form a 231 pattern. However, $\pi_3 < \pi_1 < \pi_2$ implies $\pi_1\pi_2\pi_3n1\pi_1\pi_2\pi_3n1$ contains the 1324 pattern $1\pi_2\pi_3n$. Therefore n must appear in one of the first three positions.

Let
$$\mathcal{D}_n^i(1324) = \{\sigma \in \mathcal{D}_n(1324) \mid \sigma_i = n\}$$
and let $d_n^i(1324) = |\mathcal{D}_n^i(1324)|$. We claim that $d_n^1(1324) = d_n^2(1324)$ and $d_n^3(1324) = d_{n-2}^1(1324)$ for $n \geq 6$.

First we show $d_n^1(1324) = d_n^2(1324)$ for $n \geq 6$. We claim that if $\pi\pi \in \mathcal{D}_n^2(1324)$, then π_1 and $\pi_2 = n$ can be transposed to produce a member of $\mathcal{D}_n^1(1324)$. Suppose

to the contrary that $\pi\pi \in \mathcal{D}_n^2(1324)$ but $\pi_2\pi_1\pi_3\cdots\pi_n\pi_2\pi_1\pi_3\cdots\pi_n \notin \mathcal{D}_n^1(1324)$. In this case, we know $\pi_1 < n-1$ since if $\pi_1\pi_2 = (n-1)n$, both $(n-1)$ and n can only play the role of "4" in a 1324 pattern and transposing them does not change their involvement. If $\pi_1 < n-1$ and it plays the role of a "1" in a pattern where n plays the role of "4", we must have used the first copy of π_1 and the second copy of n, so transposing them within each copy of π does not affect the existence of the 1324 patterns. The only other way for both to be involved in the same copy of 1324 that could possibly be destroyed by transposing π_1 and π_2 is for π_1 to play the role of "2" and n to play the role of "4" in a 1324 pattern in $\pi\pi$. In this case, suppose the double list beginning with $\pi_1 n$ contains 1324 but the list beginning with $n\pi_1$ avoids 1324. Since $n\pi_1\pi_3\cdots\pi_n n\pi_1\pi_3\cdots\pi_n$ avoids 1324, all digits larger than π_1 must appear in increasing order immediately after π_1 and $\pi_1 \geq n-3$. Now, a case analysis shows that any σ beginning with $(n-3)n(n-2)(n-1)$ or $(n-2)n(n-1)$ cannot have σ_1 play the role of "2" in a 1324 pattern, so it is the case that transposing π_1 and π_2 provides a bijection between $\mathcal{D}_n^1(1324)$ and $\mathcal{D}_n^2(1324)$.

To see that $\mathrm{d}_n^3(1324) = \mathrm{d}_{n-2}^1(1324)$ for $n \geq 6$, notice that if $\pi\pi \in \mathcal{D}_n^3(1324)$, then $\pi_1 = n-2$ and $\pi_2 = n-1$. We know these two numbers must appear in increasing order since 1 comes after n. If there exists i where $\pi_1 < i < \pi_2$, then $\pi_1\pi_2 in$ is a forbidden pattern and if there exists i where $\pi_2 < i < n$, then $\pi_1 i \pi_2 n$ is a forbidden pattern. Since $\pi = (n-2)(n-1)n\pi_3\cdots\pi_n$, we may delete $n-1$ and n to obtain $\pi'\pi' \in \mathcal{D}_{n-2}^1(1324)$.

It remains to show that $\mathrm{d}_n^1(1324)$ satisfies the tribonacci recurrence (and thus so do $\mathrm{d}_n^2(1324)$, $\mathrm{d}_n^3(1324)$, and $\mathrm{d}_n(1324)$). For $\sigma' \in \mathcal{D}_{n-3}^1(1324)$, replace $n-3$ with $n(n-3)(n-2)(n-1)$ to obtain $\sigma \in \mathcal{D}_n^1(1324)$. For $\sigma' \in \mathcal{D}_{n-2}^1(1324)$, replace $n-2$ with $n(n-2)(n-1)$ to obtain $\sigma \in \mathcal{D}_n^1(1324)$. For $\sigma' \in \mathcal{D}_{n-1}^1(1324)$, prepend n to the front of each copy of π to obtain $\sigma \in \mathcal{D}_n^1(1324)$. This map sends members of $\mathcal{D}_{n-3}^1(1324) \cup \mathcal{D}_{n-2}^1(1324) \cup \mathcal{D}_{n-1}^1(1324)$ to $\mathcal{D}_n^1(1324)$.

Further, each of these operations is bijective. That is, if $\sigma = \pi\pi \in \mathcal{D}_n^1(1324)$, then π either begins with $n(n-1)$, $n(n-2)(n-1)$, or $n(n-3)(n-2)(n-1)$. Indeed, if $\pi_2 \leq n-4$, then $n-1$, $n-2$, and $n-3$ appear in increasing order in π, and $(n-4)(n-2)(n-3)(n-1)$ is a 1324 pattern in σ, so $\pi_2 \geq n-3$. If $\pi_2 = n-2$ and $\pi_3 \neq n-1$, then $\pi_n = n-1$. If not, then we see all digits between π_2 and $n-1$ must be larger than all digits after $n-1$ in π to avoid a 1324 pattern where $n-1$ plays the role of "3" and n plays the role of "4". However, if $a < n-2$ is before $n-1$ in π and $b < a$ is after $n-1$ in π, then $b(n-2)a(n-1)$ is a copy of 1324 in σ. Therefore, if $\pi_2 = n-2$ and $\pi_3 \neq n-1$, then $\pi_n = n-1$. Now, since we assume $n \geq 6$, let $a < b < c$ be three digits less than $n-2$ in π. If $\pi_n = n-1$, then $a(n-2)c(n-1)$ is a 1324 pattern in σ, so it must be the case that $\pi_3 = n-1$ if $\pi_2 = n-2$. Finally, if $\pi_2 = n-3$, then $n-2$ appears before $n-1$ in π (or $(n-3)(n-1)(n-2)n$ is a 1324 pattern in σ). If $\pi_3 < (n-3)$ then $\pi_3(n-2)(n-3)(n-1)$ is a 1324 pattern

in σ. Now that we know $\pi_2 = n - 3$ implies $\pi_3 = n - 2$, a similar analysis to the case where $\pi_2 = n - 2$ shows that $\pi_4 = n - 1$ as well.

By editing appropriate prefixes, we now have a bijection between $\mathcal{D}_n^1(1324)$ and $\mathcal{D}_{n-3}^1(1324) \cup \mathcal{D}_{n-2}^1(1324) \cup \mathcal{D}_{n-1}^1(1324)$, so $d_n^1(1324)$ satisfies the tribonacci recurrence. Because $\mathcal{D}_n^1(1324)$ is in bijection with $\mathcal{D}_n^2(1324)$ and $\mathcal{D}_n^3(1324)$ is in bijection with $\mathcal{D}_{n-2}^1(1324)$, we have $d_n^2(1324)$ and $d_n^3(1324)$ also satisfy the tribonacci recurrence. Finally, since

$$d_n(1324) = d_n^1(1324) + d_n^2(1324) + d_n^3(1324),$$

$d_n(1324)$ satisfies the tribonacci recurrence as well, which is what we wanted to show. □

4. Summary

We have now completely characterized $d_n(\rho)$ where ρ is a permutation pattern of length at most 4. The corresponding results are given in Table 2. These results provide an interesting contrast to pattern-avoiding permutations. First, the only Wilf equivalences are the trivial ones. Second, the monotone pattern is the easiest pattern to avoid in the context of double lists. Finally, we obtained a variety of behaviors (constant, linear, quadratic, and exponential), as opposed to permutation pattern sequences which only grow exponentially.

pattern ρ	$d_n(\rho)$		OEIS
1342, 2431, 3124, 4213	15	$(n \geq 5)$	A010854
2143, 3412	$2n + 2$	$(n \geq 6)$	A005843
1423, 2314, 3241, 4132	$3n + 6$	$(n \geq 7)$	A008585
1432, 2341, 3214, 4123	$\frac{1}{2}n^2 + \frac{3}{2}n - 4$	$(n \geq 6)$	A052905
1243, 2134, 3421, 4312	$\frac{1}{2}n^2 + \frac{5}{2}n - 8$	$(n \geq 6)$	A183897
2413, 3142	L_{n+1}	$(n \geq 5)$	A000032
1324, 4231	$|\mathcal{D}_{n-1}(\rho)| + |\mathcal{D}_{n-2}(\rho)| + |\mathcal{D}_{n-3}(\rho)|$	$(n \geq 10)$	
1234, 4321	$2^n - n$	$(n \geq 4)$	A000325

Table 2. Formulas for $d_n(\rho)$, where $\rho \in \mathcal{S}_4$ and the sequence numbers in the far right column are from [OEIS 2015].

The variety of sequence behaviors and the complete classification for length-4 patterns are both exciting developments, but this work raises additional possibilities for future work. In particular:

(1) Is $1 \cdots n$ the easiest pattern of length n to avoid for all n? Can we characterize the hardest pattern of length n to avoid in general?

(2) All of the sequences in Table 2 have rational generating functions. Do there exist patterns ρ where the sequence $\{d_n(\rho)\}$ does not have a rational generating function?

(3) With the exception of the proof of Theorem 6, the proofs in this paper were the result of detailed case analysis. While this is a thorough treatment that reveals much about the structure of pattern-avoiding double lists, it is not the most elegant approach. What are alternate proofs of these results?

Acknowledgement

References

[Barnabei et al. 2010] M. Barnabei, F. Bonetti, and M. Silimbani, "The Eulerian numbers on restricted centrosymmetric permutations", *Pure Math. Appl.* **21**:2 (2010), 99–118. MR Zbl

[Brändén and Mansour 2005] P. Brändén and T. Mansour, "Finite automata and pattern avoidance in words", *J. Combin. Theory Ser. A* **110**:1 (2005), 127–145. MR Zbl

[Burstein 1998] A. Burstein, *Enumeration of words with forbidden patterns*, Ph.D. thesis, University of Pennsylvania, Philadelphia, PA, 1998, http://search.proquest.com/docview/304442911. MR

[Callan 2002] D. Callan, "Pattern avoidance in circular permutations", preprint, 2002. arXiv

[Conway and Guttmann 2014] A. R. Conway and A. J. Guttmann, "On the growth rate of 1324-avoiding permutations", preprint, 2014. arXiv

[Egge 2010] E. S. Egge, "Enumerating rc-invariant permutations with no long decreasing subsequences", *Ann. Comb.* **14**:1 (2010), 85–101. MR Zbl

[Ferrari 2011] L. S. Ferrari, "Centrosymmetric words avoiding 3-letter permutation patterns", *Online J. Anal. Comb.* 6 (2011), 19 pp. MR Zbl

[Jelínek and Mansour 2009] V. Jelínek and T. Mansour, "Wilf-equivalence on k-ary words, compositions, and parking functions", *Electron. J. Combin.* **16**:1 (2009), Art. ID 58. MR

[Knuth 1968] D. E. Knuth, *The art of computer programming, I: Fundamental algorithms*, 1st ed., Addison-Wesley, Reading, MA, 1968. MR Zbl

[OEIS 2015] N. Sloane, "The on–line encyclopedia of integer sequences", 2015, http://oeis.org.

[Pudwell 2010] L. Pudwell, "Enumeration schemes for words avoiding permutations", pp. 193–211 in *Permutation patterns*, London Math. Soc. Lecture Note Ser. **376**, Cambridge Univ. Press, 2010. MR Zbl

[Vella 2002/03] A. Vella, "Pattern avoidance in permutations: linear and cyclic orders", *Electron. J. Combin.* **9**:2 (2002/03), Research paper 18, 43 pp. MR Zbl

cratcd22@wclive.westminster.edu   *Department of Mathematics and Computer Science, West-*
                                  minster College, New Wilmington, PA 16172, United States

ericksosam@mnstate.edu   *Department of Mathematics, Minnesota State University*
                                  Moorhead, Moorhead, MN 56563, United States

frehiwetn@gmail.com   *Department of Mathematics, Saint Joseph's College,*
                                  Rensselaer, IN 47978, United States

lara.pudwell@valpo.edu   *Department of Mathematics and Statistics,*
                                  Valparaiso University, Valparaiso, IN 46383, United States

On a randomly accelerated particle

Michelle Nuno and Juhi Jang

(Communicated by Kenneth S. Berenhaut)

The focus of this note is to learn more about the Kolmogorov equation describing the dynamics of a randomly accelerated particle. We first explore some existing results of the Kolmogorov equation from the stochastic and differential equation points of view and discuss its solvability with and without boundary conditions. More specifically, we introduce stochastic processes and Brownian motion and we present a connection between a stochastic process and a differential equation. After looking at stochastic processes, we introduce generalized functions and derive the fundamental solution to the heat equation and to the Fokker–Planck equation. The problem with a reflecting boundary condition is also studied by using various methods such as separation of variables, self-similarity, and the reflection method.

1. Introduction

In our studies of mathematics, we will often come across different types of processes, including the stochastic process. A stochastic process is one that changes randomly with time. Even if one starts at the same point, one cannot predict how the process will evolve in the future. We can use stochastic processes to model random fluctuations. The best known example of a stochastic process is Brownian motion, which is the continuous, random movement of particles. It derives its name from Robert Brown's study [1828] of pollen floating on water; he noticed that the pollen grains moved continuously, but he could not find a pattern to their movement. Brownian motion is also a Markov process, in which future behavior depends only on the current or previous state, and all other states are irrelevant [Ibe 2013].

Later, Einstein [1905; 1926] derived a diffusion equation for the density of Brownian particles, whereas Smoluchowski [1906] created a kinetic model to represent the collision of the particles.

When dealing with stochastic processes, in particular Markov processes, a useful tool is the Chapman–Kolmogorov equation. This equation is used to determine the

transition density function for moving from one state to another. The Chapman–Kolmogorov equation is

$$p(x,t \mid y,s) = \int_{-\infty}^{+\infty} p(x,t \mid z,r)\, p(z,r \mid y,s)\, dz \quad \text{for } s < r < t. \tag{1-1}$$

This equation considers the fact that if you go from y at time s to x at time t, you must go through an intermediate point z at time r [van Kampen 1981]. In many stochastic processes, the Chapman–Kolmogorov equation is very helpful because again, stochastic processes are random processes. We cannot predict exactly where a particle will be at a given time; we can only predict the probability that the particle will be at a certain point in a given time. This applies directly when we look at Brownian motion. In the case of Brownian motion, the transition probability density function is

$$p(x,t \mid y) = \frac{1}{\sqrt{2\pi t}} e^{-(x-y)^2/(2t)} \quad \text{for } t > 0. \tag{1-2}$$

It is easy to see that p satisfies the partial differential equation (the heat equation)

$$\frac{\partial p}{\partial t} = \frac{1}{2} \frac{\partial^2 p}{\partial x^2}, \tag{1-3}$$

and the initial condition $p(x,0 \mid y) = \delta(x-y)$. Here δ is a generalized function, which we will discuss more in detail in Section 3.1. This example illustrates the connection between Brownian motion (stochastic process) and the heat equation (differential equation) via the Chapman–Kolmogorov equation.

A wider range of diffusion processes can yield diffusion equations, which are often called the Fokker–Planck equations. The Fokker–Planck equations have many different applications such as modeling Brownian motion in drift, finance, and physics [Risken 1984]. For this reason, it is worthwhile to learn about their many properties and characteristics. The focus of this note is to investigate some properties of the simplest kinetic Fokker–Planck equation, also known as the Kolmogorov equation, given by

$$\frac{\partial p}{\partial t} = -v \frac{\partial p}{\partial x} + k \frac{\partial^2 p}{\partial v^2}, \tag{1-4}$$

where

$$p = p(t,x,v) \quad \text{for } x \in \mathbb{R},\ v \in \mathbb{R},\ t > 0, \quad \text{and} \quad k > 0.$$

Here k is a diffusion coefficient. In the Kolmogorov equation, we have t, x, and v as single variables, whereas the more complicated forms of the Fokker–Planck equation consist of vectors in both x and v. It is important to look at the Kolmogorov equation first because once the simplest form has been studied, similar techniques may be applied to other forms of the equation.

Because the Fokker–Planck equation is used to model the movement of particles, it is necessary to look at some of the ways in which particles behave. In this note we will look at the case in which a particle moves randomly in a given space. The particle is not free to move as it pleases though; there is a wall, and once the particle hits the wall it is bounced back to the original space. In previous works, researchers (such as Skorohod [1961]) solved similar problems using approximation methods. In this work, we attempt to do so using separation of variables, self-similarity, and the reflection method.

2. Stochastic process of Fokker–Planck equation

We start out by determining if, like Brownian motion, the Fokker–Planck equation (1-4) comes from a stochastic process. For simplicity, we will take $k = 1$. A general form of the Fokker–Planck equation is

$$\frac{\partial p}{\partial t} = -\sum_{i=1}^{n} \frac{\partial}{\partial x_i}(b_i\, p) + \frac{1}{2}\sum_{i,j=1}^{n} \frac{\partial^2}{\partial x_i \partial x_j}(a_{ij}\, p), \tag{2-1}$$

where n is a positive integer, b_i is the drift coefficient and a_{ij} is the diffusion coefficient.

Let us first consider $n = 2$. Letting $x = x_1$ and $v = x_2$, we see that in (1-4), v is the same as b_1. Since x is not included in this term, we will form a vector $\vec{b}$ such that $\vec{b} = [x_2, 0]^T$. Notice also that in (2-1),

$$\frac{1}{2}\sum_{i,j=1}^{n=2} \frac{\partial^2}{\partial x_i x_j}(a_{ij}\, p)$$

is nonzero only when both i and j are equal to 2. Therefore $a_{11} = a_{12} = a_{21} = 0$ and $a_{22} = 2$, so we have a matrix

$$A = (a_{ij}) = \sigma\sigma^T = \begin{bmatrix} 0 & 0 \\ 0 & 2 \end{bmatrix}.$$

A stochastic differential equation for $\vec{X} = [x_1, x_2]^T$ has the form

$$d\vec{X} = \vec{b}(\vec{X}, t)\, dt + \sigma(\vec{X}, t)\, d\vec{B}. \tag{2-2}$$

Plugging in our values, we have

$$\begin{bmatrix} dx_1 \\ dx_2 \end{bmatrix} = \begin{bmatrix} x_2 \\ 0 \end{bmatrix} dt + \begin{bmatrix} 0 & 0 \\ 0 & \sqrt{2} \end{bmatrix} d\vec{B}.$$

Multiplying these out, we obtain

$$dx_1 = x_2\, dt \quad \text{and} \quad dx_2 = \sqrt{2}\, dB_2.$$

Recalling that $x = x_1, v = x_2$, and letting $dB = \xi(t) \, dt$ (white noise), we obtain

$$dx = v \, dt, \quad dv = \sqrt{2} \xi(t) \, dt.$$

We have found the stochastic differential equation for the Fokker–Planck equation.

Looking at the solution above, we see that

$$\frac{d^2 x}{dt^2} = \sqrt{2} \xi(t).$$

Therefore, the Kolmogorov equation models a randomly accelerated particle.

We can do the same with the multidimensional Kolmogorov equation with no external forces. For instance, (1-4) can be generalized as

$$\frac{\partial p}{\partial t} = -v \cdot \nabla_x p + \Delta_v p, \tag{2-3}$$

where $p = p(t, x, v)$ and $x \in \mathbb{R}^3$, $v \in \mathbb{R}^3$. Recall that

$$v \cdot \nabla_x p = v_1 \partial_{x_1} p + v_2 \partial_{x_2} p + v_3 \partial_{x_3} p. \tag{2-4}$$

Similar to the previous case, we will let $x = (x_1, x_2, x_3)$ and $v = (x_4, x_5, x_6)$. Notice $n = 6$ in this case. We see in (2-1), v_i is the same as b_i. Let

$$\vec{b} = [x_4, x_5, x_6, 0, 0, 0]^T.$$

Notice that in (2-3), the term

$$\frac{1}{2} \sum_{i,j=1}^{n=6} \frac{\partial^2}{\partial x_i \partial x_j} (a_{ij} p)$$

only exists when both i and j are equal to 4, 5, and 6. Therefore, we have a matrix A in which $a_{44} = a_{55} = a_{66} = 2$ and all other terms are equal to 0. This gives us degenerate diffusion, which is different from Brownian motion. Here, "degenerate" means that the diffusion coefficient matrix is nonnegative, but not positive definite. We also know that our vector $\vec{X} = [x_1, x_2, x_3, x_4, x_5, x_6]^T$. Recalling the general form of a stochastic process (2-2) and plugging in our vectors and multiplying them out, we obtain

$$dx_1 = x_4 \, dt, \quad dx_2 = x_5 \, dt, \quad dx_3 = x_6 \, dt,$$
$$dx_4 = \sqrt{2} \, dB_4, \quad dx_5 = \sqrt{2} \, dB_5, \quad dx_6 = \sqrt{2} \, dB_6.$$

We have once again found the stochastic differential equations, so we know that the kinetic Fokker–Planck equation (2-4) comes from a stochastic process. The result of this section is well-known and we refer to [van Kampen 1981] for more discussion on the stochastic processes and the Fokker–Planck equation.

For the rest of the note, we will study the properties of the solutions to (1-4) and (2-3) by using various methods.

3. Fundamental solutions of the Fokker–Planck equation

The fundamental solution is the solution of a particular equation with initial data at a single, concentrated point. The idea behind this is that if we have enough information about the solution of an equation at this infinitely dense point, we can draw enough information about the behavior of the equation at other points.

3.1. *Delta function and fundamental solutions.* We use the delta function (which is referred to as a generalized function) to represent the infinitely dense point. The delta function is formally defined by

$$\delta(x - \xi) = \begin{cases} 0, & x \neq \xi, \\ +\infty, & x = \xi, \end{cases}$$

such that

$$\int_a^b \delta(x - \xi)\, dx = 1 \quad \text{as long as } a < \xi < b.$$

An interesting and very helpful property is that for any function $f(x)$,

$$\int_a^b f(x)\delta(x - \xi)\, dx = f(\xi) \quad \text{if } a < \xi < b.$$

The above properties hold even if $a = -\infty$ and $b = +\infty$. Because of the information it yields, we often use the delta function as the initial condition when searching for fundamental solutions.

The definition of a fundamental solution for a linear differential operator L is

$$LF = 0, \quad F_{(t=0)} = \delta. \tag{3-1}$$

3.2. *Heat equation.* In the introduction, we presented an example of the probability density function for Brownian motion when looking at stochastic processes. In this section, we show that we can also find a solution without considering a stochastic process. For instance, we can use the Fourier transform method to give rise to the fundamental solution of the heat equation [Olver 2014]. We denote the solution as $u(t, x) = F(t, x; \xi)$ and set the initial condition to be $F(0, x; \xi) = \delta(x - \xi)$. This must satisfy the heat equation (1-3), so we know

$$\frac{\partial F}{\partial t} = \frac{\partial^2 F}{\partial x^2}.$$

We must now reconstruct the equation using the properties of linearity and the Fourier transform method. After solving this, we take the inverse Fourier transform to obtain the fundamental solution of the heat equation (1-3).

We find that

$$
\begin{aligned}
F(t, x, \xi) &= \frac{1}{\sqrt{2\pi}} \int_{-\infty}^{+\infty} e^{ik(x-\xi)-k^2 t} \, dk \\
&= \frac{1}{2\sqrt{\pi t}} e^{-(x-\xi)^2/(4t)} \quad \text{for } t > 0.
\end{aligned}
\tag{3-2}
$$

Recall the probability density function (1-2). In this section we obtained the same result, except we are off by a multiple of $\frac{1}{2}$. The reason for this is that here, we started with the diffusion coefficient $k = 1$ instead of $k = \frac{1}{2}$.

Once we have the fundamental solution of a differential equation, we can find other solutions using the convolution

$$
u(t, x) = (F * f)(t, x),
\tag{3-3}
$$

where

$$
(F * f)(t, x) = \int_{\xi \in \mathbb{R}} F(t, x, \xi) f(\xi)
$$

and with the initial condition $u(0, x) = f(x)$.

3.3. *Kolmogorov equation.* In this section, we are interested in constructing the fundamental solution to the Fokker–Planck equation (1-4) and (2-3). In fact, Kolmogoroff [1934] provided the formula for the fundamental solution to the Fokker–Planck equation, but did not give any details on the construction. After finding the solution for the Fokker–Planck equation, we will consider the case of the Kolmogorov equation.

Tanski [2004] found the fundamental solution of the Fokker–Planck equation

$$
\frac{\partial n}{\partial t} + v_x \frac{\partial n}{\partial x} + v_y \frac{\partial n}{\partial y} + v_z \frac{\partial n}{\partial z} - \alpha \left(\frac{\partial}{\partial v_x}(v_x n) + \frac{\partial}{\partial v_y}(v_y n) + \frac{\partial}{\partial v_z}(v_z n) \right)
$$
$$
= k \left(\frac{\partial^2 n}{\partial v_x^2} + \frac{\partial^2 n}{\partial v_y^2} + \frac{\partial^2 n}{\partial v_z^2} \right). \tag{3-4}
$$

He used the method of characteristics to come up with the fundamental solution of the form

$$
\begin{aligned}
G = \frac{1}{(2\pi)^6} \left(\frac{\pi}{k\sqrt{D}} \right)^3 \exp\Bigg\{ \frac{-1}{4kD} \Bigg[&\frac{1}{2\alpha}(1 - e^{-2\alpha t})(\hat{x}^2 + \hat{y}^2 + \hat{z}^2) \\
&- \left(\frac{2}{\alpha^2}(1 - e^{-\alpha t}) - \frac{1}{\alpha^2}(1 - e^{-\alpha t}) \right)(\hat{x}\hat{v}_x + \hat{y}\hat{v}_y + \hat{z}\hat{v}_z) \\
&+ \left(\frac{t}{\alpha^2} - \frac{2}{\alpha^3}(1 - e^{-\alpha t}) + \frac{1}{2\alpha^3}(1 - e^{-2\alpha t}) \right)(\hat{v}_x^2 + \hat{v}_y^2 + \hat{v}_z^2) \Bigg] \Bigg\},
\end{aligned}
\tag{3-5}
$$

where

$$\hat{x} = x - (x_0 + (v_{x0}/\alpha)(1 - e^{-\alpha t})),$$
$$\hat{y} = y - (y_0 + (v_{y0}/\alpha)(1 - e^{-\alpha t})),$$
$$\hat{z} = z - (z_0 + (v_{z0}/\alpha)(1 - e^{-\alpha t})),$$
$$D = \frac{\det(A)}{k^2},$$

and A is a matrix with

$$\det(A) = k^2 \frac{\alpha t(1 - e^{-2\alpha t}) - 2(1 - e^{-\alpha t})^2}{2\alpha^4}.$$

This matches the results of [Kolmogoroff 1934].

In our case, we would like to look at a slightly more specific equation. We look at the Fokker–Planck equation of the form

$$\partial_t p + v \cdot \nabla_x p = \Delta_v p, \tag{3-6}$$

which can be rewritten as

$$\partial_t p + v_1 \partial_{x_1} p + v_2 \partial_{x_2} p + v_3 \partial_{x_3} p = (\partial_{v_1}^2 p + \partial_{v_2}^2 p + \partial_{v_3}^2 p).$$

We follow Tanski's method in order to find the fundamental solution of our equation. The result does not follow directly from [Tanski 2004]. We have that $x = x_1, y = x_2, z = x_3$, and $v_x = v_1, v_y = v_2, v_z = v_3$, and $k = 1$. We let $N = N(t, p_1, p_2, p_3, q_1, q_2, q_3)$ be the Fourier transformation in (x, v). It is equivalent to

$$\frac{1}{(2\pi)^6} \int_{R^6} e^{-i(x_1 p_{x_1} + x_2 p_{x_2} + x_3 p_{x_3} + v_1 q_1 + v_2 q_2 + v_3 q_3)} p \, dx_1 \, dx_2 \, dx_3 \, dv_1 \, dv_2 \, dv_3.$$

In terms of N, the Fourier transform equals

$$\partial_t N - p_1 \partial_{q_1} N - p_2 \partial_{q_2} N - p_3 \partial_{q_3} N = -(q_1^2 + q_2^2 + q_3^2)N.$$

We then come up with

$$dt = \frac{dp_1}{0} = \frac{dp_2}{0} = \frac{dp_3}{0} = \frac{dq_1}{-p_1} = \frac{dq_2}{-p_2} = \frac{dq_3}{-p_3} = \frac{-dN/N}{(q_1^2 + q_2^2 + q_3^2)}.$$

Solving this we find

$$p_1 = p_{10}, \qquad p_2 = p_{20}, \qquad p_3 = p_{30},$$
$$q_1 = -p_1 t + q_{10}, \quad q_2 = -p_2 t + q_{20}, \quad q_3 = -p_3 t + q_{30},$$
$$N = N_0 e^{-\frac{1}{2}\left((p_1^2 + p_2^2 + p_3^2)\frac{1}{3}t^3 - (p_1 q_{10} + p_2 q_{20} + p_3 q_{30})t^2 + (q_{10}^2 + q_{20}^2 + q_{30}^2)t\right)}.$$

Plugging in our values for q_{10}, q_{20}, and q_{30}, we obtain

$$
\begin{aligned}
N = N_0 \exp\Big\{ -\tfrac{1}{2}\Big((p_1^2 + p_2^2 + p_3^2)\tfrac{1}{3}t^3 \\
- \big(p_1(q_1 + p_1 t) + p_2(q_2 + p_2 t) + p_3(q_3 + p_3 t)\big)t^2 \\
+ \big((q_1 + p_1 t)^2 + (q_2 + p_2 t)^2 + (q_3 + p_3 t)^2\big)t\Big)\Big\}
\end{aligned}
$$

which leaves us with

$$
N = N_0 e^{-\frac{1}{2}\left((p_1^2 + p_2^2 + p_3^2)\frac{1}{3}t^3 - (p_1 q_1 + p_2 q_2 + p_3 q_3)t^2 + (q_1^2 + q_2^2 + q_3^2)t\right)}.
$$

We take the initial density value as

$$
n_0 = \delta(x_1 - x_{10})\delta(x_2 - x_{20})\delta(x_3 - x_{30})\delta(v_1 - x_{10})\delta(v_2 - x_{20})\delta(v_3 - x_{30}).
$$

The Fourier transform of the initial density becomes

$$
N_0 = e^{-i(x_{10}p_1 + x_{20}p_2 + x_{30}p_3 + v_{10}q_1 + v_{20}q_2 + v_{30}q_3)}.
$$

Plugging in the initial values we obtain

$$
\widehat{N_0} = e^{-i(x_{10}p_1 + x_{20}p_2 + x_{30}p_3 + v_{10}(p_1 t + q_{10}) + v_{20}(p_2 t + q_{20}) + v_{30}(p_3 t + q_{30}))},
$$

which is the Fourier transform of

$$
\begin{aligned}
\widehat{n_0} = \delta(x_1 - (x_{10} + v_{10}t))\delta(x_2 - (x_{20} + v_{20}t)) \\
\delta(x_3 - (x_{30} + v_{30}t))\delta(v_1 - v_{10})\delta(v_2 - v_{20})\delta(v_3 - v_{30}).
\end{aligned}
$$

In our example, we get the matrix A to be

$$
A = \begin{bmatrix} \tfrac{1}{3}t^3 & -\tfrac{1}{2}t^2 \\ -\tfrac{1}{2}t^2 & t \end{bmatrix}.
$$

This matrix is created from the terms related to N, where a_{11} is the term coming from p_i^2, and the a_{12} and a_{21} terms are obtained by dividing the term for $p_i q_j$ in half. Finally, a_{22} is the term associated with q_i^2. Its determinant is

$$
\det(A) = \tfrac{1}{12}t^4
$$

and

$$
D = \tfrac{1}{12}t^4, \quad \text{since } D = \frac{\det(A)}{k^2} \quad \text{and} \quad k = 1.
$$

The inverse is given by

$$
A^{-1} = \frac{12}{t^4} \begin{bmatrix} t & \tfrac{1}{2}t^2 \\ \tfrac{1}{2}t^2 & \tfrac{1}{3}t^3 \end{bmatrix}.
$$

We now combine $\widehat{n_0}$ with A^{-1} to obtain

$$G = \frac{1}{(2\pi)^6}\left(\frac{\pi}{k\sqrt{D}}\right)^3 \widehat{n_0} \exp\left\{-\frac{3}{t^4}\left(t(x_1^2+x_2^2+x_3^2)-t^2(x_1v_1+x_2v_2+x_3v_3)\right.\right.$$
$$\left.\left.+\tfrac{1}{3}t^3(v_1^2+v_2^2+v_3^2)\right)\right\},$$

which gives us

$$G = \frac{1}{(2\pi)^6}\left(\frac{\pi}{k\sqrt{D}}\right)^3 \exp\left\{-\frac{3}{t^4}\left(t(\widehat{x_1}^2+\widehat{x_2}^2+\widehat{x_3}^2)-t^2(\widehat{x_1}\widehat{v_1}+\widehat{x_2}\widehat{v_2}+\widehat{x_3}\widehat{v_3})\right.\right.$$
$$\left.\left.+\tfrac{1}{3}t^3(\widehat{v_1}^2+\widehat{v_2}^2+\widehat{v_3}^2)\right)\right\}.$$

Plugging in $D = \frac{1}{12}t^4$, we have

$$G = \frac{1}{(2\pi)^6}\left(\frac{2\sqrt{3}\pi}{t^2}\right)^3 \exp\left\{-\frac{3}{t^4}\left(t(\widehat{x_1}^2+\widehat{x_2}^2+\widehat{x_3}^2)-t^2(\widehat{x_1}\widehat{v_1}+\widehat{x_2}\widehat{v_2}+\widehat{x_3}\widehat{v_3})\right.\right.$$
$$\left.\left.+\tfrac{1}{3}t^3(\widehat{v_1}^2+\widehat{v_2}^2+\widehat{v_3}^2)\right),\right\}$$

where

$$\widehat{x_1} = x_1 - (x_{10}+v_{10}t), \quad \widehat{x_2} = x_2 - (x_{20}+v_{20}t), \quad \widehat{x_3} = x_3 - (x_{30}+v_{30}t),$$
$$\widehat{v_1} = v_1 - v_{10}, \qquad\qquad \widehat{v_2} = v_2 - v_{20}, \qquad\qquad \widehat{v_3} = v_3 - v_{30}.$$

The same procedure can be performed for the Kolmogorov equation (1-4):

$$\partial_t p + v\partial_x p = \partial_v^2 p.$$

We obtain the fundamental solution

$$G = \frac{1}{(2\pi)^2}\left(\frac{2\sqrt{3}\pi}{t^2}\right)e^{-\frac{3}{t^4}\left(t\hat{x}^2-t^2\hat{x}\hat{v}+\frac{1}{3}t^3\hat{v}^2\right)}, \tag{3-7}$$

where $\hat{x} = x - (x_0+v_0t)$ and $\hat{v} = v - v_0$.

If we want to solve a problem with general initial conditions, we can do so using

$$p(t,x,v) = \iint G(t,x,v,x_0,v_0)\,p(x_0,v_0)\,\mathrm{d}x_0\,\mathrm{d}v_0. \tag{3-8}$$

This gives a representation formula for a solution to the Kolmogorov equation in the whole space.

Remark 3.1. After this work had been performed, we found out that Tanski [2008] solved the problem. We refer to [Tanski 2004; 2008] for more details on the construction of the fundamental solution of the general Fokker–Planck equations.

4. Reflecting boundary conditions

Oftentimes, particles are not free to move around as they please; they are influenced by their surroundings. This is the focus of this section. In particular, we are interested in the case where the particle is reflected back to the plane once it hits the boundary (or wall). Consider, for example, that $\{x = 0\}$ is the wall of the domain $\{x > 0, \; v \in \mathbb{R}\}$. We represent this behavior with the boundary condition

$$p(0, -v) = p(0, v) \quad \text{for all } v. \tag{4-1}$$

The first natural question is: are there any "simple solutions" of (1-4) satisfying this boundary condition? We first consider the possible stationary solutions. The equation to solve is

$$v\partial_x p = \partial_v^2 p, \tag{4-2}$$

with the condition (4-1).

4.1. *Stationary solutions.* Suppose the solution to (4-1)–(4-2) takes the form

$$p(x, v) = X(x)V(v). \tag{4-3}$$

Plugging this into (4-2), we get

$$vX'V = XV''.$$

Dividing both sides by vXV and letting this equal $-\lambda$, we get

$$\frac{X'}{X} = \frac{V''}{vV} = -\lambda.$$

Solving for X we find

$$X(x) = X_0 e^{-\lambda x},$$

where X_0 is some constant.

We now try to solve for V. Because of the boundary condition, we know that V must satisfy

$$V(v) = V(-v).$$

It will also satisfy

$$V''(v) = V''(-v).$$

Replacing these values we find

$$-\lambda v V(v) = \lambda v V(-v).$$

Using our boundary condition, we obtain

$$-\lambda v V(v) = \lambda v V(v).$$

Moving everything to one side we see that

$$-2\lambda v V(v) = 0.$$

We do not want v or $V(v)$ to equal 0; therefore $\lambda = 0$ must be true. This also means that $V'' = 0$. Integrating leads us to the solution $V(v) = av + b$. We need this equation to satisfy the boundary condition, which in turn leads us to the conclusion that $V(v) = b$.

Now that we know λ, let us solve for X. Plugging in our value of λ, we find that $X(x) = X_0$. Recall the form from (4-3). Therefore we get $p(x, v) = C$, where $C = X_0 b$. Hence we see that only constants will solve the problem.

In many cases, the total mass of particles is positive. If we view p as a probability density, then

$$\int_{x>0} \int_{v \in \mathbb{R}} p(x, v) \, dx \, dv = 1.$$

Since the domain is infinite, no constant will satisfy this criterion. There is no other interesting solution to the stationary problem by using separation of variables.

4.2. *Kummer functions.* We will try again to find a solution to (4-1)-(4-2)- by a different method. Because of the scaling invariance property of the equation, we want a solution of the form

$$p(x, v) = x^{\alpha} \phi(-v^3/(9x)).$$

When done this way, we get

$$\partial_x p = \alpha x^{\alpha-1} \phi + (v^3/(9x^2)) x^{\alpha} \phi',$$
$$\partial_v^2 p = x^{\alpha}(-3v^2/(9x))^2 \phi'' + x^{\alpha}(-6v/(9x))\phi'.$$

After some calculations, we obtain

$$z\phi'' + \left(\tfrac{2}{3} - z\right)\phi' + \alpha\phi = 0, \tag{4-4}$$

where $z = -v^3/(9x)$. This form satisfies the Kummer equations. Equation (4-4) has two independent solutions: M and U [Abramowitz and Stegun 1965].

We now examine the asymptotic behavior of the solutions to see whether the boundary conditions are satisfied by these solutions. Our boundary condition is given in (4-1): $p(0, v) = p(0, -v)$.

Taking the boundary condition into account, when x approaches 0 and $v > 0$, we notice z approaches $+\infty$, and when x approaches 0 and $v < 0$, we notice z approaches $-\infty$. Therefore, we will study the asymptotic behavior of the solution of (4-4) as z approaches $+\infty$ and $-\infty$ to match the boundary condition. We start with

the first kind of solution M. From [Abramowitz and Stegun 1965, 13.1.5], we obtain

$$M\left(-\alpha, \tfrac{2}{3}, -z\right) \approx \frac{\Gamma\left(\tfrac{2}{3}\right)}{\Gamma\left(\tfrac{2}{3} + \alpha\right)} z^\alpha \quad \text{as } z \to +\infty, \tag{4-5}$$

and from [Abramowitz and Stegun 1965, 13.1.4],

$$M\left(-\alpha, \tfrac{2}{3}, z\right) \approx \frac{\Gamma\left(\tfrac{2}{3}\right) e^z z^{-\alpha-\tfrac{2}{3}}}{\Gamma(-\alpha)} \quad \text{as } z \to +\infty. \tag{4-6}$$

The behavior as z approaches $+\infty$ differs from when z approaches $-\infty$. Therefore, the first kind of solution does not satisfy the boundary condition.

Now we will look at our second independent solution, $U(-\alpha, \tfrac{2}{3}, z)$. Recall the solution from [Abramowitz and Stegun 1965, 13.5.2]:

$$U\left(-\alpha, \tfrac{2}{3}, z\right) = z^\alpha \left\{ \sum_{n=0}^{R-1} \frac{(-\alpha)_n \left(1 - \alpha - \tfrac{2}{3}\right)_n}{n!} (-z)^{-n} + O(|z|^{-R}) \right\},$$

where $-\tfrac{3}{2}\pi < \arg(z) < \tfrac{3}{2}\pi$.

As z approaches $+\infty$, the defining behavior becomes

$$U\left(-\alpha, \tfrac{2}{3}, z\right) \approx z^\alpha.$$

Let us define a new variable S so that

$$z = -v^3/(9x) = -S^3 = (-S)^3 \quad \text{where } S \in \mathbb{R}, -\tfrac{1}{2}\pi < \arg(-S) < \tfrac{1}{2}\pi.$$

Therefore, we obtain

$$U\left(-\alpha, \tfrac{2}{3}, -S^3\right) \approx |S|^{3\alpha} \quad \text{as } S \to -\infty.$$

In order to examine the behavior as z approaches $-\infty$, we look at [Abramowitz and Stegun 1965, 13.1.3]:

$$U\left(-\alpha, \tfrac{2}{3}, z\right) = \frac{\pi}{\sin\left(\tfrac{2}{3}\pi\right)} \left\{ \frac{M\left(-\alpha, \tfrac{2}{3}, z\right)}{\Gamma\left(1 - \alpha - \tfrac{2}{3}\right)\Gamma\left(\tfrac{2}{3}\right)} - z^{1-\tfrac{2}{3}} \frac{M\left(1 - \alpha - \tfrac{2}{3}, 2 - \tfrac{2}{3}, z\right)}{\Gamma(-\alpha)\Gamma\left(2 - \tfrac{2}{3}\right)} \right\}. \tag{4-7}$$

Recall that $z = -S^3$ and the previously obtained formula (4-5). Plugging this into (4-7), we obtain

$$U\left(\alpha, \tfrac{2}{3}, -S^3\right) = \frac{\pi}{\sin\left(\tfrac{2}{3}\pi\right)} \left\{ \frac{1}{\Gamma\left(\tfrac{1}{3} - \alpha\right)\Gamma\left(\tfrac{2}{3} + \alpha\right)} + \frac{1}{\Gamma(-\alpha)\Gamma(1 + \alpha)} \right\} S^{3\alpha}.$$

We now use the following identity from [Abramowitz and Stegun 1965]:

$$\Gamma(-x)\Gamma(1 + x) = -\frac{\pi}{\sin(\pi x)},$$

which gives us

$$\Gamma\left(\tfrac{1}{3} - \alpha\right)\Gamma\left(\tfrac{2}{3} + \alpha\right) = \frac{\pi}{\sin\left(\pi\left(\tfrac{2}{3} + \alpha\right)\right)} \quad \text{and} \quad \Gamma(-\alpha)\Gamma(1 + \alpha) = -\frac{\pi}{\sin(\pi\alpha)}.$$

Recall the trigonometric identity

$$\frac{\sin\left(\pi\left(\alpha + \tfrac{2}{3}\right)\right) - \sin(\pi\alpha)}{\sin\left(\tfrac{2}{3}\pi\right)} = 2\cos\left(\pi\left(\alpha + \tfrac{1}{3}\right)\right).$$

As a result,

$$U\left(-\alpha, \tfrac{2}{3}, -S^3\right) \approx 2\cos\left(\pi\left(\alpha + \tfrac{1}{3}\right)\right)S^3 \quad \text{as } S \to +\infty.$$

If our boundary conditions are satisfied, then we have

$$2\cos\left(\pi\left(\alpha + \tfrac{1}{3}\right)\right)|S|^{3\alpha} = |S|^{3\alpha};$$

hence,

$$2\cos\left(\pi\left(\alpha + \tfrac{1}{3}\right)\right) = 1.$$

Solving for α, we find that $\alpha = 0$ or $\alpha = -\tfrac{2}{3}$.

In the case that $\alpha = 0$, we would obtain a constant, which has been already found in the previous section by separation of variables. In the case of $\alpha = -\tfrac{2}{3}$, there is a singularity near the origin. However, it turns out that it is positive and integrable near the origin. The solution

$$p(x, v) = x^{-\tfrac{2}{3}}U\left(\tfrac{2}{3}, \tfrac{2}{3}, -v^3/(9x)\right)$$

to the stationary problem (4-1)–(4-2) could be useful in studying the behavior of the solution with the boundary condition near the boundary. We refer to [Hwang et al. 2015a] for more discussion on the Kummer functions and their applications to the Kolmogorov equation (1-4).

5. Reflection method

We will now try to solve (1-4),

$$\partial_t p + v\partial_x p = \partial_v^2 p,$$

where $x > 0$, $v \in \mathbb{R}$ and $t > 0$. We also require that $p(t, x, v)$ satisfies $p(t, 0, v) = p(t, 0, -v)$ and initial data $p(0, x, v) = p_0(x, v)$ satisfies the compatibility condition $p_0(0, v) = p_0(0, -v)$.

Although we do not know the solution of this problem yet, we do know the solution on the whole real line (when $x \in \mathbb{R}$). Therefore, we will attempt to use the reflection method to solve our problem.

The main result of this section is the following.

Theorem 5.1. *Define*

$$\bar{p}(t,x,v)=\int_{-\infty}^{+\infty}\int_{0}^{+\infty}[G(t,x,v,x_0,v_0)+G(t,x,v,-x_0,-v_0)]p_0(x_0,v_0)\,dx_0\,dv_0$$

for $t > 0$, $x > 0$, $v \in \mathbb{R}$. Here G is the fundamental solution obtained in Section 3.3 and p_0 is the given initial data for our problem. Then $\bar{p}(t,x,v)$ satisfies:

(1) $\bar{p}_t + v\bar{p}_x = \bar{p}_{vv}$ *for $t > 0$, $x > 0$, $v \in \mathbb{R}$.*

(2) $\lim_{t\to 0} \bar{p}(t,x,v) = p_0(x,v)$ *for $x > 0$, $v \in \mathbb{R}$.*

(3) $\bar{p}(t,0,v) = \bar{p}(t,0,-v)$ *for $t > 0$, $v \in \mathbb{R}$.*

Proof. In order to prove the theorem, we first assume that p solves our problem and extend p to the whole space.

We let

$$\bar{q}(t,x,v) = \begin{cases} p(t,x,v), & x > 0, \\ p(t,-x,-v), & x < 0, \end{cases}$$

and let

$$\bar{q}_0(x_0,v_0) = \bar{q}(0,x,v) = \begin{cases} p_0(x,v), & x > 0, \\ p_0(-x,-v), & x < 0. \end{cases}$$

We see that $\bar{q}(t,x,v)$ satisfies our boundary conditions: plugging in 0 for x, we have

$$p(t,0,v) = p(t,0,-v) \quad \text{if } \bar{q}(t,x,v) \text{ is continuous.}$$

First, we check that $\bar{q}$ solves the problem in the whole space. We know that the equation satisfies the problem when $x > 0$, since this is our original problem. However, we must check that the second half of our solution also satisfies the problem.

When $x < 0$, we find that $\bar{q} = p(t,-x,-v)$ satisfies

$$\partial_t\bar{q}(t,x,v) = \partial_t p(t,-x,-v),$$
$$\partial_x\bar{q}(t,x,v) = -\partial_x p(t,-x,-v),$$
$$\partial_v^2\bar{q}(t,x,v) = -\partial_v^2 p(t,-x,-v).$$

On the other hand, since $-x > 0$, we have that $p(t,-x,-v)$ satisfies the equation

$$\partial_t p(t,-x,-v) + (-v)(\partial_x p(t,-x,-v)) - \partial_v^2 p(t,-x,-v) = 0,$$

which is the same as

$$\partial_t p(t,-x,-v) + (v)(-\partial_x p(t,-x,-v)) - \partial_v^2 p(t,-x,-v) = 0.$$

Now by using the above relations for the derivatives of $\bar{q}$, we see that

$$\partial_t\bar{q}(t,x,v) + v(\partial_x\bar{q}(t,x,v)) - \partial_v^2\bar{q}(t,x,v) = 0$$

for $x < 0$. Since we have seen that $\bar{q}$ solves the whole space problem, we can obtain the solution $\bar{q}(t, x, v)$ with the extended initial data $\bar{q}_0(x_0, v_0)$ by using $G(t, x, v, x_0, v_0)$, where G is the fundamental solution we obtained earlier in (3-7),

$$\bar{q}(t, x, v) = \int_{-\infty}^{+\infty} \int_{-\infty}^{+\infty} G(t, x, v, x_0, v_0) \bar{q}_0(x_0, v_0) \, dx_0 \, dv_0$$

$$= \int_{-\infty}^{+\infty} \int_{0}^{+\infty} G(t, x, v, x_0, v_0) p_0(x_0, v_0) \, dx_0 \, dv_0$$

$$+ \int_{-\infty}^{+\infty} \int_{-\infty}^{0} G(t, x, v, x_0, v_0) p_0(-x_0, -v_0) \, dx_0 \, dv_0.$$

Let $\tilde{x} = -x_0$ and $\tilde{v} = -v_0$. We get

$$\bar{q}(t, x, v) = \int_{-\infty}^{+\infty} \int_{0}^{+\infty} G(t, x, v, x_0, v_0) p_0(x_0, v_0) \, dx_0 \, dv_0$$

$$+ \int_{-\infty}^{+\infty} \int_{0}^{+\infty} G(t, x, v, -\tilde{x}, -\tilde{v}) p_0(\tilde{x}, \tilde{v}) \, d\tilde{x} \, d\tilde{v}.$$

We can now add the two parts and we obtain

$$\bar{q}(t, x, v) = \int_{-\infty}^{+\infty} \int_{0}^{+\infty} [G(t, x, v, x_0, v_0) + G(t, x, v, -x_0, -v_0)] p_0(x_0, v_0) \, dx_0 \, dv_0.$$

This is a solution to the whole space problem, but we are only looking for the solution to the half line. Therefore, we restrict the solution to $x > 0$, $v \in \mathbb{R}$, $t > 0$. It is now clear that the first two conditions in the theorem are satisfied. We must now check the third condition.

Recall our solution

$$\bar{q}(t, x, v)$$

$$= \int_{-\infty}^{+\infty} \int_{0}^{+\infty} p_0(x_0, v_0) \left[\frac{\sqrt{3}}{2\pi t^2} e^{-\frac{3}{t^4}\left(t(x-x_0-v_0 t)^2 - t^2(x-x_0-v_0 t)(v-v_0) + \frac{t^3}{3}(v-v_0)^2\right)} \right.$$

$$+ \left. \frac{\sqrt{3}}{2\pi t^2} e^{-\frac{3}{t^4}\left(t(x+x_0+v_0 t)^2 - t^2(x+x_0+v_0 t)(v+v_0) + \frac{t^3}{3}(v+v_0)^2\right)} \right] dx_0 \, dv_0.$$

Let us check if our boundary conditions are satisfied:

$$\bar{q}(t, 0, v)$$

$$= \int_{-\infty}^{+\infty} \int_{0}^{+\infty} p_0(x_0, v_0) \left[\frac{\sqrt{3}}{2\pi t^2} e^{-\frac{3}{t^4}\left(t(x_0+v_0 t)^2 - t^2(x_0+v_0 t)(v_0-v) + \frac{1}{3}t^3(v-v_0)^2\right)} \right.$$

$$+ \left. \frac{\sqrt{3}}{2\pi t^2} e^{-\frac{3}{t^4}\left(t(x_0+v_0 t)^2 - t^2(x_0+v_0 t)(v+v_0) + \frac{1}{3}t^3(v+v_0)^2\right)} \right] dx_0 \, dv_0,$$

$\bar{q}(t, 0, -v)$
$$= \int_{-\infty}^{+\infty} \int_{0}^{+\infty} p_0(x_0, v_0) \left[\frac{\sqrt{3}}{2\pi t^2} e^{-\frac{3}{t^4}\left(t(x_0+v_0 t)^2 - t^2(x_0+v_0 t)(v_0+v) + \frac{1}{3}t^3(v+v_0)^2\right)} \right.$$
$$\left. + \frac{\sqrt{3}}{2\pi t^2} e^{-\frac{3}{t^4}\left(t(x_0+v_0 t)^2 - t^2(x_0+v_0 t)(v_0-v) + \frac{1}{3}t^3(v-v_0)^2\right)} \right] dx_0 \, dv_0.$$

As we can see, both of these are equal and therefore our solution meets all three conditions. We see that $\bar{q} = \bar{p}$ and find that when $\bar{q}$ is restricted to the half line, it is $\bar{p}$ defined in the statement of the theorem. □

6. Conclusion

Our note focuses on the Kolmogorov equation and teaches us some of its important properties. We first introduced stochastic processes including Brownian motion. Next, we searched for stationary solutions to our equation. We started off by looking for a solution of the form $p(x, v) = X(x)V(v)$. When looking at this case, we found that the result is a constant. Next, we searched for a solution of self-similar type, but this time one of the form $p(x, v) = x^\alpha \phi(-v^3/(9x))$, because of the scaling invariant property of the equation. In our attempt to solve this we found that with a reflecting boundary condition, a nonconstant solution exists when $\alpha = -\frac{2}{3}$. We also found the fundamental solution to the heat equation and the Kolmogorov equation. Once we had the fundamental solution, we were able to solve the differential equation with reflecting boundary condition. We first solved the problem on the whole space and then restricted it to the half line. Now that we have completed our investigations, it would be worthwhile to see the behavior of the Kolmogorov equation with different boundary conditions. In the case of absorbing boundary conditions, we refer to [Hwang et al. 2014; 2015b]. It would be interesting to investigate the long term behavior of the solutions, particularly whether the solution to the evolution problem would converge to the stationary solution. We leave this study for future projects. In addition, it would be useful to look at some of the many applications of this multifaceted equation. These investigations would be beneficial for many fields and could provide insight to some of the more obscure areas.

Acknowledgements

References

[Abramowitz and Stegun 1965] M. Abramowitz and I. A. Stegun (editors), *Handbook of mathematical functions, with formulas, graphs, and mathematical tables*, Dover, New York, 1965. MR

[Brown 1828] R. Brown, "A brief account of microscopical observations made in the months of June, July and August 1827, on the particles contained in the pollen of plants; and on the general existence of active molecules in organic and inorganic bodies", *Philos. Mag.* (2) **4**:21 (1828), 161–173.

[Einstein 1905] A. Einstein, "Über die von der molekularkinetischen Theorie der Wärme geforderte Bewegung von in ruhenden Flüssigkeiten suspendierten Teilchen", *Ann. Phys.* **322**:8 (1905), 549–560.

[Einstein 1926] A. Einstein, *Investigations on the theory of the Brownian movement*, Dutton, New York, 1926. Zbl

[Hwang et al. 2014] H. J. Hwang, J. Jang, and J. J. L. Velázquez, "The Fokker–Planck equation with absorbing boundary conditions", *Arch. Ration. Mech. Anal.* **214**:1 (2014), 183–233. MR Zbl

[Hwang et al. 2015a] H. Hwang, J. Jang, and J. Velazquez, "On the structure of the singular set for the kinetic Fokker–Planck equations with boundaries", preprint, 2015. arXiv

[Hwang et al. 2015b] H. J. Hwang, J. Jang, and J. Jung, "On the kinetic Fokker–Planck equation in a half-space with absorbing barriers", *Indiana Univ. Math. J.* **64**:6 (2015), 1767–1804. MR Zbl

[Ibe 2013] O. C. Ibe, *Markov processes for stochastic modeling*, 2nd ed., Elsevier, Amsterdam, 2013. MR Zbl

[van Kampen 1981] N. G. van Kampen, *Stochastic processes in physics and chemistry*, 3rd ed., Lecture Notes in Mathematics **888**, Elsevier, Amsterdam, 1981. MR Zbl

[Kolmogoroff 1934] A. Kolmogoroff, "Zufällige Bewegungen (zur Theorie der Brownschen Bewegung)", *Ann. of Math.* (2) **35**:1 (1934), 116–117. MR Zbl

[Olver 2014] P. J. Olver, *Introduction to partial differential equations*, Springer, New York, 2014. MR Zbl

[Risken 1984] H. Risken, *The Fokker–Planck equation: methods of solution and applications*, Springer Series in Synergetics **18**, Springer, Berlin, 1984. MR Zbl

[Skorohod 1961] A. V. Skorohod, "Stochastic equations for diffusion processes with a boundary", *Teor. Verojatnost. i Primenen.* **6** (1961), 287–298. In Russian. MR

[von Smoluchowski 1906] M. von Smoluchowski, "Zur kinetischen Theorie der Brownschen Molekularbewegung und der Suspensionen", *Ann. der Phys.* (4) **21**:14 (1906), 756–780.

[Tanski 2004] I. Tanski, "Fundamental solution of Fokker–Planck equation", preprint, 2004. arXiv

[Tanski 2008] I. A. Tanski, "Fundamental solution of degenerated Fokker–Planck equation", preprint, 2008. arXiv

mnuno2@uci.edu   *University of California, Irvine, CA 92697, United States*

juhijang@usc.edu   *Department of Mathematics, University of Southern California, 3620 S. Vermont Ave., Los Angeles, CA 90089, United States*

Reeb dynamics of the link of the A_n singularity

Leonardo Abbrescia, I. Huq-Kuruvilla, J. Nelson and N. Sultani

(Communicated by Colin Adams)

The link of the A_n singularity, $L_{A_n} \subset \mathbb{C}^3$ admits a natural contact structure ξ_0 coming from the set of complex tangencies. The canonical contact form α_0 associated to ξ_0 is degenerate and thus has no isolated Reeb orbits. We show that there is a nondegenerate contact form for a contact structure equivalent to ξ_0 that has two isolated simple periodic Reeb orbits. We compute the Conley–Zehnder index of these simple orbits and their iterates. From these calculations we compute the positive S^1-equivariant symplectic homology groups for (L_{A_n}, ξ_0). In addition, we prove that (L_{A_n}, ξ_0) is contactomorphic to the lens space $L(n+1, n)$, equipped with its canonical contact structure ξ_{std}.

1. Introduction and main results

The classical topological theory of isolated critical points of complex polynomials relates the topology of the link of the singularity to the algebraic properties of the singularity [Milnor 1968]. More generally, the link of an irreducible affine variety $A^n \subset \mathbb{C}^N$ with an isolated singularity at $\mathbb{0}$ is defined by $L_A = A \cap S^{2N+1}_\delta$. For sufficiently small δ, the link L_A is a manifold of real dimension $2n - 1$, which is an invariant of the germ of A at $\mathbb{0}$. The links of Brieskorn varieties can sometimes be homeomorphic but not always diffeomorphic to spheres (see [Brieskorn 1966], a preliminary result which further motivated the study of such objects). Recent developments in symplectic and contact geometry have shown that the algebraic properties of a singularity are strongly connected to the contact topology of the link and symplectic topology of (the resolution of) the variety. A wide range of results demonstrating the power of investigating the symplectic and contact perspective of singularities include [Keating 2015; Kwon and van Koert 2016; McLean 2016; Ritter 2010; Seidel 2008b; Ustilovsky 1999].

In this paper we study the contact topology of the link of the A_n singularity, providing a computation of positive S^1-equivariant symplectic homology. This

is done via our construction of an explicit nondegenerate contact form and the computation of the Conley–Zehnder indices of the associated simple Reeb orbits and their iterates. Our computations show that positive S^1-equivariant symplectic homology is a free $\mathbb{Q}[u]$ module of rank equal to the number of conjugacy classes of the finite subgroup A_n of $\mathrm{SL}(2; \mathbb{C})$. This provides a concrete example of the relationship between the cohomological McKay correspondence and symplectic homology, which is work in progress by McLean and Ritter [≥ 2017]. As a result, the topological nature of the singularity is reflected by qualitative aspects of the Reeb dynamics associated to the link of the A_n singularity.

The link of the A_n singularity is defined by

$$L_{A_n} = f_{A_n}^{-1}(0) \cap S^5 \subset \mathbb{C}^3, \quad f_{A_n} = z_0^{n+1} + 2z_1 z_2. \tag{1-1}$$

It admits a natural contact structure coming from the set of complex tangencies,

$$\xi_0 := TL_{A_n} \cap J_0(TL_{A_n}).$$

The contact structure can be expressed as the kernel of the canonically defined contact form,

$$\alpha_0 = \frac{i}{2} \left(\sum_{j=0}^{m} (z_j d\bar{z}_j - \bar{z}_j dz_j) \right) \Bigg|_{L_{A_n}}.$$

The contact form α_0 is degenerate and hence not appropriate for computing Floer-theoretic invariants as the periodic orbits of the Reeb vector field defined by

$$\alpha_0(R_{\alpha_0}) = 1, \quad \iota_{R_{\alpha_0}} d\alpha_0 = 0$$

are not isolated.

Our first result is the construction of a nondegenerate contact form α_ϵ such that $(L_{A_n}, \ker \alpha_0)$ and $(L_{A_n}, \ker \alpha_\epsilon)$ are contactomorphic. Define the Hamiltonian on $\mathbb{C}^3$ by

$$H : \mathbb{C}^3 \to \mathbb{R},$$
$$(z_0, z_1, z_2) \mapsto |z|^2 + \epsilon(|z_1|^2 - |z_2|^2),$$

where ϵ is chosen so that $H > 0$ on S^5. We will show

$$\alpha_\epsilon = \frac{1}{H} \left[\frac{(n+1)i}{8} (z_0 d\bar{z}_0 - \bar{z}_0 dz_0) + \frac{i}{4} (z_1 d\bar{z}_1 - \bar{z}_1 dz_1 + z_2 d\bar{z}_2 - \bar{z}_2 dz_2) \right] \tag{1-2}$$

is a nondegenerate contact form. We also find the simple Reeb orbits of R_{α_ϵ} and compute the associated Conley–Zehnder index with respect to the canonical trivialization of $\mathbb{C}^3$ of their iterates.

Theorem 1.1. *The 1-form α_ϵ is a nondegenerate contact form for L_{A_n} such that $(L_{A_n}, \ker \alpha_0)$ and $(L_{A_n}, \ker \alpha_\epsilon)$ are contactomorphic. The Reeb orbits of R_{α_ϵ} are*

defined by

$$\gamma_+(t) = (0, e^{2i(1+\epsilon)t}, 0), \quad 0 \le t \le \pi/(1+\epsilon),$$

$$\gamma_-(t) = (0, 0, e^{2i(1-\epsilon)t}), \quad 0 \le t \le \pi/(1-\epsilon).$$

The Conley–Zehnder index for $\gamma = \gamma_\pm^N$ in $0 \le t \le N\pi/(1 \pm \epsilon)$ is

$$\mu_{CZ}(\gamma_\pm^N) = 2\left(\left\lfloor \frac{2N}{(n+1)(1 \pm \epsilon)} \right\rfloor + \left\lfloor \frac{N(1 \mp \epsilon)}{1 \pm \epsilon} \right\rfloor - \left\lfloor \frac{2N}{1 \pm \epsilon} \right\rfloor\right) + 2N + 1. \quad (1\text{-}3)$$

Remark 1.2. If ϵ is chosen such that $0 < \epsilon \ll 1/N$ then (1-3) can be simplified to

$$\mu_{CZ}(\gamma_-^N) = 2\left\lfloor \frac{2N}{(n+1)(1-\epsilon)} \right\rfloor + 1,$$

$$\mu_{CZ}(\gamma_+^N) = 2\left\lfloor \frac{2N}{(n+1)(1+\epsilon)} \right\rfloor + 1. \quad (1\text{-}4)$$

The proof of Theorem 1.1 is obtained by adapting methods of Ustilovsky [1999] to obtain α_ϵ and to compute the Conley–Zehnder indices. The Conley–Zehnder index is a Maslov index for arcs of symplectic matrices and is defined in Section 2D. These paths of matrices are obtained by linearizing the flow of the Reeb vector field along the Reeb orbit and restricting to ξ_0. To better understand the spread of the Reeb orbits and their iterates in various indices, we have the following example.

Example 1.3. Let $n = 2$ and $0 < \epsilon \ll \frac{1}{10}$. Then

$$\mu_{CZ}(\gamma_-) = 1, \quad \mu_{CZ}(\gamma_+) = 1,$$
$$\mu_{CZ}(\gamma_-^2) = 3, \quad \mu_{CZ}(\gamma_+^2) = 3,$$
$$\mu_{CZ}(\gamma_-^3) = 5, \quad \mu_{CZ}(\gamma_+^3) = 3,$$
$$\mu_{CZ}(\gamma_-^4) = 5, \quad \mu_{CZ}(\gamma_+^4) = 5,$$
$$\mu_{CZ}(\gamma_-^5) = 7, \quad \mu_{CZ}(\gamma_+^5) = 7,$$
$$\mu_{CZ}(\gamma_-^6) = 9, \quad \mu_{CZ}(\gamma_+^6) = 7,$$
$$\mu_{CZ}(\gamma_-^7) = 9, \quad \mu_{CZ}(\gamma_+^7) = 9.$$

It is interesting to note that the spread of integers is not uniform between $\mu_{CZ}(\gamma_-^N)$ and $\mu_{CZ}(\gamma_+^N)$, and where these jumps in index occur. However, we see that there are $n = 2$ Reeb orbits with Conley–Zehnder index 1 and $n + 1 = 3$ orbits with Conley–Zehnder index $2k + 1$ for each $k \ge 1$.

Remark 1.4. Extrapolating this to all values of n and N demonstrates that the numerology of the Conley–Zehnder index realizes the number of free homotopy classes of L_{A_n}. Recall $[\Sigma L_{A_n}] = \pi_0(\Sigma L_{A_n}) = \pi_1(L_{A_n})/\{\text{conjugacy classes}\}$ and $H_1(L_{A_n}, \mathbb{Z}) = \mathbb{Z}_{n+1}$. The information that the $(n+1)$-th iterate of $\gamma_\pm$ is the first

contractible Reeb orbit is also encoded in the above formulas. Qualitative aspects of the Reeb dynamics reflect this topological information in the following computation of a Floer-theoretic invariant of the contact structure ξ_0.

Theorem 1.1 allows us to easily compute positive S^1-equivariant symplectic homology SH_*^{+,S^1}. Symplectic homology is a Floer-type invariant of symplectic manifolds with contact-type boundary; see [Seidel 2008a]. Under additional assumptions, one can prove that the positive S^1-equivariant symplectic homology SH_*^{+,S^1} is in fact an invariant of the contact structure; see [Gutt 2015, Theorems 1.2 and 1.3; Bourgeois and Oancea 2012, Section 4.1.2]. Because of the behavior of the Conley–Zehnder index in Theorem 1.1, we can directly compute $SH_*^{+,S^1}(L_{A_n}, \xi_0)$ and conclude that it is a contact invariant. As a result, the underlying topology of the manifold determines qualitative aspects of any Reeb vector field associated to a contact form defining ξ_0.

Theorem 1.5. *The positive S^1-equivariant symplectic homology of (L_{A_n}, ξ_0) is*

$$SH_*^{+,S^1}(L_{A_n}, \xi_0) = \begin{cases} \mathbb{Q}^n, & * = 1, \\ \mathbb{Q}^{n+1}, & * \geq 3 \text{ and odd}, \\ 0, & * \text{ else}. \end{cases}$$

Proof. To obtain a contact invariant from SH_*^{+,S^1} we need to show in dimension 3 that all contractible Reeb orbits γ satisfy $\mu_{CZ}(\gamma) \geq 3$; see [Gutt 2015, Theorems 1.2 and 1.3; Bourgeois and Oancea 2012, Section 4.1.2]. The first iterate of $\gamma_\pm$ which is contractible is the $(n+1)$-th iterate, and by Theorem 1.1, will always satisfy $\mu_{CZ}(\gamma_\pm) \geq 3$.

If α is a nondegenerate contact form such that the Conley–Zehnder indices of all periodic Reeb orbits are lacunary, meaning they contain no two consecutive numbers, then we can appeal to [Gutt 2015, Theorem 1.1]. This result of Gutt allows us to conclude that over $\mathbb{Q}$-coefficients the differential for $SH^{S^1,+}$ vanishes. In light of Theorem 1.1 we obtain the above result. $\square$

Remark 1.4 yields the following corollary of Theorem 1.5, indicating a Floer-theoretic interpretation of the McKay correspondence [Ito and Reid 1996] via the Reeb dynamics of the link of the A_n singularity. The A_n singularity is the singularity of $f_{A_n}^{-1}(0)$, where f_{A_n} is described as (1-1). This is equivalent to its characterization as the absolutely isolated double point quotient singularity of $\mathbb{C}^2/A_n$, where A_n is the cyclic subgroup of SL(2; $\mathbb{C}$); see Section 4A. The cyclic group A_n acts on $\mathbb{C}^2$ by $(u, v) \mapsto (e^{2\pi i/(n+1)}u, e^{2\pi in/(n+1)}v)$.

Corollary 1.6. *The positive S^1-equivariant symplectic homology $SH_*^{+,S^1}(L_{A_n}, \xi_0)$ is a free $\mathbb{Q}[u]$ module of rank equal to the number of conjugacy classes of the finite subgroup A_n of* SL(2; $\mathbb{C}$).

Remark 1.7. The ongoing work of Nelson [2015; ≥ 2017] and Hutchings and Nelson [2014; ≥ 2017] is needed in order to work under the assumption that a related Floer-theoretic invariant, cylindrical contact homology is a well-defined contact invariant of (L_{A_n}, ξ_0). Once this is complete, the index calculations provided in Theorem 1.1 show that positive S^1-equivariant symplectic homology and cylindrical contact homology agree up to a degree shift.

Bourgeois and Oancea [2012] prove that there are restricted classes of contact manifolds for which one can prove that cylindrical contact homology (with a degree shift) is isomorphic to the positive part of S^1-equivariant symplectic homology when both are defined over $\mathbb{Q}$-coefficients. Their isomorphism relies on having transversality for a generic choice of J, which is presently the case for unit cotangent bundles DT^*L such that dim $L \geq 5$ or when L is Riemannian manifold which admits no contractible closed geodesics [Bourgeois and Oancea 2015]. Our computations confirm that their results should hold for many more closed contact manifolds.

Our final result is an explicit proof that the singularity (L_{A_n}, ξ_0) and the lens space $(L(n + 1, n), \xi_{std})$ are contactomorphic. The lens space

$$L(n + 1, n) = S^3 / \big((u, v) \sim (e^{2\pi i/(n+1)} u, e^{2\pi ni/(n+1)} v) \big)$$

admits a contact structure, which is induced by the one on S^3 and can be expressed as the kernel of the contact form

$$\lambda_{std} = \tfrac{1}{2} i (u d\bar{u} - \bar{u} du + v d\bar{v} - \bar{v} dv).$$

Theorem 1.8. *The link of the A_n singularity $(L_{A_n}, \xi_0 = \ker \alpha_0)$ and the lens space $(L(n + 1, n), \xi_{std} = \ker \lambda_{std})$ are contactomorphic.*

Theorems 1.5 and 1.8 allow us to reprove the following result of Kwon and van Koert [2016]. Since (L_{A_n}, ξ_0) and $(L(n + 1, n), \xi_{std})$ are contactomorphic and $SH_*^{S^1,+}$ is a contact invariant, $SH_*^{S^1,+}(L(n + 1, n), \xi_{std}) = SH_*^{S^1,+}(L_{A_n}, \xi_0)$.

Theorem 1.9 [Kwon and van Koert 2016, Appendix A]. *The positive S^1-equivariant symplectic homology of $(L(n + 1, n), \xi_{std})$ is*

$$SH_*^{+,S^1}(L(n + 1, n), \xi_{std}) = \begin{cases} \mathbb{Q}^n, & * = 1, \\ \mathbb{Q}^{n+1}, & * \geq 3 \text{ and odd}, \\ 0, & * \text{ else}. \end{cases}$$

Their proof relies on the nondegenerate contact form on $(L(n + 1, n), \xi_{std})$. If a_1, a_2 are any rationally independent positive real numbers then

$$\lambda_{a_1,a_2} = \frac{i}{2} \sum_{j=1}^{2} a_j (z_j d\bar{z}_j - \bar{z}_j dz_j)$$

is a nondegenerate contact form for $(L(n+1, n), \xi_{std})$. The simple Reeb orbits on $L(n+1, n)$ are given by

$$\gamma_1 = (e^{it/a_1}, 0), \quad 0 \leq t \leq (2a_1\pi)/(n+1),$$
$$\gamma_2 = (0, e^{it/a_2}), \quad 0 \leq t \leq (2a_2\pi)/(n+1),$$

which descend from the simple isolated Reeb orbits on S^3. Again, the $n+1$ different free homotopy classes associated to this lens space are realized by covers of the isolated Reeb orbits γ_i for $i = 1$ or 2. The Conley–Zehnder index for γ_1^N is

$$\mu_{CZ}(\gamma_1^N) = 2\left(\left\lfloor \frac{N}{n+1} \right\rfloor + \left\lfloor \frac{Na_1}{(n+1)a_2} \right\rfloor\right) + 1, \tag{1-5}$$

with a similar formula holding for γ_2^N.

Outline. The necessary background is given in Section 2. The construction of a nondegenerate contact form and the proof of Theorem 1.1 is given in Section 3. The proof of Theorem 1.8 is given in Section 4.

2. Background

In this section we recall all the necessary symplectic and contact background which is needed to prove Theorems 1.1 and 1.8.

2A. *Contact structures.* First we recall some notions from contact geometry.

Definition 2.1. Let M be a manifold of dimension $2n + 1$. A *contact structure* is a maximally nonintegrable hyperplane field $\xi = \ker \alpha \subset TM$.

Remark 2.2. The kernel of a 1-form α on M^{2n+1}, $\xi = \ker \alpha$, is a contact structure whenever

$$\alpha \wedge (d\alpha)^n \neq 0,$$

which is equivalent to the condition that $d\alpha$ be nondegenerate on ξ.

Note that the contact structure is unaffected when we multiply the contact form α by any positive or negative function on M. We say that two contact structures $\xi_0 = \ker \alpha_0$ and $\xi_1 = \ker \alpha_1$ on a manifold M are *contactomorphic* whenever there is a diffeomorphism $\psi : M \to M$ such that ψ sends ξ_0 to ξ_1,

$$\psi_*(\xi_0) = \xi_1.$$

If a diffeomorphism $\psi : M \to M$ is in fact a contactomorphism then there exists a nonzero function $g : M \to \mathbb{R}$ such that $\psi^*\alpha_1 = g\alpha_0$. Finding an explicit contactomorphism often proves to be a rather difficult and messy task, but an application of Moser's argument yields Gray's stability theorem, which essentially states that there are no nontrivial deformations of contact structures on a fixed closed manifold.

First we give the statement of Moser's theorem, which says that one cannot vary a symplectic structure by perturbing it within its cohomology class. Recall that a *symplectic structure* on a smooth manifold W^{2n} is a nondegenerate closed 2-form $\omega \in \Omega^2(W)$.

Theorem 2.3 (Moser's theorem, [McDuff and Salamon 1998, Theorem 3.17]). *Let W be a closed manifold and suppose that ω_t is a smooth family of cohomologous symplectic forms on W. Then there is a family of diffeomorphisms Ψ_t of W such that*

$$\Psi_0 = \mathrm{id}, \quad \psi_t^* \omega_t = \omega_0.$$

The aforementioned contact analogue of Moser's theorem is Gray's stability theorem, stated formally below.

Theorem 2.4 (Gray's stability theorem, [Geiges 2008, Theorem 2.2.2]). *Let ξ_t, $t \in [0, 1]$, be a smooth family of contact structures on a closed manifold V. Then there is an isotopy $(\psi_t)_{t \in [0,1]}$ of V such that*

$$\psi_{t*}(\xi_0) = \xi_t \quad \textit{for each } t \in [0, 1].$$

Next we give the most basic example of a contact structure.

Example 2.5. Consider $\mathbb{R}^{2n+1}$ with coordinates $(x_1, y_1, \ldots, x_n, y_n, z)$ and the 1-form

$$\alpha = dz + \sum_{j=1}^{n} x_j dy_j.$$

Then α is a contact form for $\mathbb{R}^{2n+1}$. The contact structure $\xi = \ker \alpha$ is called the standard contact structure on $\mathbb{R}^{2n+1}$.

As in symplectic geometry, a variant of Darboux's theorem holds. This states that locally all contact structures are diffeomorphic to the standard contact structure on $\mathbb{R}^{2n+1}$.

A contact form gives rise to a unique Hamiltonian-like vector field as follows.

Definition 2.6. For any contact manifold $(M, \xi = \ker \alpha)$ the *Reeb vector field* R_α is defined to be the unique vector field determined by α,

$$\iota(R_\alpha)d\alpha = 0, \quad \alpha(R_\alpha) = 1.$$

We define the Reeb flow of R_α by $\varphi_t : M \to M$, $\dot{\varphi}_t = R_\alpha(\varphi_t)$.

The first condition says that R_α points along the unique null direction of the form $d\alpha$ and the second condition normalizes R_α. Because

$$\mathcal{L}_{R_\alpha}\alpha = d\iota_{R_\alpha}\alpha + \iota_{R_\alpha}d\alpha,$$

the flow of R_α preserves the form α and hence the contact structure ξ. Note that if one chooses a different contact form $f\alpha$, the corresponding vector field $R_{f\alpha}$ is very different from R_α, and its flow may have quite different properties.

A *Reeb orbit* γ of period T associated to R_α is defined to be a path $\gamma : \mathbb{R}/T\mathbb{Z} \to M$ given by an integral curve of R_α. That is,

$$\frac{d\gamma}{dt} = R_\alpha \circ \gamma(t), \quad \gamma(0) = \gamma(T).$$

Two Reeb orbits

$$\gamma_1, \ \gamma_0 : \mathbb{R}/T\mathbb{Z} \to M$$

are considered equivalent if they differ by reparametrization, i.e., precomposition with a translation of $\mathbb{R}/T\mathbb{Z}$.

The N-fold cover γ^N is defined to be the composition of $\gamma_\pm$ with $\mathbb{R}/NT\mathbb{Z} \to \mathbb{R}/T\mathbb{Z}$. A *simple Reeb orbit* is one such that $\gamma : \mathbb{R}/T\mathbb{Z} \to M$ is injective.

Remark 2.7. Since Reeb vector fields are autonomous, the terminology "simple Reeb orbit γ" refers to the entire equivalence class of orbits, and likewise for its iterates.

A Reeb orbit γ is said to be *nondegenerate* whenever the linearized return map

$$d(\varphi_T)_{\gamma(0)} : \xi_{\gamma(0)} \to \xi_{\gamma(T)=\gamma(0)}$$

has no eigenvalue equal to 1. A *nondegenerate contact form* is one whose Reeb orbits are all nondegenerate and hence isolated. Note that since the Reeb flow preserves the contact structure, the linearized return map is symplectic.

Next we briefly review the canonical contact form on S^3 and its Reeb dynamics.

Example 2.8 (canonical Reeb dynamics on the 3-sphere). If we define the function $f : \mathbb{R}^4 \to \mathbb{R}$,

$$f(x_1, y_1, x_2, y_2) = x_1^2 + y_1^2 + x_2^2 + y_2^2,$$

then $S^3 = f^{-1}(1)$. Recall that the canonical contact form on $S^3 \subset \mathbb{R}^4$ is given to be

$$\lambda_0 := -\tfrac{1}{2}df \circ J = (x_1dy_1 - y_1dx_1 + x_2dy_2 - y_2dx_2)|_{S^3}. \qquad (2\text{-}1)$$

The Reeb vector field is given by

$$R_{\lambda_0} = \left(x_1\frac{\partial}{\partial y_1} - y_1\frac{\partial}{\partial x_1} + x_2\frac{\partial}{\partial y_2} - y_2\frac{\partial}{\partial x_2} \right)$$

$$= (-y_1, x_1, -y_2, x_2). \qquad (2\text{-}2)$$

Equivalently we may reformulate these using complex coordinates by identifying $\mathbb{R}^4$ with $\mathbb{C}^2$ via

$$u = x_1 + iy_1, \quad v = x_2 + iy_2.$$

We obtain
$$\lambda_0 = \tfrac{1}{2}i(ud\bar{u} - \bar{u}du + vd\bar{v} - \bar{v}dv)|_{S^3},$$
and
$$R_{\lambda_0} = i\left(u\frac{\partial}{\partial u} - \bar{u}\frac{\partial}{\partial \bar{u}} + v\frac{\partial}{\partial v} - \bar{v}\frac{\partial}{\partial \bar{v}}\right) \tag{2-3}$$
$$= (iu, iv).$$

The second expression for R_{λ_0} follows from (2-2) since $iu = (-y_1, x_1)$ and $iv = (-y_2, x_2)$.

To see that the orbits of R_{λ_0} define the fibers of the Hopf fibration, recall that a fiber through a point
$$(u, v) = (x_1 + iy_1, x_2 + iy_2) \in S^3 \subset \mathbb{C}^2$$
can be parameterized as
$$\varphi(t) = (e^{it}u, e^{it}v), \quad t \in \mathbb{R}. \tag{2-4}$$

We compute the time derivative of the fiber
$$\dot{\varphi}(0) = (iu, iv) = (ix_1 - y_1, ix_2 - y_2).$$

Expressed as a real vector field on $\mathbb{R}^4$, which is tangent to S^3, this is the Reeb vector field R_{λ_0} as it appears in (2-3), so the Reeb flow does indeed define the Hopf fibration.

2B. *Hypersurfaces of contact type.* Another notion that we need from symplectic and contact geometry is that of a hypersurface of contact type in a symplectic manifold. The following notion of a Liouville vector field allows us to define hypersurfaces of contact type. Liouville vector fields will be used to understand the Reeb dynamics of the nondegenerate contact form α_1 as well as to construct the contactomorphism between (L_{A_n}, ξ_0) and $(L(n+1, n), \xi_{\text{std}})$.

Definition 2.9. A *Liouville vector field* Y on a symplectic manifold (W, ω) is a vector field satisfying
$$\mathcal{L}_Y\omega = \omega.$$

The flow ψ_t of such a vector field is conformal symplectic, i.e., $\psi_t^*(\omega) = e^t\omega$. The flow of these fields is volume expanding, so such fields may only exist locally on compact manifolds.

Whenever there exists a Liouville vector field Y defined in a neighborhood of a compact hypersurface Q of (W, ω), which is transverse to Q, we can define a contact 1-form on Q by
$$\alpha := \iota_Y\omega.$$

Proposition 2.10 [McDuff and Salamon 1998, Proposition 3.58]. *Let* (W, ω) *be a symplectic manifold and* $Q \subset W$ *a compact hypersurface. Then the following are equivalent*:

(i) *There exists a contact form* α *on* Q *such that* $d\alpha = \omega|_Q$.

(ii) *There exists a Liouville vector field* $Y : U \to TW$ *defined in a neighborhood* U *of* Q, *which is transverse to* Q.

If these conditions are satisfied then Q *is said to be of* contact type.

We will need the following application of Gray's stability theorem to hypersurfaces of contact type to prove Theorem 1.8 in Section 4.

Lemma 2.11 [Geiges 2008, Lemma 2.1.5]. *Let* Y *be a Liouville vector field on a symplectic manifold* (W, ω). *Suppose that* M_1 *and* M_2 *are hypersurfaces of contact type in* W. *Assume that there is a smooth function*

$$h : W \to \mathbb{R} \tag{2-5}$$

*such that the time-*1 *map of the flow of* hY *is a diffeomorphism from* M_1 *to* M_2. *Then this diffeomorphism is in fact a contactomorphism from* $(M_1, \ker \iota_Y \omega|_{TM_1})$ *to* $(M_2, \ker \iota_Y \omega|_{TM_2})$.

2C. *Symplectization.* The symplectization of a contact manifold is an important notion in defining Floer-theoretic theories like symplectic and contact homology. It will also be used in our calculation of the Conley–Zehnder index. Let $(M, \xi = \ker \alpha)$ be a contact manifold. The *symplectization* of $(M, \xi = \ker \alpha)$ is given by the manifold $\mathbb{R} \times M$ and symplectic form

$$\omega = e^t (d\alpha - \alpha \wedge dt) = d(e^t \alpha).$$

Here t is the coordinate on $\mathbb{R}$, and it should be noted that α is interpreted as a 1-form on $\mathbb{R} \times M$, as we identify α with its pullback under the projection $\mathbb{R} \times M \to M$.

Any contact structure ξ may be equipped with a complex structure J such that (ξ, J) is a complex vector bundle. This set is nonempty and contractible. There is a unique canonical extension of the almost complex structure J on ξ to an $\mathbb{R}$-invariant almost complex structure $\tilde{J}$ on $T(\mathbb{R} \times M)$, whose existence is due to the splitting,

$$T(\mathbb{R} \times M) = \mathbb{R}\frac{\partial}{\partial t} \oplus \mathbb{R}R_\alpha \oplus \xi. \tag{2-6}$$

Definition 2.12 (canonical extension of J to $\tilde{J}$ on $T(\mathbb{R} \times M)$). Let $[a, b; v]$ be a tangent vector where $a, b \in \mathbb{R}$ and $v \in \xi$. We can extend $J : \xi \to \xi$ to $\tilde{J} : T(\mathbb{R} \times M) \to T(\mathbb{R} \times M)$ by

$$\tilde{J}[a, b; v] = [-b, a, Jv].$$

Thus $\tilde{J}|_\xi = J$ and $\tilde{J}$ acts on $\mathbb{R}\partial/\partial t \oplus \mathbb{R}R_\alpha$ in the same manner as multiplication by i acts on $\mathbb{C}$, namely $J\partial/\partial t = R_\alpha$.

2D. *The Conley–Zehnder index.*

The Conley–Zehnder index μ_{CZ} is a Maslov index for arcs of symplectic matrices which assigns an integer $\mu_{CZ}(\Phi)$ to every path of symplectic matrices $\Phi : [0, T] \to \mathrm{Sp}(n)$, with $\Phi(0) = \mathbb{1}$. In order to ensure that the Conley–Zehnder index assigns the same integer to homotopic arcs, one must also stipulate that 1 is not an eigenvalue of the endpoint of this path of matrices, i.e., $\det(\mathbb{1} - \Phi(T)) \neq 0$. We define the following set of continuous paths of symplectic matrices that start at the identity and end on a symplectic matrix that does not have 1 as an eigenvalue:

$$\Sigma^*(n) = \{\Phi : [0, T] \to \mathrm{Sp}(2n) : \Phi \text{ is continuous, } \Phi(0) = \mathbb{1}, \text{ and } \det(\mathbb{1} - \Phi(T)) \neq 0\}.$$

The Conley–Zehnder index is a functor satisfying the following properties, and is uniquely determined by the homotopy, loop, and signature properties.

Theorem 2.13 [Robbin and Salamon 1993, Theorem 2.3, Remark 5.4; Gutt 2014, Theorem 2, Propositions 8 and 9]. *There exists a unique functor μ_{CZ} called the* Conley–Zehnder index *that assigns the same integer to all homotopic paths Ψ in $\Sigma^*(n)$,*

$$\mu_{CZ} : \Sigma^*(n) \to \mathbb{Z},$$

such that the following hold:

(1) *Homotopy*: *The Conley–Zehnder index is constant on the connected components of $\Sigma^*(n)$.*

(2) *Naturalization*: *For any paths $\Phi, \Psi : [0, 1] \to \mathrm{Sp}(2n)$,*

$$\mu_{CZ}(\Phi\Psi\Phi^{-1}) = \mu_{CZ}(\Psi).$$

(3) *Zero*: *If $\Psi(t) \in \Sigma^*(n)$ has no eigenvalues on the unit circle for $t > 0$, then $\mu_{CZ}(\Psi) = 0$.*

(4) *Product*: *If $n = n' + n''$, identify $\mathrm{Sp}(2n') \oplus \mathrm{Sp}(2n'')$ with a subgroup of $\mathrm{Sp}(2n)$ in the obvious way. For $\Psi' \in \Sigma^*(n')$ and $\Psi'' \in \Sigma^*(n'')$, we have $\mu_{CZ}(\Psi' \oplus \Psi'') = \mu_{CZ}(\Psi') + \mu_{CZ}(\Psi'')$.*

(5) *Loop*: *If Φ is a loop at $\mathbb{1}$, then $\mu_{CZ}(\Phi\Psi) = \mu_{CZ}(\Psi) + 2\mu(\Phi)$, where μ is the* Maslov Index.

(6) *Signature*: *If $S \in M(2n)$ is a symmetric matrix with $\|S\| < 2\pi$ and $\Psi(t) = \exp(J_0 S t)$, then $\mu_{CZ}(\Psi) = \frac{1}{2}\mathrm{sgn}(S)$.*

The linearized Reeb flow of γ yields a path of symplectic matrices

$$d(\varphi_t)_{\gamma(0)} : \xi_{\gamma(0)} \to \xi_{\gamma(t) = \gamma(0)}$$

for $t \in [0, T]$, where T is the period of γ.

Thus we can compute the Conley–Zehnder index of $d\varphi_t$, $t \in [0, T]$. This index is typically dependent on the choice of trivialization τ of ξ along γ which was used in linearizing the Reeb flow. However, if $c_1(\xi; \mathbb{Z}) = 0$ we can use the existence of an (almost) complex volume form on the symplectization to obtain a global means of linearizing the flow of the Reeb vector field. The choice of a complex volume form is parametrized by $H^1(\mathbb{R} \times M; \mathbb{Z})$, so an absolute integral grading is only determined up to the choice of volume form. See [Nelson $\geq$ 2017, §1.1.1].

We define

$$\mu_{CZ}^\tau(\gamma) := \mu_{CZ}(\{d\varphi_t\}|_{t \in [0,T]}).$$

In the case at hand we will be able to work in the ambient space of $(\mathbb{C}^3, J_0)$, and use a canonical trivialization of $\mathbb{C}^3$.

2E. *The canonical contact structure on Brieskorn manifolds.* The A_n link is an example of a Brieskorn manifold, which are defined generally by

$$\Sigma(\boldsymbol{a}) = \left\{ (z_0, \ldots, z_m) \in \mathbb{C}^{m+1} \Big| f := \sum_{j=0}^m z_j^{a_j} = 0, \, a_j \in \mathbb{Z}_{>0} \text{ and } \sum_{j=0}^m |z_j|^2 = 1 \right\}.$$

The link of the A_n singularity after a linear change of variables is $\Sigma(n+1, 2, 2)$ for $n > 3$; see (3-1). Brieskorn gave a necessary and sufficient condition on $\boldsymbol{a}$ for $\Sigma(\boldsymbol{a})$ to be a topological sphere, and means to show when these yield exotic differentiable structures on the topological $(2n-1)$-sphere in [Brieskorn 1966]. A standard calculus argument [Geiges 2008, Lemma 7.1.1] shows that $\Sigma(\boldsymbol{a})$ is always a smooth manifold.

In the mid 1970s, Brieskorn manifolds were found to admit a canonical contact structure, given by their set of complex tangencies,

$$\xi_0 = T\Sigma \cap J_0(T\Sigma),$$

where J_0 is the standard complex structure on $\mathbb{C}^{m+1}$. The contact structure ξ_0 can be expressed as $\xi_0 = \ker \alpha_0$ for the canonical 1-form

$$\alpha_0 := (-d\rho \circ J_0)|_\Sigma = \frac{i}{4} \left(\sum_{j=0}^m (z_j d\bar{z}_j - \bar{z}_j dz_j) \right)\Big|_\Sigma,$$

where $\rho = (\|z\|^2 - 1)/4$. A proof of this fact may be found in [Geiges 2008, Theorem 7.1.2]. The Reeb dynamics associated to α_0 are difficult to understand. There is a more convenient contact form α_1 constructed by Ustilovsky [1999, Lemma 4.1.2] via the following family.

Proposition 2.14 [Geiges 2008, Proposition 7.1.4]. *The 1-form*

$$\alpha_t = \frac{i}{4} \sum_{j=0}^{m} \frac{1}{1-t+t/a_j}(z_j d\bar{z}_j - \bar{z}_j dz_j)$$

is a contact form on $\Sigma(\boldsymbol{a})$ for each $t \in [0, 1]$.

Via Gray's stability theorem we obtain the following corollary.

Corollary 2.15. *For all $t \in (0, 1]$, the contact manifold $(\Sigma(\boldsymbol{a}), \ker \alpha_0)$ is contactomorphic to $(\Sigma(\boldsymbol{a}), \ker \alpha_t)$.*

Next, the Reeb dynamics associated to $\alpha_1 = \frac{1}{4}i \sum_{j=0}^{m} a_j(z_j d\bar{z}_j - \bar{z}_j dz_j)$ are computed.

Remark 2.16. While α_1 is degenerate, one can still easily check that the Reeb vector field associated to α_1 is given by

$$R_{\alpha_1} = 2i \sum_{j=0}^{m} \frac{1}{a_j}\left(z_j \frac{\partial}{\partial z_j} - \bar{z}_j \frac{\partial}{\partial \bar{z}_j}\right) = 2i\left(\frac{z_0}{a_0}, \ldots, \frac{z_m}{a_m}\right).$$

Indeed, one computes

$$df(R_{\alpha_1}) = f(\boldsymbol{z}) \quad \text{and} \quad d\rho(R_{\alpha_1}) = 0.$$

This shows that R_{α_1} is tangent to $\Sigma(\boldsymbol{a})$. The defining equations for the Reeb vector field are satisfied since

$$\alpha_1(R_{\alpha_1}) \equiv 1 \quad \text{and} \quad \iota_{R_{\alpha_1}} d\alpha_1 = -d\rho,$$

with the latter form being zero on the $T_p\Sigma(\boldsymbol{a})$. The flow of R_{α_1} is given by

$$\varphi_t(z_0, \ldots, z_m) = (e^{2it/a_0}, \ldots, e^{2it/a_m}).$$

All the orbits of the Reeb flow are closed, and the flow defines an effective S^1-action on $\Sigma(\boldsymbol{a})$.

In the next section we perturb α_1 to a nondegenerate contact form.

3. Proof of Theorem 1.1

3A. *Constructing a nondegenerate contact form.* Here, we adapt a method used by Ustilovsky [1999, §4] to obtain a nondegenerate contact form α_ϵ on L_{A_n} whose kernel is contactomorphic to ξ_0. Ustilovsky's methods yielded a nondegenerate contact form on Brieskorn manifolds of the form $\Sigma(p, 2, \ldots, 2)$, which are diffeomorphic to S^{4m+1}.

We define the change of coordinates to go from $\Sigma(n+1, 2, 2)$ with defining function $f = z_0^{n+1} + z_1^2 + z_2^2$ to L_{A_n} with defining function $f_{A_n} = w_0^{n+1} + 2w_1w_2$:

$$\Psi(w_0, w_1, w_2) = \Big(\underbrace{w_0}_{:=z_0}, \underbrace{\tfrac{\sqrt{2}}{2}(w_1 + w_2)}_{:=z_1}, \underbrace{\tfrac{\sqrt{2}}{2}(-iw_1 + iw_2)}_{:=z_2} \Big). \qquad (3\text{-}1)$$

We obtain

$$\Psi^* f(z_0, z_1, z_2) = w_0^{n+1} + 2w_1w_2. \qquad (3\text{-}2)$$

Then the pull-back of

$$\frac{\alpha_1}{2} = \frac{i}{8} \sum_{j=0}^{m} a_j(z_j d\bar{z}_j - \bar{z}_j dz_j)$$

is given by

$$\frac{\Psi^*\alpha_1}{2} = \frac{(n+1)i}{8}(w_0 d\bar{w}_0 - \bar{w}_0 dw_0) + \frac{i}{4}(w_1 d\bar{w}_1 - \bar{w}_1 dw_1 + w_2 d\bar{w}_2 - \bar{w}_2 dw_2).$$

We now construct the Hamiltonian function

$$H(w) = |w|^2 + \epsilon(|w_1|^2 - |w_2|^2).$$

We choose $0 < \epsilon < 1$ such that $H(w)$ is positive on S^5, and define the contact form

$$\alpha_\epsilon = \Psi^*\alpha_1/(2H). \qquad (3\text{-}3)$$

Remark 3.1. The above shows that $(\Sigma(n+1, 2, 2), \ker\alpha_1)$ is contactomorphic to $(\Psi(\Sigma(n+1, 2, 2)), \ker\alpha_\epsilon)$. Moreover $L_{A_n} = \Psi(\Sigma(n+1, 2, 2))$, where L_{A_n} was defined in (1-1).

Proposition 3.2. *The Reeb vector field for* α_ϵ *is*

$$R_{\alpha_\epsilon} = \frac{4i}{n+1}w_0\frac{\partial}{\partial w_0} - \frac{4i}{n+1}\bar{w}_0\frac{\partial}{\partial \bar{w}_0} + 2i(1+\epsilon)\Big(w_1\frac{\partial}{\partial w_1} - \bar{w}_1\frac{\partial}{\partial \bar{w}_1}\Big)$$

$$+ 2i(1-\epsilon)\Big(w_2\frac{\partial}{\partial w_2} - \bar{w}_2\frac{\partial}{\partial \bar{w}_{2j}}\Big)$$

$$= \Big(\frac{4i}{n+1}w_0, 2i(1+\epsilon)w_1, 2i(1-\epsilon)w_2\Big). \qquad (3\text{-}4)$$

Remark 3.3. The second formulation of the Reeb vector field is equivalent to the first in the above proposition via the standard identification of $\mathbb{R}^4$ with $\mathbb{C}^2$, as explained in Example 2.8, (2-3).

Before proving Proposition 3.2 we need the following lemma.

Lemma 3.4. *On $\mathbb{C}^3$, the vector field*

$$X(w) = \frac{1}{2}\left(\sum_{j=0}^{2} w_j \frac{\partial}{\partial w_j} + \overline{w}_j \frac{\partial}{\partial \overline{w}_j}\right) \tag{3-5}$$

is a Liouville vector field for the symplectic form

$$\omega_1 = \frac{d(\Psi^*\alpha_1)}{2} = \frac{i(n+1)}{4}dw_0 \wedge d\overline{w}_0 + \frac{i}{2}\sum_{j=1}^{2} dw_j \wedge d\overline{w}_j.$$

The Hamiltonian vector field X_H of H with respect to ω_1 is $-R_{\alpha_\epsilon}$, as in (3-4).

Proof. Recall that the condition to be a Liouville vector field is $\mathcal{L}_X \omega_1 = \omega_1$. We show this with Cartan's formula, given as

$$\mathcal{L}_X \omega_1 = \iota_X d\omega_1 + d(\iota_X \omega_1)$$
$$= d(\iota_X \omega_1).$$

We do the explicit calculation for the first term and the rest easily follows:

$$d\left(\frac{i(n+1)}{4}d\omega_0 \wedge d\overline{\omega}_0\left(\frac{1}{2}\left(w_0\frac{\partial}{\partial w_0} + \overline{w}_0\frac{\partial}{\partial \overline{w}_0}\right), \cdot\right)\right)$$
$$= d\left(\frac{i(n+1)}{8}w_0 d\overline{w}_0 - \overline{w}_0 dw_0\right)$$
$$= \frac{i(n+1)}{8}(dw_0 \wedge d\overline{w}_0 - d\overline{w}_0 \wedge dw_0)$$
$$= \frac{i(n+1)}{4}dw_0 \wedge d\overline{w}_0,$$

so $X(w)$ is indeed a Liouville vector field for ω_1.

Next we prove that $\omega_1(-R_{\alpha_\epsilon}, \cdot) = dH(\cdot)$. First we calculate dH:

$$dH = \left(\sum_{j=0}^{2} w_j d\overline{w}_j + \overline{w}_j dw_j\right) + \epsilon(w_1 d\overline{w}_1 + \overline{w}_1 dw_1 - w_2 d\overline{w}_2 - \overline{w}_2 dw_2).$$

Then we compare the coefficients of dH to the coefficients of $\omega_1(-R_{\alpha_\epsilon}, \cdot)$ associated to each term, $(dw_i \wedge d\overline{w}_i)$. The $(dw_0 \wedge d\overline{w}_0)$ term is

$$\frac{i(n+1)}{4}dw_0 \wedge d\overline{w}_0\left(-\frac{4i}{n+1}w_0\frac{\partial}{\partial w_0} + \frac{4i}{n+1}\overline{w}_0\frac{\partial}{\partial \overline{w}_0}, \cdot\right)$$
$$= \frac{i(n+1)}{4}\left(-\frac{4i}{n+1}w_0 d\overline{w}_0 - \frac{4i}{n+1}\overline{w}_0 dw_0\right)$$
$$= w_0 d\overline{w}_0 + \overline{w}_0 dw_0.$$

The $(dw_1 \wedge d\overline{w}_1)$ term is

$$\tfrac{1}{2}idw_1 \wedge d\overline{w}_1\left(-2i(1+\epsilon)w_1\frac{\partial}{\partial w_1} + 2i(1+\epsilon)\overline{w}_1\frac{\partial}{\partial \overline{w}_1}\right)$$

$$= \tfrac{1}{2}i(-2i(1+\epsilon)w_1d\overline{w}_1 - 2i(1+\epsilon)\overline{w}_1dw_1)$$

$$= (1+\epsilon)w_1d\overline{w}_1 + (1+\epsilon)\overline{w}_1dw_1.$$

The $(dw_2 \wedge d\overline{w}_2)$ term is obtained in a similar way. Summing the terms yields $\omega_1(-R_{\alpha_\epsilon}, \cdot) = dH(\cdot)$. □

Proof of Proposition 3.2. First we show that $X_H = -R_{\alpha_\epsilon}$ is tangent to the link $\Psi(\Sigma(n+1, 2, 2))$. We compute

$$(\Psi_* df)(R_{\alpha_\epsilon}) = ((n+1)w_0^n dw_0 + 2w_1 dw_2 + 2w_2 dw_1)(R_{\alpha_\epsilon})$$

$$= 4iw_0^{n+1} + 4i(1-\epsilon)w_1w_2 + 4i(1+\epsilon)w_1w_2$$

$$= 4i(\Psi^* f)$$

$$= 0.$$

The last equality is because $\Psi^* f$ is constant along $\Psi(\Sigma(n+1, 2, 2))$. Now we have to show that $\tfrac{1}{2}\Psi^*\alpha_1(X_H) = -H$. We have

$$\tfrac{1}{2}\Psi^*\alpha_1(\cdot) = \iota_X\omega_1(\cdot) = \omega_1(X(w), \cdot) = -\omega(\cdot, X(w)),$$

$$\tfrac{1}{2}\Psi^*\alpha_1(X_H) = -\omega(X_H, X(w)) = -dH(X(w))$$

$$= -|w|^2 - \epsilon(|w_1|^2 - |w_2|^2)$$

$$= -H.$$

From these, we conclude

$$\alpha_\epsilon(X_H) = -\frac{1}{H}H = -1,$$

$$d\alpha_\epsilon(X_H, \cdot) = -\frac{1}{2H^2}(dH \wedge \Psi^*\alpha_1)(X_H, \cdot) + \frac{1}{2H}d\Psi^*\alpha_1(X_H, \cdot)$$

$$= -\frac{1}{2H^2}dH(X_H)\Psi^*\alpha_1(\cdot) + \frac{1}{2H^2}\Psi^*\alpha_1(X_H)dH(\cdot) + \frac{1}{H}\omega(X_H, \cdot)$$

$$= -\frac{1}{2H^2}\omega_1(X_H, X_H)\Psi^*\alpha_1(\cdot) - \frac{1}{H}dH(\cdot) + \frac{1}{H}dH(\cdot)$$

$$= 0.$$

By Lemma 3.4, we know $-X_H = R_{\alpha_\epsilon}$ so the result follows. □

3B. *Isolated Reeb orbits.* In this short section, we prove the following proposition.

Proposition 3.5. *The only simple periodic Reeb orbits of R_{α_ϵ} are nondegenerate and defined by*

$$\gamma_+(t) = (0, e^{2i(1+\epsilon)t}, 0), \quad 0 \le t \le \pi/(1+\epsilon),$$
$$\gamma_-(t) = (0, 0, e^{2i(1-\epsilon)t}), \quad 0 \le t \le \pi/(1+\epsilon).$$

Proof. The flow of

$$R_{\alpha_\epsilon} = \left(\frac{4i}{n+1} w_0, 2i(1+\epsilon)w_1, 2i(1-\epsilon)w_2 \right)$$

is given by

$$\varphi_t(w_0, w_1, w_2) = \left(e^{4it/(n+1)} w_0, e^{2i(1+\epsilon)t} w_1, e^{2i(1-\epsilon)t} w_2 \right).$$

Since ϵ is small and irrational, the only possible periodic trajectories are

$$\gamma_0(t) = (e^{4i/(n+1)t}, 0, 0),$$
$$\gamma_+(t) = (0, e^{2i(1+\epsilon)t}, 0),$$
$$\gamma_-(t) = (0, 0, e^{2i(1-\epsilon)t}).$$

It is important to note that the first trajectory does not lie in $\Psi(\Sigma(n+1, 2, 2))$, but rather on the total space $\mathbb{C}^3$. This is because the point $\gamma_0(0) = (1, 0, 0)$ is not a zero of $f_{A_n} = w_0^{n+1} + 2w_1 w_2$.

Next we need to check that the linearized return maps $d\phi|_\xi$ associated to γ_+ and γ_- have no eigenvalues equal to 1. We consider the first orbit γ_+ of period $\pi/(1+\epsilon)$, as a similar argument applies to the return flow associated to γ_-. The differential of its total return map is

$$d\varphi_T = \begin{pmatrix} e^{4iT/(n+1)} & 0 & 0 \\ 0 & 1 & 0 \\ 0 & 0 & e^{2i(1-\epsilon)T} \end{pmatrix} \Bigg|_{T=\pi/(1+\epsilon)}.$$

Since ϵ is a small irrational number, the total return map only has one eigenvalue which is 1. The eigenvector associated to the eigenvalue which is 1 is in the direction of the Reeb orbit γ^+, but since we are restricting the return map to ξ, we can conclude that γ_+ is nondegenerate. $\square$

3C. *Computation of the Conley–Zehnder index.* To compute the Conley–Zehnder indices of the Reeb orbits in Theorem 1.1 we use the same method as shown in [Ustilovsky 1999], extending the Reeb flow to give rise to a symplectomorphism of $\mathbb{C}^3 \setminus \{0\}$. This permits us to do the computations in $\mathbb{C}^3$, equipped with the

symplectic form

$$\omega_1 = \frac{d(\Psi^*\alpha_1)}{2} = \frac{i(n+1)}{4} dw_0 \wedge d\overline{w}_0 + \frac{i}{2} \sum_{j=1}^{2} dw_j \wedge d\overline{w}_j.$$

We may equip the contact structure ξ_0 with the symplectic form $\omega = d\alpha_1$ instead of $d\alpha_\epsilon$ when computing the Conley–Zehnder indices. This is because $\ker \alpha_\epsilon = \ker \alpha_1 = \xi_0$, as $\alpha_\epsilon = (1/H)\alpha_1$ with $H > 0$ and because $\omega|_\xi = H d\alpha_\epsilon|_\xi$ and H is constant along Reeb trajectories.

Our first proposition shows that we can construct a standard symplectic basis for the symplectic complement

$$\xi^\omega = \{v \in \mathbb{C}^3 : \omega(v, w) = 0 \text{ for all } w \in \xi\}$$

of ξ in $\mathbb{C}^3$. As a result, $c_1(\xi^\omega) = 0$. Since $c_1(\mathbb{C}^3) = 0$, we know $c_1(\xi) = 0$. Thus we may compute the Conley–Zehnder indices in the ambient space $\mathbb{C}^3$ and use additivity of the Conley–Zehnder index under direct sums of symplectic paths to compute it in ξ.

Proposition 3.6. *There exists a standard symplectic basis for the symplectic complement ξ^ω with respect to $\omega = d\alpha_1$.*

Proof. Notice that $\xi^\omega = \mathrm{span}(X_1, Y_1, X_2, Y_2)$, where

$$X_1 = (\overline{w}_0^n, \overline{w}_1, \overline{w}_2), \quad Y_1 = iX_1,$$
$$X_2 = R_\epsilon, \quad\quad\quad\quad Y_2 = w.$$

We make this into a symplectic standard basis for ξ^ω via a Gram–Schmidt process. The new basis is given by

$$\tilde{X}_1 = \frac{X_1}{\sqrt{\omega(X_1, Y_2)}}, \quad \tilde{Y}_1 = \frac{Y_1}{\sqrt{\omega(X_1, Y_1)}} = i\tilde{X}_1,$$

$$\tilde{X}_2 = X_2, \quad\quad\quad \tilde{Y}_2 = Y_2 - \frac{\omega(X_1, Y_2)Y_1 - \omega(Y_1, Y_2)X_1}{\omega(X_1, Y_1)}$$

$$= Y_2 - \frac{n-1}{2} w_0^{n+1} w(X_1, Y_1) X_1.$$

This is a standard basis for the symplectic vector space ξ^ω; i.e., the form ω in this basis is given by

$$\begin{pmatrix} \begin{pmatrix} 0 & 1 \\ 1 & 0 \end{pmatrix} & \\ & \begin{pmatrix} 0 & 1 \\ 1 & 0 \end{pmatrix} \end{pmatrix}. \qquad \square$$

Now we are ready to prove the Conley–Zehnder index formula in Theorem 1.1.

Proposition 3.7. *The Conley–Zehnder index for $\gamma = \gamma_\pm^N$ in $0 \le t \le N\pi/(1 \pm \epsilon)$ is*

$$\mu_{CZ}(\gamma_\pm^N) = 2\left(\left\lfloor \frac{2N}{(n+1)(1\pm\epsilon)} \right\rfloor + \left\lfloor \frac{N(1\mp\epsilon)}{1\pm\epsilon} \right\rfloor - \left\lfloor \frac{2N}{1\pm\epsilon} \right\rfloor\right) + 2N + 1. \quad (3\text{-}6)$$

Proof. The Reeb flow φ which we introduced in the previous section can be extended to a flow on $\mathbb{C}^3$, which we also denote by φ. The action of the extended Reeb flow on $\mathbb{C}^3$ is given by

$$d\varphi_t(w)\tilde{X}_1 = e^{4it}\tilde{X}_1(\varphi_t(w)), \quad d\varphi_t(w)\tilde{Y}_1 = e^{4it}\tilde{Y}_1(\varphi_t(w)),$$
$$d\varphi_t(w)\tilde{X}_2 = \tilde{X}_2(\varphi_t(w)), \quad d\varphi_t(w)\tilde{Y}_2 = \tilde{Y}_2(\varphi_t(w)).$$

Define

$$\Phi := d\varphi_t|_{\mathbb{C}^3} = \operatorname{diag}(e^{4i/(n+1)t}, e^{2i(1+\epsilon)t}, e^{2i(1-\epsilon)t}).$$

We can now use the additivity of the Conley–Zehnder index under direct sums of symplectic paths, Theorem 2.13(4) to get

$$\mu_{CZ}(\gamma_\pm) = \mu_{CZ}(\Phi) - \mu_{CZ}(\Phi_{\xi^\omega}),$$

where

$$\Phi_{\xi^\omega} := d\varphi_t|_{\xi^\omega} = \operatorname{diag}(e^{4it}, 1). \quad (3\text{-}7)$$

The right-hand side of (3-7) is easily computed via the crossing form; see [Robbin and Salamon 1993, Remark 5.4]. In particular we have

$$\mu_{CZ}\left(\{e^{it}\}|_{t\in[0,T]}\right) = \begin{cases} T/\pi, & T \in 2\pi\mathbb{Z}, \\ 2\lfloor T/2\pi \rfloor + 1, & \text{otherwise.} \end{cases}$$

Thus for $\{\Phi(t)\} = \{e^{4it/(n+1)} \oplus e^{2it(1+\epsilon)} \oplus e^{2it(1-\epsilon)}\}$ with $0 \le t \le T$ we obtain

$$\mu_{CZ}(\Phi) = \begin{cases} 4T/((n+1)\pi), & T \in \frac{1}{2}(n+1)\pi\mathbb{Z}, \\ 2\lfloor 2T/((n+1)\pi) \rfloor + 1, & T \notin \frac{1}{2}(n+1)\pi\mathbb{Z}, \end{cases}$$
$$+ \begin{cases} 2T(1+\epsilon)/\pi, & T \in \pi/(1+\epsilon)\mathbb{Z}, \\ 2\lfloor T(1+\epsilon)/\pi \rfloor + 1, & T \notin \pi/(1+\epsilon)\mathbb{Z}, \end{cases}$$
$$+ \begin{cases} 2T(1-\epsilon)/\pi, & T \in \pi/(1-\epsilon)\mathbb{Z}, \\ 2\lfloor T(1-\epsilon)/\pi \rfloor + 1, & T \notin \pi/(1-\epsilon)\mathbb{Z}. \end{cases}$$

Likewise for Φ_{ξ^ω} with $0 \le t \le T$ we obtain

$$\mu_{CZ}(\Phi_{\xi^\omega}) = \begin{cases} 4T/\pi, & T \in \pi/2\mathbb{Z}, \\ 2\lfloor 2T/\pi \rfloor + 1, & T \notin \pi/2\mathbb{Z}. \end{cases}$$

Hence we get that the Conley–Zehnder index for $\gamma_\pm^N$ in $0 \le t \le N\pi/(1\pm\epsilon)$ is given by

$$\mu_{CZ}(\gamma_\pm^N) = 2\left(\left\lfloor \frac{2N}{(n+1)(1\pm\epsilon)} \right\rfloor + \left\lfloor \frac{N(1\mp\epsilon)}{1\pm\epsilon} \right\rfloor - \left\lfloor \frac{2N}{1\pm\epsilon} \right\rfloor\right) + 2N + 1. \quad (3\text{-}8)$$

This completes the proof.   □

4. Proof of Theorem 1.8

This section proves that (L_{A_n}, ξ_0) and $(L(n+1, n), \xi_{\text{std}})$ are contactomorphic. This is done by constructing a 1-parameter family of contact manifolds via a canonically defined Liouville vector field and applying Gray's stability theorem.

4A. Contact geometry of $(L(n+1, n), \xi_{\text{std}})$. The lens space $L(n+1, n)$ is obtained via the quotient of S^3 by the binary cyclic subgroup $A_n \subset \text{SL}(2, \mathbb{C})$. The subgroup A_n is given by the action of $\mathbb{Z}_{n+1}$ on $\mathbb{C}^2$ defined by

$$\begin{pmatrix} u \\ v \end{pmatrix} \mapsto \begin{pmatrix} e^{2\pi i/(n+1)} & 0 \\ 0 & e^{2n\pi i/(n+1)} \end{pmatrix} \begin{pmatrix} u \\ v \end{pmatrix}.$$

The following exercise shows that $L(n+1, n)$ is homeomorphic to L_{A_n}. This construction will be needed later in another proof, so we explain it here to set up the notation.

The origin is the only fixed point of the A_n action on $\mathbb{C}^2$ and hence is an isolated quotient singularity of $\mathbb{C}^2/A_n$. We can represent $\mathbb{C}^2/A_n$ as a hypersurface of $\mathbb{C}^3$ as follows. Consider the monomials

$$z_0 := uv, \quad z_1 := \tfrac{1}{\sqrt{2}} i u^{n+1}, \quad z_2 := \tfrac{1}{\sqrt{2}} i v^{n+1}.$$

These are invariant under the action of A_n and satisfy the equation $z_0^{n+1} + 2z_1 z_2 = 0$. Recall that

$$f_{A_n}(z_0, z_1, z_2) = z_0^{n+1} + 2z_1 z_2 \quad \text{and} \quad L_{A_n} = S^5 \cap \{f_{A_n}^{-1}(0)\}.$$

Moreover,

$$\begin{aligned} \tilde{\varphi} : \mathbb{C}^2 &\to \mathbb{C}^3, \\ (u, v) &\mapsto (uv, \tfrac{1}{\sqrt{2}} i u^{n+1}, \tfrac{1}{\sqrt{2}} i v^{n+1}), \end{aligned} \tag{4-1}$$

descends to the map

$$\varphi : \mathbb{C}^2/A_n \to \mathbb{C}^3,$$

which sends $\varphi(\mathbb{C}^2/A_n)$ homeomorphically onto the hypersurface $f_{A_n}^{-1}(0)$.

Rescaling away from the origin of $\mathbb{C}^3$ yields a homeomorphism between $\varphi(S^3/A_n)$ and L_{A_n}. As 3-manifolds which are homeomorphic are also diffeomorphic [Moise 1952], we obtain the following proposition.

Proposition 4.1. $L(n+1, n)$ is diffeomorphic to L_{A_n}.

Remark 4.2. In order to prove that two manifolds are contactomorphic, one must either construct an explicit diffeomorphism or make use of Gray's stability theorem. Sadly, φ is not a diffeomorphism onto its image when $u = 0$ or $v = 0$. As the above

diffeomorphism is only known to exist abstractly, we will need to appeal the latter method to prove that (L_{A_n}, ξ_0) and $(L(n+1, n), \xi_{std})$ are contactomorphic. As a result, this proof is rather involved.

Our application of Gray's stability theorem uses the flow of a Liouville vector field to construct a 1-parameter family of contactomorphisms. First we prove that $L(n+1, n)$ is a contact manifold whose contact structure descends from the quotient of S^3.

Consider the standard symplectic form on $\mathbb{C}^2$ given by

$$\begin{aligned} \omega_{\mathbb{C}^2} &= d\lambda_{\mathbb{C}^2}, \\ \lambda_{\mathbb{C}^2} &= \tfrac{1}{2}i(u d\bar{u} - \bar{u} du + v d\bar{v} - \bar{v} dv). \end{aligned} \tag{4-2}$$

The following proposition shows that λ_0 restricts to a contact form on $L(n+1, n)$. We define $\ker \lambda = \xi_{std}$ on $L(n+1, n)$.

Proposition 4.3. *The vector field*

$$Y_0 = \frac{1}{2}\left(u\frac{\partial}{\partial u} + \bar{u}\frac{\partial}{\partial \bar{u}} + v\frac{\partial}{\partial v} + \bar{v}\frac{\partial}{\partial \bar{v}}\right)$$

is a Liouville vector field on $(\mathbb{C}^2/A_n, \omega_{\mathbb{C}^2})$ away from the origin and transverse to $L(n+1, n)$.

Proof. We have that $\mathbb{C}^2/A_n$ is a smooth manifold away from the origin because 0 is the only fixed point by the action of A_n. Write

$$S^3/A_n = \{(u, v) \in \mathbb{C}^2/A_n : |u|^2 + |v|^2 = 1\}.$$

Then $L(n+1, n) = S^3/A_n$ is a regular level set of $g(u, v) = |u|^2 + |v|^2$ Choose a Riemannian metric on $\mathbb{C}^2/A_n$ and note that

$$Y_0 = \tfrac{1}{4}\nabla g.$$

Thus Y_0 is transverse to $L(n+1, n)$. Since

$$\mathcal{L}_{Y_0}\omega_{\mathbb{C}^2} = d(i_{Y_0}d\lambda_{\mathbb{C}^2}) = \omega_{\mathbb{C}^2},$$

we may conclude that Y_0 is indeed a Liouville vector field on $(\mathbb{C}^2/A_n, \omega_{\mathbb{C}^2})$ away from the origin. Thus by Proposition 2.10, $L(n+1, n)$ is a hypersurface of contact type in $\mathbb{C}^2/A_n$. $\square$

4B. *The proof that (L_{A_n}, ξ_0) and $(L(n+1, n), \xi_{std})$ are contactomorphic.* First we set up L_{A_n} and $\varphi(L(n+1, n))$ as hypersurfaces of contact type in $\{f_{A_n}^{-1}(0)\} \setminus \{0\}$. Define $\rho : \mathbb{C}^3 \to \mathbb{R}$ by

$$\rho(z) = \tfrac{1}{4}|z|^2 - 1 = \tfrac{1}{4}z_0\bar{z}_0 + \cdots + z_2\bar{z}_2 - 1.$$

The standard symplectic structure on $\mathbb{C}^3$ is given by

$$\omega_{\mathbb{C}^3} = \tfrac{1}{2}i(dz_0 \wedge d\bar{z}_0 + \cdots + dz_2 \wedge d\bar{z}_2).$$

Moreover,

$$Y = \nabla\rho = \frac{1}{2}\sum_{j=0}^{2} z_j \frac{\partial}{\partial z_j} + \bar{z}_j \frac{\partial}{\partial \bar{z}_j} \tag{4-3}$$

is a Liouville vector field for $(\mathbb{C}^3, \omega_{\mathbb{C}^3})$. We define

$$\lambda_{\mathbb{C}^3} = \iota_Y \omega_{\mathbb{C}^3}.$$

A standard calculation analogous to the proof of Proposition 4.3 shows that Y is a Liouville vector field on $(\{f_{A_n}^{-1}(0)\} \setminus \{0\}, \omega_{\mathbb{C}^3})$.

Remark 4.4. Both $\varphi(L(n+1,n))$ and L_{A_n} are hypersurfaces of contact type in $(\{f_{A_n}^{-1}(0)\} \setminus \{0\}, \omega_{\mathbb{C}^3})$. Note that $\varphi(L(n+1,n))$ is in fact transverse to the Liouville vector field Y because

$$\varphi(L(n+1,n)) = \varphi(\{|u|^2 + |v|^2 = 1\}/A_n)$$
$$= \varphi(\{|u|^4 + 2|u|^2|v|^2 + |v|^4 = 1\}/A_n)$$
$$= \{2|z_0|^2 + 4^{1/(n+1)}|z_1|^{4/(n+1)} + 4^{1/(n+1)}|z_2|^{4/(n+1)} = 1\} \cap f_{A_n}^{-1}(0).$$

We will want $\varphi(L(n+1,n))$ and L_{A_n} to be disjoint in $\{f_{A_n}^{-1}(0)\}$. This is easily accomplished by rescaling r in the definition of the link.

Definition 4.5. Define

$$L_{A_n}^r = f_{A_n}^{-1}(0) \cap S_r^5,$$

with the assumption that r has been chosen so that $\varphi(L(n+1,n))$ and $L_{A_n}^r$ are disjoint in $\{f_{A_n}^{-1}(0)\}$ and so that the flow of the Liouville vector field Y "hits" $\varphi(L(n+1,n))$ before $L_{A_n}^r$.

The first result is the following lemma, which provides a 1-parameter family of diffeomorphic manifolds starting on $\varphi(L(n+1,n))$ and ending on $L_{A_n}^r$. First we set up some notation. Let

$$\psi_t : \mathbb{R} \times X \to X$$

be the flow of Y and $\psi_t(z) = \gamma_z(t)$ the unique integral curve passing through $z \in \varphi(L(n+1,n))$ at time $t = 0$. For any integral curve γ of Y we consider the initial value problem

$$\gamma'(t) = Y(\gamma(t)) \quad \text{and} \quad \gamma(0) = z \in \varphi(L(n+1,n)). \tag{4-4}$$

By means of the implicit function theorem and the properties of the Liouville vector field Y we can prove the following claim.

Lemma 4.6. *For every γ_z, there exists a $\tau(z) \in \mathbb{R}_{>0}$ such that $\gamma_z(\tau(z)) \in L^r_{A_n}$. The choice of $\tau(z)$ varies smoothly for each $z \in \varphi(L(n+1, n))$.*

Proof. In order to apply the implicit function theorem, we must show for all (t, z) with $\rho \circ \gamma = 0$ that

$$\frac{\partial(\rho \circ \gamma)}{\partial t} \neq 0.$$

Note that $\rho \circ \gamma$ is smooth. By the chain rule,

$$\frac{\partial(\rho \circ \gamma)}{\partial t}\bigg|_{(s,p)} = \operatorname{grad} \rho|_{\gamma(s,p)} \cdot \dot{\gamma}|_{(s,p)},$$

where $\dot{\gamma}|_{(s,p)} = \partial \gamma / \partial t|_{(s,p)}$.

If $\operatorname{grad} \rho|_{\gamma(s,p)} \cdot \dot{\gamma}|_{(s,p)} = 0$, then $\operatorname{grad} \rho$ is not transverse along $\{(\rho \circ \gamma)(s, p) = 0\}$ or $\dot{\gamma}|_{(s,p)} = 0$, since $\operatorname{grad} \rho \neq 0$. By construction, $\operatorname{grad} \rho = \nabla \rho$ is a Liouville vector field transverse to $L^r_{A_n}$. Furthermore, the conformal symplectic nature of a Liouville vector field implies that for any integral curve γ satisfying the initial value problem given by (4-4), $\dot{\gamma}|_{(s,p)} \neq 0$. Thus we see that the conditions for the implicit function theorem are satisfied and our claim is proven. $\square$

Remark 4.7. The time $\tau(z)$ can be normalized to 1 for each z, yielding a 1-parameter family of diffeomorphic contact manifolds (M_t, ζ_t) for $0 \leq t \leq 1$ given by

$$M_t = \psi_t\big(\varphi(L(n+1, n))\big), \quad \zeta_t = TM_t \cap J_{\mathbb{C}^3}(TM_t),$$

where

$$M_0 = \psi_0\big(\varphi(L(n+1, n))\big) = \varphi(L(n+1, n)), \quad M_1 = \psi_1\big(\varphi(L(n+1, n))\big) = L_{A_n}.$$

Moreover, we can relate the standard contact structure on $L(n+1, n)$ under the image of φ. To avoid excessive parentheses, we use S^3/A_n in place of $L(n+1, n)$ in this lemma.

Lemma 4.8. *On $\varphi(S^3/A_n)$,*

$$\varphi_*(\xi_{\mathrm{std}}) = T(\varphi(S^3/A_n)) \cap J_{\mathbb{C}^3}\big(T(\varphi(S^3/A_n))\big).$$

Proof. Since $A_n \subset \mathrm{SL}(2, \mathbb{C})$, we have

$$\tilde{\varphi}(J_{\mathbb{C}^2} TS^3) = J_{\mathbb{C}^3}(T\tilde{\varphi}(S^3)).$$

Examining $\varphi_*(\xi_{\mathrm{std}})$ yields

$$\begin{aligned}
\varphi_*(T(S^3/A_n) \cap J_{\mathbb{C}^2} T(S^3/A_n)) &= \tilde{\varphi}_*(TS^3 \cap J_{\mathbb{C}^2}(TS^3)) = \tilde{\varphi}_*(TS^3) \cap \tilde{\varphi}_*(J_{\mathbb{C}^2}(TS^3)) \\
&= \tilde{\varphi}_*(TS^3) \cap J_{\mathbb{C}^3}\tilde{\varphi}_*(TS^3) = T\tilde{\varphi}(S^3) \cap J_{\mathbb{C}^3}(T\tilde{\varphi}(S^3)) \\
&= T(\varphi(S^3/A_n)) \cap J_{\mathbb{C}^3}(T\varphi(S^3/A_n)). \qquad \square
\end{aligned}$$

Lemmas 4.6 and 4.8 in conjunction with Remark 4.7 and Lemma 2.11 yield the following proposition.

Proposition 4.9. *The image of the lens space* $(\varphi(L(n+1, n)), \varphi_* \xi_{\mathrm{std}})$ *is contactomorphic to* (L_{A_n}, ξ_0).

It remains to show that $(\varphi(L(n+1, n)), \varphi_* \xi_{\mathrm{std}})$ and $(L(n+1, n), \xi_{\mathrm{std}})$ are contactomorphic. To accomplish this, we use Moser's lemma to prove the following lemma.

Lemma 4.10. *The manifolds* $(\mathbb{C}^2 \setminus \{0\}, d\lambda_{\mathbb{C}^2})$ *and* $(\mathbb{C}^2 \setminus \{0\}, d\tilde{\varphi}^* \lambda_{\mathbb{C}^3})$ *are contactomorphic.*

Proof. Consider the family of 2-forms

$$\omega_t = (1-t)\omega_{\mathbb{C}^2} + t\tilde{\varphi}^* \omega_{\mathbb{C}^3}$$

for $0 \le t \le 1$. Then ω_t is exact because Y_0 and Y are Liouville vector fields for $\mathbb{C}^2 \setminus 0$ equipped with the symplectic forms $\omega_{\mathbb{C}^2}$ and $\omega_{\mathbb{C}^3}$ respectively; thus $d\lambda_t = \omega_t$ for

$$\lambda_t = (1-t)\lambda_{\mathbb{C}^2} + t\tilde{\varphi}^*(\lambda_{\mathbb{C}^3})$$

for $0 \le t \le 1$. We claim that λ_t is a family of contact forms for each $t \in [0, 1]$.

We compute

$$\frac{2}{i}\tilde{\varphi}^* d\lambda_{\mathbb{C}^3} = d(uv) \wedge d(\overline{uv}) + d(u^{n+1}) \wedge d(\bar{u}^{n+1}) + d(v^{n+1}) \wedge d(\bar{v}^{n+1})$$
$$= ((n+1)^2 |u|^{2n} + |v|^2) du \wedge d\bar{u} + 2\Re(u\bar{v} dv \wedge d\bar{u})$$
$$+ ((n+1)^2 |v|^{2n} + |u|^2) dv \wedge d\bar{v}.$$

Since ω_t is exact for each $t \in [0, 1]$, we know $d(\omega_t) = 0$ for each $t \in [0, 1]$. Moreover, a simple calculation reveals that $\omega_t \wedge \omega_t$ is a volume form on $\mathbb{C}^2$ for each $t \in [0, 1]$. Thus we may conclude that ω_t is a symplectic form for each $t \in [0, 1]$. Applying Moser's argument, Theorem 2.3, yields the desired result. $\square$

This yields the desired corollary.

Corollary 4.11. *The manifolds* $(L(n+1, n), \ker \lambda_{\mathbb{C}^2})$ *and* $(L(n+1, n), \ker \varphi^* \lambda_{\mathbb{C}^3})$ *are contactomorphic.*

Proof. Let $\phi : (\mathbb{C}^2 \setminus \{0\}, d\lambda_{\mathbb{C}^2})$ and $(\mathbb{C}^2 \setminus \{0\}, d\tilde{\varphi}^* \lambda_{\mathbb{C}^3})$ be the symplectomorphism, which exists by Lemma 4.10. It induces the desired contactomorphism. On $\mathbb{C}^2 \setminus \{0\}$,

$$\phi^* d(\varphi^* \lambda_{\mathbb{C}^3}) = d\lambda_{\mathbb{C}^2};$$

thus,

$$d\phi^*(\varphi^* \lambda_{\mathbb{C}^3}) = d\lambda_{\mathbb{C}^2}.$$

So on $L(n+1, n)$,

$$\phi_*(\xi_{\mathrm{std}}) = \phi_*(\ker \lambda_{\mathbb{C}^2}) = \ker \varphi_* \lambda_{\mathbb{C}^3} = \varphi_* \xi_{\mathrm{std}}.$$

Proposition 4.9 and Corollary 4.11 complete the proof of Theorem 1.8. □

Acknowledgements

References

[Bourgeois and Oancea 2012] F. Bourgeois and A. Oancea, "S^1-equivariant symplectic homology and linearized contact homology", preprint, 2012. To appear in *Int. Math. Res. Not.* arXiv

[Bourgeois and Oancea 2015] F. Bourgeois and A. Oancea, "Erratum to: An exact sequence for contact- and symplectic homology", *Invent. Math.* **200**:3 (2015), 1065–1076. MR Zbl

[Brieskorn 1966] E. Brieskorn, "Beispiele zur Differentialtopologie von Singularitäten", *Invent. Math.* **2** (1966), 1–14. MR Zbl

[Geiges 2008] H. Geiges, *An introduction to contact topology*, Cambridge Studies in Advanced Mathematics **109**, Cambridge University Press, 2008. MR Zbl

[Gutt 2014] J. Gutt, "Generalized Conley–Zehnder index", *Ann. Fac. Sci. Toulouse Math.* (6) **23**:4 (2014), 907–932. MR Zbl

[Gutt 2015] J. Gutt, "The positive equivariant symplectic homology as an invariant for some contact manifolds", preprint, 2015. arXiv

[Hutchings and Nelson 2014] M. Hutchings and J. Nelson, "Cylindrical contact homology for dynamically convex contact forms in three dimensions", preprint, 2014. To appear in *J. Symplectic Geom.* arXiv

[Hutchings and Nelson ≥ 2017] M. Hutchings and J. Nelson, "Invariance and an integral lift of cylindrical contact homology for dynamically convex contact forms", In preparation.

[Ito and Reid 1996] Y. Ito and M. Reid, "The McKay correspondence for finite subgroups of SL(3, ℂ)", pp. 221–240 in *Higher-dimensional complex varieties* (Trento, 1994), edited by M. Andreatta and T. Peternell, de Gruyter, Berlin, 1996. MR Zbl

[Keating 2015] A. Keating, "Homological mirror symmetry for hypersurface cusp singularities", preprint, 2015. arXiv

[Kwon and van Koert 2016] M. Kwon and O. van Koert, "Brieskorn manifolds in contact topology", *Bull. Lond. Math. Soc.* **48**:2 (2016), 173–241. MR Zbl

[McDuff and Salamon 1998] D. McDuff and D. Salamon, *Introduction to symplectic topology*, 2nd ed., Oxford University Press, 1998. MR Zbl

[McLean 2016] M. McLean, "Reeb orbits and the minimal discrepancy of an isolated singularity", *Invent. Math.* **204**:2 (2016), 505–594. MR Zbl

[McLean and Ritter ≥ 2017] M. McLean and A. Ritter, "The cohomological McKay correspondence and symplectic homology", In preparation.

[Milnor 1968] J. Milnor, *Singular points of complex hypersurfaces*, Annals of Mathematics Studies **61**, Princeton University Press, 1968. MR Zbl

[Moise 1952] E. E. Moise, "Affine structures in 3-manifolds, V: The triangulation theorem and Hauptvermutung", *Ann. Math.* **56**:2 (1952), 96–114. MR Zbl

[Nelson 2015] J. Nelson, "Automatic transversality in contact homology, I: Regularity", *Abh. Math. Semin. Univ. Hambg.* **85**:2 (2015), 125–179. MR Zbl

[Nelson ≥ 2017] J. Nelson, "Automatic transversality in contact homology, II: Invariance and computations", In preparation.

[Ritter 2010] A. F. Ritter, "Deformations of symplectic cohomology and exact Lagrangians in ALE spaces", *Geom. Funct. Anal.* **20**:3 (2010), 779–816. MR Zbl

[Robbin and Salamon 1993] J. Robbin and D. Salamon, "The Maslov index for paths", *Topology* **32**:4 (1993), 827–844. MR Zbl

[Seidel 2008a] P. Seidel, "A biased view of symplectic cohomology", pp. 211–253 in *Current developments in mathematics, 2006*, edited by B. Mazur et al., Int. Press, Somerville, MA, 2008. MR Zbl

[Seidel 2008b] P. Seidel, *Fukaya categories and Picard–Lefschetz theory*, European Mathematical Society, Zürich, 2008. MR Zbl

[Ustilovsky 1999] I. Ustilovsky, "Infinitely many contact structures on S^{4m+1}", *Internat. Math. Res. Notices* **14** (1999), 781–791. MR Zbl

leonardo@math.msu.edu   *Department of Mathematics, Michigan State University, 1016 Chester Rd., Apt. B14, Lansing, MI 48912, United States*

ih2271@columbia.edu   *Department of Mathematics, Columbia University, 2920 Broadway, 6580 Lerner Hall, New York, NY 10027, United States*

nelson@math.columbia.edu   *Institute for Advanced Study, Columbia University, 2990 Broadway, Room 509, MC 4403, New York, NY 10027, United States*

njs2155@columbia.edu   *Department of Mathematics, Columbia University, 2920 Broadway, 6580 Lerner Hall, New York, NY 10027, United States*

msp

The vibration spectrum of
two Euler–Bernoulli beams
coupled via a dissipative joint

Chris Abriola, Matthew P. Coleman, Aglika Darakchieva and Tyler Wales

(Communicated by Kenneth S. Berenhaut)

The asymptotic estimation of the vibration spectrum for a system of two identical Euler–Bernoulli beams coupled via each of the four standard types of linear dissipative joint has been solved for the case when one beam is clamped and the other beam is free at the outer ends. Here, we generalize those results and solve the problem for all 40 combinations of energy-conserving end conditions. We provide both asymptotic and numerical results, and we compare the various systems with an eye toward determining which configurations lead to asymptotically equivalent vibration spectra.

1. Introduction

The design of large or complex structures — bridges, airplanes, robots, buildings, machinery, etc. — entails the joining or coupling of smaller, simpler components, which often can be modeled as beams, plates, or shells. These couplings may include active or passive damping mechanisms for the damping of unwanted vibrations. Successful design requires a knowledge of the system's vibration spectrum, i.e., the set of its natural frequencies of vibration.

There are four standard linear models for describing the vibration of beams — the Euler–Bernoulli, Rayleigh, shear, and Timoshenko beams. Of these, the Euler–Bernoulli is the simplest, with each of the others incorporating one or more physical effects neglected by the Euler–Bernoulli model. Despite the better accuracy of these latter models, the Euler–Bernoulli is accurate enough to be the model of choice for a multitude of physical applications. In addition, the most commonly utilized models for plates and shells are those based on the same assumptions as those governing the Euler–Bernoulli beam. Indeed, given its simplicity and applicability, the Euler-Bernoulli beam may be thought of as the most universal element in structural dynamics.

In this paper, we consider the vibration of a system consisting of two identical Euler–Bernoulli beams, coupled end to end by each of four standard types of dissipative joint, and satisfying any of the standard energy-conserving boundary conditions at each end. Our intent is to estimate and classify the vibration spectrum for all 40 possible configurations (four joint conditions and ten sets of end conditions.)

The problem of serially connected Euler–Bernoulli beams seems first to have been treated in [Chen et al. 1987], while the specific problem here was solved in [Chen et al. 1989] for the case involving a so-called type I joint with clamped-free end conditions. The authors employ an asymptotic method in order to compute the spectrum analytically, and provide numerical results for comparison. In addition, they provide physical models for the four joint types (three being special cases, involving only some of the *damping parameters*), and present some early experimental results. In [Chen et al. 1988], the authors provide more experimental results and, after smoothing this data, show good agreement with the results from [Chen et al. 1989].

Krantz and Paulsen [1991] generalize to a great extent the asymptotic results in [Chen et al. 1989]. They again treat the case with clamped-free end conditions, but they consider all four types of joints. In addition, they allow for an arbitrary number of beams of arbitrary length! Finally, in [Chen and Zhou 1990], an alternate solution of the problem in [Chen et al. 1989] is provided, using the elegant asymptotic *wave propagation method* (WPM) of Keller and Rubinow [1960].

In this paper, we consider the case of two identical Euler–Bernoulli beams subject to any of the four types of joint conditions, as given in [Chen et al. 1989], and we generalize by considering all possible combinations of energy-conserving end conditions. We employ WPM in order to derive analytic/asymptotic results, and the Legendre–Tau spectral method for numerical comparisons. These are the first numerical results that we know of for Euler–Bernoulli systems with types II, III and IV joints, and the first asymptotic results for systems without clamped-free end conditions. The asymptotic results allow us easily to compare the vibration spectra for all 40 configurations, permitting us to categorize them, in order to see which configurations may be equivalent insofar as they lead to identical vibration spectra.

This paper is organized as follows: In Section 2, we present the problem and, in Section 3, it is recast in dimensionless form; WPM is applied and the asymptotic results are presented in Section 4, with a brief discussion of the results in Section 5. In Section 6, the numerical results and comparisons are presented.

2. The problem

As mentioned, we consider the problem of two identical Euler–Bernoulli beams, connected by any of the four standard dissipative joints, as presented in [Chen et al. 1989]. We have, then, an Euler–Bernoulli beam equation satisfied along each beam:

$$mw_{1tt} + EIw_{1xxxx} = 0, \quad -L < x < 0, \ t > 0,$$
$$mw_{2tt} + EIw_{2xxxx} = 0, \quad 0 < x < L, \ t > 0.$$

Here, $w_j(x, t)$, $j = 1, 2$, is the transverse displacement along beam j, E is the constant Young's modulus, I is the constant (vertical) moment of inertia, and m is the constant linear mass density.

In addition, we have the joint conditions:

Type I:
$$M_2(0, t) = M_1(0, t),$$
$$V_2(0, t) = V_1(0, t),$$
$$w_{2t}(0, t) - w_{1t}(0, t) = k_1^2 V_1(0, t) + c_1 M_1(0, t),$$
$$w_{2xt}(0, t) - w_{1xt}(0, t) = c_2 V_1(0, t) - k_2^2 M_1(0, t);$$

Type II:
$$w_2(0, t) = w_1(0, t),$$
$$M_2(0, t) = M_1(0, t),$$
$$V_2(0, t) - V_1(0, t) = k_1^2 w_{1x}(0, t) + c_1 M_1(0, t),$$
$$w_{2xt}(0, t) - w_{1xt}(0, t) = c_2 w_{1t}(0, t) - k_2^2 M_1(0, t);$$

Type III:
$$w_2(0, t) = w_1(0, t),$$
$$w_{2x}(0, t) = w_{1x}(0, t),$$
$$V_2(0, t) - V_1(0, t) = k_1^2 w_{1t}(0, t) + c_1 w_{1xt}(0, t),$$
$$M_2(0, t) - M_1(0, t) = c_2 w_{1t}(0, t) - k_2^2 w_{1xt}(0, t);$$

Type IV:
$$w_{2x}(0, t) = w_{1x}(0, t),$$
$$V_2(0, t) = V_1(0, t),$$
$$w_{2t}(0, t) - w_{1t}(0, t) = k_1^2 V_1(0, t) + c_1 w_{1xt}(0, t),$$
$$M_2(0, t) - M_1(0, t) = c_2 V_1(0, t) - k_2^2 w_{1xt}(0, t);$$

where $M_j(x, t)$ is the bending moment, and $V_j(x, t)$ the shear force, along beam j. The *damping constants* k_1^2, k_2^2, c_1 and c_2 ensure dissipation of energy so long as

$$k_1^2 + k_2^2 > 0 \quad \text{and} \quad k_1^2\alpha^2 + k_2^2\beta^2 + (c_1 - c_2)\alpha\beta > 0 \quad \forall \alpha, \beta \in \mathbb{R}$$

[Chen and Zhou 1990]. For the sake of convenience, we assume throughout the paper that $k_1 \neq 0$ (corresponding to "type a" joints in [Krantz and Paulsen 1991]) and that $k_1^2 k_2^2 + c_1 c_2 > 0$. (It is easy to show that $k_1^2 k_2^2 + c_1 c_2 \geq 0$, with equality if and only if $c_1 = -c_2 = \pm k_1 k_2$.)

Finally, at the left end of the first beam, we have one of the energy-conserving boundary conditions

$$\text{clamped (C):} \quad w_1(-L, t) = w_{1x}(-L, t) = 0,$$
$$\text{simply supported (S):} \quad w_1(-L, t) = w_{1xx}(-L, t) = 0,$$
$$\text{roller supported (R):} \quad w_{1x}(-L, t) = w_{1xxx}(-L, t) = 0,$$
$$\text{free (F):} \quad w_{1xx}(-L, t) = w_{1xxx}(-L, t) = 0,$$

and similarly at the right end of the second beam. Thus, we have the following ten combinations of boundary conditions to consider:

$$\text{C-C,} \quad \text{C-S,} \quad \text{C-R,} \quad \text{C-F,} \quad \text{S-S,} \quad \text{S-R,} \quad \text{S-F,} \quad \text{R-R,} \quad \text{R-F,} \quad \text{F-F.}$$

We note here that, in order for a *joint* to exist, at least one of the variables w (or w_t), w_x (or w_{xt}), M or V must be discontinuous. In addition, at most one of each pair of *conjugate variables* (w and V, w_x and M) can be discontinuous. Thus, types I–IV do, indeed, represent the most general situation for linear joints [Pilkey 1969].

3. Dimensionless form

We first separate variables,

$$w_j(x, t) = e^{-i\xi^2 t} v_j(x), \quad j = 1, 2,$$

and introduce the new variables

$$y = \frac{x}{L}, \quad u_j(y) = \frac{v_j(x)}{L}, \quad j = 1, 2.$$

Also, in order to apply WPM, we let $y \to -y$ along the second beam, as it is convenient to have both beams on the same y-interval. The resulting dimensionless ODEs are

$$u_j^{(4)}(y) - k^4 u_j(y) = 0, \quad -1 < y < 0, \ j = 1, 2, \tag{1}$$

where

$$k^2 = \sqrt{\frac{m}{EI}} L^2 \xi^2.$$

The new joint conditions are:

Type I:

$$u_2''(0) - u_1''(0) = 0,$$
$$u_2'''(0) + u_1'''(0) = 0,$$
$$ik^2[u_2(0) - u_1(0)] - p_{11} u_1'''(0) - q_{11} u_1''(0) = 0,$$
$$ik^2[u_2'(0) + u_2'(0)] - p_{12} u_1''(0) + q_{12} u_1'''(0) = 0;$$

Type II:
$$u_2(0) - u_1(0) = 0,$$
$$u_2''(0) - u_1''(0) = 0,$$
$$u_2'''(0) + u_1'''(0) + ik^2 p_{21} u_1(0) + q_{21} u_1''(0) = 0,$$
$$ik^2[u_2'(0) + u_1'(0)] - p_{22} u_1'''(0) + ik^2 q_{22} u_1(0) = 0;$$

Type III:
$$u_2(0) - u_1(0) = 0,$$
$$u_2'(0) + u_1'(0) = 0,$$
$$u_2''(0) - u_1''(0) + ik^2 p_{31} u_1'(0) - ik^2 q_{31} u_1(0) = 0,$$
$$u_2'''(0) + u_1'''(0) + ik^2 p_{32} u_1(0) + ik^2 q_{32} u_1'(0) = 0;$$

Type IV:
$$u_2'(0) + u_1'(0) = 0,$$
$$u_2'''(0) + u_1'''(0) = 0,$$
$$ik^2[u_2(0) - u_1(0)] - p_{41} u_1'''(0) - ik^2 q_{41} u_1'(0) = 0,$$
$$u_2''(0) - u_1''(0) + ik^2 p_{42} u_1'(0) - q_{42} u_1(0) = 0.$$

Here, the constants p_{ij} and q_{ij}, where $i = 1, 2, 3, 4$, $j = 1, 2$, are given by:

Type I:
$$p_{11} = \frac{k_1^2 \sqrt{mEI}}{L}, \quad p_{12} = k_2^2 L \sqrt{mEI}, \quad q_{11} = c_1 \sqrt{mEI}, \quad q_{12} = c_2 \sqrt{mEI};$$

Type II:
$$p_{21} = \frac{k_1^2 L}{\sqrt{mEI}}, \quad p_{22} = k_2^2 L \sqrt{mEI}, \quad q_{21} = c_1 L, \quad q_{22} = c_2 L;$$

Type III:
$$p_{31} = \frac{k_1^2}{L\sqrt{mEI}}, \quad p_{32} = \frac{k_2^2 L}{\sqrt{mEI}}, \quad q_{31} = \frac{c_1}{\sqrt{mEI}}, \quad q_{32} = \frac{c_2}{\sqrt{mEI}};$$

Type IV:
$$p_{41} = \frac{k_1^2 \sqrt{mEI}}{L}, \quad p_{42} = \frac{k_2^2}{L\sqrt{mEI}}, \quad q_{41} = \frac{c_1}{L}, \quad q_{42} = \frac{c_2}{L}.$$

Note that $k_1^2 \alpha^2 + k_2^2 \beta^2 + (c_1 - c_2)\alpha\beta \geq 0$ if and only if

$$p_{j1}\alpha^2 + p_{j2}\beta^2 + (q_{j1} - q_{j2})\alpha\beta \geq 0, \quad j = 1, 2, 3, 4.$$

For $j = 1, 2$, the new boundary conditions are

$$\text{C: } u_j(-1) = u_j'(-1) = 0,$$

$$\text{S: } u_j(-1) = u_j''(-1) = 0,$$

$$\text{R: } u_j'(-1) = u_j'''(-1) = 0,$$

$$\text{F: } u_j''(-1) = u_j'''(-1) = 0.$$

4. Asymptotic estimation of vibration frequencies by WPM

Applying WPM to the problem is identical to writing the general solutions of the ODEs (1) as

$$u(x) = \begin{bmatrix} u_1(x) \\ u_2(x) \end{bmatrix} = \begin{bmatrix} A_1 \\ A_2 \end{bmatrix} e^{ikx} + \begin{bmatrix} B_1 \\ B_2 \end{bmatrix} e^{-ikx} + \begin{bmatrix} C_1 \\ C_2 \end{bmatrix} e^{kx} + \begin{bmatrix} D_1 \\ D_2 \end{bmatrix} e^{-k(x+1)}$$

$$= \begin{bmatrix} A_3 \\ A_4 \end{bmatrix} e^{ik(x+1)} + \begin{bmatrix} B_3 \\ B_4 \end{bmatrix} e^{-ik(x+1)} + \begin{bmatrix} C_1 \\ C_2 \end{bmatrix} e^{kx} + \begin{bmatrix} D_1 \\ D_2 \end{bmatrix} e^{-k(x+1)}, \quad (2)$$

applying the joint conditions to the first expression in (2) and the boundary conditions to the second expression in (2). Here, we follow Chen and Zhou [1990] and stipulate that $\mathrm{Re}(k) \geq 0$ (else, we just replace k by $-k$). Applying the boundary conditions, neglecting the terms of $\mathbb{O}(e^{-k})$, and eliminating D_1 and D_2 leads to

$$\begin{bmatrix} A_3 \\ A_4 \end{bmatrix} = \begin{bmatrix} a & 0 \\ 0 & b \end{bmatrix} \begin{bmatrix} B_3 \\ B_4 \end{bmatrix} = R_2 \begin{bmatrix} B_3 \\ B_4 \end{bmatrix}. \quad (3)$$

Here, a and b depend on the boundary conditions, as follows:

$$a = b = i : \text{C-C, C-F, F-F,}$$

$$a = b = 1 : \text{R-R,} \quad a = b = -1 : \text{S-S,} \quad a = -1, b = 1 : \text{S-R,}$$

$$a = i, b = 1 : \text{C-R,} \quad a = i, b = -1 : \text{C-S,} \quad a = 1, b = i : \text{R-F,} \quad a = -1, b = i : \text{S-F,}$$

where, e.g., C-F signifies that the first beam is clamped at the left end and the second beam is free at the right end.

Next, we apply the joint conditions, again neglecting terms of $\mathbb{O}(e^{-k})$, and eliminate C_1 and C_2. The result is a relationship of the form

$$M_1(k) \begin{bmatrix} B_1 \\ B_2 \end{bmatrix} = M_2(k) \begin{bmatrix} A_1 \\ A_2 \end{bmatrix}, \quad (4)$$

where each matrix M_j is 2×2. Solving for $\begin{bmatrix} B_1 \\ B_2 \end{bmatrix}$, we have

$$\begin{bmatrix} B_1 \\ B_2 \end{bmatrix} = M_1^{-1}(k) M_2(k) \begin{bmatrix} A_1 \\ A_2 \end{bmatrix} = R_1(k) \begin{bmatrix} A_1 \\ A_2 \end{bmatrix}, \quad (5)$$

for which we find it more convenient to write

$$\begin{bmatrix} B_1 \\ B_2 \end{bmatrix} = \frac{1}{\det M_1(k)} R_1'(k) \begin{bmatrix} A_1 \\ A_2 \end{bmatrix}. \tag{6}$$

For the sake of completeness, we provide R_1' and $\det M_1$ for each of the four joints:

Type I:

$$\det M_1 = 2(1+i)p_{11}k^2 + i(p_{11}p_{12} + q_{11}q_{12} + 8)k + 2(-1+i)p_{12} = t_{11},$$

$$R_1' = \begin{bmatrix} u+v & w+z \\ w-z & u-v \end{bmatrix} = T_{11},$$

where

$$u = 2ip_{11}k^2 - (p_{11}p_{12} + q_{11}q_{12})k - 2ip_{12}, \quad v = 2(q_{11} - q_{12})k,$$
$$w = 2p_{11}k^2 + 8ik - 2p_{12}, \qquad\qquad\qquad z = 2(q_{11} + q_{12})k.$$

Type II:

$$\det M_1 = 8ik^2 + 2(-1+i)(p_{21} + p_{22} + q_{21} + q_{22})k - 2(p_{21}p_{22} + q_{21}q_{22}),$$

$$R_1' = \begin{bmatrix} -v & 2u \\ 2u & -v \end{bmatrix},$$

where

$$u = 4ik^2 + [-(p_{21} + p_{22}) + i(q_{21} + q_{22})]k,$$
$$v = 2[i(p_{21} + p_{22}) - (q_{21} + q_{22})]k - 2(p_{21}p_{22} + q_{21}q_{22}).$$

Type III:

$$\det M_1 = 2(1+i)p_{31}k^2 + i(p_{31}p_{32} + q_{31}q_{32})k + 2(-1+i)p_{32} = t_{31},$$

$$R_1' = \begin{bmatrix} u+v & w-z \\ w+z & u-v \end{bmatrix} = T_{31},$$

where

$$u = 2ip_{31}k^2 - (p_{31}p_{32} + q_{31}q_{32})k - 2ip_{32}, \quad v = -2(q_{31} - q_{32})k,$$
$$w = 2p_{31}k^2 + 8ik - p_{32}, \qquad\qquad\qquad z = 2(q_{31} + q_{32})k.$$

Type IV:

$$\det M_1 = -2i(p_{41}p_{42} + q_{41}q_{42})k^2 + 2(1-i)(p_{41} + p_{42} + q_{41} + q_{42})k + 8,$$

$$R_1' = \begin{bmatrix} -u & -2v \\ -2v & -u \end{bmatrix},$$

where

$$u = 2i(p_{41}p_{42} + q_{41}q_{42})k^2 + 2[-(p_{41} + p_{42}) + i(q_{41} + q_{42})]k,$$
$$v = [i(p_{41} + p_{42}) - (q_{41} + q_{42})]k - 4.$$

Now, we also see from the general solution (2) that

$$\begin{bmatrix} A_1 \\ A_2 \end{bmatrix} = \begin{bmatrix} A_3 \\ A_4 \end{bmatrix} e^{ik}, \quad \begin{bmatrix} B_1 \\ B_2 \end{bmatrix} = \begin{bmatrix} B_3 \\ B_4 \end{bmatrix} e^{-ik}. \tag{7}$$

Combining (3), (5), and (7) then gives us

$$\begin{bmatrix} B_1 \\ B_2 \end{bmatrix} = R_1(k) \begin{bmatrix} A_1 \\ A_2 \end{bmatrix} = R_1(k) e^{ik} \begin{bmatrix} A_3 \\ A_4 \end{bmatrix}$$

$$= R_1(k) e^{ik} R_2 \begin{bmatrix} B_3 \\ B_4 \end{bmatrix} = R_1(k) e^{ik} R_2 e^{ik} \begin{bmatrix} B_1 \\ B_2 \end{bmatrix}. \tag{8}$$

Thus, we are to find those values of k for which

$$\det \left[e^{2ik} R_1(k) R_2 - I \right] = 0$$

or

$$\det \left[R_1' R_2 - e^{-2ik} (\det M_1(k)) I \right] = \det \left[R_1' R_2 - \lambda I \right] = 0.$$

Thus, we need only compute the eigenvalues of $R_1'(k) R_2$.

It is easy to see that, if we identify $p_{11} \to p_{31}$, $p_{12} \to p_{32}$, $q_{11} \to q_{31}$, $q_{12} \to q_{32}$, we have $t_{31} = t_{11}$ and $T_{31} = (T_{11})^T$. Thus, $R_{11}' R_2$ and $R_{13}' R_2$ will have the same eigenvalues, and the spectra for the types I and III joints are identical for each R_2; i.e., given any set of end/boundary conditions, the types I and III joints have identical spectra, *asymptotically*. This generalizes the result in [Krantz and Paulsen 1991] where they show that these spectra are identical in the case of C-F end conditions.

Continuing the analysis, in each case the matrix $R_1'(k) R_2$ will have two eigenvalues, $\lambda_1(k)$ and $\lambda_2(k)$. It is easy to show, as in [Chen and Zhou 1990], that these eigenvalues are distinct. It follows that, in each case, there will be two streams or branches of frequencies, satisfying

$$\lambda_j(k) = e^{-2ik} \det M_1(k) \quad \text{or} \quad e^{-2ik} = \frac{\lambda_j(k)}{\det M_1(k)}, \quad j = 1, 2, \tag{9}$$

where each $\lambda_j(k)$ and $\det M_1(k)$ are quadratic polynomials in k. Thus, as (9) is unwieldy, we follow [Chen and Zhou 1990] and we use the first-degree Taylor approximation

$$\frac{a_1 k^2 + b_1 k + c_1}{a_2 k^2 + b_2 k + c_2} = \frac{a_1}{a_2} + \frac{a_2 b_1 - a_1 b_2}{a_2^2} \frac{1}{k} + \mathbb{O}\left(\frac{1}{k^2}\right). \tag{10}$$

Applying (10) to (9) yields an equation of the form

$$e^{-2ik} = d_1 \left(1 - d_2 \frac{1}{k}\right) + \mathbb{O}\left(\frac{1}{k^2}\right), \quad |d_1| = 1, \tag{11}$$

and, taking the (complex) log of (11) and using the Taylor approximation

$$\ln\left(1 - d_2\frac{1}{k} + \mathbb{O}\left(\frac{1}{k^2}\right)\right) = -d_2\frac{1}{k} + \mathbb{O}\left(\frac{1}{k^2}\right),$$

we have

$$-2ik = -d_2\frac{1}{k} + i(\arg d_1 - 2n\pi) + \mathbb{O}\left(\frac{1}{k^2}\right), \quad n = 0, 1, 2, \ldots. \tag{12}$$

We note here that the choice of $-2n\pi$ is based on our earlier assumption that $\mathrm{Re}(k) \geq 0$. We rewrite (12) as a quadratic equation, realizing that multiplying by k will add an extraneous root of $\mathbb{O}(1/k)$, and after also employing the Taylor approximation

$$\sqrt{1+\epsilon} = 1 + \tfrac{1}{2}\epsilon + \mathbb{O}(\epsilon^2),$$

we arrive at

$$-ik^2 = -d_2 - \left(\tfrac{1}{2}\arg d_1 - n\pi\right)^2 i + \mathbb{O}\left(\frac{1}{k}\right).$$

Here, we provide the expressions for $-ik^2$ for all 40 cases:

Type I:

   $a = b$ (C-C, C-F, F-F, S-S, R-R, F-F):

$$-ik^2 = -\frac{p_{11}p_{12} + q_{11}q_{12}}{2p_{11}} - \left(\tfrac{1}{2}\arg a - n\pi\right)^2 i,$$

$$-ik^2 = -\frac{4}{p_{11}} - \left(\tfrac{1}{2}\arg(-a) - n\pi\right)^2 i;$$

   $a = -b = -1$ (S-R):

$$-ik^2 = -(4p_{11})^{-1}[p_{11}p_{12} + q_{11}q_{12} + 8 - 2\sqrt{2}(q_{11} - q_{12})i] - \left(\tfrac{1}{8}\pi - n\pi\right)^2 i,$$

$$-ik^2 = -(4p_{11})^{-1}[p_{11}p_{12} + q_{11}q_{12} + 8 + 2\sqrt{2}(q_{11} - q_{12})i] - \left(\tfrac{5}{8}\pi - n\pi\right)^2 i;$$

   $a = 1, b = i$ (R-F):

$$-ik^2 = -(4\sqrt{3}p_{11})^{-1}[(\sqrt{3}+1)(p_{11}p_{12} + q_{11}q_{12}) + 4i(q_{11} - q_{12}) + 8(\sqrt{3} - 1)]$$
$$- \left(\tfrac{1}{12}\pi - n\pi\right)^2 i,$$

$$-ik^2 = -(4\sqrt{3}p_{11})^{-1}[(\sqrt{3}-1)(p_{11}p_{12} + q_{11}q_{12}) - 4i(q_{11} - q_{12}) + 8(\sqrt{3} + 1)]$$
$$- \left(\tfrac{5}{12}\pi - n\pi\right)^2 i;$$

$\underline{a = -1, b = i \text{ (S-F)}}$:

$$-ik^2 = -(4\sqrt{3}\,p_{11})^{-1}[(\sqrt{3}+1)(p_{11}p_{12}+q_{11}q_{12})-4i(q_{11}-q_{12})+8(\sqrt{3}-1)]$$
$$-\left(\tfrac{1}{3}\pi - n\pi\right)^2 i,$$
$$-ik^2 = -(4\sqrt{3}\,p_{11})^{-1}[(\sqrt{3}-1)(p_{11}p_{12}+q_{11}q_{12})+4i(q_{11}-q_{12})+8(\sqrt{3}+1)]$$
$$-\left(\tfrac{2}{3}\pi - n\pi\right)^2 i;$$

$\underline{a = i, b = 1 \text{ (C-R)}}$:

$$-ik^2 = -(4\sqrt{3}\,p_{11})^{-1}[(\sqrt{3}+1)(p_{11}p_{12}+q_{11}q_{12})-4i(q_{11}-q_{12})+8(\sqrt{3}-1)]$$
$$-\left(\tfrac{1}{12}\pi - n\pi\right)^2 i,$$
$$-ik^2 = -(4\sqrt{3}\,p_{11})^{-1}[(\sqrt{3}-1)(p_{11}p_{12}+q_{11}q_{12})+4i(q_{11}-q_{12})+8(\sqrt{3}+1)]$$
$$-\left(\tfrac{5}{12}\pi - n\pi\right)^2 i;$$

$\underline{a = i, b = -1 \text{ (C-S)}}$:

$$-ik^2 = -(4\sqrt{3}\,p_{11})^{-1}[(\sqrt{3}+1)(p_{11}p_{12}+q_{11}q_{12})+4i(q_{11}-q_{12})+8(\sqrt{3}-1)]$$
$$-\left(\tfrac{1}{3}\pi - n\pi\right)^2 i,$$
$$-ik^2 = -(4\sqrt{3}\,p_{11})^{-1}[(\sqrt{3}-1)(p_{11}p_{12}+q_{11}q_{12})-4i(q_{11}-q_{12})+8(\sqrt{3}+1)]$$
$$-\left(\tfrac{2}{3}\pi - n\pi\right)^2 i.$$

Type III: This is the same as type I, with $p_{1j} \to p_{3j}$, $q_{1j} \to q_{3j}$, $j = 1, 2$.

Type II:

$\underline{a = b \text{ (C-C, C-F, S-S, R-R, F-F)}}$:

$$-ik^2 = -\tfrac{1}{2}[p_{21} + p_{22} + i(q_{21} + q_{22})] - \left(\tfrac{1}{2}\arg a - n\pi\right)^2 i,$$
$$-ik^2 = -\left(\tfrac{1}{2}\arg(-a) - n\pi\right)^2 i;$$

$\underline{a = -b = -1 \text{ (S-R)}}$:

$$-ik^2 = -\tfrac{1}{4}[p_{21} + p_{22} + i(q_{21} + q_{22})] - \left(\tfrac{1}{4}\pi - n\pi\right)^2 i,$$
$$-ik^2 = -\tfrac{1}{4}[p_{21} + p_{22} + i(q_{21} + q_{22})] - \left(\tfrac{3}{4}\pi - n\pi\right)^2 i;$$

$\underline{a = i, b = 1 \text{ (C-R)}; a = 1, b = i \text{ (R-F)}}$:

$$-ik^2 = -\tfrac{1}{8}(2 + \sqrt{2})[p_{21} + p_{22} + i(q_{21} + q_{22})] - \left(\tfrac{1}{8}\pi - n\pi\right)^2 i,$$
$$-ik^2 = -\tfrac{1}{8}(2 - \sqrt{2})[p_{21} + p_{22} + i(q_{21} + q_{22})] - \left(\tfrac{5}{8}\pi - n\pi\right)^2 i;$$

<u>$a = i$, $b = -1$ (C-S); $a = -1$, $b = i$ (S-F):</u>

$$-ik^2 = -\tfrac{1}{8}(2 + \sqrt{2})[p_{21} + p_{22} + i(q_{21} + q_{22})] - \left(\tfrac{3}{8}\pi - n\pi\right)^2 i,$$
$$-ik^2 = -\tfrac{1}{8}(2 - \sqrt{2})[p_{21} + p_{22} + i(q_{21} + q_{22})] - \left(\tfrac{7}{8}\pi - n\pi\right)^2 i.$$

<u>Type IV:</u>

<u>$a = b$ (C-C, C-F, S-S, R-R, F-F):</u>

$$-ik^2 = -2\frac{p_{41} + p_{42} + i(q_{41} + q_{42})}{p_{41}p_{42} + q_{41}q_{42}} - \left(\tfrac{1}{2}\arg a - n\pi\right)^2 i,$$
$$-ik^2 = -\left(\tfrac{1}{2}\arg a - n\pi\right)^2 i;$$

<u>$a \neq b$ (C-S, C-R, S-R, S-F, R-F):</u>

$$-ik^2 = -\frac{p_{41} + p_{42} + i(q_{41} + q_{42})}{p_{41}p_{42} + q_{41}q_{42}} - \left(\tfrac{1}{2}\arg a - n\pi\right)^2 i,$$
$$-ik^2 = -\frac{p_{41} + p_{42} + i(q_{41} + q_{42})}{p_{41}p_{42} + q_{41}q_{42}} - \left(\tfrac{1}{2}\arg b - n\pi\right)^2 i.$$

5. Discussion of asymptotic results

Again, we begin by noting that, for each set of end conditions, the type I and type III joints are asymptotically equivalent. This agrees with what is found in [Krantz and Paulsen 1991] for C-F end conditions.

We see also that, for many choices of the end conditions, the damping rates for the type II and type IV joints are asymptotically equivalent. Specifically, for those cases satisfying $a = b$, there is an asymptotically undamped branch, while, for the other branch, we need only choose our damping constants so that

$$p_{21} = \frac{4p_{41}}{p_{41}p_{42} + q_{41}q_{42}}, \qquad \text{etc.}$$

We have a similar equivalence for the case $a = -b = -1$ (S-R).

It is of particular interest that, in so many cases, for each type of joint, a term of the form $q_{j1} - q_{j2}$ or $q_{j1} + q_{j2}$ appears in $\mathrm{Im}(-ik^2)$. Thus, there are examples where the q_{j1} and q_{j2} affect the "frequency part" of the eigenfrequencies. Indeed, a term of this form appears in all cases except for those where there is a type I or type III joint and end conditions satisfying $a = b$. Thus, this behavior would not have been encountered in [Chen and Zhou 1990]. These terms *are* encountered in [Krantz and Paulsen 1991]; however, they seem to be discarded.

More specifically, in computing the damping rates, [Krantz and Paulsen 1991] arrives at a correct term similar to

$$p_{j1} + p_{j2} + i(q_{j1} + q_{j2}),$$

and then arrives at the, again correct, damping rate of

$$- \text{Re}[p_{j1} + p_{j2} + i(q_{j1} + q_{j2})].$$

However, the $i(q_{j1} + q_{j2})$ part is then dropped from consideration; although, as we shall see below, these efforts do show up in the numerical results. This does, however, seem to be an easy fix for Krantz and Paulsen [1991, p. 399].

6. Numerical results and comparisons

We have applied the Legendre–Tau spectral method to the problem. The problem is recast so that each beam has domain $-1 \le x \le 1$, after which we approximate u_1 and u_2 by

$$u_1(x) = \sum_{n=0}^{N} a_n P_n(x), \quad u_2(x) = \sum_{n=0}^{N} b_n P_n(x), \tag{13}$$

where P_n is the Legendre polynomial of degree n [Gottlieb and Orszag 1977]. Computations were performed within MATLAB, and also using Fortran 90 on a laptop. Computations at $N = 40$ and $N = 42$ show that all results in the table below converge to at least five decimal places.

In each table, we present the first 20 eigenfrequencies. We note here that, although we have only negative imaginary parts in our asymptotic results, in fact the conjugate of each eigenfrequency also is an eigenfrequency. In the following example, we list only those with positive imaginary parts.

In our first example, we compare numerical results for a type I and a type III joint, with C-F end conditions, for $q_{j1} = q_{j2} = 0$, and for various values of $p_{11} = p_{31}$ and $p_{12} = p_{32}$. The results appear in Tables 1–3.

The purpose here is threefold — to compare the numerical results for type I and type III joints (remembering that we have shown them to be asymptotically equivalent), to compare the numerical and asymptotic results, of course, and to see what happens when we vary the "dominant" damping parameters, p_{ij}.

For Table 1, we have taken $p_{11} = p_{31} = p_{12} = p_{32} = 1$. The first thing we must point out is the very close match between the type I and type III numerical results. We shall see similar behavior in the remaining results examining types I and III (Tables 2–4).

We also are surprised to see such a good match between the numerical and asymptotic results at this low end of the spectrum. Indeed, from the second eigenfrequency on, it is clear that the numerical spectrum already has split into the expected two branches or streams.

For Table 2, we have let $p_{11} = p_{31} = 2$ and $p_{12} = p_{32} = 0.5$. Again, we have a very close match between types I and III, and a close match between the numerical and asymptotic results.

type I numerical		type III numerical		WPM	
Re	Im	Re	Im	Re	Im
−0.49507	0.77898	−0.49507	0.77898		
−0.53772	5.5070	−0.53772	5.5070	−0.5	5.5517
−3.6704	20.562	−3.6704	20.562	−4.0	22.207
−0.49979	30.205	−0.49979	30.205	−0.5	30.226
−3.8734	60.711	−3.8734	60.711	−4.0	61.685
−0.49981	74.625	−0.49981	74.625	−0.5	74.639
−3.9307	120.20	−3.9307	120.20	−4.0	120.90
−0.49989	138.78	−0.49989	138.78	−0.5	138.79
−3.9561	199.31	−3.9561	199.31	−4.0	199.86
−0.49992	222.67	−0.49992	222.67	−0.5	222.68
−3.9697	298.10	−3.9697	298.10	−4.0	298.56
−0.49995	326.31	−0.49995	326.31	−0.5	326.31
−3.9778	416.61	−3.9777	416.61	−4.0	416.99
−0.49996	449.68	−0.49997	449.68	−0.5	449.68
−3.9830	554.83	−3.9829	554.83	−4.0	555.17
−0.49997	592.79	−0.49999	592.79	−0.5	592.79
−3.9866	712.79	−3.9866	712.79	−4.0	713.08
−0.49997	755.64	−0.49987	755.64	−0.5	755.64
−3.9889	890.47	−3.9901	890.47	−4.0	890.73
−0.50000	938.22	−4.9987	938.22	−0.5	938.23

Table 1. Types I and III joints, C-F end conditions, with $p_{11} = p_{12} = 1$, $q_{11} = q_{12} = 0$.

For Table 3, we have $p_{11} = p_{31} = 0.5$ and $p_{12} = p_{32} = 2$. Here, once more, the match for types I and III is very close. Meanwhile, the convergence of the numerical to the asymptotic results is somewhat slower than in the previous two tables, especially for the branch with real part equaling -8. Indeed, this slower but smooth convergence is seen quite clearly in Figure 1, where we have plotted the data from Table 3.

For Table 4, we continue to consider types I and III joints and C-F end conditions, with $p_{11} = p_{31} = p_{12} = p_{32} = 1$ but with $q_{11} = q_{31} = 0.5$ and $q_{12} = q_{32} = 0.7$. Once again, the types I and III results are an excellent match. In addition, the smooth convergence of the numerical to the asymptotic results is similar to that in the previous example, and can be seen clearly in Figure 2.

Given the excellent agreement between the type I and type III numerical results, we are curious as to "how equivalent" they actually are. We have tried to compare the determinant equations for the exact solutions, but so far we have had no luck.

type I numerical		type III numerical		WPM	
Re	Im	Re	Im	Re	Im
−1.7301	1.1041	−1.7300	1.1041		
−0.28489	5.5602	−0.28489	5.5602	−0.25	5.5517
−1.9703	21.818	−1.9702	21.818	−2.0	22.207
−0.25005	30.221	−0.25005	30.220	−0.25	30.226
−1.9856	61.556	−1.9856	61.445	−2.0	61.685
−0.24998	75.635	−0.24998	74.635	−0.25	74.639
−1.9917	120.73	−1.9917	120.72	−2.0	120.90
−0.24999	138.79	−0.24999	138.79	−0.25	138.79
−1.9946	199.72	−1.9946	199.72	−2.0	199.86
−0.24999	222.68	−0.24999	222.68	−0.25	222.68
−1.9963	298.44	−1.9963	298.44	−2.0	298.56
−0.24999	326.31	−0.24999	326.31	−0.25	326.13
−1.9973	416.90	−1.9973	416.90	−2.0	418.99
−0.25000	449.68	−0.25000	449.68	−0.25	449.68
−1.9979	555.08	−1.9979	555.08	−2.0	555.17
−0.25000	592.79	−0.24999	592.79	−0.25	592.79
−1.9983	713.00	−1.9983	713.00	−2.0	713.08
−0.25000	755.64	−0.25004	755.64	−0.25	755.64
−1.9989	890.67	−1.9984	890.67	−2.0	890.73
−0.25000	938.23	−0.25003	938.23	−0.25	938.23

Table 2. Types I and III joints, C-F end conditions, with $p_{11} = 2$, $p_{12} = 0.5$, $q_{11} = q_{12} = 0$.

For Table 5, we consider a type II joint with C-F end conditions. The purpose here is to investigate the behavior of the "undamped" branch, the contribution of q_{21} and q_{22} to the imaginary parts of the eigenfrequencies, and, of course, again to compare the numerical and asymptotic results.

Here, we let $p_{21} = p_{22} = 1$. The first two columns give the numerical results, and the next two columns the asymptotic results for the case where $q_{21} = q_{22} = 0$. We see here that the numerical real parts for the "undamped" branch are very small and, in most cases, are negative, as expected. For those that are not negative (the fifth, seventh and thirteenth eigenfrequencies), we assume that it is due to the numerical approximation. In addition, the match between the numerical and asymptotic results is again quite good, even as early as the second eigenfrequency. This can also be seen clearly in Figure 3, where we have plotted these results.

The last four columns are arranged as are the first four, but here we have let $q_{21} = 0.5$ and $q_{22} = 0.7$. We note that the effect of these values on the imaginary

type I numerical		type III numerical		WPM	
Re	Im	Re	Im	Re	Im
−0.41842	0.79717	−0.41842	0.79717		
−1.0353	5.3641	−1.0353	5.3641	−1.0	5.5517
−3.8189	17.042	−3.8189	17.042	−8.0	22.207
−0.99732	30.143	−0.99732	30.143	−1.0	30.226
−6.6452	57.777	−6.6452	57.777	−8.0	61.685
−0.99849	74.584	−0.99849	74.584	−1.0	74.639
−7.3547	118.07	−7.3547	118.07	−8.0	120.90
−0.99909	138.75	−0.99909	138.75	−1.0	138.79
−7.6154	197.65	−7.6154	197.65	−8.0	199.86
−0.99940	222.65	−0.99940	222.65	−1.0	222.68
−7.7423	296.75	−7.7423	296.75	−8.0	298.56
−0.99957	326.29	−0.99957	326.29	−1.0	326.13
−7.8144	415.45	−7.8144	415.46	−8.0	418.99
−0.99968	449.66	−0.99969	449.66	−1.0	449.68
−7.8598	553.83	−7.8595	553.83	−8.0	555.17
−0.99977	592.77	−0.99980	592.77	−1.0	592.79
−7.8901	711.90	−7.8905	711.91	−8.0	713.08
−0.99976	755.62	−0.99947	755.62	−1.0	755.64
−7.9105	889.67	−7.9140	889.68	−8.0	890.73
−0.99981	938.20	−0.99924	938.22	−1.0	938.23

Table 3. Types I and III joints, C-F end conditions, with $p_{11} = 0.5$, $p_{12} = 2$, $q_{11} = q_{12} = 0$.
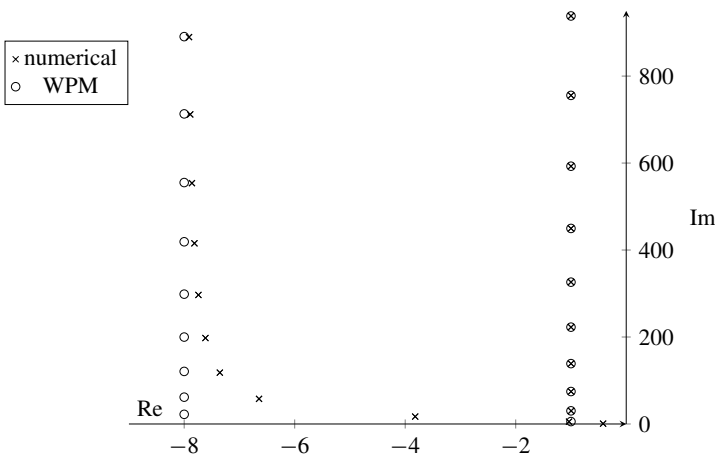
Figure 1. Plot of the vibration frequencies from Table 3.

type I numerical		type III numerical		WPM	
Re	Im	Re	Im	Re	Im
−0.45378	0.76895	−0.45378	0.76895		
−0.95917	5.2515	−0.95917	5.2515	−1.35	5.5517
−3.6112	17.067	−3.6112	17.067	−8.0	22.207
−1.0664	29.951	−1.0664	29.951	−1.35	30.226
−6.5928	57.645	−6.5928	57.645	−8.0	61.685
−1.1599	74.377	−1.1599	74.377	−1.35	74.639
−7.3698	117.99	−7.3698	117.99	−8.0	120.90
−1.2226	138.56	−1.2226	138.56	−1.35	138.79
−7.6396	197.61	−7.6396	197.61	−8.0	199.86
−1.2611	222.48	−1.2611	222.48	−1.35	222.68
−7.7645	296.72	−7.7645	296.72	−8.0	298.56
−1.2853	326.14	−1.2853	325.14	−1.35	326.13
−7.8331	415.44	−7.8331	415.44	−8.0	418.99
−1.3012	449.53	−1.3012	449.53	−1.35	449.68
−7.8751	553.82	−7.8751	553.82	−8.0	555.17
−1.3119	592.65	−1.3120	592.65	−1.35	592.79
−7.9026	711.89	−7.9028	711.89	−8.0	713.08
−1.3197	755.51	−1.3196	755.52	−1.35	755.64
−7.9225	889.67	−7.9222	889.67	−8.0	890.73
−1.3253	938.12	−1.3251	938.11	−1.35	938.23

Table 4. Types I and III joints, C-F end conditions, with $p_{11} = p_{12} = 1$, $q_{11} = 0.5$, $q_{12} = 0.7$.
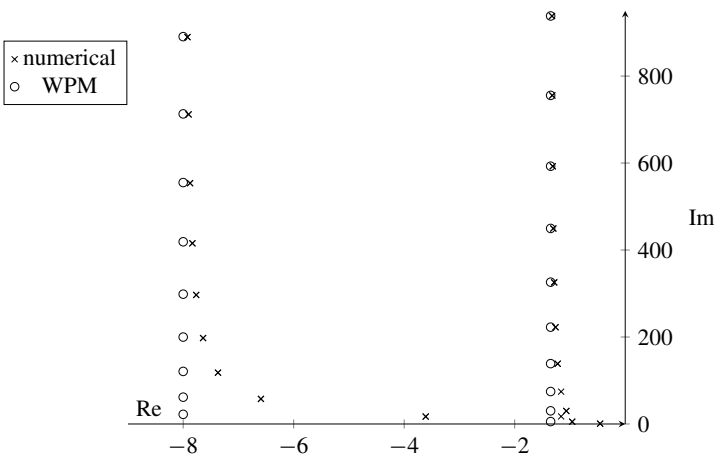
Figure 2. Plot of the vibration frequencies from Table 4.

| type II joint							
$q_{11} = q_{12} = 0$				$q_{11} = 0.5, q_{12} = 0.7$			
numerical		WPM		numerical		WPM	
Re	Im	Re	Im	Re	Im	Re	Im
-0.21945	0.82672	0.0	0.61685	-0.16897	0.72184	0.0	0.61685
-1.0236	5.5617	-1.0	5.5517	-0.95445	6.1571	-1.0	6.1577
$-7.6 \cdot 10^{-4}$	15.424	0.0	15.421	$-6.6 \cdot 10^{-4}$	15.424	0.0	15.421
-1.0025	30.234	-1.0	30.226	-0.98966	30.834	-1.0	30.826
$1.4 \cdot 10^{-6}$	49.964	0.0	49.965	$-1.3 \cdot 10^{-6}$	49.965	0.0	49.965
-1.0011	74.642	-1.0	74.639	-0.99584	75.242	-1.0	75.239
$3.4 \cdot 10^{-10}$	104.25	0.0	104.25	$1.1 \cdot 10^{-9}$	104.25	0.0	104.25
-1.0006	138.70	-1.0	138.79	-0.99777	139.39	-1.0	139.39
$-1.3 \cdot 10^{-8}$	178.27	0.0	178.27	$-1.1 \cdot 10^{-8}$	178.27	0.0	178.27
-1.0004	222.68	-1.0	222.68	-0.99861	223.28	-1.0	223.28
$-9.5 \cdot 10^{-8}$	272.03	0.0	272.03	$-7.5 \cdot 10^{-8}$	272.03	0.0	272.03
-1.0003	326.31	-1.0	326.31	-0.99905	326.91	-1.0	326.91
$2.2 \cdot 10^{-8}$	385.53	0.0	385.53	$3.8 \cdot 10^{-7}$	385.53	0.0	385.53
-1.0002	449.68	-1.0	449.68	-0.99930	450.28	-1.0	450.28
$-5.3 \cdot 10^{-8}$	518.77	0.0	518.77	$-5.4 \cdot 10^{-7}$	518.77	0.0	518.77
-1.0001	592.79	-1.0	592.79	-0.99947	593.39	-1.0	593.39
$-8.1 \cdot 10^{-6}$	671.75	0.0	671.75	$-7.6 \cdot 10^{-6}$	671.75	0.0	671.75
-1.0002	755.64	-1.0	755.64	-0.99970	756.24	-1.0	756.24
$-8.5 \cdot 10^{-6}$	844.47	0.0	844.47	$-2.2 \cdot 10^{-5}$	844.48	0.0	844.47
-1.0002	938.23	-1.0	938.23	-0.99972	938.84	-1.0	938.83

Table 5. Type II joint, C-F end conditions, with $p_{11} = p_{12} = 1$, $q_{11} = q_{12} = 0$, and $p_{11} = p_{12} = 1$, $q_{11} = 0.5$, $q_{12} = 0.7$.

parts of the eigenfrequencies of the "damped" branch should be

$$\frac{q_{21} + q_{22}}{2} = 0.6 \qquad (14)$$

and, indeed, this is what we see in the numerical results. Here, again, and in Figure 4, we see a strong match between the numerical and asymptotic results.

Table 6 is arranged exactly as Table 5, but here we consider, instead, a type IV joint, with $p_{41} = p_{42} = 1$. As before, $q_{41} = q_{42} = 0$ for the first four columns, while $q_{41} = 0.5$ and $q_{42} = 0.7$ for the last four. Once more, we provide the first twenty eigenfrequencies. For the $q_{41} = q_{42} = 0$ results, the asymptotic results occur in pairs with equal imaginary parts, and we can see from the table and from Figure 5, where these data are plotted, that the numerical results are approaching the same behavior asymptotically. For the case $q_{41} = 0.5$, $q_{42} = 0.7$, we again see the effect of nonzero
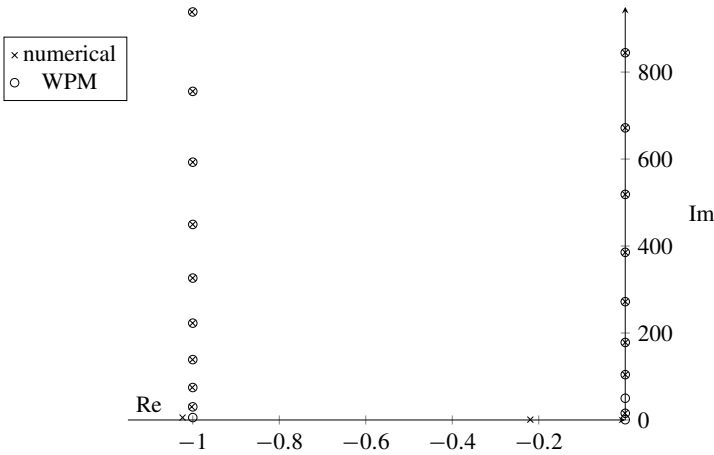
Figure 3. Plot of the vibration frequencies from Table 5 for the case $q_{11} = q_{12} = 0$.
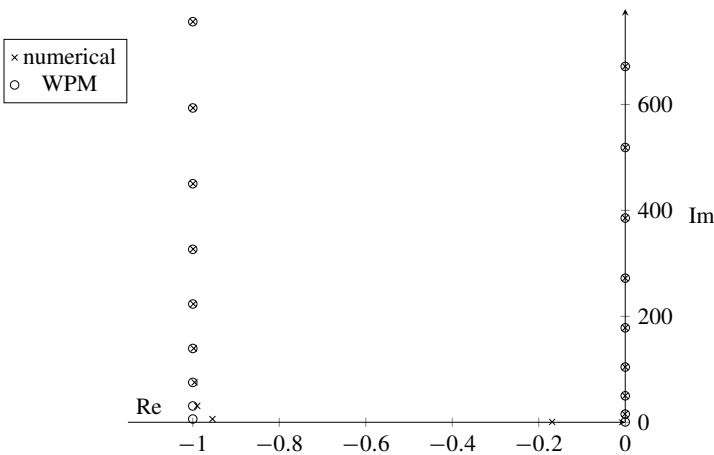
Figure 4. Plot of the vibration frequencies from Table 5 for the case $q_{11} = 0.5$, $q_{12} = 0.7$.

q-values on the imaginary part of the "damped" branch. Here, the effect is

$$\frac{q_{41} + q_{42}}{p_{41} p_{42} + q_{41} q_{42}} = 1.7778. \tag{15}$$

We plot these results in Figure 6, where, although it is difficult to see the effects of the nonzero q-values, we can see, again, a very good match between the asymptotic and numerical results.

We realize that the damping parameters we have used may not be physically realistic. Indeed, in other work, we have seen that, for realistic data, the convergence

type IV joint							
$q_{41} = q_{42} = 0$				$q_{41} = 0.5,\ q_{42} = 0.7$			
numerical		WPM		numerical		WPM	
Re	Im	Re	Im	Re	Im	Re	Im
$3.3 \cdot 10^{-16}$	0.0000			$7.8 \cdot 10^{-16}$	0.0000		
-0.46155	0.53410			-0.26096	0.45158		
$-4.2 \cdot 10^{-2}$	5.5592	0.0	5.5517	$-2.3 \cdot 10^{-2}$	5.5606	0.0	5.5517
-4.0964	6.6697	-4.0	5.5517	-2.3443	7.6742	-2.96	7.3295
$-1.2 \cdot 10^{-4}$	30.226	0.0	30.226	$-7.0 \cdot 10^{-5}$	30.226	0.0	30.226
-4.1652	30.395	-4.0	30.226	-2.8528	32.136	-2.96	32.004
$-1.2 \cdot 10^{-4}$	74.639	0.0	74.639	$-1.5 \cdot 10^{-7}$	74.639	0.0	74.639
-4.0704	74.698	-4.0	74.639	-2.9217	76.474	-2.96	76.417
$-2.1 \cdot 10^{-10}$	138.79	0.0	138.79	$2.3 \cdot 10^{-9}$	138.79	0.0	138.79
-4.0382	138.82	-4.0	138.79	-2.9415	140.60	-2.96	140.57
$-1.4 \cdot 10^{-8}$	222.68	0.0	222.68	$-2.4 \cdot 10^{-10}$	222.68	0.0	222.68
-4.0239	222.70	-4.0	222.68	-2.9498	224.48	-2.96	224.46
$-3.5 \cdot 10^{-8}$	326.31	0.0	326.31	$-5.0 \cdot 10^{-8}$	326.31	0.0	326.31
-4.0163	326.33	-4.0	326.31	-2.9540	328.10	-2.96	328.09
$-8.7 \cdot 10^{-8}$	449.68	0.0	449.68	$-2.7 \cdot 10^{-7}$	449.68	0.0	449.68
-4.0118	449.69	-4.0	449.68	-2.9565	451.47	-2.96	451.46
$-3.2 \cdot 10^{-7}$	592.79	0.0	592.79	$1.2 \cdot 10^{-7}$	592.79	0.0	592.79
-4.0090	592.80	-4.0	592.79	-2.9581	594.58	-2.96	594.57
$1.8 \cdot 10^{-6}$	755.64	0.0	755.64	$3.6 \cdot 10^{-6}$	755.64	0.0	755.64
-4.0071	755.65	-4.0	755.64	-2.9592	757.42	-2.96	757.42

Table 6. Type IV joint, C-F end conditions, with $p_{11} = p_{12} = 1$, $q_{11} = q_{12} = 0$, and $p_{11} = p_{12} = 1$, $q_{11} = 0.5$, $q_{12} = 0.7$.

of the numerical to the asymptotic results sometimes takes much longer. However, we have not been able to find realistic parameters in the literature. In particular, in the two papers which give experimental results [Chen et al. 1988; 1989], the physical parameters have not been determined, and the comparison with the asymptotic results is based instead on a very clever use of the patterns that result from looking at various differences between the eigenfrequencies.

Finally, we should mention that, in order to utilize the *wave propagation method* in its current form, it is necessary that the possible wave speeds are the same along each beam, thus the assumption here and in the references that each of the physical parameters m, E, and I is the same for each beam. We can generalize a bit, given that the wave speeds actually depend only on the ratio EI/m, so we need only have the ratio be the same for each beam. Once this condition is not met, however, the problem becomes far more difficult — indeed, we have found nothing in the literature regarding an asymptotic analysis of this problem.
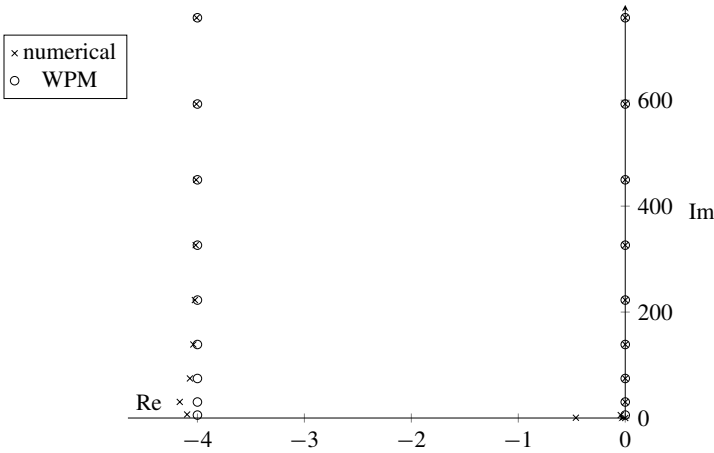
Figure 5. Plot of the vibration frequencies from Table 6 for the case $q_{41} = q_{42} = 0$.
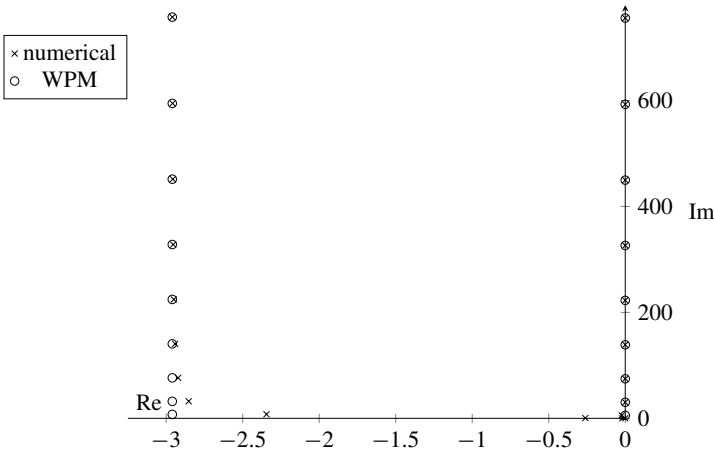
Figure 6. Plot of the vibration frequencies from Table 6 for the case $q_{41} = 0.5$, $q_{42} = 0.7$.

References

[Chen and Zhou 1990] G. Chen and J. Zhou, "The wave propagation method for the analysis of boundary stabilization in vibrating structures", *SIAM J. Appl. Math.* **50**:5 (1990), 1254–1283. MR Zbl

[Chen et al. 1987] G. Chen, M. C. Delfour, A. M. Krall, and G. Payre, "Modeling, stabilization and control of serially connected beams", *SIAM J. Control Optim.* **25**:3 (1987), 526–546. MR Zbl

[Chen et al. 1988] G. Chen, S. G. Krantz, D. L. Russell, C. E. Wayne, H. H. West, and J. Zhou, "Modelling, analysis and testing of dissipative beam joints — experiments and data smoothing", *Math. Comput. Modelling* **11** (1988), 1011–1016. MR

[Chen et al. 1989] G. Chen, S. G. Krantz, D. L. Russell, C. E. Wayne, H. H. West, and M. P. Coleman, "Analysis, designs, and behavior of dissipative joints for coupled beams", *SIAM J. Appl. Math.* **49**:6 (1989), 1665–1693. MR

[Gottlieb and Orszag 1977] D. Gottlieb and S. A. Orszag, *Numerical analysis of spectral methods: theory and applications*, CBMS-NSF Regional Conference Series in Applied Mathematics **26**, SIAM, Philadelphia, PA, 1977. MR Zbl

[Keller and Rubinow 1960] J. B. Keller and S. I. Rubinow, "Asymptotic solution of eigenvalue problems", *Ann. Phys.* **9**:1 (1960), 24–75. Zbl

[Krantz and Paulsen 1991] S. G. Krantz and W. H. Paulsen, "Asymptotic eigenfrequency distributions for the N-beam Euler–Bernoulli coupled beam equation with dissipative joints", *J. Symbolic Comput.* **11**:4 (1991), 369–418. MR Zbl

[Pilkey 1969] W. D. Pilkey, "Analysis for the response of structural members", Research Institute Project J6094, Illinois Institute of Technology, 1969.

christopher.abriola@gmail.com   *Department of Mathematics and Statistics, University of New Hampshire, Durham, NH 03824, United States*

mcoleman@fairfield.edu   *Department of Mathematics and Computer Science, Fairfield University, Fairfield, CT 06824, United States*

aglika.darakchieva@uconn.edu   *Department of Mathematics, University of Connecticut, Storrs, CT 06269, United States*

tylermwales@gmail.com   *Department of Mathematics, Louisiana State University, Baton Rouge, LA 70803, United States*

msp

msp

Loxodromes on hypersurfaces of revolution

Jacob Blackwood, Adam Dukehart and Mohammad Javaheri

(Communicated by Gaven Martin)

A loxodrome is a curve that makes a constant angle with the meridians. We use conformal maps and the notion of parallel transport in differential geometry to investigate loxodromes on hypersurfaces of revolution and their spiral behavior near a pole.

1. Introduction

Loxodromes appear historically as mathematical tools in navigation, since they provide efficient navigation routes from one point to another by making a constant *course angle* with the meridians. Even modern technology relies on the ability to calculate loxodromes [Alexander 2004]. Loxodromes are best understood via conformal maps, maps that preserve angles locally. For example, the Mercator projection map is a conformal map under which the meridians and curves of constant latitude (parallels) are mapped to vertical and horizontal lines. A curve making a constant angle with vertical lines as it crosses them is itself a straight line; therefore, the Mercator projection map represents loxodromes as straight lines. As another example of a conformal map, consider the stereographic projection which maps the meridians and parallels to lines through the origin (radial lines) and circles centered at the origin. The curves that make a constant angle with the radial lines are the well-known logarithmic spirals. In other words, the stereographic projection maps loxodromes to logarithmic spirals.

The construction of loxodromes on the sphere and oblate-spheroidal surfaces, which approximate the shape of the earth, has been investigated previously [Bennett 1996; Carlton-Wippern 1992; Smart 1946; Williams 1950]. Spheres and spheroids are examples of surfaces of revolution that we now define. Let $\eta(t) = (u(t), v(t))$, where $t \in (a, b)$, be a curve in the half-plane $H = \{(x, y, 0) \in \mathbb{R}^3 : y > 0\}$. By rotating the *profile curve* $\eta(t)$ around the x-axis in $\mathbb{R}^3$, one obtains a surface of revolution parametrized as

$$x = u(t), \quad y = v(t) \cos \theta, \quad z = v(t) \sin \theta, \quad \text{where } t \in (a, b), \ \theta \in [0, 2\pi).$$

The *meridians* of the surface are the curves of constant θ, while the *parallels* of the surface are the curves of constant t. A curve on S is called a loxodrome of S if it makes a constant angle with the meridians of S as it crosses them.

In Section 2, we derive the parametric equations of loxodromes on a surface of revolution. We also define a stereographic projection on a given surface of revolution that maps loxodromes to logarithmic spirals in the plane. Finally, we study the distances along loxodromes as well as the spiral behavior of loxodromes near a pole.

In Section 3, we consider the case where the profile curve is a Jordan curve (and so the resulting surface of revolution is a torus). In particular, we study closed loxodromes and their density in the set of all loxodromes. We also show that loxodromes are geodesics in a suitable metric on the surface.

Hypersurfaces of revolution are important and interesting geometric objects, and they have been studied extensively by geometers [Coll and Harrison 2013; do Carmo and Dajczer 1983; Zhang 2012]. In Section 4, we give a definition of loxodromes on hypersurfaces of revolution. As an example, we also find parametric equations of loxodromes on higher-dimensional spheres.

2. The loxodrome equation

Suppose that the profile curve of a surface of revolution S is given by $y = f(x)$, where $f(x)$ is a differentiable function on the interval $(a, b) \subseteq \mathbb{R}$ such that $f(x) > 0$ for all $x \in (a, b)$. Then S is parametrized by the cylindrical map

$$r(x, \theta) = \langle x, \ f(x) \cos \theta, \ f(x) \sin \theta \rangle.$$

Let

$$\gamma(x) = \langle x, \ f(x) \cos \theta(x), \ f(x) \sin \theta(x) \rangle$$

be a loxodrome that makes a constant angle ψ_0 with the meridians. The tangent vector to the meridian $r(x, \theta)$, where θ is constant, is given by

$$\boldsymbol{a} = \frac{\partial}{\partial x} r(x, \theta) = \langle 1, \ f'(x) \cos \theta, \ f'(x) \sin \theta \rangle,$$

while the tangent vector to γ at $x \in (a, b)$ is given by

$$\boldsymbol{b} = \frac{d}{dx} \gamma(x) = \langle 1, \ f'(x) \cos \theta - f(x) \theta'(x) \sin \theta, \ f'(x) \sin \theta + f(x) \theta'(x) \cos \theta \rangle.$$

The constant-angle constraint gives $(\boldsymbol{a} \cdot \boldsymbol{b})^2 = \|\boldsymbol{a}\|^2 \|\boldsymbol{b}\|^2 \cos^2(\psi_0)$, which yields

$$1 + (f'(x))^2 = \big(1 + (f'(x))^2 + (f(x)\theta'(x))^2\big) \cos^2(\psi_0).$$

After solving for $\theta'(x)$ and integrating, one has

$$\theta(x) = \tan(\psi_0) A(x), \tag{2-1}$$

where

$$A(x) = \int_c^x \frac{\sqrt{1 + (f'(x))^2}}{f(x)} \, dx + C, \qquad (2\text{-}2)$$

with constants $c \in (a, b)$ and $C \in \mathbb{R}$.

2.1. *The conformal stereographic projection.*

The stereographic projection on the sphere has the property that it is conformal and it maps meridians and parallels to lines through the origin and circles centered at the origin respectively. We now describe a map with the same properties on the surface of revolution S with the profile curve $y = f(x)$. Let

$$L(r, s) = \langle \ln(r^2 + s^2), \arctan(s/r) \rangle$$

and

$$F(x, \theta) = \langle A^{-1}(x), f(A^{-1}(x)) \cos \theta, f(A^{-1}(x)) \sin \theta \rangle,$$

where $A(x)$ is given by (2-2).

We claim that the composition $T = F \circ L$ is a conformal map from an open subset of $\mathbb{R}^2$ to S. The map L is the logarithmic conformal mapping such that L^{-1} maps the horizontal and vertical lines in the (x, θ)-plane to lines through the origin and circles centered at the origin respectively. The map F is also a conformal map that maps the horizontal and vertical lines in the (x, θ)-plane to meridians and parallels on the surface S. To see this, we note that with $g(x) = A^{-1}(x)$, one has

$$F_x = \langle g'(x), f' \circ g(x)g'(x) \cos \theta, f' \circ g(x)g'(x) \sin \theta \rangle, \qquad (2\text{-}3)$$

$$F_\theta = \langle 0, -f \circ g(x) \sin \theta, f \circ g(x) \cos \theta \rangle. \qquad (2\text{-}4)$$

Therefore,

$$\begin{bmatrix} F_x \cdot F_x & F_x \cdot F_\theta \\ F_\theta \cdot F_x & F_\theta \cdot F_\theta \end{bmatrix} = \begin{bmatrix} (g'(x))^2 (1 + (f' \circ g(x))^2) & 0 \\ 0 & (f \circ g(x))^2 \end{bmatrix}. \qquad (2\text{-}5)$$

For F to be a conformal map from the (x, θ)-plane to the surface of revolution S, the matrix in (2-5) must be a multiple of the identity matrix. By (2-2), one has

$$g'(x) = (A^{-1})'(x) = \frac{1}{A'(g(x))} = \frac{f(g(x))}{\sqrt{1 + f'(g(x))^2}},$$

which implies that the matrix (2-5) is a multiple of identity; hence F is a conformal map. It follows that T, being a composition of conformal maps, is a conformal map. Moreover, T^{-1} maps the meridians and parallels of S to lines through the origin and circles centered at the origin respectively. Therefore, every loxodrome on S is mapped under T^{-1} to a logarithmic spiral in the (r, s)-plane.

A feature of the logarithmic spiral is its infinite spiraling around the origin. We now study this spiral behavior of loxodromes in more detail.
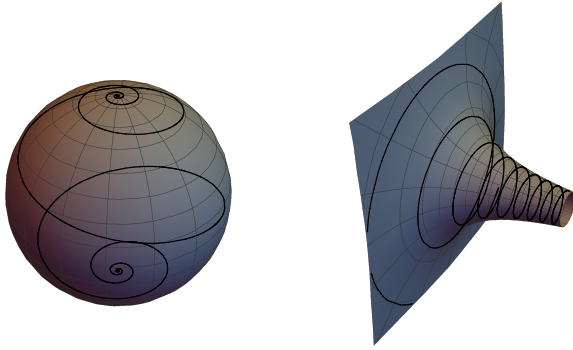
Figure 1. Left: spiral at a point. Right: spiral at infinity.

Theorem 1. *Let $y = f(x)$ be differentiable on the interval $(a, b) \subseteq \mathbb{R}$ and suppose that $\lim_{x \to b^-} f(x) = 0$ or ∞. Let $\gamma(x) = (x, f(x)\cos\theta(x), f(x)\sin\theta(x))$ be a loxodrome, where $\theta(x)$ is given by (2-2) with $\tan(\psi_0) \neq 0$. Then*

$$\lim_{x \to b^-} \theta(x) = \pm\infty, \tag{2-6}$$

where the plus or minus sign is determined by $\mathrm{sign}(\tan(\psi_0))$.

Proof. Let $c \in (a, b)$. Then

$$|\theta(x) - \theta(c)| = \left| \tan(\psi_0) \int_c^x \frac{\sqrt{1 + (f'(x))^2}}{f(x)} \, dx \right| \geq |\tan(\psi_0)| \int_c^x \left| \frac{f'(x)}{f(x)} \right| dx$$

$$\geq |\tan(\psi_0)| \, |\ln f(c) - \ln f(x)| \to \infty,$$

as $x \to b^-$, since $\lim_{x \to b^-} f(x) = 0$ or ∞, and in either case $|\ln f(x)| \to \infty$. $\square$

In the next theorem, we compute distances along loxodromes. We denote the length of a curve γ by $\ell(\gamma)$ and the length of the graph of a function f by $\ell(f)$.

Theorem 2. *Let $y = f(x)$ be a differentiable positive function on the interval $(a, b) \subseteq \mathbb{R}$, and let $\gamma(x) = \langle x, f(x)\cos\theta(x), f(x)\sin\theta(x) \rangle$ be a loxodrome, where $\theta(x)$ is given by (2-2). Then*

$$\ell(\gamma) = |\sec(\psi_0)| \ell(f) = |\sec(\psi_0)| \int_a^b \sqrt{1 + (f'(x))^2} \, dx. \tag{2-7}$$

Proof. By (2-1), we have

$$\|\gamma'(x)\|^2 = 1 + (f'(x)\cos\theta - f(x)\theta'(x)\sin\theta)^2 + (f'(x)\sin\theta + f(x)\theta'(x)\cos\theta)^2$$

$$= 1 + (f'(x))^2 + (f(x)\theta'(x))^2$$

$$= 1 + (f'(x))^2 + \tan^2(\psi_0)(1 + (f'(x))^2)$$

$$= \sec^2(\psi_0)(1 + (f'(x))^2),$$

which implies (2-7). $\square$
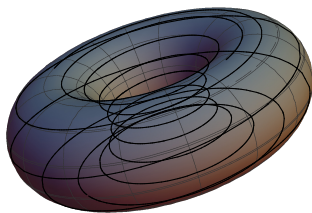
Figure 2. A toric loxodrome.

3. Loxodromes on the torus

Let C be a simple plane curve parametrized by arc length, $C(t) = (x(t), y(t))$, where $x(t)$ and $y(t)$ are differentiable functions of $t \in (a, b)$ and $y(t) > 0$ for all $t \in (a, b)$. Rotating C around the x-axis yields a surface of revolution with the parametrization

$$u(t, \theta) = \langle x(t), \ y(t) \cos \theta, \ y(t) \sin \theta \rangle. \tag{3-1}$$

Suppose that

$$\eta(t) = \langle x(t), \ y(t) \cos \theta(t), \ y(t) \sin \theta(t) \rangle$$

is a loxodrome. A similar calculation to that the previous section implies

$$\theta(t) = \tan(\psi_0) B(t), \tag{3-2}$$

where

$$B(t) = \int \frac{dt}{y(t)}. \tag{3-3}$$

In the next theorem, we discuss closed loxodromes on surfaces of revolution with periodic profile curves.

Theorem 3. *Let $C(t) = \langle x(t), y(t) \rangle$, $y(t) > 0$, be a simple closed differentiable curve parametrized by the arc length and with period $T > 0$, i.e., $C(t + T) = C(t)$ for all $t \in \mathbb{R}$. Let S be the surface of revolution with profile curve $C(t)$. Let $\eta(t)$ be a loxodrome on S, making a constant angle ψ_0 with the meridians of S. Then $\eta(t)$ is a closed curve if and only if*

$$\tan(\psi_0) \cdot \frac{1}{2\pi} \int_0^T \frac{dt}{y(t)} \in \mathbb{Q}. \tag{3-4}$$

In particular, closed loxodromes on S are dense in the set of all loxodromes. In addition, if a loxodrome is not closed, then the loxodrome is dense in S.

Proof. Since C is parametrized by arc length, we have from (3-2) that

$$\theta(mT + t) - \theta(t) = \tan(\psi_0) \int_t^{mT+t} \frac{dt}{y(t)} = m \tan(\psi_0) \int_0^T \frac{dt}{y(t)}. \tag{3-5}$$

For $\eta(t)$ to be a closed curve, we must have $\theta(mT + t) - \theta(t) = 2n\pi$ for some integers m, n with $m \neq 0$. It follows that

$$m \tan(\psi_0) \int_0^T \frac{dt}{y(t)} = 2\pi n,$$

which is equivalent to (3-4).

The set of angles ψ_0 for which (3-4) holds is dense in $\mathbb{R}$, and so the set of periodic loxodromes is dense among all loxodromes on S.

Next, suppose that $\eta(t)$ is not closed, and so (3-4) fails. It follows from (3-5) that $\theta(mT + t) - \theta(t) = 2\pi m\lambda$, where λ is a fixed irrational number. By Kronecker's approximation theorem, the set $\{2\pi m\lambda \pmod{2\pi} : m \in \mathbb{Z}\}$ is dense in the interval $[0, 2\pi)$. Therefore, the set $\{\eta(mT + t) : m \in \mathbb{Z}\}$ is dense in the parallel obtained by rotating $\eta(t)$ around the x-axis. In other words, if η intersects a parallel of S then it is dense in that parallel of S. Since η intersects every parallel of S, we conclude that η is dense in S. $\qquad \square$

The flat metric on the torus has the property that every geodesic (paths that are locally of shortest length) is either periodic or dense in the torus. This resembles the property we discussed in Theorem 3 for loxodromes of S. In fact, there exists a metric on S for which the loxodromes are exactly the geodesics. The metric is simply the pullback of the Euclidean flat metric on $\mathbb{R}^2$ by the map R^{-1}, where

$$R(s, \theta) = \langle x(B^{-1}(s)), \ y(B^{-1}(s)) \cos \theta, \ y(B^{-1}(s)) \sin \theta \rangle,$$

where $B(t)$ is defined by (3-3).

4. Hypersurfaces of revolution

In this section, we give a definition of loxodromes on hypersurfaces of revolution. Let M be an $(n-2)$-dimensional submanifold of $\mathbb{R}^{n-1} \times \{0\} \subseteq \mathbb{R}^n$, and consider a local parametrization of M

$$\langle \boldsymbol{x}, 0 \rangle = \langle x_1, \ldots, x_{n-1}, 0 \rangle : \mathcal{U} \to \mathbb{R}^n, \tag{4-1}$$

where $\mathcal{U} \subseteq \{\langle x_1, \ldots, x_{n-1}, 0 \rangle : x_{n-1} > 0\}$ is open. There is a natural embedding of $M \times \mathbb{S}^1$ in $\mathbb{R}^n$ defined by

$$\langle \boldsymbol{x}, 0, \theta \rangle \mapsto R(\boldsymbol{x}, \theta) = \langle x_1, \ldots, x_{n-2}, x_{n-1} \cos \theta, x_{n-1} \sin \theta \rangle. \tag{4-2}$$

We call this embedded $(n-1)$-dimensional submanifold S of $\mathbb{R}^n$ the hypersurface of revolution and call M the *profile manifold*. By the meridians of S we mean the submanifolds of S given by the images of $R(\boldsymbol{x}, \theta)$ for constant θ-values. We denote the meridians of S by M_θ, where $\theta \in \mathbb{R}$.

Let $\gamma : (a, b) \to N$ be a smooth curve so that

$$\gamma(t) = \langle x_1(t), \ldots, x_{n-2}(t), x_{n-1}(t)\cos\theta(t), x_{n-1}(t)\sin\theta(t)\rangle.$$

To be a loxodrome on S, we require the curve γ to have the property that its relative position to the meridians stays constant. We need to be able to compare the relative position of $\gamma(t)$ to $M_{\theta(t)}$ for different values of t. To do this, one uses the isomorphism $M_\theta \to M$ to bring the position and velocity vectors along γ back on M. One obtains the curve $\eta(t) = R(\gamma(t), -\theta(t)) = \langle x(t), 0\rangle$ on M and the vector field

$$V(t) = R(\gamma'(t), -\theta(t)) = \langle x'(t), x_{n-1}(t)\theta'(t)\rangle \tag{4-3}$$

along η. Therefore, to compare the relative positions of $\gamma(t)$ to $M_{\theta(t)}$ at different values of t, we instead compare $V(t)$ along $\eta(t)$ on M at different t-values. This requires a way of comparing the geometry of M at different points along the curve $\eta(t)$, which is exactly what parallel transport along η can do. Let ∇ denote the connection on M induced by the Euclidean metric on $\mathbb{R}^n$. We define a loxodrome $\gamma(t)$, where $t \in (a, b)$, by the equation

$$\nabla_{\eta'(t)} V(t) = 0 \quad \text{for all } t \in (a, b).$$

From (4-3), we have $V(t) = \eta'(t) + x_{n-1}(t)\psi'(t)\vec{N}$, where $\vec{N} = \langle 0, \ldots, 0, 1\rangle$, the unit normal vector to $\mathbb{R}^{n-1} \times \{0\}$. It follows that

$$
\begin{aligned}
0 = \nabla_{\eta'(t)} V(t) &= \nabla_{\eta'(t)}\big(\eta'(t) + x_{n-1}(t)\psi'(t)\vec{N}\big) \\
&= \nabla_{\eta'(t)}\eta'(t) + \frac{d}{dt}(x_{n-1}(t)\psi'(t))\vec{N} + x_{n-1}\psi'(t)\nabla_{\eta'(t)}\vec{N} \\
&= \nabla_{\eta'(t)}\eta'(t) + \frac{d}{dt}(x_{n-1}(t)\psi'(t))\vec{N},
\end{aligned}
$$

which is equivalent to the pair of equations

$$
\begin{cases}
\nabla_{\eta'(t)}\eta'(t) = 0, \\
\psi'(t)x_{n-1}(t) = c,
\end{cases}
\tag{4-4}
$$

where c is a constant. The first equation in the coupled system (4-4) is the geodesic equation, and the second equation gives the angle of rotation along the geodesic η. In other words, each loxodrome on S is obtained by rotating a geodesic of M by the angle $\psi(t) = k\int dt/x_{n-1}(t)$, where k is a constant and $x_{n-1}(t)$ is the $(n-1)$-th component of the geodesic. Note that our definition of loxodrome is consistent with the definition of loxodrome on surfaces, since on a surface $\eta(t) = \gamma(t)$ and the second equation in (4-4) is the same as (3-2).

Example 4. The $(n-1)$-dimensional sphere $\mathbb{S}^{n-1}$ is a hypersurface of revolution with profile manifold $\mathbb{S}^{n-2}$. To obtain the parametric equations of an arbitrary loxodrome on $\mathbb{S}^{n-1}$, we first need to find the parametric equations of an arbitrary geodesic

on $\mathbb{S}^{n-2}$. Geodesics on $\mathbb{S}^{n-2}$ are the great circles. Each great circle is the intersection of the sphere with a two-dimensional plane $\mathcal{P}$ that passes through the origin. Choose an orthonormal basis $\{\boldsymbol{u}, \boldsymbol{v}\}$ in $\mathcal{P}$. Then the great circle $\mathbb{S}^2 \cap \mathcal{P}$ can be parametrized as

$$\gamma(\theta) = \boldsymbol{u} \cos\theta + \boldsymbol{v} \sin\theta, \quad 0 \le \theta \le 2\pi.$$

From (4-4), we must have

$$\psi'(\theta) = \frac{c}{u_{n-1} \cos\theta + v_{n-1} \sin\theta} = A \cdot \sec(\theta + \theta_0),$$

where A and θ_0 are constants that depend on u_{n-1}, v_{n-1}. It follows that

$$\psi(\theta) = A \ln|\sec(\theta + \theta_0) + \tan(\theta + \theta_0)| + B,$$

and consequently, the general equation of a loxodrome on $\mathbb{S}^3$ is given by

$$x_i(\theta) = u_i \cos\theta + v_i \sin\theta, \quad 1 \le i \le n - 2,$$
$$x_{n-1}(\theta) = (u_{n-1} \cos\theta + v_{n-1} \sin\theta) \cos\big(A \ln|\sec(\theta + \theta_0) + \tan(\theta + \theta_0)| + B\big),$$
$$x_n(\theta) = (u_{n-1} \cos\theta + v_{n-1} \sin\theta) \sin\big(A \ln|\sec(\theta + \theta_0) + \tan(\theta + \theta_0)| + B\big).$$

References

[Alexander 2004] J. Alexander, "Loxodromes: a rhumb way to go", *Math. Mag.* **77**:5 (2004), 349–356. MR Zbl

[Bennett 1996] G. G. Bennett, "Practical rhumb line calculations on the spheroid", *J. Navigation* **49**:1 (1996), 112–119.

[Carlton-Wippern 1992] K. C. Carlton-Wippern, "On loxodromic navigation", *J. Navigation* **45**:2 (1992), 292–297.

[do Carmo and Dajczer 1983] M. do Carmo and M. Dajczer, "Rotation hypersurfaces in spaces of constant curvature", *Trans. Amer. Math. Soc.* **277**:2 (1983), 685–709. MR Zbl

[Coll and Harrison 2013] V. Coll and M. Harrison, "Hypersurfaces of revolution with proportional principal curvatures", *Adv. Geom.* **13**:3 (2013), 485–496. MR Zbl

[Smart 1946] W. M. Smart, "On a problem in navigation", *Monthly Not. Roy. Astr. Soc.* **106** (1946), 124–127. MR Zbl

[Williams 1950] J. E. D. Williams, "Loxodromic distances on the terrestrial spheroid", *J. Navigation* **3**:2 (1950), 133–140.

[Zhang 2012] Z. Zhang, "Remarks on hypersurfaces of revolution in Euclidean space $\mathbb{R}^{n+1}$", *Inter. J. Pure Appl. Math.* **77**:5 (2012), 595–604.

jm20blac@siena.edu   *School of Science, Siena College, 515 Loudon Road, Loudonville, NY 12211, United States*

am06duke@siena.edu   *School of Science, Siena College, 515 Loudon Road, Loudonville, NY 12211, United States*

mjavaheri@siena.edu   *School of Science, Siena College, 515 Loudon Road, Loudonville, NY 12211, United States*

msp

Existence of positive solutions for
an approximation of stationary mean-field games

Nojood Almayouf, Elena Bachini, Andreia Chapouto, Rita Ferreira,
Diogo Gomes, Daniela Jordão, David Evangelista Junior,
Avetik Karagulyan, Juan Monasterio, Levon Nurbekyan,
Giorgia Pagliar, Marco Piccirilli, Sagar Pratapsi, Mariana Prazeres,
João Reis, André Rodrigues, Orlando Romero, Maria Sargsyan,
Tommaso Seneci, Chuliang Song, Kengo Terai, Ryota Tomisaki,
Hector Velasco-Perez, Vardan Voskanyan and Xianjin Yang

(Communicated by Kenneth S. Berenhaut)

Here, we consider a regularized mean-field game model that features a low-order regularization. We prove the existence of solutions with positive density. To do so, we combine a priori estimates with the continuation method. In contrast with high-order regularizations, the low-order regularizations are easier to implement numerically. Moreover, our methods give a theoretical foundation for this approach.

1. Prologue

On August 22, 2015, eighteen young mathematicians (B.Sc. and M.Sc. students) arrived at King Abdullah University of Science and Technology (KAUST) in Thuwal, Kingdom of Saudi Arabia. They were participants in the first KAUST summer camp in applied partial differential equations. Among them were Argentinians, Armenians, Chinese, Italians, Japanese, Mexicans, Portuguese, and Saudis. For many of them, this was their first time abroad. All were looking forward to the following three weeks.

We designed the summer camp to give an intense hands-on three-week Ph.D. experience. It comprised courses, seminars, a project, and a final presentation. The

project was an essential component of the summer camp, and its main outcome is the present paper. Our objectives were to introduce students to an active research topic, teach effective paper writing techniques, and develop their presentation skills. Numerous challenges lay ahead. First, we had three weeks to achieve these goals. Second, students had distinct backgrounds. Third, we planned to study a research-level problem, not a simple exercise.

We selected a problem in mean-field games, a recent and active area of research. The primary goal was to prove the existence of solutions of a system of partial differential equations. To avoid unnecessary technicalities, we considered the one-dimensional case, where the partial differential equations become ordinary differential equations. The project involved partial differential equation methods that are usually taught in advanced courses: a priori estimate methods, the infinite-dimensional implicit function theorem, and the continuation method. In spite of the elementary nature of the proofs, the results presented here are a relevant and original contribution to the theory of mean-field games.

We divided the students into five groups and assigned tasks to each of them. Roughly, each of the sections of this paper corresponds to a task. The students were given a rough statement of the results to be proven, and their task was to figure out the appropriate assumptions, the precise statements, and the proofs. The work of the different groups had to be coordinated to make sure that the assumptions, results, and proofs fit nicely with each other and that duplicate work was avoided. Several KAUST graduate students and postdocs were of invaluable help in this regard.

This project would not have been possible within such a short time frame without the use of new technologies. The paper was written in a collaborative fashion using the platform Authorea that allowed all the groups to work simultaneously. In this way, all groups had access to the latest version of the assumptions and to the current statements of the theorems and propositions. Each group could easily comment and make corrections on other group's work.

This project illustrates how research in mathematics can be a collaborative experience even with a large number of participants. Moreover, it gave each of the students in the summer camp a glimpse of real research in mathematics. Finally, this was the first experience for the Ph.D. students and postdocs who helped in this project in mentoring and advising students. This summer camp was a unique and valuable experience for all participants whose results we share in this paper.

2. Introduction

Mean-field game (MFG) theory is the study of strategic decision making in large populations of small interacting individuals who are also called agents or players. The MFG framework was developed in the engineering community by Caines,

Huang, and Malhamé [Huang et al. 2006; 2007] and in the mathematical community by Lasry and Lions [2006a; 2006b; 2007]. These games model the behavior of rational agents who play symmetric differential games. In these problems, each player chooses their optimal strategy in view of global (or macroscopic) statistical information on the ensemble of players. This approach leads to novel problems in nonlinear equations. Current research topics are the applications of MFGs (including, for example, growth theory in economics and environmental policy), mathematical problems related to MFGs (existence, uniqueness, and regularity questions), and numerical methods in the MFGs framework (discretization, convergence, and efficient implementation).

Here, we consider the following problem:

Problem 1. Let $\mathbb{T} = \mathbb{R}/\mathbb{Z}$ denote the one-dimensional torus, identified with the interval $[0, 1]$ whenever convenient. Fix a C^2 Hamiltonian, $H : \mathbb{R} \to \mathbb{R}$, and a continuous potential, $V : \mathbb{T} \to \mathbb{R}$. Let α and ϵ be positive numbers with $\epsilon \leq 1$ for definedness. Find $u, m \in C^2(\mathbb{T})$ satisfying $m > 0$ and

$$\begin{cases} u - u_{xx} + H(u_x) + V(x) = m^\alpha + \epsilon(m - m_{xx}), \\ m - m_{xx} - (H'(u_x)m)_x = 1 - \epsilon(u - u_{xx}). \end{cases} \quad (2\text{-}1)$$

In this problem, m is the distribution of players and $u(x)$ is the value function for a typical player in the state x. We stress that the condition $m > 0$ is an essential component of the problem. So, if (u, m) solves Problem 1, we require m to be strictly positive. We will show the existence of solutions to this problem under suitable assumptions on the Hamiltonian that are described in Section 3. An example that satisfies those assumptions is $H(p) = (1 + p^2)^{\gamma/2}$ with $1 < \gamma < 2$ and any $V : \mathbb{T} \to \mathbb{R}$ of class C^2.

When $\epsilon = 0$, (2-1) becomes

$$\begin{cases} u - u_{xx} + H(u_x) + V(x) = m^\alpha, \\ m - m_{xx} - (H'(u_x)m)_x = 1. \end{cases} \quad (2\text{-}2)$$

The system in (2-2) is a typical MFG model similar to the one introduced in [Lasry and Lions 2006a]. The Legendre transform of the Hamiltonian, H, given by $L(v) = \sup_p -pv - H(p)$ is the cost in units of time that an agent incurs by choosing to move with a drift v; the potential V accounts for spatial preferences of the agents; the term m^α encodes congestion effects.

The MFG models proposed in [Lasry and Lions 2006a; 2006b] consist of a system of partial differential equations that have (2-2) as a particular case. The current literature covers a broad range of problems, including stationary problems [Gomes et al. 2012; 2014; Gomes and Ribeiro 2013; Gomes and Sánchez Morgado 2014; Pimentel and Voskanyan 2015], heterogeneous populations [Cirant 2015], time-dependent models [Cardaliaguet et al. 2015; Gomes et al. 2015; 2016; Gomes

and Pimentel 2015; 2016; Porretta 2014; 2015], congestion problems [Gomes and Mitake 2015; Graber 2015], and obstacle-type problems [Gomes and Patrizi 2015]. For a recent account of the theory of MFGs, we suggest the survey paper [Gomes and Saúde 2014] and the course [Lions 2012].

The system in (2-1) arises as an approximation of (2-2) that preserves monotonicity properties. Monotonicity-preserving approximations to MFG systems were introduced in [Ferreira and Gomes 2015]. In that paper, the authors consider mean-field games in dimension $d \geq 1$, which include the following example:

$$\begin{cases} u - \Delta u + H(Du, x) + V(x) = m^\alpha + \epsilon(m + \Delta^{2q} m) + \beta_\epsilon(m), \\ m - \Delta m - \operatorname{div}(D_p H(Du, x) m) = 1 - \epsilon(u + \Delta^{2q} u), \end{cases} \tag{2-3}$$

where q is a large enough integer, and β_ϵ is a suitable penalization that satisfies $\beta_\epsilon(m) \to -\infty$ as $m \to 0$. Then, as $\epsilon \to 0$, the solutions of (2-3) converge to solutions of (2-2). Yet, from the perspective of numerical methods, both the high-order degree of (2-3) and the singularity caused by the penalty, β_ϵ, are unsatisfactory due to a poor conditioning of discretizations. Here, we investigate a low-order regularization that may be more suitable for computational problems.

A fundamental difficulty in the analysis of (2-1) is the nonnegativity of m. The Fokker–Planck equation in (2-2) has a maximum principle, and, consequently, $m \geq 0$ for any solution of (2-2). Due to the coupling, this property is not evident in the corresponding equation in (2-1). The previous regularization in (2-3) relies on a penalty that forces the positivity of m. This mechanism does not exist in (2-1), and we are not aware of any general method to prove the existence of positive solutions of (2-1).

Our main result is the following theorem.

Theorem 2.1. *Suppose that Assumptions 1–7 hold* (*see Section 3*). *Then, there exists $\epsilon_0 > 0$ such that for all $0 < \epsilon < \epsilon_0$, Problem 1 admits a $C^{2,1/2}$ solution (u, m).*

Theorem 2.1 introduces a low-order regularization procedure for (2-2) for which existence of solutions can be established without penalty terms. Because high-order regularization methods and penalty terms create serious difficulties in the numerical implementation, this result is relevant to the numerical approximation of (2-2). Moreover, we believe that the techniques we consider here can be extended to higher-dimensional problems.

To prove the main result, we use the continuation method. The first step is to establish a priori estimates for the solutions of (2-1). Then, we replace the potential V by λV for $0 \leq \lambda \leq 1$. For $\lambda = 0$, which corresponds to $V = 0$ in (2-1), we determine an explicit solution. The a priori estimates give that the set Λ of values λ for which (2-1) has a solution is a closed set. Finally, we apply an infinite-dimensional version of the implicit function theorem to show that Λ is relatively open in $[0, 1]$. This proves the existence of solutions.

The remainder of this paper is structured as follows. We discuss the main assumptions in Section 3. Next, in Section 4, we start our study of (2-1) by considering the case $V = 0$ and constructing an explicit solution. Sections 5–9 are devoted to a priori estimates for solutions of (2-1). These estimates include energy and second-order bounds, discussed respectively in Sections 5 and 6, Hölder and $C^{2,1/2}$ estimates, addressed respectively in Sections 7 and 8, and lower bounds on m, given in Section 9. Next, we lay out the main results needed for the implicit function theorem. We introduce the linearized operator in Section 10 and discuss its injectivity and surjectivity properties. Finally, the proof of Theorem 2.1 is presented in Section 11.

3. Main assumptions

We start by recalling that $C^{2,1/2}(\mathbb{T})$ is the space of all functions in $C^2(\mathbb{T})$ whose second derivative is $\frac{1}{2}$-Hölder continuous.

To prove Theorem 2.1, we need to introduce various assumptions that are natural in this class of problems. These encode distinct properties of the Hamiltonian in a convenient way. We begin by stating a polynomial growth condition for the Hamiltonian.

Assumption 1. There exist positive constants, C_1, C_2, C_3, and $\gamma > 1$, such that for all $p \in \mathbb{R}$, the Hamiltonian H satisfies

$$-C_1 + C_2|p|^\gamma \le H(p) \le C_1 + C_3|p|^\gamma.$$

For convex Hamiltonians, the expression $pH'(p) - H(p)$ is the Lagrangian written in momentum coordinates. The next assumption imposes polynomial growth in this quantity.

Assumption 2. There exist positive constants, $\tilde{C}_1$, $\tilde{C}_2$, and $\tilde{C}_3$, such that for all $p \in \mathbb{R}$, we have

$$-\tilde{C}_1 + \tilde{C}_2|p|^\gamma \le pH'(p) - H(p) \le \tilde{C}_1 + \tilde{C}_3|p|^\gamma.$$

Because we look for solutions $(u, m) \in C^{2,1/2}(\mathbb{T}) \times C^{2,1/2}(\mathbb{T})$ of Problem 1, we require in Assumptions 3 and 5 more regularity for V and H.

Assumption 3. The potential V is of class C^2.

Because the Hamilton–Jacobi equation in (2-2) arises from an optimal control problem, it is natural to suppose that the Hamiltonian H is convex.

Assumption 4. H is convex.

Assumption 5. The Hamiltonian H is of class C^4.

Here, we work with subquadratic Hamiltonians. Accordingly, we impose the following condition on γ.

Assumption 6. The constant γ satisfies $\gamma < 2$.

Finally, we state a growth condition on the derivative of the Hamiltonian. The exponent γ is the same as in Assumptions 1 and 2. This is a natural growth condition that the model $H(p) = (1 + |p|^2)^{\gamma/2}$ satisfies.

Assumption 7. There exists a positive constant, $\bar{C}$, such that for all $p \in \mathbb{R}$, we have

$$|H'(p)| \le \bar{C}(1 + |p|^{\gamma-1}).$$

4. The $V = 0$ case

To prove Theorem 2.1, we use the continuation method. More precisely, we consider system (2-1) with V replaced by λV for $0 \le \lambda \le 1$. Next, we show the existence of the solution for all $0 \le \lambda \le 1$. As a starting point, we study the $\lambda = 0$ case; that is, $V = 0$. We show that (2-1) admits a solution in this particular instance.

Proposition 4.1. *Suppose that $V = 0$. Then, there exists an $\epsilon_0 > 0$ such that for all $0 < \epsilon < \epsilon_0$, Problem 1 admits a solution (u, m).*

Proof. We look for constant solutions (u, m). In this case, we have $u_x = u_{xx} = m_x = m_{xx} = 0$. Accordingly, (2-1) reduces to

$$\begin{cases} u + H(0) = m^\alpha + \epsilon m, \\ m = 1 - \epsilon u. \end{cases}$$

In the previous system, solving the first equation for u and replacing the resulting expression into the second, we get

$$\epsilon m^\alpha + (1 + \epsilon^2)m - 1 - \epsilon H(0) = 0. \tag{4-1}$$

We set $g(m) = \epsilon m^\alpha + (1 + \epsilon^2)m - 1 - \epsilon H(0)$, so that (4-1) reads $g(m) = 0$. Next, we notice that $g(0) = -1 - \epsilon H(0)$. For small enough $\epsilon_0 > 0$ and for all $0 < \epsilon < \epsilon_0$, we have $g(0) < 0$. On the other hand, if we take a constant $C > |H(0)|$, we have

$$g(1 + \epsilon C) > 1 + \epsilon C - 1 - \epsilon H(0) = \epsilon(C - H(0)) > 0.$$

Because $0 < 1 + \epsilon C$, by the intermediate value theorem, there exists a constant $m_0 \in]0, 1 + \epsilon C[$ such that $g(m_0) = 0$. Then, setting $u_0 = (1 - m_0)/\epsilon$, we conclude that the pair (u_0, m_0) satisfies the requirements. $\square$

Remark 4.2. Note that if $H(0) > 0$, then $g(0) < 0$ and $g(1 + \epsilon C) > 0$. In this case, the previous proposition holds for all $\epsilon > 0$.

5. Energy estimates

MFG systems such as (2-2) admit many a priori estimates. Among those, energy estimates stand out for their elementary proof — the multiplier method. Here, we apply this method to (2-1).

Proposition 5.1. *Suppose that Assumptions 1 and 2 hold. Let (u, m) solve Problem 1. Then,*

$$\int_0^1 m^{\alpha+1}\,dx + \int_0^1 |u_x|^{\gamma}(1+m)\,dx + \epsilon \int_0^1 (u^2 + m^2 + u_x^2 + m_x^2)\,dx \le C, \quad (5\text{-}1)$$

where C is a universal positive constant depending only on the constants in Assumptions 1 and 2 and on $\|V\|_{L^{\infty}}$.

Proof. We begin by multiplying the first equation in (2-1) by $(1+\epsilon-m)$ and the second one by u. Adding the resulting expressions and integrating, we get

$$\int_0^1 \left[(1+\epsilon)H(u_x)+m(u_x H'(u_x)-H(u_x))\right] dx$$

$$+\int_0^1 m^{\alpha+1}\,dx+\epsilon\int_0^1 (u^2+m^2+u_x^2+m_x^2)\,dx$$

$$=-\epsilon\int_0^1 u\,dx+\int_0^1 (m-1-\epsilon)V(x)\,dx+(1+\epsilon)\int_0^1 m^{\alpha}\,dx+\epsilon(1+\epsilon)\int_0^1 m\,dx, \quad (5\text{-}2)$$

where we used integration by parts and the periodicity of u and m to obtain

$$\int_0^1 mu_{xx}\,dx - \int_0^1 um_{xx}\,dx = 0,$$

$$\int_0^1 u_{xx}\,dx = u_x\big|_0^1 = 0, \qquad \int_0^1 m_{xx}\,dx = m_x\big|_0^1 = 0,$$

$$\int_0^1 mm_{xx}\,dx = -\int_0^1 m_x^2\,dx, \qquad \int_0^1 uu_{xx}\,dx = -\int_0^1 u_x^2\,dx,$$

$$\int_0^1 u(H'(u_x)m)_x\,dx = -\int_0^1 u_x H'(u_x)m\,dx.$$

Next, we observe that by Assumptions 1 and 2, and using the fact that $0 < \epsilon \le 1$, we have

$$\int_0^1 \left[(1+\epsilon)H(u_x) + m(H'(u_x)u_x - H(u_x))\right] dx$$

$$\ge \int_0^1 [-2C_1 - \tilde{C}_1 m + K_0|u_x|^{\gamma}(1+m)]\,dx, \quad (5\text{-}3)$$

where $K_0 := \min\{C_2, \tilde{C}_2\}$.

From (5-2) and (5-3), it follows that

$$
\int_0^1 K_0 |u_x|^\gamma (1+m)\,dx + \int_0^1 m^{\alpha+1}\,dx + \epsilon \int_0^1 (u^2 + m^2 + u_x^2 + m_x^2)\,dx
$$
$$
\leq \frac{\epsilon}{2}\int_0^1 u^2\,dx + \frac{1}{2} + (\|V\|_\infty + 2 + \tilde{C}_1)\int_0^1 m\,dx + 2\int_0^1 m^\alpha\,dx + 2(\|V\|_\infty + C_1), \quad (5\text{-}4)
$$

where we also used the estimates $2u \leq u^2 + 1$ and $0 < \epsilon \leq 1$.

Finally, we observe that for every $\delta_1, \delta_2 > 0$, there exist constants, K_1 and K_2, such that

$$
\int_0^1 m^\alpha\,dx \leq \delta_1 \int_0^1 m^{\alpha+1}\,dx + K_1, \quad \int_0^1 m\,dx \leq \delta_2 \int_0^1 m^{\alpha+1}\,dx + K_2. \quad (5\text{-}5)
$$

Consequently, taking $\delta_1 = \frac{1}{8}$ and $\delta_2 = 1/(4(\|V\|_\infty + 2 + \tilde{C}_1))$ in (5-5) and using the resulting estimates in (5-4), we conclude that (5-1) holds. □

Corollary 5.2. *Suppose that Assumptions 1 and 2 hold. Let (u, m) solve Problem 1. Then,*

$$
\int_0^1 m\,dx \leq C,
$$

where C is a universal positive constant depending only on the constants in Assumptions 1 and 2 and on $\|V\|_{L^\infty}$.

Proof. Due to (5-1) and because m is positive,

$$
\int_0^1 m^{\alpha+1}\,dx \leq C,
$$

where C is a universal positive constant depending only on the constants in Assumptions 1 and 2 and on $\|V\|_{L^\infty}$. Consequently, using Young's inequality, we have

$$
\int_0^1 m\,dx \leq \frac{1}{\alpha+1}\int_0^1 m^{\alpha+1}\,dx + \frac{\alpha}{\alpha+1} \leq \frac{C}{\alpha+1} + \frac{\alpha}{\alpha+1}. \quad \square
$$

6. Second-order estimates

We proceed in our study of (2-1) by examining another technique to obtain a priori estimates. These estimates give additional control over high-order norms of the solutions.

Proposition 6.1. *Suppose that Assumption 3 holds. Let (u, m) solve Problem 1. Then, we have*

$$
\int_0^1 (H''(u_x)u_{xx}^2 m + \alpha m^{\alpha-1} m_x^2)\,dx + \epsilon \int_0^1 (m_x^2 + m_{xx}^2 + u_x^2 + u_{xx}^2)\,dx \leq C, \quad (6\text{-}1)
$$

where $C > 0$ denotes a universal constant depending only on $\|V\|_{C^2}$. Moreover, under Assumption 4,

$$\int_0^1 \alpha m^{\alpha-1} m_x^2 \, dx + \epsilon \int_0^1 (m_x^2 + m_{xx}^2 + u_x^2 + u_{xx}^2) \, dx \leq C. \tag{6-2}$$

Proof. To simplify the notation, we represent by C any positive constant that depends only on $\|V\|_{C^2}$ and whose value may change from one instance to another.

Multiplying the first equation in (2-1) by m_{xx} and the second one by u_{xx} yields

$$(u - u_{xx} + H(u_x) + V(x))m_{xx} = (m^\alpha + \epsilon(m - m_{xx}))m_{xx},$$

$$(m - m_{xx} - (H'(u_x)m)_x)u_{xx} = (1 - \epsilon(u - u_{xx}))u_{xx}.$$

Subtracting the above equations integrated over $[0, 1]$ gives

$$\int_0^1 (um_{xx} - mu_{xx} + u_{xx}) \, dx + \int_0^1 [H(u_x)m_{xx} + (H'(u_x)m)_x u_{xx}] \, dx$$

$$+ \int_0^1 V(x)m_{xx} \, dx - \int_0^1 m^\alpha m_{xx} \, dx + \epsilon \int_0^1 (-mm_{xx} + m_{xx}^2 - uu_{xx} + u_{xx}^2) \, dx = 0. \tag{6-3}$$

Next, we evaluate each of the integrals above. Using the integration by parts formula and the periodicity of boundary conditions, we have

$$\int_0^1 (um_{xx} - mu_{xx} + u_{xx}) \, dx = 0. \tag{6-4}$$

In addition,

$$\int_0^1 [(H'(u_x)m)_x u_{xx} + H(u_x)m_{xx}] \, dx$$

$$= \int_0^1 [H''(u_x)mu_{xx}^2 + (H(u_x))_x m_x + (H(u_x))m_{xx}] \, dx$$

$$= \int_0^1 H''(u_x)mu_{xx}^2 \, dx. \tag{6-5}$$

Furthermore, we have

$$-\int_0^1 m^\alpha m_{xx} \, dx = \int_0^1 \alpha m^{\alpha-1} m_x^2 \, dx \tag{6-6}$$

and

$$\int_0^1 -Vm_{xx} \, dx = -\int_0^1 V_{xx}m \, dx \leq \int_0^1 |V_{xx}|m \, dx \leq C \int_0^1 m \, dx \leq C, \tag{6-7}$$

where we used Corollary 5.2.

Finally,

$$\epsilon \int_0^1 (-mm_{xx} + m_{xx}^2 - uu_{xx} + u_{xx}^2)\, dx = \epsilon \int_0^1 (m_x^2 + m_{xx}^2 + u_x^2 + u_{xx}^2)\, dx. \quad (6\text{-}8)$$

Using (6-3)–(6-8), we get

$$\int_0^1 H''(u_x)mu_{xx}^2\, dx + \int_0^1 \alpha m^{\alpha-1}m_x^2\, dx$$
$$+ \epsilon \int_0^1 (m_x^2 + m_{xx}^2 + u_x^2 + u_{xx}^2)\, dx = -\int_0^1 Vm_{xx} \le C.$$

This completes the proof of (6-1). To conclude the proof of Proposition 6.1, we observe that Assumption 4 implies that H'' is a nonnegative function, which together with (6-1) gives (6-2). □

7. Hölder continuity

We recall that Morrey's theorem in one dimension [Evans 1998] gives the following result.

Proposition 7.1. *Let* $f \in C^1(\mathbb{T})$. *Then,*

$$|f(x) - f(y)| \le \|f_x\|_{L^2}|x - y|^{1/2} \quad \forall x, y \in \mathbb{T}.$$

Proposition 7.2. *Suppose that Assumptions 1–4 hold. Let* (u, m) *solve Problem 1. Then,* u, u_x, m, *and* m_x *are* $\frac{1}{2}$-*Hölder continuous functions with* L^∞-*norms and Hölder constants bounded by* $C/\sqrt{\epsilon}$, *where* C *is a universal constant depending only on the constants in Assumptions 1 and 2 and on* $\|V\|_{C^2}$.

Proof. By Proposition 5.1, we have that

$$\epsilon \int_0^1 (m^2 + u^2 + m_x^2 + u_x^2)\, dx \le C, \quad (7\text{-}1)$$

where C is a universal constant depending only on the constants in Assumptions 1 and 2 and on $\|V\|_{L^\infty}$.

According to Proposition 7.1, we have

$$|u(x) - u(y)| \le \|u_x\|_{L^2}|x - y|^{1/2} \quad \forall x, y \in \mathbb{T}. \quad (7\text{-}2)$$

Moreover, combining the bound on $\|u\|_{L^2}$ given by (7-1), the mean-value theorem for definite integrals, and the Hölder continuity given by (7-2), we get the L^∞ bound on u. A similar inequality holds for m. Next, we observe that Proposition 6.1 (see (6-2)) gives bounds for $\|u_{xx}\|_{L^2}$ and $\|m_{xx}\|_{L^2}$ of the same type as (7-1). Accordingly, the functions u_x and m_x are also $\frac{1}{2}$-Hölder continuous, and their L^∞ norms are

bounded by $C/\sqrt{\epsilon}$, where C depends only on the constants in Assumptions 1 and 2 and on $\|V\|_{C^2}$. □

Remark 7.3. Consider Problem 1 with V replaced by λV for some $\lambda \in [0, 1]$. By revisiting the proofs of Propositions 5.1 and 6.1, we can readily check that the bounds stated in these propositions are uniform with respect to $\lambda \in [0, 1]$. More precisely, (5-1), (6-1), and (6-2) are still valid for a universal positive constant C that depends only on the constants in Assumptions 1 and 2 and on $\|V\|_{C^2}$. In particular, Proposition 7.2 remains unchanged.

8. Higher regularity

The bounds in the previous section give Hölder regularity for any solution (u, m) of Problem 1 and for its derivatives (u_x, m_x). Here, we use (2-1) to improve this result and prove Hölder regularity for u_{xx} and m_{xx}.

Proposition 8.1. *Suppose that Assumptions 1–5 hold. Let (u, m) solve Problem 1. Then $(u, m) \in C^{2,1/2}(\mathbb{T}) \times C^{2,1/2}(\mathbb{T})$.*

Proof. Solving for $m - m_{xx}$ in the second equation of (2-1) and replacing the resulting expression in the first equation yields

$$[1+\epsilon^2+\epsilon H''(u_x)m]u_{xx} = (1+\epsilon^2)u + H(u_x) - \epsilon + V(x) - m^\alpha - \epsilon H'(u_x)m_x. \quad (8\text{-}1)$$

Because H is convex, we have $H''(u_x) \geq 0$. Consequently, $1 + \epsilon^2 + \epsilon H''(u_x)m \geq 1 > 0$. This allows us to rewrite (8-1) as

$$u_{xx} = \frac{(1+\epsilon^2)u + H(u_x) - \epsilon + V(x) - m^\alpha - \epsilon H'(u_x)m_x}{1 + \epsilon^2 + \epsilon H''(u_x)m}. \quad (8\text{-}2)$$

Because u, m, u_x, and m_x are $\frac{1}{2}$-Hölder continuous and because H and H' are locally Lipschitz functions, it follows that

$$(1 + \epsilon^2)u + H(u_x) - \epsilon + V(x) - m^\alpha - \epsilon H'(u_x)m_x$$

is also $\frac{1}{2}$-Hölder continuous. Similarly, due to Assumption 5, $1+\epsilon^2+\epsilon H''(u_x)m$ is also $\frac{1}{2}$-Hölder continuous and bounded from below by 1. Therefore, u_{xx} is $\frac{1}{2}$-Hölder continuous; thus, $u \in C^{2,1/2}(\mathbb{T})$.

Finally, we observe that the second equation in (2-1) is equivalent to

$$m_{xx} = m + \epsilon(u - u_{xx}) - 1 - H''(u_x)mu_{xx} - H'(u_x)m_x. \quad (8\text{-}3)$$

Hence, analogous arguments to those used above yield that m_{xx} is also $\frac{1}{2}$-Hölder continuous. Thus, $m \in C^{2,1/2}(\mathbb{T})$. □

9. Lower bounds on m

Here, we establish our last a priori estimate, which gives lower bounds on m. We begin by proving an auxiliary result.

Lemma 9.1. *Suppose that Assumptions 1–4, 6, and 7 hold. Let (u, m) solve Problem 1. Then, $\|\epsilon(u - u_{xx})\|_\infty \leq C\epsilon^{1-\gamma/2}$, where C is a universal positive constant depending only on the constants in Assumptions 1, 2, and 7 and on $\|V\|_{C^2}$.*

Proof. To simplify the notation, C represents a positive constant depending only on the constants in Assumptions 1, 2, and 7 and on $\|V\|_{C^2}$ and whose value may change from one instance to another.

Note that $\max\{\epsilon^{1/2}, \epsilon, \epsilon^{2-\gamma/2}, \epsilon^{3/2}, \epsilon^2\} \leq \epsilon^{1-\gamma/2}$ because $0 < 1 - \frac{1}{2}\gamma < \frac{1}{2}$ (see Assumption 6).

By Proposition 7.2, we have that $\|u\|_\infty \leq C/\sqrt{\epsilon}$. Thus,

$$\|\epsilon u\|_\infty \leq C\epsilon^{1-\gamma/2}. \tag{9-1}$$

Next, we examine $\|\epsilon u_{xx}\|_\infty$. The identity (8-2) and the condition $1 + \epsilon^2 + \epsilon H''(u_x)m > 1$ give

$$\|\epsilon u_{xx}\|_\infty \leq \|\epsilon(1 + \epsilon^2)u\|_\infty + \|\epsilon H(u_x)\|_\infty$$
$$+ \epsilon^2 + \|\epsilon V\|_\infty + \|\epsilon m^\alpha\|_\infty + \|\epsilon^2 H'(u_x)m_x\|_\infty. \tag{9-2}$$

By (9-1) and by the boundedness of V, it follows that

$$\|\epsilon(1 + \epsilon^2)u\|_\infty + \epsilon^2 + \|\epsilon V\|_\infty \leq C\epsilon^{1-\gamma/2}.$$

According to Propositions 5.1 and 6.1, we have

$$\int_0^1 m^{\alpha+1}\, dx \leq C \quad \text{and} \quad \int_0^1 \alpha m^{\alpha-1}m_x^2\, dx = \frac{4\alpha}{(\alpha+1)^2}\int_0^1 (m^{(\alpha+1)/2})_x^2\, dx \leq C.$$

The first integral guarantees that there exists $x_0 \in \mathbb{T}$ such that $m^{(\alpha+1)/2}(x_0) \leq C$. Then, because $m > 0$ and because $m \in C^1(\mathbb{T})$, the second integral together with Proposition 7.1 implies that for all $x \in \mathbb{T}$,

$$0 < m^\alpha(x) = (m^{\alpha/2}(x))^2 \leq \left(m^{(\alpha+1)/2}(x) - m^{(\alpha+1)/2}(x_0) + m^{(\alpha+1)/2}(x_0) + 1\right)^2 \leq C.$$

Hence, $\|\epsilon m^\alpha\|_\infty \leq C\epsilon^{1-\gamma/2}$.

Assumption 1 and Proposition 7.2 give

$$|H(u_x)| \leq C(1 + \epsilon^{-\gamma/2}).$$

This implies that $\|\epsilon H(u_x)\|_\infty \leq C\epsilon^{1-\gamma/2}$.

Combining Assumption 7 with Proposition 7.2 gives the bound

$$|H'(u_x)| \leq C(1 + \epsilon^{-(\gamma-1)/2}).$$

By Proposition 7.2, we have that $|m_x| \leq C/\sqrt{\epsilon}$. Therefore,

$$\|\epsilon^2 H'(u_x)m_x\|_\infty \leq C\epsilon^{1-\gamma/2}.$$

Collecting all the estimates proved above, we conclude from (9-1) and (9-2) that

$$\|\epsilon(u - u_{xx})\|_\infty \leq C\epsilon^{1-\gamma/2}. \qquad \square$$

Proposition 9.2. *Suppose that Assumptions 1–4, 6, and 7 hold. Let*

$$\bar\epsilon_0 := \left(\frac{1}{2C}\right)^{2/(2-\gamma)},$$

where C is the constant given by Lemma 9.1. Let (u, m) solve Problem 1 with $0 < \epsilon < \min\{1, \bar\epsilon_0\}$. Then, there exists $\bar m > 0$ such that $m > \bar m$ on $\mathbb{T}$. Moreover, $\bar m$ is a universal constant depending only on the constants in Assumptions 1, 2, and 7, on $\|V\|_{C^2}$, and on ϵ.

Proof. Multiplying the second equation in (2-1) by $1/m$ and integrating with respect to x in $[0, 1]$, we obtain

$$\int_0^1 \left(1 - \frac{m_{xx}}{m} - \frac{(H'(u_x)m)_x}{m}\right) dx = \int_0^1 \left(\frac{1}{m} - \epsilon\frac{u - u_{xx}}{m}\right) dx. \qquad (9\text{-}3)$$

Integration by parts and periodicity yield

$$\int_0^1 \frac{m_{xx}}{m} dx = \int_0^1 \frac{m_x^2}{m^2} dx.$$

Then, (9-3) can be rewritten as

$$\int_0^1 \left(\frac{1}{m} + \frac{m_x^2}{m^2}\right) dx = 1 + \int_0^1 \frac{\epsilon(u - u_{xx})}{m} dx - \int_0^1 \frac{(H'(u_x)m)_x}{m} dx.$$

Next, we estimate the right-hand side of this identity. By Lemma 9.1, for $0 < \epsilon < \bar\epsilon_0$, we have $\|\epsilon(u - u_{xx})\|_\infty < \frac{1}{2}$. Consequently,

$$\int_0^1 \left(\frac{1}{2m} + \frac{m_x^2}{m^2}\right) dx \leq 1 + \left|\int_0^1 \frac{(H'(u_x)m)_x}{m} dx\right| = 1 + \left|\int_0^1 H'(u_x)\frac{m_x}{m} dx\right|, \qquad (9\text{-}4)$$

where in the last equality we used the integration by parts formula and the periodicity of u_x. In view of Cauchy's inequality, we conclude that

$$\left|\int_0^1 H'(u_x)\frac{m_x}{m} dx\right| \leq \int_0^1 \left|H'(u_x)\frac{m_x}{m}\right| dx \leq \int_0^1 \left(\frac{(H'(u_x))^2}{2} + \frac{m_x^2}{2m^2}\right) dx. \qquad (9\text{-}5)$$

Invoking Assumptions 6 and 7, we obtain the estimates

$$(H'(u_x))^2 \leq \bar C^2(1 + |u_x|^{\gamma-1})^2 \leq 2\bar C^2(1 + |u_x|^{2(\gamma-1)}) \leq 2\bar C^2(2 + |u_x|^2)$$

in $\mathbb{T}$. These estimates, (9-4), (9-5), and Proposition 5.1 yield

$$\int_0^1 \left(\frac{1}{2m} + \frac{m_x^2}{2m^2} \right) dx \leq 1 + \bar{C}^2 (2 + C/\epsilon).$$

Consequently, for $\tilde{C} = 2 + 2\bar{C}^2(2 + C/\epsilon)$, we obtain the bounds

$$\int_0^1 \frac{1}{m} \, dx \leq \tilde{C} \quad \text{and} \quad \int_0^1 \frac{m_x^2}{m^2} \, dx = \int_0^1 (\ln(m))_x^2 \, dx \leq \tilde{C}.$$

The first bound implies that there exists $x_0 \in \mathbb{T}$ such that $1/(m(x_0)) \leq \tilde{C} + 1$; that is, $\ln(m(x_0)) \geq -\ln(\tilde{C}+1)$. The second bound, together with Proposition 7.1, implies that for all $x \in \mathbb{T}$, the value of $|\ln(m(x)) - \ln(m(x_0))| \leq \sqrt{\tilde{C}}$. Hence, for all $x \in \mathbb{T}$,

$$m(x) \geq e^{-\sqrt{\tilde{C}} - \ln(\tilde{C}+1)}. \qquad \square$$

Remark 9.3. As in Remark 7.3, the statement of Proposition 9.2 remains unchanged if we replace V by λV for some $\lambda \in [0, 1]$ in Problem 1.

10. The linearized operator

Consider the functional, F, defined for $(u, m, \lambda) \in C^{2,1/2}(\mathbb{T}) \times C^{2,1/2}(\mathbb{T}; \,]0, \infty[) \times [0, 1]$ by

$$F(u, m, \lambda) = \begin{bmatrix} u - u_{xx} + H(u_x) + \lambda V - m^\alpha - \epsilon(m - m_{xx}) \\ m - m_{xx} - (H'(u_x)m)_x - 1 + \epsilon(u - u_{xx}) \end{bmatrix}. \tag{10-1}$$

Note that under Assumption 5, the functional F is a C^1 map between $C^{2,1/2}(\mathbb{T}) \times C^{2,1/2}(\mathbb{T}; \,]0, \infty[) \times [0, 1]$ and $C^{0,1/2}(\mathbb{T}) \times C^{2,1/2}(\mathbb{T})$.

To prove Theorem 2.1, we use the continuation method and show that for every $\lambda \in [0, 1]$, the equation

$$F(u, m, \lambda) = 0 \tag{10-2}$$

has a solution, $(u, m) \in C^{2,1/2}(\mathbb{T}) \times C^{2,1/2}(\mathbb{T}; \,]0, \infty[)$. Theorem 2.1 then follows by taking $\lambda = 1$ and by observing that system (2-1) is equivalent to $F(u, m, 1) = 0$.

The implicit function theorem plays a crucial role in proving the solvability of (10-2). To use this theorem, for each $\lambda \in [0, 1]$, we introduce the linearized operator L of $F(\cdot, \cdot, \lambda)$ at $(u, m) \in C^{2,1/2}(\mathbb{T}) \times C^{2,1/2}(\mathbb{T}; \,]0, \infty[)$; that is,

$$\begin{aligned} L(f, v) &= \frac{\partial F}{\partial \mu}(u + \mu v, m + \mu f, \lambda)\big|_{\mu=0} \\ &= \begin{bmatrix} v - v_{xx} + H'(u_x)v_x - \alpha m^{\alpha-1} f - \epsilon(f - f_{xx}) \\ f - f_{xx} - (H''(u_x)v_x m + H'(u_x)f)_x + \epsilon(v - v_{xx}) \end{bmatrix} \end{aligned} \tag{10-3}$$

for $(f, v) \in C^{2,1/2}(\mathbb{T}) \times C^{2,1/2}(\mathbb{T})$. Under Assumption 5 and because $(u, m) \in C^{2,1/2}(\mathbb{T}) \times C^{2,1/2}(\mathbb{T}; \,]0, \infty[)$, the operator L defines a map from $C^{2,1/2}(\mathbb{T}) \times$

$C^{2,1/2}(\mathbb{T})$ into $C^{0,1/2}(\mathbb{T}) \times C^{0,1/2}(\mathbb{T})$. Moreover, this map is continuous and linear. Next, we show that it is also an isomorphism between $C^{2,1/2}(\mathbb{T}) \times C^{2,1/2}(\mathbb{T})$ and $C^{0,1/2}(\mathbb{T}) \times C^{0,1/2}(\mathbb{T})$.

Proposition 10.1. *Suppose that Assumptions 4 and 5 hold. Fix $\lambda \in [0, 1]$ and assume that $(u, m) \in C^{2,1/2}(\mathbb{T}) \times C^{2,1/2}(\mathbb{T};]0, \infty[)$ satisfies $F(u, m, \lambda) = 0$. Then, the operator L given by (10-3) is an isomorphism between $C^{2,1/2}(\mathbb{T}) \times C^{2,1/2}(\mathbb{T})$ and $C^{0,1/2}(\mathbb{T}) \times C^{0,1/2}(\mathbb{T})$.*

Proof. To prove the proposition, we begin by applying the Lax–Milgram theorem in $H^1(\mathbb{T}) \times H^1(\mathbb{T})$, after which we bootstrap additional regularity. Here, we endow $H^1(\mathbb{T}) \times H^1(\mathbb{T})$ with the inner product

$$\langle (\theta_1, \theta_2), (\bar{\theta}_1, \bar{\theta}_2) \rangle_{H^1(\mathbb{T}) \times H^1(\mathbb{T})} = \int_0^1 (\theta_1 \bar{\theta}_1 + \theta_2 \bar{\theta}_2 + \theta_{1x} \bar{\theta}_{1x} + \theta_{2x} \bar{\theta}_{2x}) \, dx$$

for $(\theta_1, \theta_2), (\bar{\theta}_1, \bar{\theta}_2) \in H^1(\mathbb{T}) \times H^1(\mathbb{T})$.

Consider the bilinear form $B : (H^1(\mathbb{T}) \times H^1(\mathbb{T})) \times (H^1(\mathbb{T}) \times H^1(\mathbb{T})) \to \mathbb{R}$ defined for $(v, f), (w_1, w_2) \in H^1(\mathbb{T}) \times H^1(\mathbb{T})$ by

$$B\left(\begin{pmatrix} v \\ f \end{pmatrix}, \begin{pmatrix} w_1 \\ w_2 \end{pmatrix} \right)$$

$$= \int_0^1 (f + \epsilon v) w_1 \, dx + \int_0^1 [f_x + H''(u_x) v_x m + H'(u_x) f + \epsilon v_x] w_{1x} \, dx$$

$$- \int_0^1 [v + H'(u_x) v_x - \alpha m^{\alpha-1} f - \epsilon f] w_2 \, dx + \int_0^1 (\epsilon f_x - v_x) w_{2x} \, dx.$$

Note that if $(v, f) \in C^{2,1/2}(\mathbb{T}) \times C^{2,1/2}(\mathbb{T})$, then

$$B\left(\begin{pmatrix} v \\ f \end{pmatrix}, \begin{pmatrix} w_1 \\ w_2 \end{pmatrix} \right) = \int_0^1 [-L_1(f, v) w_2 + L_2(f, v) w_1] \, dx, \qquad (10\text{-}4)$$

where L_1 and L_2 are the first and second components of L, respectively.

Next, we prove that B is coercive and bounded in $H^1(\mathbb{T}) \times H^1(\mathbb{T})$. Fix $(v, f), (w_1, w_2) \in H^1(\mathbb{T}) \times H^1(\mathbb{T})$. Using the integration by parts formula and the periodicity of v and f, we obtain

$$B\left(\begin{pmatrix} v \\ f \end{pmatrix}, \begin{pmatrix} v \\ f \end{pmatrix} \right) = \int_0^1 [\alpha m^{\alpha-1} f^2 + H''(u_x) v_x^2 m + \epsilon (v^2 + v_x^2 + f^2 + f_x^2)] \, dx.$$

Because $H'' \geq 0$ by Assumption 4 and because $m > 0$, we have

$$B\left(\begin{pmatrix} v \\ f \end{pmatrix}, \begin{pmatrix} v \\ f \end{pmatrix} \right) \geq \epsilon \left\| \begin{pmatrix} v \\ f \end{pmatrix} \right\|_{H^1(\mathbb{T}) \times H^1(\mathbb{T})}^2,$$

which proves the coercivity of B.

Because m, u, and H are $C^{2,1/2}$-functions on the compact set $[0, 1]$, we have that m, u, m_x, u_x, u_{xx}, H, $H'(u_x)$, and $H''(u_x)$ are bounded. Therefore, there exists a positive constant, C, that depends only on these bounds and for which

$$\left| B\left(\begin{pmatrix} v \\ f \end{pmatrix}, \begin{pmatrix} w_1 \\ w_2 \end{pmatrix} \right) \right| \le C \left\| \begin{pmatrix} v \\ f \end{pmatrix} \right\|_{H^1(\mathbb{T}) \times H^1(\mathbb{T})} \left\| \begin{pmatrix} w_1 \\ w_2 \end{pmatrix} \right\|_{H^1(\mathbb{T}) \times H^1(\mathbb{T})},$$

where we also used Hölder's inequality. This proves the boundedness of B.

Finally, we fix $b = (b_1, b_2) \in C^{0,1/2}(\mathbb{T}) \times C^{0,1/2}(\mathbb{T})$, and we consider the bounded and linear functional $G : H^1(\mathbb{T}) \times H^1(\mathbb{T}) \to \mathbb{R}$ defined for $(w_1, w_2) \in H^1(\mathbb{T}) \times H^1(\mathbb{T})$ by

$$G \begin{pmatrix} w_1 \\ w_2 \end{pmatrix} = \int_0^1 (-b_1 w_2 + b_2 w_1) \, dx.$$

By the Lax–Milgram theorem, there exists a unique $(v, f) \in H^1(\mathbb{T}) \times H^1(\mathbb{T})$ such that for all $(w_1, w_2) \in H^1(\mathbb{T}) \times H^1(\mathbb{T})$, we have

$$B\left(\begin{pmatrix} v \\ f \end{pmatrix}, \begin{pmatrix} w_1 \\ w_2 \end{pmatrix} \right) = G \begin{pmatrix} w_1 \\ w_2 \end{pmatrix}.$$

This is equivalent to saying that for all $(w_1, w_2) \in H^1(\mathbb{T}) \times H^1(\mathbb{T})$,

$$B\left(\begin{pmatrix} v \\ f \end{pmatrix}, \begin{pmatrix} -w_2 \\ w_1 \end{pmatrix} \right) = G \begin{pmatrix} -w_2 \\ w_1 \end{pmatrix} = \int_0^1 (-b_1 w_1 - b_2 w_2) \, dx.$$

From this and (10-4), we conclude that $L(f, v) = b$ has a unique weak solution $(f, v) \in H^1(\mathbb{T}) \times H^1(\mathbb{T})$. Because $b \in C^{0,1/2}(\mathbb{T}) \times C^{0,1/2}(\mathbb{T})$ is arbitrary, L is injective. To prove surjectivity, it suffices to check that the weak solution of $L(f, v) = b$ is in $C^{2,1/2}(\mathbb{T}) \times C^{2,1/2}(\mathbb{T})$. This higher regularity follows from a bootstrap argument.

Fix $b = (b_1, b_2) \in C^{0,1/2}(\mathbb{T}) \times C^{0,1/2}(\mathbb{T})$ and let $(f, v) \in H^1(\mathbb{T}) \times H^1(\mathbb{T})$ be the weak solution of $L(f, v) = b$ given by the Lax–Milgram theorem. Then, we have the following identity in the weak sense:

$$v_{xx} = \frac{g}{1 + \epsilon^2 + \epsilon H''(u_x) m}, \tag{10-5}$$

where

$$g = v(1 + \epsilon^2) + H'(u_x) v_x - \alpha m^{\alpha-1} f - \epsilon v_x (H'(u_x) m)_x \\ - \epsilon (H'(u_x) f)_x - \epsilon b_2 - b_1 \in L^2(\mathbb{T}).$$

We recall that $1 + \epsilon^2 + \epsilon H''(u_x) m > 1$. Hence, $v_{xx} \in L^2(\mathbb{T})$, and so $v \in H^2(\mathbb{T})$. Moreover, because

$$f_{xx} = f - (H''(u_x) v_x m)_x - (H'(u_x) f)_x + \epsilon(v - v_{xx}) - b_2 \tag{10-6}$$

in the weak sense, similar arguments yield $f_{xx} \in L^2(\mathbb{T})$ and $f \in H^2(\mathbb{T})$.

So far, $(f, v) \in C^{1,1/2}(\mathbb{T}) \times C^{1,1/2}(\mathbb{T})$. This implies that $g \in C^{0,1/2}(\mathbb{T})$. Then, using the fact that $1 + \epsilon^2 + \epsilon H''(u_x)m$ also belongs to $C^{0,1/2}(\mathbb{T})$ and is bounded from below by 1, from (10-5) it follows that $v_{xx} \in C^{0,1/2}(\mathbb{T})$. Consequently, in view of (10-6), $f_{xx} \in C^{0,1/2}(\mathbb{T})$. Hence, $(f, v) \in C^{2,1/2}(\mathbb{T}) \times C^{2,1/2}(\mathbb{T})$. Therefore, the unique solution given by the Lax–Milgram theorem is a strong solution with $C^{2,1/2}$ regularity. Thus, L is surjective. Because L is injective and surjective, it is an isomorphism. $\qquad\square$

11. Proof of the main theorem

In this last section, we prove Theorem 2.1. We assume that $\epsilon > 0$ satisfies $\epsilon < \min\{1, \epsilon_0, \bar{\epsilon}_0\}$, where ϵ_0 and $\bar{\epsilon}_0$ are given by Propositions 4.1 and 9.2, respectively.

Let F be the functional defined in (10-1). For each $\lambda \in [0, 1]$, consider the problem of finding $(u, m) \in C^{2,1/2}(\mathbb{T}) \times C^{2,1/2}(\mathbb{T}; \,]0, \infty[)$ satisfying (10-2). From Propositions 4.1 and 8.1, such a pair (u, m) exists for $\lambda = 0$. Next, using the continuation method, we prove that this is true not only for $\lambda = 0$ but also for all $\lambda \in [0, 1]$.

More precisely, let Λ be the set of values $\lambda \in [0, 1]$ for which (10-2) has a solution $(u, m) \in C^{2,1/2}(\mathbb{T}) \times C^{2,1/2}(\mathbb{T})$ with $m \geq \bar{m}$ in $\mathbb{T}$, where $\bar{m} > 0$ is given by Proposition 9.2. Note that $\bar{m}$ does not depend on λ (see Remark 9.3). As we just argued, Λ is a nonempty set. In the subsequent two propositions, we show that Λ is a closed and open subset of $[0, 1]$. Consequently, $\Lambda = [0, 1]$.

Proposition 11.1. *Suppose that Assumptions 1–7 hold. Then, Λ is a closed subset of $[0, 1]$.*

Proof. Let $(\lambda^n)_{n\in\mathbb{N}} \subset \Lambda$ and $\lambda \in [0, 1]$ be such that $\lim_{n\to\infty} \lambda^n = \lambda$. We claim that $\lambda \in \Lambda$.

By definition of Λ, for each $n \in \mathbb{N}$, there exists $(u^n, m^n) \in C^{2,1/2}(\mathbb{T}) \times C^{2,1/2}(\mathbb{T})$ satisfying (10-2) and $m^n \geq \bar{m}$ in $\mathbb{T}$. Then, by Proposition 7.2 (also see Remark 7.3), $(u^n)_{n\in\mathbb{N}}$, $(m^n)_{n\in\mathbb{N}}$, $(u_x^n)_{n\in\mathbb{N}}$, and $(m_x^n)_{n\in\mathbb{N}}$ are uniformly bounded in $C^{0,1/2}(\mathbb{T})$. Consequently, by the Arzelà–Ascoli theorem, we can find $(u, m, \tilde{u}, \tilde{m}) \in C^{0,1/2}(\mathbb{T}) \times C^{0,1/2}(\mathbb{T}) \times C^{0,1/2}(\mathbb{T}) \times C^{0,1/2}(\mathbb{T})$ such that, up to a subsequence that we do not relabel,

$$\lim_{n\to\infty} \|(u^n, m^n, u_x^n, m_x^n) - (u, m, \tilde{u}, \tilde{m})\|_\infty = 0. \qquad (11\text{-}1)$$

We now recall that if $(w^n)_{n\in\mathbb{N}}$ is a sequence of differentiable functions on $[0, 1]$ such that $(w^n)_{n\in\mathbb{N}}$ converges uniformly to some w on $[0, 1]$ and such that $(w_x^n)_{n\in\mathbb{N}}$ converges uniformly on $[0, 1]$, then $w_x = \lim_{n\to\infty} w_x^n$ on $[0, 1]$. Consequently, by (11-1), we have $\tilde{u} = u_x$ and $\tilde{m} = m_x$.

Next, we show that $(u_{xx}^n)_{n\in\mathbb{N}}$ and $(m_{xx}^n)_{n\in\mathbb{N}}$ are also uniformly convergent sequences on [0, 1]. In view of (8-2), we have for every $n \in \mathbb{N}$,

$$u_{xx}^n = \frac{(1+\epsilon^2)u^n + H(u_x^n) - \epsilon + \lambda^n V(x) - (m^n)^\alpha - \epsilon H'(u_x^n)m_x^n}{1 + \epsilon^2 + \epsilon H''(u_x^n)m^n}. \qquad (11\text{-}2)$$

By Assumption 5 and by the uniform convergence of $(u^n, m^n, \lambda^n, u_x^n, m_x^n)_{n\in\mathbb{N}}$ to $(u, m, \lambda, u_x, m_x)$ on [0, 1], it follows from (11-2) that $(u_{xx}^n)_{n\in\mathbb{N}}$ converges uniformly on [0, 1]. Then, the limit of $(u_{xx}^n)_{n\in\mathbb{N}}$ is necessarily u_{xx}. Analogous arguments (see (8-3)) give that $(m_{xx}^n)_{n\in\mathbb{N}}$ converges uniformly to m_{xx} on [0, 1]. Thus, $(u, m) \in C^{2,1/2}(\mathbb{T}) \times C^{2,1/2}(\mathbb{T};]0, \infty[)$. Moreover, $\lim_{n\to\infty} F(u^n, m^n, \lambda^n) = F(u, m, \lambda)$. Finally, because for all $n \in \mathbb{N}$, the functional $F(u^n, m^n, \lambda^n) = 0$ and $m^n \geq \bar{m}$ in $\mathbb{T}$, we have that $F(u, m, \lambda) = 0$ and $m \geq \bar{m}$ in $\mathbb{T}$. Hence, $\lambda \in \Lambda$. □

Proposition 11.2. *Suppose that Assumptions 1–7 hold. Then, Λ is an open subset of* [0, 1].

Proof. Let $\lambda_0 \in \Lambda$. Then, there exists $(u_0, m_0) \in C^{2,1/2}(\mathbb{T}) \times C^{2,1/2}(\mathbb{T})$ satisfying $F(u_0, m_0, \lambda_0) = 0$ and $m_0 \geq \bar{m}$ in $\mathbb{T}$. By Proposition 10.1 and by the implicit function theorem in Banach spaces (see, for example, [Dieudonné 1960]), we can find $\delta > 0$ such that, for every $\lambda^* \in]\lambda - \lambda_0, \lambda + \lambda_0[$, there exists $(u^*, m^*) \in C^{2,1/2}(\mathbb{T}) \times C^{2,1/2}(\mathbb{T})$ satisfying $F(u^*, m^*, \lambda^*) = 0$ and $m^* \geq \bar{m}$ in $\mathbb{T}$. Moreover, the implicit function theorem also guarantees that the map $\lambda^* \mapsto m^*$ is continuous. Hence, if δ is small enough, we have $m^* > 0$ in $\mathbb{T}$. Then, Proposition 9.2 gives $m^* > \bar{m}$ in $\mathbb{T}$. Therefore, $\lambda^* \in \Lambda$ and, consequently, Λ is open. □

Finally, we sum up the proof of our main result.

Proof of Theorem 2.1. Let $\epsilon > 0$ be such that $\epsilon < \min\{1, \epsilon_0, \bar{\epsilon}_0\}$, where ϵ_0 is given by Proposition 4.1 and where $\bar{\epsilon}_0$ is given by Proposition 9.2.

Propositions 11.1 and 11.2 give that Λ is a relatively open and closed set in [0, 1]. It is a nonempty set due to Propositions 4.1, 8.1, and 9.2. Hence, $\Lambda = [0, 1]$. Finally, we observe that Theorem 2.1 corresponds to the $\lambda = 1$ case. □

Acknowledgements

References

[Cardaliaguet et al. 2015] P. Cardaliaguet, P. J. Graber, A. Porretta, and D. Tonon, "Second order mean field games with degenerate diffusion and local coupling", *NoDEA Nonlinear Differential Equations Appl.* **22**:5 (2015), 1287–1317. MR Zbl

[Cirant 2015] M. Cirant, "Multi-population mean field games systems with Neumann boundary conditions", *J. Math. Pures Appl.* (9) **103**:5 (2015), 1294–1315. MR Zbl

[Dieudonné 1960] J. Dieudonné, *Foundations of modern analysis*, Pure and applied mathematics **10**, Academic Press, New York, 1960. Reprinted 1969 as v. 1 of *Treatise on analysis*. MR Zbl

[Evans 1998] L. C. Evans, *Partial differential equations*, Graduate Studies in Mathematics **19**, American Mathematical Society, Providence, RI, 1998. MR Zbl

[Ferreira and Gomes 2015] R. Ferreira and D. Gomes, "Existence of weak solutions to stationary mean-field games through variational inequalities", Preprint, 2015. arXiv

[Gomes and Mitake 2015] D. A. Gomes and H. Mitake, "Existence for stationary mean-field games with congestion and quadratic Hamiltonians", *NoDEA Nonlinear Differential Equations Appl.* **22**:6 (2015), 1897–1910. MR Zbl

[Gomes and Patrizi 2015] D. A. Gomes and S. Patrizi, "Obstacle mean-field game problem", *Interfaces Free Bound.* **17**:1 (2015), 55–68. MR Zbl

[Gomes and Pimentel 2015] D. A. Gomes and E. Pimentel, "Time-dependent mean-field games with logarithmic nonlinearities", *SIAM J. Math. Anal.* **47**:5 (2015), 3798–3812. MR Zbl

[Gomes and Pimentel 2016] D. A. Gomes and E. Pimentel, "Local regularity for mean-field games in the whole space", *Minimax Theory Appl.* **1**:1 (2016), 65–82. MR Zbl

[Gomes and Ribeiro 2013] D. Gomes and R. Ribeiro, "Mean field games with logistic population dynamics", in *52nd IEEE Conference on Decision and Control* (Florence), IEEE, Piscataway, NJ, 2013.

[Gomes and Sánchez Morgado 2014] D. Gomes and H. Sánchez Morgado, "A stochastic Evans–Aronsson problem", *Trans. Amer. Math. Soc.* **366**:2 (2014), 903–929. MR Zbl

[Gomes and Saúde 2014] D. A. Gomes and J. Saúde, "Mean field games models — a brief survey", *Dyn. Games Appl.* **4**:2 (2014), 110–154. MR

[Gomes et al. 2012] D. A. Gomes, G. E. Pires, and H. Sánchez-Morgado, "A-priori estimates for stationary mean-field games", *Netw. Heterog. Media* **7**:2 (2012), 303–314. MR Zbl

[Gomes et al. 2014] D. A. Gomes, S. Patrizi, and V. Voskanyan, "On the existence of classical solutions for stationary extended mean field games", *Nonlinear Anal.* **99** (2014), 49–79. MR Zbl

[Gomes et al. 2015] D. A. Gomes, E. A. Pimentel, and H. Sánchez-Morgado, "Time-dependent mean-field games in the subquadratic case", *Comm. Partial Differential Equations* **40**:1 (2015), 40–76. MR Zbl

[Gomes et al. 2016] D. A. Gomes, E. Pimentel, and H. Sánchez-Morgado, "Time-dependent mean-field games in the superquadratic case", *ESAIM Control Optim. Calc. Var.* **22**:2 (2016), 562–580. MR Zbl

[Graber 2015] J. Graber, "Weak solutions for mean field games with congestion", Preprint, 2015. arXiv

[Huang et al. 2006] M. Huang, R. P. Malhamé, and P. E. Caines, "Large population stochastic dynamic games: closed-loop McKean–Vlasov systems and the Nash certainty equivalence principle", *Commun. Inf. Syst.* **6**:3 (2006), 221–251. MR Zbl

[Huang et al. 2007] M. Huang, P. E. Caines, and R. P. Malhamé, "Large-population cost-coupled LQG problems with nonuniform agents: individual-mass behavior and decentralized ϵ-Nash equilibria", *IEEE Trans. Automat. Control* **52**:9 (2007), 1560–1571. MR

[Lasry and Lions 2006a] J.-M. Lasry and P.-L. Lions, "Jeux à champ moyen, I: le cas stationnaire", *C. R. Math. Acad. Sci. Paris* **343**:9 (2006), 619–625. MR Zbl

[Lasry and Lions 2006b] J.-M. Lasry and P.-L. Lions, "Jeux à champ moyen, II: horizon fini et contrôle optimal", *C. R. Math. Acad. Sci. Paris* **343**:10 (2006), 679–684. MR Zbl

[Lasry and Lions 2007] J.-M. Lasry and P.-L. Lions, "Mean field games", *Jpn. J. Math.* **2**:1 (2007), 229–260. MR Zbl

[Lions 2012] P. Lions, "Course on mean-field games", 2012, http://www.ima.umn.edu/2012-2013/ sw11.12-13.12/.

[Pimentel and Voskanyan 2015] E. Pimentel and V. Voskanyan, "Regularity for second-order stationaty mean-field games", Preprint, 2015. To appear in *Indiana Univ. Math. J.* arXiv

[Porretta 2014] A. Porretta, "On the planning problem for the mean field games system", *Dyn. Games Appl.* **4**:2 (2014), 231–256. MR Zbl

[Porretta 2015] A. Porretta, "Weak solutions to Fokker–Planck equations and mean field games", *Arch. Ration. Mech. Anal.* **216**:1 (2015), 1–62. MR Zbl

nojoud16@gmail.com	*Effat University, Jeddah 23523, Saudi Arabia*
elena.bachini@studenti.unipd.it	*Department of Mathematics, University of Padova, I-35121 Padova, Italy*
a_chapouto@hotmail.com	*University of Coimbra, 5400-000 Chaves, Portugal*
rita.ferreira@kaust.edu.sa	*CEMSE Division, King Abdullah University of Science and Technology (KAUST), Thuwal 23955-6900, Saudi Arabia*
diogo.gomes@kaust.edu.sa	*CEMSE Division, King Abdullah University of Science and Technology (KAUST), Thuwal 23955-6900, Saudi Arabia*
daniela.jordao@hotmail.com	*University of Coimbra, 3001-501 Coimbra, Portugal*
davidsevangelista@gmail.com	*CEMSE Division, King Abdullah University of Science and Technology (KAUST), Thuwal 23955-6900, Saudi Arabia*
bbavo96@yahoo.com	*Faculty of Mathematics and Mechanics, Yerevan State University, Republic of Armenia, Yerevan, 0025, 1 Alex Manoogian, 0025 Yerevan, Armenia*
laterio@gmail.com	*University of Buenos Aires, 1414CKS Buenos Aires, Argentina*
levonnurbekian@gmail.com	*CEMSE Division, King Abdullah University of Science and Technology (KAUST), Thuwal 23955-6900, Saudi Arabia*
pagliagiorgia37@gmail.com	*University of Verona, I-37045 Legnago, Italy*
piccio991@hotmail.it	*University of Rome Tor Vergata, I-35121 Padova, Italy*
sagar.dipak@gmail.com	*University of Coimbra, 4465-040 S. Mamede de Infesta, Portugal*

mariana.prazeres.1@kaust.edu.sa   *CEMSE Division, King Abdullah University of Science and Technology (KAUST), Thuwal 23955-6900, Saudi Arabia*

joao.feliciodosreis@kaust.edu.sa   *CEMSE Division, King Abdullah University of Science and Technology (KAUST), Thuwal 23955-6900, Saudi Arabia*

amr_aac@hotmail.com   *University of Coimbra, 3040-109 Coimbra, Portugal*

orlando_andres2005@hotmail.com

    University of Lisbon, 9000-690 Funchal, Portugal

maria_sargsyan@edu.aua.am   *American University of Armenia, 0025 Yerevan, Armenia*

ttoommxx@gmail.com   *University of Verona, via Brunelleschi 1, I-37178 Verona, Italy*

larrysong@zju.edu.cn   *MIT, Cambridge, MA 02140, United States*

ken5terai@akane.waseda.jp   *Waseda University, Saitama 338-0001, Japan*

ryota-tomisaki@fuji.waseda.jp   *Waseda University, 210-10 Nase, Totsuka, Yokohama 245-00051, Japan*

bigquantum@ciencias.unam.mx   *National Autonomous University of Mexico, Cerro Copor #16, Campestre Churubusco, 02100 Mexico City,, Mexico*

vartanvos@gmail.com   *CEMSE Division, King Abdullah University of Science and Technology (KAUST), Thuwal 23955-6900, Saudi Arabia*

xianjin.yang@kaust.edu.sa   *CEMSE Division, King Abdullah University of Science and Technology (KAUST), Thuwal 23955-6900, Saudi Arabia*

Discrete dynamics of contractions on graphs

Olena Ostapyuk and Mark Ronnenberg

(Communicated by Martin Bohner)

We study the dynamical behavior of functions on vertices of a graph that are contractions in the graph metric. We show that the fixed point set of such functions must be convex. If a function has no fixed points and the graph is a tree, we prove that every dynamical cycle must have an even period and the function behaves eventually like a symmetry.

1. Introduction

This work was inspired by dynamics of analytic functions on the unit disk. The key property of such functions is the point-invariant Schwarz lemma, i.e., that analytic functions are contractions in the hyperbolic metric of the disk. This property allows the proof of various results about iteration of analytic functions; see, for example, the survey paper [Poggi-Corradini 2011].

Our purpose is to study dynamics of contractions in a discrete setting. In particular, we study dynamics on finite graphs (in most cases, trees). A connected graph can be considered as a discrete metric space of vertices with the *graph metric*. Let $G = (V, E)$ be a finite, connected, simple graph with the set of vertices V and the set of edges E. Then for all vertices $x, y \in V$, we say the distance between x and y, denoted $d(x, y)$, is the number of edges in the shortest path connecting x to y. Such path is called a *geodesic*. Note that trees as metric spaces are 0-hyperbolic [Anderson 1999], so we expect them to have some similar properties to the unit disk with hyperbolic metric.

We wish to study contractions (in the graph metric) on the vertices of a graph. Let f be a function on the vertices of G to the vertices of G. We say f is a *contraction* if, for all vertices $x, y \in V$, we have $d(f(x), f(y)) \leq d(x, y)$. We will need some terminology from dynamics. Let f be a function. We denote by $f^{\circ n}(x) = f \circ f \circ f \circ \cdots \circ f(x)$ (n terms) the n-th *iterate* of f. If for some point x and some positive integer n, we have $f^{\circ n}(x) = x$, then we say x is a periodic point, x lies on a *dynamical cycle* of f of period n, or that x lies on a *dynamical n-cycle*

of f. If $f(x) = x$, we say x is a *fixed point* of f. We use the term *dynamical cycle* to distinguish these cycles from the graph cycles.

It is easy to show by induction that, given a contraction f, the map $f^{\circ n}$ is also a contraction for any positive integer n. Dynamical cycles and fixed points will be the main focus of our study.

2. Fixed point sets

Our goal is to characterize the set of fixed points of a contraction on graph vertices. Note that in the general case, the fixed point set can be empty:

Example 2.1. Let G_1 be a graph with four vertices x, y, z, w. Let f be a function on the vertices of G_1 defined by $f(x) = y$, $f(y) = z$, $f(z) = w$, and $f(w) = x$. Then $\{x, y, z, w\}$ forms a dynamical 4-cycle of f (see Figure 1). The map f is clearly a contraction since for all $a, b \in \{x, y, w, z\}$, we have $d(f(a), f(b)) = d(a, b)$. In this case, the set of fixed points of f is empty.

Example 2.2. Let G_2 be a graph with vertices $x_0, x_1, x_2, y_0, y_1, z_0$ and z_1 as shown in Figure 2. Let f be a contraction on the vertices of G_2 such that x_0, x_1, x_2 are fixed by f, and $\{y_0, y_1\}$ and $\{z_0, z_1\}$ are dynamical 2-cycles of f.

Note that one main difference between the two examples is that for any two vertices in G_2, the geodesic connecting them is unique, whereas this is not the case with G_1. Notice also that for any two fixed points in G_2, the geodesic connecting them contains only fixed points.
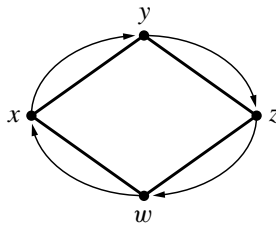
Figure 1. Dynamical 4-cycle.
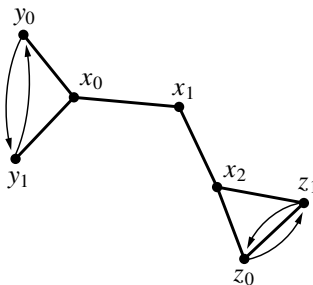
Figure 2. Cycles and fixed points.
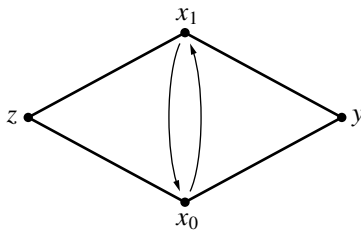
Figure 3. The graph G_3 with nonunique geodesics.

Definition 2.3. Let $G = (V, E)$ be a graph and let $H \subset V$. We say H is *convex* if for any two vertices in H, the geodesic connecting them contains only vertices in H. (See, for example, [Gross and Yellen 2006].)

Thus in Example 2.2, the set of fixed points of f is convex. In fact, this is true in general:

Theorem 2.4. *Let $G = (V, E)$ be a graph such that the geodesic between any two vertices is unique. Let f be a contraction on the vertices of G. Then the set of fixed points of f is convex.*

Proof. Let $x, y \in V$ be fixed by f. Let L be the unique geodesic connecting them. Let $z \in L$. We need to show that $f(z) = z$. We will first show that $f(z) \in L$ and it will follow that $f(z) = z$.

By way of contradiction, suppose $f(z) \notin L$. Then there exist unique geodesics connecting x to $f(z)$ and y to $f(z)$, respectively. We can concatenate these geodesics to construct a walk K connecting x to y, so the length of K is $d(x, f(z)) + d(f(z), y)$ and the length of L is $d(x, z) + d(z, y)$. Since f is a contraction and x and y are fixed points, we have $d(f(z), x) \leq d(z, x)$ and $d(f(z), y) \leq d(z, y)$. Then it follows that $d(x, f(z)) + d(f(z), y) \leq d(x, z) + d(z, y)$. If $d(x, f(z)) + d(f(z), y) = d(x, z) + d(z, y)$, then L is not a unique geodesic between x and y, a contradiction. If $d(x, f(z)) + d(f(z), y) < d(x, z) + d(z, y)$, then K is shorter than L, which is also a contradiction. Thus it must be that $z \in L$.

Now we will show $f(z) = z$. Suppose $f(z) \neq z$. Since $f(z)$ lies on the geodesic L connecting x to y, we have $d(x, z) + d(z, y) = d(x, f(z)) + d(f(z), y) = d(x, y)$. We can assume without loss of generality that $d(x, f(z)) < d(x, z)$, in which case we obtain $d(y, f(z)) = d(x, y) - d(x, f(z)) > d(x, y) - d(x, z) = d(y, z)$, contradicting the fact that f is a contraction. Thus we conclude that $f(z) = z$. $\square$

Note that if for any two points in G the geodesic connecting them is not unique then the conclusion of Theorem 2.4 does not necessarily hold, as can be seen in the following counterexample.

Example 2.5. Let G_3 be a graph with vertices x_0, x_1, y and z as shown in Figure 3. Let f be a contraction such that the vertices z and y are fixed and the points x_0 and x_1 form a dynamical 2-cycle. Note that the geodesic connecting z to y is

not unique, since the path from z to y through x_0 is the same length as the path through x_1. Despite the fact that z and y are fixed and that x_0, x_1 lie on the geodesics connecting them, x_0 and x_1 are clearly not fixed. Thus the conclusion of Theorem 2.4 does not hold in this case.

Corollary 2.6. *Let $G = (V, E)$ be a graph such that for any two vertices in G the geodesic connecting them is unique. Let f be a contraction on V. Suppose f has a dynamical cycle J of period k. Let z be a point which lies on the geodesic connecting two consecutive points in J. Then z lies on a dynamical cycle whose period divides k.*

Proof. Let $x, y \in J$. Let $z \in V$ such that z lies on the geodesic between x and y. Since J is a dynamical cycle of period k, we know $f^{\circ k}(x) = x$ and $f^{\circ k}(y) = y$. Thus x and y are fixed by the k-th iterate of f. Since f is a contraction, any iterate of f is also a contraction. Thus Theorem 2.4 applied to $f^{\circ k}$ implies $f^{\circ k}(z) = z$. So z must lie on a dynamical cycle whose period divides k. □

Now we will consider a particular case when the graph is a tree. For any tree, a path connecting any two points is unique, hence geodesics are unique, so Theorem 2.4 holds. But the converse is also true for trees: any convex set of vertices will be a fixed point set for some contraction.

We will need the following property of a tree structure: in a tree, a concatenation of two geodesics from x to y and from y to z is either a geodesic from x to z or a walk that follows the geodesic connecting x to y until the first common point of the two geodesics, y', then follows the geodesic from y' to y, then goes back to y' along the same geodesic and finally follows the geodesic from y' to z. Note that concatenation of geodesics from x to y' and from y' to z will form a geodesic that connects x to z.

Proposition 2.7. *Let $T = (V, E)$ be a tree and $H \subset V$ be convex set. Then there exists a contraction f such that H is the fixed point set of f.*

Proof. Given H, we define the desired contraction f as follows: for all $x \in V$, $f(x) = y$, where $y \in H$ is the closest vertex to x in H; see Figure 4. Note that such a y is unique. Indeed, suppose $y_1, y_2 \in H$ are at the same shortest distance from $x \notin H$. Apply the property mentioned above the proposition to the concatenation of geodesics connecting y_1 to x and x to y_2. If it is a geodesic, then $x \in H$, which is a contradiction. If instead there is a common point y', then $y' \in H$ and it is closer to x than y_1 and y_2 are, again a contradiction. Thus the point y is unique and the function f is well-defined. Also, H is clearly fixed point set of f.

Now we need to show that f is a contraction. Let $f(x_1) = y_1$ and $f(x_2) = y_2$. Consider a walk following the geodesic from x_1 to y_1, then from y_1 to y_2. If there is a common point of these geodesics other than y_1, then this point is in H and within a shorter distance to x_1 than y_1, which contradicts the construction of y_1. So the
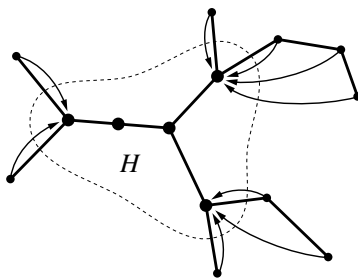
Figure 4. Constructing the contraction f for a given convex subset of vertices H.

concatenation of these two geodesics is the geodesic from x_1 to y_2. Similarly, the geodesic from y_1 to x_2 passes through y_2, and finally, the geodesic from x_1 to x_2 is just a concatenation of those from x_1 to y_1, y_1 to y_2 and y_2 to x_1. So we have

$$d(x_1, x_2) = d(x_1, y_1) + d(y_1, y_2) + d(y_2, x_2) \geq d(y_1, y_2),$$

and f is a contraction. □

3. Contractions with no fixed points

In the previous section, we characterized the set of fixed points of a contraction on the vertices of a graph with unique geodesics, in particular a tree. Next we want to consider the case when a contraction has no fixed points. Then there must exist a dynamical cycle. We will use the following property of periodic points:

Lemma 3.1. *Let G be a finite graph, and f be a contraction on vertices of G. If x and y are two periodic points of f (not necessarily from the same dynamical cycle), then $d(f(x), f(y)) = d(x, y)$.*

Proof. Assume x belongs to a dynamical m-cycle and y belongs to a dynamical n-cycle. Let K be a common multiple of m and n. Then we have

$$d(x, y) \geq d(f(x), f(y)) \geq \cdots \geq d(f^{\circ K}(x), f^{\circ K}(y)) = d(x, y).$$

So all inequalities must be, in fact, equalities and in particular, $d(f(x), f(y)) = d(x, y)$. □

Now let us introduce some notation. Let $G = (V, E)$ be a graph and f a contraction on V. Let $J \subset V$ be a dynamical cycle of f. Then we denote by J' the set of all vertices which lie on geodesics connecting consecutive points in J, together with the vertices in J.

Theorem 3.2. *Let T be a finite tree. Let f be a contraction on the vertices of T. If f has no fixed points, then f has a dynamical 2-cycle such that the points in the cycle are connected by an edge. Moreover, such a cycle is unique.*

Proof. Suppose f has no fixed points. Since the number of vertices of T is finite, every vertex of T either lies on a dynamical cycle of period greater than 1 or is eventually mapped into one. Let k be the smallest period of all dynamical cycles of f. Let J be a dynamical cycle of period k such that the distance between consecutive points in J is least among all dynamical cycles of f of period k. We want to show that $k = 2$.

We claim that for $k > 2$ there must exist two geodesics connecting consecutive points in J that intersect at a point other than their endpoints. If not, the points in J' would form a graph cycle, which is a contradiction since T is a tree. Thus there must exist two geodesics which intersect at a point which is not one of their endpoints.

Suppose two nonconsecutive geodesics intersect at some point y. Then we claim that there must exist two consecutive geodesics which intersect at point z which is not one of their endpoints. Indeed, if we start from the point y of intersection of two nonconsecutive geodesics and follow one of the geodesics to the point x_j on the cycle J, then follow the next geodesic to the point $x_{j+1} = f(x_j)$, and so on, we will eventually return to the point y. Since the graph is a tree, the walk constructed this way must go over each edge in this walk at least twice. In particular, there must exist a vertex w which is farthest away from y on this walk and an edge $\{w, z\}$ such that our walk will follow the edge from z to w and then immediately return to z through the same edge. Note that w must be an endpoint of two consecutive geodesics, because one geodesic cannot follow the same edge twice. Then z lies on the intersection of two consecutive geodesics.

Without loss of generality, let x_0, x_1, x_2 be the endpoints of the two consecutive geodesics constructed above. By Corollary 2.6, z must lie on a dynamical cycle whose period divides k, but since k is the smallest possible cycle length, z must lie on a dynamical k-cycle.

Since f is a contraction and x_0, x_1, x_2 are points on a dynamical cycle, f must map the geodesic from x_0 to x_1 bijectively to the geodesic from x_1 to x_2. Since z lies on the geodesic from x_0 to x_1, the point $f(z)$ must lie on the geodesic from x_1 to x_2. Thus both z and $f(z)$ lie on the geodesic from x_1 to x_2 and we have $d(z, f(z)) < d(x_1, x_2) = d(x_0, x_1)$. So we have found a dynamical k-cycle $\{z, f(z), \dots, f^{\circ(k-1)}(z)\}$ such that the distance between two consecutive points in this cycle is less than $d(x_0, x_1)$.

This contradicts the way we selected J, so k must be equal to 2 and the geodesic from x_0 to x_1, which is the same as the geodesic from x_1 to x_0, must contain no other points. This means there is a dynamical 2-cycle $\{x_0, x_1\}$ and x_0 and x_1 are connected by an edge.

Now we need prove that such a dynamical 2-cycle is unique. Let $\{y_0, y_1\}$ be another such cycle. Without loss of generality assume that the distance a between x_0 and y_0 is the shortest among all distances from a point in $\{x_0, x_1\}$ to a point in $\{y_0, y_1\}$. Now consider x_1; it is connected to x_0 by an edge. If x_1 lies on the geodesic from x_0
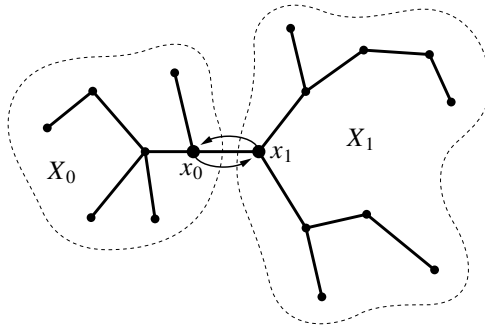
Figure 5. Unique 2-cycle $\{x_0, x_1\}$ and sets X_0 and X_1.

to y_0, then $d(x_1, y_0) < d(x_0, y_0)$, which contradicts the choice of x_0, y_0. Otherwise, the geodesic from y_0 to x_1 follows the geodesic from y_0 to x_0 and then the edge connecting x_0 to x_1, so $d(y_0, x_1) = a + 1$. Similarly, $d(x_0, y_1) = a + 1$, and finally, $d(x_1, y_1) = a + 2$. But then $d(x_1, y_1) = d(f(x_0), f(y_0)) > d(x_0, y_0)$, which contradicts the assumption that f is a contraction. $\square$

It will in fact turn out that every dynamical cycle of a contraction with no fixed points has even period. To prove this, we will need the following corollary to Theorem 3.2. Let us introduce the following notation. Let $\{x_0, x_1\}$ be the points in the 2-cycle constructed in Theorem 3.2. We let X_0 denote the set of all points which are within shorter distance to x_0 than to x_1. Similarly we let X_1 denote the set of all points which are within shorter distance to x_1 than to x_0; see Figure 5.

Corollary 3.3. *Let T be a finite tree and f a contraction on the vertices of T such that f has no fixed points. Let $\{x_0, x_1\}$ be the unique dynamical 2-cycle, where x_0 and x_1 are connected by an edge. Then for all vertices z that lie on any dynamical cycle, if $z \in X_0$ (respectively X_1), then $f(z) \in X_1$ (respectively X_0).*

Proof. Let z lie on a dynamical cycle and $z \in X_0$. By way of contradiction, suppose $f(z) \in X_0$. Let $a = d(z, x_0)$; then $d(z, x_1) = a + 1$. By Lemma 3.1, $d(f(z), x_1) = a$, and since $f(z) \in X_0$, we must have $d(f(z), x_0) < d(f(z), x_1) = a$. But by Lemma 3.1 again, $d(f(z), x_0) = d(f(z), f(x_1)) = d(z, x_1) = a + 1$, which is a contradiction. So $f(z) \in X_1$. $\square$

Note that if z is not a periodic point, then the above claim does not hold.

Example 3.4. Let T be a tree with vertices x_0, x_1 and z such that there are edges between x_0 and x_1 and between x_0 and z, and f be a contraction such that $\{x_0, x_1\}$ forms a dynamical 2-cycle and $f(z) = x_0$ (see Figure 6). Then f has no fixed points, and x_0 and x_1 form the unique 2-cycle connected by an edge. Since $f(z) = x_0$, we have $z \in X_0$ and also $f(z) \in X_0$. Thus we see that if a point z is in X_0 but does not lie on a dynamical cycle, it is not necessarily true that $f(z) \in X_1$.
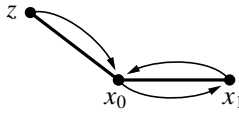
Figure 6

Now we are ready to prove the following:

Theorem 3.5. *Let T be a finite tree and f a contraction on the vertices of T such that f has no fixed points. Then every dynamical cycle of f has even period.*

Proof. Since f has no fixed points, f has a dynamical 2-cycle $\{x_0, x_1\}$ whose points are connected by an edge and sets of vertices X_0 and X_1 as defined above. Let $\{y_0, y_1, \ldots, y_{n-1}\}$ be a dynamical n-cycle of f. Without loss of generality, suppose $y_0 \in X_0$. Then by Corollary 3.3, we have $y_1 \in X_1$, and in general, $y_{2k} \in X_0$ and $y_{2k+1} \in X_1$. If n is odd, then $y_0 = f(y_{n-1}) \in X_1$, which is a contradiction to $y_0 \in X_0$. Hence every dynamical cycle of f has even period. $\qquad\square$

If a contraction f on the vertices of a tree T has no fixed points, then f eventually behaves like a symmetry. More precisely:

Theorem 3.6. *Let $T = (V, E)$ be a finite tree and f a contraction on V without fixed points. Then there exists a subset H of V and a nonnegative integer N such that $f^{\circ N}(V) = H$ and f is a symmetry on the connected subgraph induced by H. In particular, there is an edge in the subgraph such that two connected components obtained by removing this edge are isomorphic graphs and f is an isomorphism.*

Proof. Since T is finite and has no fixed points, each vertex of T will be mapped eventually to a point on a dynamical cycle. Thus there exists N such that $f^{\circ N}(V) = H$ contains only periodic points of f. Note that by Corollary 2.6, the subgraph induced by H is connected. Let $\{x_0, x_1\}$ be the unique dynamical 2-cycle whose points are connected by an edge. Then by Corollary 3.3, for all $z \in H \cap X_0$, we have $f(z) \in H \cap X_1$ and for all $z \in H \cap X_1$, we have $f(z) \in H \cap X_0$. Moreover, since all points in H are periodic, f bijectively maps $H \cap X_0$ to $H \cap X_1$. Now we need to show that any two vertices y, z in $H \cap X_0$ are connected by an edge if and only if $f(y)$ and $f(z)$ are connected by an edge. But being connected by an edge is equivalent to $d(y, z) = 1$, and since by Lemma 3.1, $d(y, z) = d(f(y), f(z))$, the required conclusion follows. $\qquad\square$

4. Conclusion

Note that in the classical case of the unit disk in the complex plane, any analytic self-map of the disk always has a fixed point in the closed disk. This is the consequence of the classical Denjoy–Wolff theorem (see, for example, [Abate 1989]

and references therein). In our study, a contraction without fixed points must behave like a symmetry. Symmetries are contractions in the unit disk, but they are not analytic (in fact, they are anticonformal, i.e., they preserve the value of angles, but change their orientation). So we can say that our result agrees with the classical case.

References

[Abate 1989] M. Abate, *Iteration theory of holomorphic maps on taut manifolds*, Mediterranean Press, Rende, 1989. MR Zbl

[Anderson 1999] J. W. Anderson, *Hyperbolic geometry*, Springer, London, 1999. MR Zbl

[Gross and Yellen 2006] J. L. Gross and J. Yellen, *Graph theory and its applications*, 2nd ed., Chapman & Hall/CRC, Boca Raton, FL, 2006. MR Zbl

[Poggi-Corradini 2011] P. Poggi-Corradini, "Iteration in the disk and the ball: a survey of the role of hyperbolic geometry", *Anal. Math. Phys.* **1**:4 (2011), 289–310. MR Zbl

ostapyuk@math.uni.edu   *Department of Mathematics, University of Northern Iowa, Cedar Falls, IA 50614-0506, United States*

ronnemaa@uni.edu   *Department of Mathematics, University of Northern Iowa, Cedar Falls, IA 50614-0506, United States*

Tiling annular regions with skew and T-tetrominoes

Amanda Bright, Gregory J. Clark, Charles Lundon, Kyle Evitts,
Michael P. Hitchman, Brian Keating and Brian Whetter

(Communicated by Arthur T. Benjamin)

In this paper, we study tilings of annular regions in the integer lattice by skew
and T-tetrominoes. We demonstrate the tileability of most annular regions by
the given tile set, enumerate the tilings of width-2 annuli, and determine the tile
counting group associated to this tile set and the family of all width-2 annuli.

1. Introduction

The first question in the mathematics of tilings is this: can a given region be tiled
by a given set of tiles? By tiled, we mean that the region can be covered without
gaps or overlaps by copies of the tiles in the tile set. If the answer is "yes", the
proof is often a single picture, which is satisfying to be sure. However, if the
answer is "no", the proof is often more interesting mathematically. Over the last
25 years, mathematical tools drawing on subjects in the undergraduate mathematics
curriculum have been developed to answer in the negative the tileability question in
many interesting cases (see, for instance, [Conway and Lagarias 1990; Korn 2004;
Pak 2000; Thurston 1990]).

Other tiling questions have received attention as well, such as enumeration
questions (how many different tilings are possible?) and connectivity questions (how
must any two tilings of a region be related?). In 2000, an abelian group called the tile
counting group was introduced in [Pak 2000] to encode information about such rela-
tionships, and this group has been found for several tile sets and families of regions
(see, e.g., [Moore and Pak 2002; Muchnik and Pak 1999; Pak 2000; Korn 2004]).

We consider the tile set $\mathcal{T}$ in Figure 1 consisting of four T-tetrominoes (tiles t_1
through t_4) and four skew tetrominoes (tiles t_5 through t_8). We refer to the first
four tiles as T-tiles, and the others as skew tiles. The regions we consider are
annular regions in the integer lattice. For positive integers a, b, and n we define
the annular region $A_n(a, b)$ to be the region in the integer lattice obtained from an
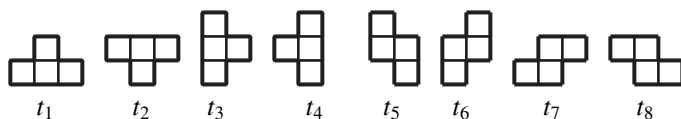
Figure 1. The tile set $\mathcal{T}$ consisting of T- and skew tetrominoes.
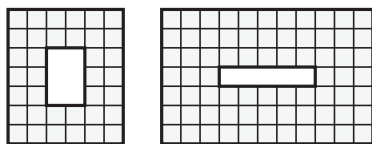
Figure 2. The annular regions $A_2(3, 2)$ and $A_3(1, 5)$.

$(a + 2n) \times (b + 2n)$ rectangle by removing the central $a \times b$ rectangle. We may think of $A_n(a, b)$ as an annulus of width-n units wrapped around an $a \times b$ rectangle. For instance, $A_2(3, 2)$ and $A_3(1, 5)$ are pictured in Figure 2. Certainly no annulus with width-$n = 1$ may be tiled by $\mathcal{T}$, so we assume $n \geq 2$. For an integer $n \geq 2$, let $\mathcal{A}_n$ represent all width-n annuli, and $\mathcal{A} = \bigcup_{n=2}^{\infty} \mathcal{A}_n$.

With respect to this tile set and family of regions, we prove three main results. We solve the tileability question for most annular regions with Theorem 9, and we enumerate tilings of width-2 annuli in Theorem 5. In Section 3 we address the question of how tilings of a given width-2 annulus must be related. As noted above, the tile counting group is an abelian group that gives information about such relations, and we determine the tile counting group associated to $\mathcal{T}$ and width-2 annuli in Theorem 8. We define the tile counting group in its generality and provide some illustration of it in Section 3 prior to the proof of Theorem 8.

The tile set $\mathcal{T}$ has been considered in other papers. For instance, [Lester 2012] solves the tileability question for rectangles with respect to $\mathcal{T}$, and [Korn 2004] looks at the tile counting group for a subset of $\mathcal{T}$ with respect to rectangles. Much is known about tile invariants and the tile counting group for tile sets over simply connected regions (see, for instance, [Conway and Lagarias 1990; Korn 2004; Moore and Pak 2002; Muchnik and Pak 1999; Pak 2000; Sheffield 2002; Thurston 1990]), but less is known for families of multiply connected regions, and this motivates our decision to study annular regions. The annular regions offer some control over the additional variation in possible tiling patterns that emerge beyond those found in rectangular regions. Finally, we note that our proofs are somewhat ad hoc, making use of the geometry of the annuli.

2. Tiling width-2 annular regions

Notice that the tile set $\mathcal{T}$ contains all rotations of each tile in the set, where by rotation we mean rotation by an integer multiple of $\pi/2$ radians, a rotation that
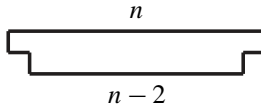
Figure 3. An extended-T of length n, denoted by X_n.

Figure 4. Tiling extended-Ts of odd length.

keeps the tile in the integer lattice. Any rotation of an annular region produces an annular region, and the set $\mathcal{T}$ tiles $A_n(a, b)$ if and only if it tiles $A_n(b, a)$. Further, note that horizontal or vertical reflection of a tiling of the annulus $A_n(a, b)$ will produce a distinct tiling of the same annulus $A_n(a, b)$.

It turns out that all width-2 annuli are tileable by $\mathcal{T}$, a fact we prove en route to enumerating the tilings of a given $A_2(a, b)$. To make this count it is first helpful to consider the extended-T.

Definition 1. Let $n \geq 3$. An *extended-T of length n*, denoted X_n, is any rotation of a region formed by removing the two corner squares from the bottom row of a $2 \times n$ rectangle.

We note that an extended-T has area $2n - 2$, so if n is even, the area of X_n is not divisible by 4, and hence X_n is not tileable by $\mathcal{T}$. However, an extended-T with odd length is more interesting with respect to the tile set $\mathcal{T}$.

Lemma 2. *Suppose $n \geq 3$ is odd. The following hold for the extended-T X_n:*

(i) *X_n is tileable by $\mathcal{T}$.*

(ii) *Any tiling of X_n by $\mathcal{T}$ uses an odd number of T-tiles.*

(iii) *The number of ways in which $\mathcal{T}$ can tile X_n is $2^{(n-3)/2}$.*

Proof. (i): For odd $n \geq 3$, the extended-T X_n as oriented in Figure 4 (left) may be tiled by placing the T-tile t_2 followed by $(n - 3)/2$ copies of the skew tile t_7.

(ii): We proceed by strong induction. X_3 can only be tiled by a single T-tile of the same shape as X_3. Now suppose any tiling of X_k uses an odd number of T-tiles for all odd $3 \leq k \leq n$. We show that any tiling of X_{n+2} also requires an odd number of T-tiles. In a given tiling of X_{n+2}, which we assume for the sake of argument is oriented as in Figure 4 (right), the left-most square may be covered with either the skew tile t_8 or the T-tile t_2. If it is covered by t_8 then the remaining region is an extended-T of length n, which requires an odd number of T-tiles by the inductive hypothesis. It follows that the tiling of X_{n+2} uses an odd number of T-tiles as well.
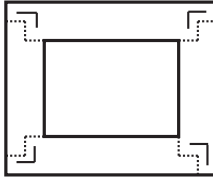
Figure 5. Any tiling of $A_2(a, b)$ can be decomposed into four extended-Ts, its T-structure.

Now suppose the left-most square of X_{n+2} is covered by t_2 instead. If no other T-tiles are present, then we're done. Otherwise, we proceed from left to right in the tiling until the next T-tile is found. Notice that as we proceed from left to right, if the next tile is not a T it must be the skew t_7. Notice further that the next T-tile placed will have to be the horizontal T-tile t_1. At this point, the shape of the untiled portion of the region is an extended-T of the form X_k for some odd $k < n$, as suggested in Figure 4 (right). Any tiling of the remaining portion requires an odd number of T-tiles by the inductive hypothesis, and it follows that the tiling of X_{n+2} itself uses an odd number of T-tiles.

(iii): This enumeration problem boils down to first picking the number of T-tiles used, which must be an odd number by (ii), and next picking the order in which skew and T-tiles are placed from left to right in the tiling of X_n. Once the number of T-tiles has been chosen, and the order of their placement has been chosen, the resulting tiling of X_n is uniquely determined. Thus the number of ways of tiling X_n is

$$\sum_{\substack{k=1 \\ k \text{ is odd}}}^{m} \binom{m}{k} = 2^{m-1}.$$

Here, $m = (n-1)/2$, the number of total tiles needed to tile X_n. $\qquad\square$

Lemma 3. *If α is a tiling of $A_2(a, b)$ by $\mathcal{T}$ then α may be viewed as the disjoint union of tilings of four extended-Ts.*

Proof. Note that in any attempt to tile the annular region $A_2(a, b)$, the corners must be covered by a tile. Both skew and T-tiles partially fill a corner in an L shape. Not all such configurations of these L-shapes can lead to valid tilings; however, it is necessary for any complete tiling of the region to have this structure. No matter how these L-shapes are arranged they allow us to uniquely decompose the region into four extended-Ts, as suggested in Figure 5. $\qquad\square$

We call such a decomposition of an annulus into four extended-Ts a *T-structure* for that annulus.
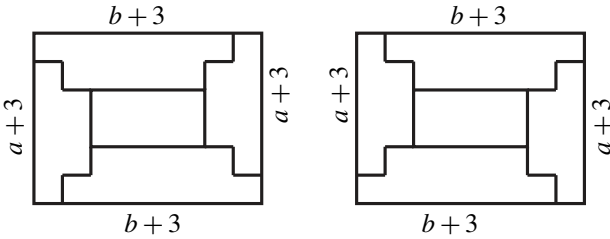
Figure 6. T-structures in the case a, b are even.
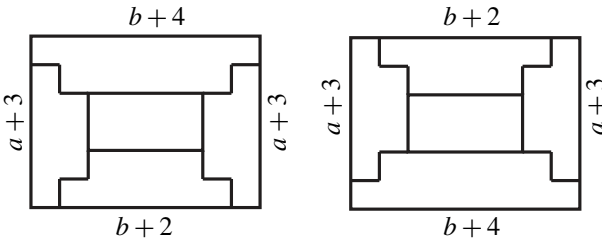
Figure 7. T-structures in the case a is even, b is odd.

Lemma 4. *There are exactly two T-structures for the annulus $A_2(a, b)$ in which each extended-T has odd length.*

Proof. We will consider three cases, according to the parities of a and b.

Case 1: Suppose a and b are both even. In this case, the use of an extended-T of length $a + 1$ or $b + 1$ would leave uncovered squares in the region, so we must use extended-Ts of length $a + 3$ and $b + 3$. There are only two possible ways to arrange extended-Ts of this length to cover the region; see Figure 6.

Case 2: Suppose a is even and b is odd (the case a odd and b even is handled by rotational symmetry). In this case, we must use two extended-Ts of length $a + 3$ in our T-structure. This forces us to use one extended-T of length $b + 4$ and one of length $b + 2$ in order to cover the annulus and obtain the correct parity for the extended-Ts. Figure 7 depicts the two possible T-structures.

Case 3: Suppose a and b are odd. To obtain the correct parity for each extended-T, we must use lengths of $a + 2$, $a + 4$, $b + 2$, or $b + 4$. Note that if we pick our vertical extended-Ts such that one has length $a + 2$ and the other has length $a + 4$, then this would force each horizontal extended-T to have length $b + 3$. However, this would be an extended-T of even length and therefore untileable. Thus the vertical (and therefore horizontal) extended-Ts must have the same length. This leads us to two possible configurations, as in Figure 8. □

We observe that because any width-2 annulus may be decomposed into odd length extended Ts, it follows that any width-2 annulus is tileable by $\mathcal{T}$. We can count
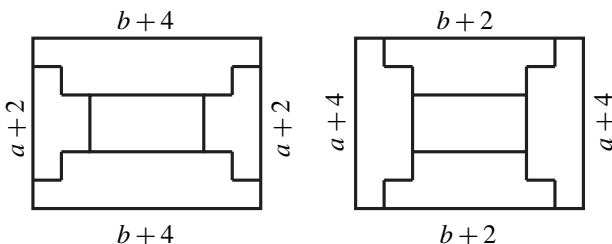
Figure 8. T-structures in the case a, b are odd.

the number of possible tilings of $A_2(a, b)$, thanks to the restrictions on possible T-structures.

Theorem 5. *The number of ways of tiling $A_2(a, b)$ by $\mathcal{T}$ is 2^{a+b+1}.*

Proof. We may consider three cases, based on the parities of a and b. We will show the calculations for the case where a and b are even. The other cases are analogous.

By Lemma 4, each horizontal extended-T in an allowable T-structure has length $b + 3$. By Lemma 2(iii), the number of ways to tile a horizontal extended-T of this length is $2^{b/2}$. Similarly, the number of ways of tiling one of the vertical extended-Ts is $2^{a/2}$. Thus the total number of ways to tile $A_2(a, b)$ is

$$2 \cdot 2^{b/2} \cdot 2^{b/2} \cdot 2^{a/2} \cdot 2^{a/2} = 2^{a+b+1},$$

since we have two T-structures and two horizontal and two vertical extended-Ts. $\square$

3. The tile counting group for width-2 annuli

We now turn to the question of how any two tilings of an annular region $A_2(a, b)$ by $\mathcal{T}$ must be related. Some mathematical machinery is necessary to address this question, and we take time here to develop this machinery for the reader's convenience.

Suppose a region Γ can be tiled by a tile set $\mathcal{T}$. It may be that Γ can be tiled in more than one way, and it is reasonable to ask how these tilings, or indeed any two tilings of Γ, must be related.

Suppose the tile set $\mathcal{T} = \{\tau_1, \tau_2, \ldots, \tau_n\}$ consists of n tiles, and each tile in $\mathcal{T}$ has the same area (that is, it is comprised of the same number of squares). If α represents a particular tiling by $\mathcal{T}$ of a region Γ, we let $a_i(\alpha)$ equal the number of copies of tile τ_i that appears in the tiling. There are certain relations among the $a_i(\alpha)$ that hold for all tilings of a given region, and any such relation is called a *tile invariant* [Pak 2000].

One relation is an area invariant: since all tiles in $\mathcal{T}$ have the same area, for any tiling α of any region Γ, the linear combination $\sum_{i=1}^{n} a_i(\alpha)$ is constant. The value of the constant depends only on the region, not the particular tiling, and its value equals the total number of tiles needed to tile the region. A typical tile invariant

has the form

$$\sum_{i=1}^{n} k_i a_i(\alpha) = c(\Gamma),$$

where $c(\Gamma)$ is a constant, each k_i is an integer, and the equality may be taken (mod m) for some n. As the value of the constant is independent of the particular tiling, and depends only on the region Γ, it is often cleaner to drop the α from the notation, in which case a tile invariant might be written as

$$2a_1 + a_2 - a_3 \equiv c(\Gamma) \pmod 4,$$

which in this case would mean that for any tiling of Γ, twice the number of copies of τ_1 plus the number of copies of τ_2 minus the number of copies of τ_3 is constant modulo 4.

The tile counting group $G(\mathcal{T}, \mathcal{R})$ associated to a tile set $\mathcal{T}$ and a collection of regions $\mathcal{R}$ was introduced in [Pak 2000] as a way to record in the form of a group the different tile invariants associated to a tile set and a family of regions. This group is defined as follows. To any tiling α of a region $\Gamma \in \mathcal{R}$ we associate an element w_α in the abelian group $\mathbb{Z}^n$ given by $w_\alpha = (a_1(\alpha), a_2(\alpha), \ldots, a_n(\alpha))$. We call w_α a *tile vector*. Now, if α and β are two tilings of the same region $\Gamma \in \mathcal{R}$, we call $w_\alpha - w_\beta$ a *difference vector*. In this setting we may view a tile invariant as a linear function from $\mathbb{Z}^n$ to $\mathbb{Z}$ (or possibly $\mathbb{Z}_m$) that maps each difference vector to 0. Let H denote the normal subgroup of $\mathbb{Z}^n$ generated by all possible difference vectors obtainable from our family of regions $\mathcal{R}$ and our tile set $\mathcal{T}$.

The *tile counting group* is then the quotient group

$$G(\mathcal{T}, \mathcal{R}) = \mathbb{Z}^n / H.$$

It seems that as we include more regions in our family $\mathcal{R}$, thus allowing for more difference vectors (from more regions that can be tiled in more than one way), the size of H will grow, and thus the size of the tile counting group will shrink. However, the tile counting group can stabilize rather quickly as you grow the number of regions in the family. Computations of tile counting groups can be difficult in general. Some computations can be found in [Hitchman 2015; Korn 2004; Moore and Pak 2002; Muchnik and Pak 1999; Pak 2000]. Before computing $G(\mathcal{T}, \mathcal{A}_2)$, we consider an example.

Suppose $\mathcal{T}_3$ consists of the ribbon tile trominoes as pictured in Figure 9, and $\mathcal{R}$ consists of a single region, the 3×3 square. This square has six tilings by $\mathcal{T}_3$, given in Figure 9. Tilings 3 and 1 give us difference vector $(1, 1, 1, 0) - (3, 0, 0, 0) = (-2, 1, 1, 0)$, and tilings 5 and 3 give us difference vector $(0, 1, 1, 1) - (1, 1, 1, 0) = (-1, 0, 0, 1)$. One can check that all other difference vectors from pairs of tilings
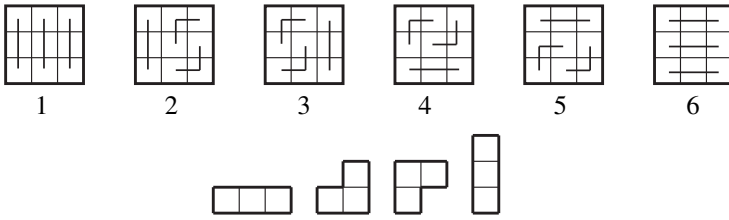
Figure 9. Tilings of a 3×3 square by ribbon tile trominoes.

taken from this collection are integer linear combinations of these two. Thus H is generated by $v_1 = (-2, 1, 1, 0)$ and $v_2 = (-1, 0, 0, 1)$.

We use two tile invariants to calculate the tile counting group. First, we have the area invariant: in any of the six tilings, we have that $a_1 + a_2 + a_3 + a_4$ is constant (equal to 3); second, we note that $a_2 - a_3$ is constant in all six tilings. Alternatively, these are tile invariants because for any difference vector $w_\alpha - w_\beta = (c_1, c_2, c_3, c_4)$, we know $c_1 + c_2 + c_3 + c_4 = 0$ and $c_2 - c_3 = 0$. The latter invariant is the Conway–Lagarias invariant [1990].

We claim the tile counting group $G(\mathcal{T}_3, \{[3 \times 3]\})$ is isomorphic to $\mathbb{Z}^2$. To see this, let $\phi : \mathbb{Z}^4 \to \mathbb{Z}^2$ be defined by $\phi(a, b, c, d) = (a + b + c + d, b - c)$. First note that ϕ is a group homomorphism and it is a surjection since we can map onto the generators of $\mathbb{Z}^2$: $\phi(1, 0, 0, 0) = (1, 0)$ and $\phi(-1, 1, 0, 0) = (0, 1)$. Second, we show $\ker \phi \subseteq H$: if $g = (a, b, c, d) \in \ker \phi$, then $b = c$, so $g = (a, b, b, d)$ where $a = -2b - d$ so

$$g = (-2b - d, b, b, d)$$
$$= (-2b, b, b, 0) + (-d, 0, 0, d)$$
$$= b(-2, 1, 1, 0) + d(-1, 0, 0, 1)$$
$$= bv_1 + dv_2.$$

It follows that $g \in H$. Third, $H \subseteq \ker \phi$ since $\phi(v_1) = (0, 0)$ and $\phi(v_2) = (0, 0)$. Thus, by the first isomorphism theorem $G(\mathcal{T}_3, \mathcal{R}) = \mathbb{Z}^4 / H \simeq \mathbb{Z}^2$.

Remarkably, the tile counting group here does not shrink if $\mathcal{R}$ grows to include all simply connected regions. That is, the two tile invariants used as the coordinate functions of ϕ persist as we expand $\mathcal{R}$. Conway and Lagarias [1990] introduced combinatorial group theoretic methods for deriving their tile invariant. Their inventive methods have motivated much research in tiling problems, including the development of the tile counting group itself. The Conway–Lagarias invariant is also revisited from a topological perspective in [Hitchman 2015], as is the tile counting group itself.

We now turn to the computation of $G(\mathcal{T}, \mathcal{A}_2)$. We begin again with extended-Ts. Figure 10 shows so-called "local moves" one may perform on a tiling of a horizontal
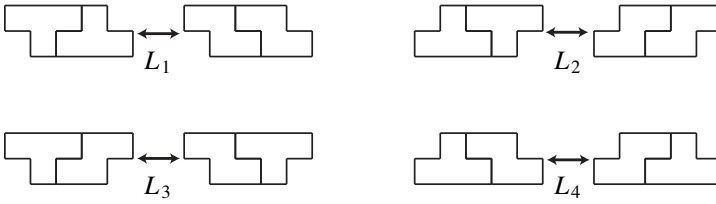
Figure 10. The set $\mathcal{L}$ of local moves on horizontal extended-T regions.

extended-T to produce a new tiling. That is, in each case, we may replace a local, two-tile configuration with a different configuration to generate a new tiling of the extended-T.

In general, a set of regions $\mathcal{R}$ has a *local move property* with respect to a tile set $\mathcal{T}$ if there exists a set of local moves, $\mathcal{L}$, such that every region $\Gamma \in \mathcal{R}$ has the feature that given any two tilings of Γ by $\mathcal{T}$, one can be made to match the other by a finite sequence of local moves.

Lemma 6. *The family of horizontal extended-Ts has a local move property with respect to the tile set $\mathcal{T}$, using the four local moves in the set $\mathcal{L} = \{L_1, L_2, L_3, L_4\}$ in Figure 10.*

Proof. Suppose $n \geq 3$ is odd, and α is a tiling of X_n, a horizontal extended-T oriented as in Figure 3. We show that α, by a finite number of local moves from $\mathcal{L}$, can be transformed into the tiling of X_n consisting of a single T-tile followed by $(n-3)/2$ copies of the skew t_7, as suggested in Figure 4 (left). It will then follow that any two tilings of X_n can be made to match by making local moves from $\mathcal{L}$. First, note that moves L_3 and L_4 tell us that T-and skew tiles "commute". By application of moves L_3 and L_4, we may convert the tiling α to one that consists of some number of T-tiles followed by some number of skew tiles. As observed in Lemma 2(ii), the number of T-tiles used in the tiling must be odd. Moves L_1 and L_2 may then be made to reduce the number of T-tiles two at a time until the number of T-tiles used is one. The $(n-3)/2$ skews now present in the tiling must all be copies of tile t_7 in order to have a valid tiling. □

We note that an analogous result holds for vertical extended-T regions: for tilings by $\mathcal{T}$, the family of vertical extended-Ts has a local move property with respect to four local moves, which correspond to the moves in Figure 11.
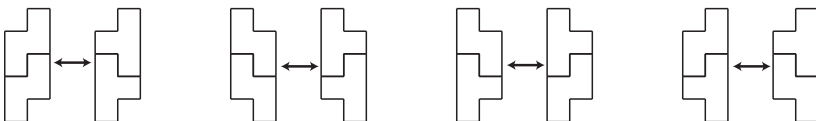
Figure 11. Local moves on vertical extended-T regions.
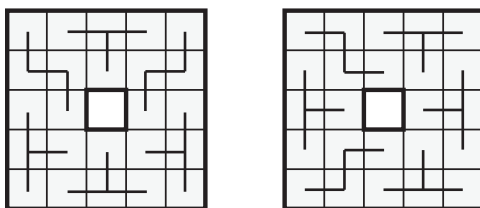
Figure 12. Two tilings of $A_2(1, 1)$ generate $v_5 = (0, 0, 0, 0, 1, 1, -1, -1)$.

One can show that the collection $\mathcal{A}_2$ does not have a local move property, essentially due to the fact that local moves cannot account for different T-structures among tilings.

The local moves on horizontal extended-Ts produce two distinct difference vectors in the subgroup H, the subgroup of $\mathbb{Z}^8$ generated by all difference vectors. Consider two tilings of $A_2(a, b)$ that differ by a single application of an L_1-move. We let v_1 denote the difference vector in this case, and note

$$v_1 = (1, 1, 0, 0, 0, 0, 0, -2).$$

Two tilings of $A_2(a, b)$ that differ by a single L_3-move or by a single L_4-move will generate the difference vector

$$v_2 = (0, 0, 0, 0, 0, 0, 1, -1).$$

Two tilings that differ by an L_2-move will produce the difference vector

$$(1, 1, 0, 0, 0, 0, -2, 0),$$

which equals $v_1 - 2v_2$, so it is a consequence of v_1 and v_2.

By a similar argument, two tilings that differ by some combination of the four vertical local moves in Figure 11 will have a difference vector that is a consequence of these two:

$$v_3 = (0, 0, 1, 1, -2, 0, 0, 0) \quad \text{and} \quad v_4 = (0, 0, 0, 0, 1, -1, 0, 0).$$

These four vectors do not quite generate H. For instance,

$$v_5 = (0, 0, 0, 0, 1, 1, -1, -1),$$

the difference vector determined by the two tilings of $A_2(1, 1)$ in Figure 12 is not a linear combination of the first four. This difference vector arises from tilings having distinct T-structures. It turns out that these five difference vectors generate H.

Lemma 7. *The subgroup H is generated by the five difference vectors*

$$v_1 = (1, 1, 0, 0, 0, 0, 0, -2),$$
$$v_2 = (0, 0, 0, 0, 0, 0, 1, -1),$$
$$v_3 = (0, 0, 1, 1, -2, 0, 0, 0),$$
$$v_4 = (0, 0, 0, 0, 1, -1, 0, 0),$$
$$v_5 = (0, 0, 0, 0, 1, 1, -1, -1).$$

Proof. Let H' be the normal subgroup of $\mathbb{Z}^8$ generated by the five difference vectors v_i. We show $H = H'$, where H is the normal subgroup generated by *all* difference vectors stated in the lemma. Clearly $H' \subseteq H$, and it remains to show that $H \subseteq H'$. Suppose α and β are two tilings of $A_2(a, b)$, and consider the difference vector $w_\alpha - w_\beta$. If these tilings have the same T-structures, then each tiling may be viewed as the tiling of a disjoint union of four extended-Ts of identical sizes, so one can be made to look like the other by a sequence of our local moves on extended-Ts. Thus, the difference vector $w_\alpha - w_\beta$ is in H'.

Now suppose α and β have distinct T-structures. Again, we consider cases based on the parities of a and b.

Case 1: Assume a and b are even, and α and β are tilings with distinct T-structures, given in Figure 6. Notice that in both T-structures, extended-Ts of the same orientation have the same size. This ensures that the difference vector $w_\alpha - w_\beta$ is a consequence of v_1, v_2, v_3, v_4, so it is in H'.

Case 2: Assume a is even and b is odd, and α and β represent tilings having distinct T-structures (the case a is odd and b is even is handled analogously). The tiling α can be transformed to a tiling α' with the same T-structure as α but having just a single T-tetromino in each extended-T as indicated in Figure 13. In particular, the single T-tetromino is either the bottommost or leftmost tile in the tiling of the extended-T, depending on its orientation. The rest of each extended-T is tiled by some number of copies of a single skew. Since α' was obtained from α by local moves within extended-Ts, $w_\alpha - w_{\alpha'} \in H'$. Similarly, β can be transformed to a tiling β' having the same T-structure but consisting of just one T-tetromino in each extended-T (at left or bottom), and $w_\beta - w_{\beta'} \in H'$. Furthermore, $w_{\alpha'} - w_{\beta'} = (0, 0, 0, 0, 0, 0, -1, 1) = -v_2$, which is also in H'. It follows that $w_\alpha - w_\beta$ is in H'.

Case 3: Assume a and b are odd, and α and β represent tilings having distinct T-structures. We may convert to tilings α' and β' as we did in Case 2, resulting in tilings with just one T-tile in each extended-T (see Figure 14). Then

$$w_{\alpha'} - w_{\beta'} = (0, 0, 0, 0, 1, 1, -1, -1) = v_5.$$
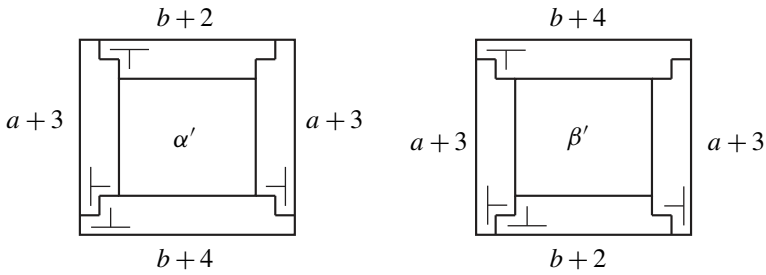
Figure 13. The difference vector for tilings with different T-structures in the (even) × (odd) case.
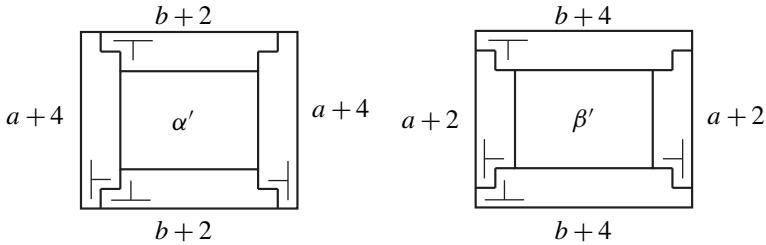
Figure 14. The difference vector for tilings with different T-structures in the (odd) × (odd) case.

Since
$$w_\alpha - w_\beta = (w_\alpha - w_{\alpha'}) + (w_{\alpha'} - w_{\beta'}) + (w_{\beta'} - w_\beta)$$
is the sum of three elements in H', it follows that $w_\alpha - w_\beta \in H'$.

Thus, $H' = H$. That is, the normal subgroup H is generated by the difference vectors v_1, v_2, v_3, v_4, and v_5.   □

With a local move property on extended-T regions and the subgroup H in hand, we can write down various tile invariants. Of course, we have the area invariant: for any tiling α of a region Γ in $\mathcal{A}_2$ we have

$$\sum_{i=1}^{8} a_i = c(\Gamma).$$

Two other tile invariants arise by focusing on the horizontal and vertical T-tetrominoes present in any tiling of $A_2(a, b)$. In particular, we have

$$a_2 - a_1 = d(\Gamma),$$
$$a_4 - a_3 = e(\Gamma).$$

The first of these invariants says that the difference in the number of horizontal T-tiles used in any tiling of a given annulus is constant; the second says the same for the difference of vertical T-tiles used.

Also, the total number of horizontal tiles used in any tiling of a given $A_2(a, b)$ must be constant, modulo 2. That is,

$$a_1 + a_2 + a_7 + a_8 \equiv k(\Gamma) \pmod{2}.$$

We now prove that all tile invariants are consequences of these four.

Theorem 8. *The tile counting group $G(\mathcal{T}, \mathcal{A}_2)$ is isomorphic to $\mathbb{Z}^3 \times \mathbb{Z}_2$.*

Proof. We use the tile invariants above to define $\phi : \mathbb{Z}^8 \to \mathbb{Z}^3 \times \mathbb{Z}_2$ as

$$\phi(c_1, c_2, \ldots, c_8) = \left(\sum_{i=1}^{8} c_i, c_2 - c_1, c_4 - c_3, [c_1 + c_2 + c_7 + c_8]_2 \right),$$

where $[k]_n$ represents the residue of k modulo n

The reader can check that ϕ is a homomorphism. To see that ϕ is a surjection, suppose $h \in \mathbb{Z}^3 \times \mathbb{Z}_2$. We want to show that there exists some $g \in \mathbb{Z}^8$ such that $\phi(g) = h$. Since $h \in \mathbb{Z}^3 \times \mathbb{Z}_2$, we know $h = (w, x, y, z)$, where $w, x, y \in \mathbb{Z}$ and $z \in \mathbb{Z}_2$.

Further suppose that $z = x + b$, where $b \in \mathbb{Z}$. In other words, $h = (w, x, y, [x+b]_2)$. Let $g = (0, x, 0, y, 0, w - (x+b+y), 0, b) \in \mathbb{Z}^8$. We have that $\phi(g) = h$ as desired, and it follows that ϕ is surjective.

Next we show $\ker \phi = H$. To see that $H \subseteq \ker \phi$, suppose $g \in H$. Observe that each $v_i \in \ker \phi$ for $i = 1, \ldots, 5$. It follows directly that $g \in \ker \phi$ since ϕ is a homomorphism.

Now suppose that $g = (c_1, c_2, \ldots, c_8) \in \ker \phi$. Then $c_2 - c_1 = 0$ and $c_4 - c_3 = 0$. Hence, $c_1 = c_2$ and $c_3 = c_4$. We also know that

$$0 \equiv c_1 + c_2 + c_7 + c_8 \equiv 2c_1 + c_7 + c_8 \equiv c_7 + c_8 \pmod{2}.$$

That is, $c_7 + c_8$ is even, and $c_7 \equiv c_8 \pmod{2}$. Furthermore, we know that

$$\sum_{i=1}^{8} c_i = 2c_1 + 2c_3 + c_5 + c_6 + c_7 + c_8 = 0,$$

from which it follows that $c_5 \equiv c_6 \pmod{2}$ as well. In other words, if $g \in \ker \phi$, then g has the form $g = (c_1, c_1, c_3, c_3, c_5, c_6, c_7, c_8)$, where $c_5 \equiv c_6 \pmod{2}$ and $c_7 \equiv c_8 \pmod{2}$.

With g expressed in such a way, it is possible to express g as a linear combination of the difference vectors $v_1, \ldots, v_5$. Indeed, if we let $m = c_3 + \frac{1}{2}(c_5 + c_6)$ (which is an integer since $c_5 + c_6$ is even), then

$$g = c_1 v_1 + (c_7 + m)v_2 + c_3 v_3 + (m - c_6)v_4 + m v_5.$$

Thus, $g \in H$, as desired. $\square$

4. Extensions and remarks

In this section we consider width-n annuli for general n.

Theorem 9. *Let $A_n(a, b)$ be an annular region with $n \geq 2$. Then $\mathcal{T}$ tiles $A_n(a, b)$ if one of these conditions holds*:

  (i) *n is even.*

 (ii) *$n = 3$, with $a \equiv b$ (mod 2), and a and b are not both divisible by four.*

(iii) *$n \geq 5$ is odd and $a \equiv b$ (mod 2).*

Proof. (i): We have already seen that $\mathcal{T}$ tiles any width-2 annulus, and if $A_n(a, b)$ can be tiled by $\mathcal{T}$ then so can $A_{n+2}(a, b)$, since $A_{n+2}(a, b)$ may be viewed as the disjoint union of $A_n(a, b)$ and $A_2(a + 2n, b + 2n)$. It follows inductively that $A_n(a, b)$ can be tiled by $\mathcal{T}$ for any even $n \geq 2$, and we have tilings for all the regions for (i).

(ii): If $n \geq 3$ is odd, observe that $A_n(a, b)$ has area divisible by 4 if and only if $a \equiv b$ (mod 2). Figure 15 shows tilings of $A_3(1, 1)$, $A_3(1, 3)$, $A_3(3, 3)$, $A_3(2, 2)$, and $A_3(2, 4)$. One can then use reflections and rotations of the width-3 "expander" region in Figure 16 to effectively increase the a-dimension and the b-dimension of any of the tilings in Figure 15 by an integer multiple of 4 units. This can be achieved by inserting the expander regions as needed along the bold face seams given in the tilings of Figure 15. For instance, Figure 17 demonstrates how to extend the tiling of $A_3(1, 3)$ in Figure 15 to a tiling of the annulus $A_3(5, 7)$. Along each side of the annulus we may insert a width-3 expander region at the bold faced seam, indicated by an arrow to increase the length and width dimensions of the annulus by 4. Of course, we could have chosen to insert expander regions in just the vertical sides to obtain a tiling of $A_3(5, 3)$ or just the horizontal sides to obtain a tiling of $A_3(1, 7)$. In this way, we may generate tilings for all the regions for (ii).
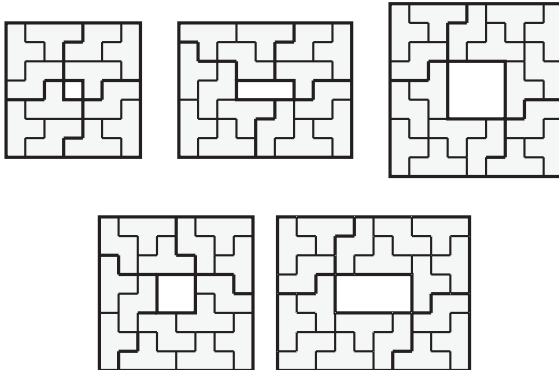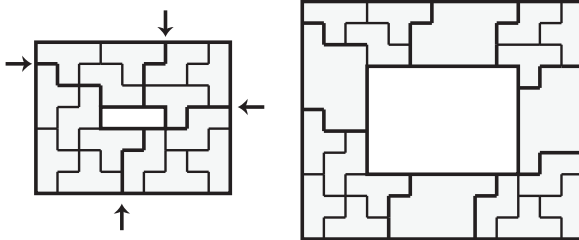

Figure 15. Tilings of $A_3(1, 1)$, $A_3(1, 3)$, $A_3(3, 3)$, $A_3(2, 2)$, and $A_3(2, 4)$.
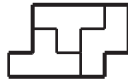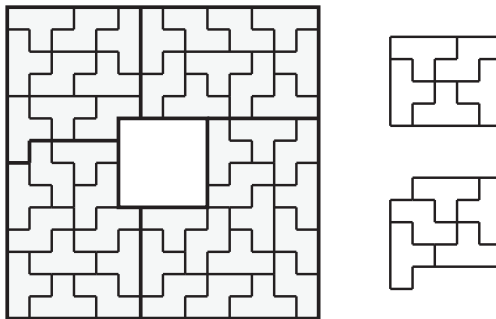
Figure 16. Tiling a width-3 expander region.

Figure 17. Extending a tiling of $A_3(1, 3)$ to a tiling of $A_3(5, 7)$.

(iii): Figure 18 shows a tiling of $A_5(4, 4)$ and width-5 expander regions. From these pieces, we may construct a tiling of $A_5(a, b)$ when a and b are both multiples of 4. Other regions $A_5(a, b)$ in which $a \equiv b \pmod 2$ may be viewed as the union of an $A_3(a, b)$ region and an $A_2(a + 6, b + 6)$ region, both of which may be tiled, so all $A_5(a, b)$ in which $a \equiv b \pmod 2$ may be tiled by $\mathcal{T}$. Finally, for odd $n \geq 7$, the region $A_n(a, b)$ may be viewed as the disjoint union of annuli $A_5(a, b)$ and $A_k(a + 10, b + 10)$, where $k \geq 2$ is even. If $a \equiv b \pmod 2$ then both these regions can be tiled by $\mathcal{T}$ so $A_n(a, b)$ can be tiled by $\mathcal{T}$ as well. Thus we have tilings of all the regions for (iii). $\qquad\square$

We believe the converse to Theorem 9 holds as well. That is, if we suppose $A_n(a, b)$ has area divisible by 4, then we claim that $\mathcal{T}$ fails to tile $A_n(a, b)$ if and only if $n = 3$ and $a \equiv b \equiv 0 \pmod 4$. At the time of this writing, the proof that $A_3(4, 4)$ cannot be tiled by $\mathcal{T}$ is a brute force effort that involves tracking down all the scenarios for placing tiles, an argument comparable to the proof in [Lester

Figure 18. Tiling $A_5(4, 4)$, and width-5 expander regions.

2012] that $\mathcal{T}$ does not tile the 6×6 rectangle. That $\mathcal{T}$ tiles none of the regions $A_3(a, b)$ for $a, b \equiv 0 \pmod 4$ follows again by a brute force argument appealing to the geometry of the width-3 annuli. An elegant nonexistence proof using tile invariants remains elusive. For instance, there exists a signed tiling of $A_3(4, 4)$ by $\mathcal{T}$, which means no coloring argument exists to demonstrate the nontileability of $A_3(4, 4)$ by $\mathcal{T}$.

Enumeration and connectivity questions remain open for width-3 annuli. In fact, except for the area invariant, none of the tile invariants that hold for $\mathcal{A}_2$ persist when we pass to $\mathcal{A}_3$. Consider the invariant $a_2 - a_1$ over $\mathcal{A}_2$, and look again at the tiling of $A_3(1, 3)$ in Figure 15. In this tiling $a_2 - a_1 = 4 - 2 = 2$, but if we reflect this tiling about a horizontal axis we obtain a second tiling of $A_3(1, 3)$ in which $a_2 - a_1 = 2 - 4 = -2$. So, $a_2 - a_1$ is no longer a tile invariant if we pass to width-3 annuli. These two tilings of $A_3(1, 3)$ may be rotated by $\pi/2$ to show that $a_4 - a_3$ is no longer invariant over $\mathcal{A}_3$. Finally, consider the tile invariant that $a_1 + a_2 + a_7 + a_8$ is constant modulo 2, for tilings of regions in $\mathcal{A}_2$. The tiling of $A_3(2, 2)$ in Figure 15 uses eight horizontal tiles and seven vertical tiles. So, the given tiling gives $a_1 + a_2 + a_7 + a_8 \equiv 0 \pmod 2$. But if we rotate this tiling by $\pi/2$ we obtain a new tiling of the same annulus, $A_3(2, 2)$, that now has seven horizontal tiles so that $a_1 + a_2 + a_7 + a_8 \equiv 1 \pmod 2$ in this second tiling.

Finally, determining $G(\mathcal{T}, \mathcal{A}_n)$ for $n > 2$ remains open.

References

[Conway and Lagarias 1990] J. H. Conway and J. C. Lagarias, "Tiling with polyominoes and combinatorial group theory", *J. Combin. Theory Ser. A* **53**:2 (1990), 183–208. MR Zbl

[Hitchman 2015] M. P. Hitchman, "The topology of tile invariants", *Rocky Mountain J. Math.* **45**:2 (2015), 539–563. MR Zbl

[Korn 2004] M. R. Korn, *Geometric and algebraic properties of polyomino tilings*, Ph.D. thesis, MIT, 2004, http://hdl.handle.net/1721.1/16628. MR

[Lester 2012] C. Lester, "Tiling with T and skew tetrominoes", *Querqus: Linfield Journal of Undergraduate Research* **1**:3 (2012).

[Moore and Pak 2002] C. Moore and I. Pak, "Ribbon tile invariants from the signed area", *J. Combin. Theory Ser. A* **98**:1 (2002), 1–16. MR Zbl

[Muchnik and Pak 1999] R. Muchnik and I. Pak, "On tilings by ribbon tetrominoes", *J. Combin. Theory Ser. A* **88**:1 (1999), 188–193. MR Zbl

[Pak 2000] I. Pak, "Ribbon tile invariants", *Trans. Amer. Math. Soc.* **352**:12 (2000), 5525–5561. MR Zbl

[Sheffield 2002] S. Sheffield, "Ribbon tilings and multidimensional height functions", *Trans. Amer. Math. Soc.* **354**:12 (2002), 4789–4813. MR Zbl

[Thurston 1990] W. P. Thurston, "Conway's tiling groups", *Amer. Math. Monthly* **97**:8 (1990), 757–773. MR Zbl

amanda.m.bright@nga.mil   *Department of Mathematics, University of Missouri-Columbia, Columbia, MO 65211, United States*

gjclark@math.sc.edu   *Department of Mathematics, University of South Carolina, Columbia, SC 29208, United States*

chuckl@linfield.edu   *Department of Mathematics, Linfield College, McMinnville, OR 97128, United States*

kevitts@uoregon.edu   *Department of Mathematics, University of Oregon, Eugene, OR 97403, United States*

mhitchm@linfield.edu   *Department of Mathematics, Linfield College, McMinnville, OR 97128, United States*

blkeatin@calpoly.edu   *Department of Mathematics, California Polytechnic State University, San Luis Obispo, CA 93407, United States*

bmwhetter@gmail.com   *Department of Mathematics, Western Washington University, Bellingham, WA 98225, United States*

A bijective proof of a q-analogue of the sum of cubes using overpartitions

Jacob Forster, Kristina Garrett, Luke Jacobsen and Adam Wood

(Communicated by Jim Haglund)

We present a q-analogue of the sum of cubes, give an interpretation in terms of overpartitions, and provide a combinatorial proof. In addition, we note a connection between a generating function for overpartitions and the q-Delannoy numbers.

1. Introduction

The formula for the sum of the first n cubes,

$$\sum_{k=1}^{n} k^3 = \binom{n+1}{2}^2,\tag{1}$$

is well known and has been proven using various methods. Benjamin and Orrison [2002] gave two combinatorial proofs. More recently, Garrett and Hummel [2004] proved a q-analogue of (1) using integer partitions. (A q-analogue is an expression involving q-binomial coefficients — see Section 2.3 on the next page — and reducing to the given expression when $q \to 1^-$.) In this paper, we give an alternate q-analogue of (1) and provide a bijective proof using overpartitions. The first section is devoted to an introduction to partition theory and establishing necessary notation and facts for our work. Then we state and explain a generating function for overpartitions and relate it to the Delannoy numbers. In the last section we give our q-analogue and provide a combinatorial proof.

2. Background

In this section, we introduce aspects of partition theory that are relevant to our work. For further reading, see [Andrews 1976; Corteel and Lovejoy 2004].

2.1. *Partitions.*

Definition 1. A partition λ of a positive integer n is a nonincreasing sequence of positive integers $\lambda_1, \lambda_2, \ldots, \lambda_k$ such that $\sum_{i=1}^{k} \lambda_i = n$. The λ_i are called the parts of the partition.

As an example, consider $n = 4$. The five distinct partitions of 4 are

$$4, \ 31, \ 22, \ 211, \ 1111.$$

One method of displaying partitions graphically is with Ferrers shapes. A Ferrers shape of a partition $\lambda = \lambda_1, \lambda_2, \ldots, \lambda_k$, where $\lambda_i \geq \lambda_{i+1}$, is a left-justified array of cells with λ_i cells in row i of the shape and $i = 1$ defined as the top row. Below is the Ferrers shape for the partition $\lambda = 31$:

2.2. *Overpartitions.*

Definition 2. An overpartition λ is a partition $\lambda_1, \lambda_2, \ldots, \lambda_k$ in which the first occurrence of a given part size may be overlined.

Below are the fourteen distinct overpartitions of $n = 4$:

$$4, \bar{4}, 31, \bar{3}1, 3\bar{1}, \bar{3}\bar{1}, 22, \bar{2}2, 211, \bar{2}11, 21\bar{1}, \bar{2}1\bar{1}, 1111, \bar{1}111.$$

Overpartitions can also be graphically represented using Ferrers shapes by letting the last cell of the rows corresponding to overlined parts be shaded. For example, the Ferrers shape for the overpartition $\lambda = \bar{3}1$ is

2.3. *Partitions in a $k \times (n - k)$ box.* In order to discuss partitions whose Ferrers shapes fit inside of a $k \times (n - k)$ box, we must first introduce the q-binomial coefficient. The q-binomial coefficient is defined as

$$\begin{bmatrix} n \\ k \end{bmatrix}_q = \frac{\prod_{i=n-k+1}^{n}(1 - q^i)}{\prod_{i=1}^{k}(1 - q^i)},$$

and is a q-analogue of the binomial coefficient. It is well known that

$$g_{n,k}(q) = \begin{bmatrix} n \\ k \end{bmatrix}_q$$

is the generating function for the number of partitions whose Ferrers shapes fit inside of a $k \times (n - k)$ box. This generating function can be easily shown to satisfy the recurrence relation

$$g_{n,k}(q) = q^k g_{n-1,k}(q) + g_{n-1,k-1}(q),$$

which is a q-analogue of the binomial coefficient recurrence. Note that, in this case, the empty partition is included in the set of partitions that fit inside the $k \times (n-k)$ box.

3. Overpartitions in a $2 \times (n-1)$ box

For our main theorem, we are interested in counting the number of overpartitions whose Ferrers shape fits in a $2 \times (n-1)$ box. The generating function for the number of partitions in a $2 \times (n-1)$ box is $\left[\begin{smallmatrix} n+1 \\ 2 \end{smallmatrix} \right]_q$. In this section, we give an analogy of this generating function for overpartitions. We will discuss the recurrence relation for overpartitions that fit in a $k \times (n-k)$ box and then use it to verify a generating function for the number of overpartitions that fit in a $2 \times (n-1)$ box.

3.1. *Recurrence relation for overpartitions.* We will first discuss the general case of overpartitions in a $k \times (n-k)$ box and then consider the case of a $2 \times (n-1)$ box. Let $\bar{p}_{n,k}$ denote the number of overpartitions that can fit in a $k \times (n-k)$ box. Then, $\bar{p}_{n,k}$ satisfies the recurrence relation

$$\bar{p}_{n,k} = \bar{p}_{n-1,k} + \bar{p}_{n-1,k-1} + \bar{p}_{n-2,k-1}. \tag{2}$$

We will explain each term in the recurrence relation. Note that, given a $k \times (n-k)$ box, this recurrence relation indicates that there are three possible disjoint ways of transforming the $k \times (n-k)$ box which, when taken together, describe all possible overpartitions that can fit inside a $k \times (n-k)$ box. These disjoint cases can be easily seen by considering the largest part of an overpartition, λ, in a $k \times (n-k)$ box and are as follows:

(i) $\mathrm{lp}(\lambda) < n-k$. Then the other parts of the overpartition must be less than or equal to $\mathrm{lp}(\lambda)$. This situation describes the number of overpartitions in a $k \times (n-k-1)$ box.

(ii) $\mathrm{lp}(\lambda) = n-k$ and $\mathrm{lp}(\lambda)$ is not overlined. Then the other parts of the overpartition are less than or equal to $n-k$. Thus, this collection of overpartitions is equivalent to the number of overpartitions in a $(k-1) \times (n-k)$ box.

(iii) $\mathrm{lp}(\lambda) = n-k$ and $\mathrm{lp}(\lambda)$ is overlined. Then the other parts of the overpartition must be less than $(n-k)$. Hence, this case is equivalent to the number of overpartitions that fit inside of a $(k-1) \times (n-k-1)$ box.

These cases are shown in Figure 1.

Hence, the three disjoint cases of the recurrence relation cover all possible cases of overpartitions that can fit in a $k \times (n-k)$ box.

To be useful when verifying the generating function in question, (2) must be written in terms of q. That is, let $G(n, k, q)$ be the generating function for the
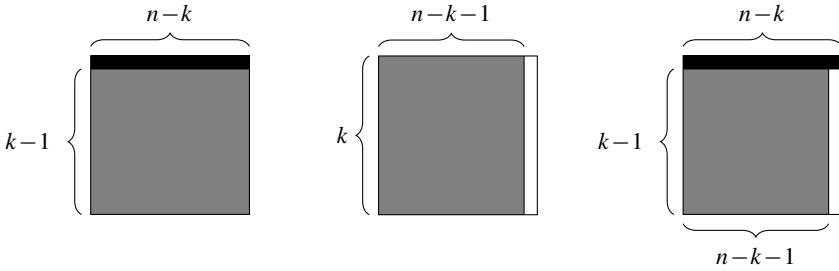
Figure 1. Illustration of the three cases for the recurrence relation. The dimensions of all of the boxes are $k \times (n-k)$. Black denotes a fixed part, gray denotes that the portion can be filled with all possible overpartitions, and white corresponds to empty space. Left: $\mathrm{lp}(\lambda) < n-k$. Middle: $\mathrm{lp}(\lambda) = n-k$ and $\mathrm{lp}(\lambda)$ is not overlined. Right: $\mathrm{lp}(\lambda) = n-k$ and $\mathrm{lp}(\lambda)$ is overlined.

number of overpartitions that fit in a $k \times (n-k)$ box. Then,

$$G(n, k, q) = G(n-1, k, q) + q^{n-k} G(n-1, k-1, q) + q^{n-k} G(n-2, k-1, q).$$

In the case of overpartitions in $2 \times (n-1)$ box, we have the recurrence relation

$$G(n+1, 2, q) = G(n, 2, q) + q^{n-1} G(n, 1, q) + q^{n-1} G(n-1, 1, q). \quad (3)$$

We now give the generating function.

Lemma 3. *Let n be a positive integer and $|q| < 1$. Then $f(q) = (2q + 2q^2)\left[\begin{smallmatrix} n \\ 2 \end{smallmatrix}\right]_q + 1$ is the generating function for overpartitions that fit inside of a $2 \times (n-1)$ box.*

It can be shown that $f(q)$ satisfies (3); therefore, Lemma 3 holds.

3.2. *The q-analogue of Delannoy numbers.* Now that we have verified our generating function for the number of overpartitions in a $2 \times (n-1)$ box, we will draw a connection between Lemma 3 and the Delannoy numbers.

Definition 4. Let m, n be positive integers. The Delannoy numbers $D(m, n)$ are the number of lattice paths from $(0, 0)$ to (m, n) in which only east, north, and northeast steps are allowed.

It is easy to see that when we consider the cells above the path drawn from $(0, 0)$ to (m, n) as a Ferrers shape, the Delannoy numbers are equal to the number of overpartitions that fit inside of a $m \times n$ box. Note that in this model, the northeast steps correspond to overlined, and thus shaded, cells.

Example 5. Consider a 2×4 box. The following is a lattice path in this box:
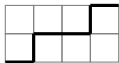

This lattice path corresponds to the Ferrers shape
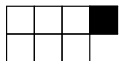
and thus the overpartition $\bar{4}3$.

Example 6. Consider another lattice path in a 2×4 box:

This lattice path corresponds to the Ferrers shape

and thus the partition 31.

Lemma 7. *Let n be a positive integer and $|q| < 1$. The generating function for overpartitions that fit inside a $2 \times (n-1)$ box, $g(q) = (2q + 2q^2)\left[{n+1 \atop 2}\right]_q + 1$, is a q-analogue of the Delannoy numbers, $D(2, n-1)$.*

Proof. As per the definition of a q-analogue, we first take the limit as $q \to 1^-$ of $g(q)$ to find the expression that our generating function generalizes in terms of q. Therefore, we see

$$\lim_{q \to 1^-} (2q + 2q^2)\left[{n \atop 2}\right]_q + 1 = 4\binom{n}{2} + 1 = 2n(n-1) + 1.$$

Next, we must show that this result, $2n(n-1) + 1$, is indeed the expression for the Delannoy numbers $D(2, n-1)$. According to [Pan 2015], a formula for the Delannoy numbers is

$$D(n, k) = \sum_{d=0}^{n} 2^d \binom{k}{d}\binom{n}{d}.$$

Therefore, in this case, we have

$$D(2, n-1) = \sum_{d=0}^{2} \binom{n-1}{d}\binom{2}{d},$$

which readily simplifies to

$$D(2, n-1) = 2n(n-1) + 1.$$

Ergo, we have equality and the generating function $g(q) = (2q + 2q^2)\left[{n+1 \atop 2}\right]_q + 1$ is a q-analogue of the Delannoy numbers $D(2, n-1)$. $\square$

4. A q-analogue of the sum of cubes

In [Garrett and Hummel 2004], the authors give a q-analogue of the sum of cubes and a bijective proof using partitions. We give another q-analogue of the sum of cubes and provide a bijective proof with a similar method, but using overpartitions.

Theorem 8. *Let n be a positive integer and let $|q| < 1$. Then,*

$$\sum_{i=1}^{n} 2q^{i-1}\left(\frac{1-q^{i-1}}{1-q}\right)^2\left(\left(\frac{1-q^{i-2}}{1-q}\right)+\left(\frac{1-q^i}{1-q}\right)\right) = (2q+2q^2)\begin{bmatrix}n\\2\end{bmatrix}_q^2. \quad (4)$$

Note that, taking the limit as $q \to 1^-$, we obtain

$$\sum_{i=1}^{n} i^3 = \binom{n+1}{2}^2.$$

Thus, the above theorem is a q-analogue of the sum of cubes.

Bijective proof. We will prove Theorem 8 by interpreting the terms combinatorially and finding a weight-preserving bijection between two sets of overpartitions. Let R be a set of pairs of overpartitions, (λ, μ), where λ is a nonempty overpartition that fits inside a $2 \times (n-1)$ box and μ is a partition that fits inside a $2 \times (n-2)$ box. It follows that $f(q) = \sum_{(\lambda,\mu)\in R} q^{|\lambda|+|\mu|}$ is a generating function for R and is equal to the right-hand side of (4).

Given a positive integer n, let L be a set of tuples, $(v, a, b) \cup (v, a, b')$, where the allowed values of v, a, b, and b' are:

- v is an overpartition into two parts, where the largest part is equal to at most $n-1$ and can be overlined and the smallest part is at most $n-2$ and cannot be overlined.
- $0 \le a \le n-2$.
- $0' \le b' \le (n-3)'$.
- $0 \le b \le n-1$.

Let $\ell = (v, a, b) \in L$. Then $g(q) = \sum_{\ell \in L} q^{|\ell|}$, where $|\ell| = |v| + a + b$ is a generating function for L and is equal to the left-hand side.

We will now define a bijection between the finite sets R and L. Then, we can show that $f(q) = g(q)$; therefore, (4) holds. So, let $\phi : R \to L$, where $\phi(\lambda, \mu) = (v, a, b)$ and define ϕ in cases:

<u>Case 1</u>: $\lambda_1 > \mu_1$.

(a) $\lambda_2 \ne 0$, and λ_2 is not overlined.
   (i) If λ_1 is not overlined, then $\phi(\lambda, \mu) = ((\lambda_1)(\lambda_2 - 1), \mu_2, \mu_1 + 1)$.
   (ii) If λ_1 is overlined, then $\phi(\lambda, \mu) = ((\overline{\lambda_1})(\lambda_2 - 1), \mu_2, \mu_1 + 1)$.

(b) λ_2 is overlined or $\lambda_2 = 0$.

    (i) If λ_1 is not overlined, then $\phi(\lambda, \mu) = ((\lambda_1)(\lambda_2), \mu_1, \mu_2)$.

    (ii) If λ_1 is overlined, then $\phi(\lambda, \mu) = ((\overline{\lambda_1})(\lambda_2), \mu_1, \mu_2)$.

<u>Case 2</u>: $\lambda_1 \leq \mu_1$.

(a) λ_2 is not overlined.

    (i) If λ_1 is not overlined, then $\phi(\lambda, \mu) = ((\mu_1 + 1)(\mu_2), \lambda_2, (\lambda_1 - 1)')$.

    (ii) If λ_1 is overlined, then $\phi(\lambda, \mu) = ((\overline{\mu_1 + 1})(\mu_2), \lambda_2, (\lambda_1 - 1)')$.

(b) λ_2 is overlined.

    (i) If λ_1 is not overlined, then $\phi(\lambda, \mu) = ((\mu_1 + 1)(\mu_2), \lambda_1, (\lambda_2 - 1)')$.

    (ii) If λ_1 overlined, then $\phi(\lambda, \mu) = ((\overline{\mu_1 + 1})(\mu_2), \lambda_1, (\lambda_2 - 1)')$.

To prove that ϕ is a bijection, one can show that it is one-to-one and onto. It is easier, however, to construct its inverse. We can define $\phi^{-1} : L \to R$ by the following cases, starting with the case of whether b is primed or not primed.

<u>Case 1</u>: b is not primed.

(a) $a \geq b$.

    (i) If v_1 is not overlined, then $\phi^{-1}(v, a, b) = (v, (a)(b))$.

    (ii) If v_1 is overlined, then $\phi^{-1}(v, a, b) = (v, (a)(b))$.

(b) $a < b$.

    (i) If v_1 is not overlined, then $\phi^{-1}(v, a, b) = ((v_1)(v_2 + 1), (b - 1)(a))$.

    (ii) If v_1 is overlined, then $\phi^{-1}(v, a, b) = ((v_1)(v_2 + 1), (b - 1)(a))$.

<u>Case 2</u>: b is primed.

(a) $a \geq b + 2$.

    (i) If v_1 is not overlined, then $\phi^{-1}(v, a, b) = ((a)(b + 1), (v_1 - 1)(v_2))$.

    (ii) If v_1 is overlined, then $\phi^{-1}(v, a, b) = ((\bar{a})(b + 1), (v_1 - 1)(v_2))$.

(b) $a < b + 2$.

    (i) If v_1 is not overlined, then $\phi^{-1}(v, a, b) = ((b + 1)(a), (v_1 - 1)(v_2))$.

    (ii) If v_1 is overlined, then $\phi^{-1}(v, a, b) = ((\overline{b + 1})(a), (v_1 - 1)(v_2))$.

The details of verifying that ϕ and ϕ^{-1} are inverses are not hard and are left to the reader. However, we will conclude the combinatorial proof with two examples of ϕ and ϕ^{-1} to help make the bijection clearer.

Example 9. Let $(\lambda, \mu) = (54, 22)$. First, we find i. We have $\lambda_1 > \mu_1$, so $i = 5 + 1 = 6$. For ϕ, we are in Case 1(a)(i), so $\phi(\lambda, \mu) = ((\lambda_1)(\lambda_2 - 1), \mu_2, \mu_1 + 1)$. Therefore, $\phi(54, 22) = (53, 2, 3)$. Note that $|\lambda| + |\mu| = 9 + 4 = 13$ and $|v| + a + b = 8 + 2 + 3 = 13$. Next, we act on (v, a, b) with the inverse. We are in Case 1(b)(i), so $\phi^{-1}(v, a, b) = ((v_1)(v_2 + 1), (b - 1)(a))$. So, $\phi^{-1}(53, 2, 3) = (54, 22)$.

Example 10. Let $(\lambda, \mu) = (\bar{2}1, 41)$. First, we find i. We have $\lambda_1 \le \mu_1$, so $i = 4 + 2 = 6$. For ϕ, we are in Case 2(a)(ii), so $\phi(\lambda, \mu) = ((\overline{\mu_1 + 1})(\mu_2), \lambda_2, (\lambda_1 - 1)')$. Therefore, $\phi(\bar{2}1, 41) = (\bar{5}1, 1, 1')$. Note that $|\lambda| + |\mu| = 3 + 5 = 8$ and $|v| + a + b = 6 + 1 + 1 = 8$. Next, we act on (v, a, b) with the inverse. We are in Case 2(b)(ii), so $\phi^{-1}(v, a, b) = ((\overline{b + 1})(a), (v_1 - 1)(v_2))$. So, $\phi^{-1}(\bar{5}1, 1, 1') = (\bar{2}1, 41)$.

5. Conclusion

Although the specific case of overpartitions whose Ferrers shape fits in a $2 \times (n - 1)$ box is central to the proof presented here, extending this idea to the general case of a $k \times (n - k)$ box would be useful. This general work could lead to q-analogues of other expressions. In particular, investigating q-analogues for the sums of other integer powers is a natural extension of our work.

6. Acknowledgments

References

[Andrews 1976] G. E. Andrews, *The theory of partitions*, Addison-Wesley, Reading, MA, 1976. MR Zbl

[Benjamin and Orrison 2002] A. T. Benjamin and M. E. Orrison, "Two quick combinatorial proofs", *Coll. Math. J.* **33**:5 (2002), 406–408.

[Corteel and Lovejoy 2004] S. Corteel and J. Lovejoy, "Overpartitions", *Trans. Amer. Math. Soc.* **356**:4 (2004), 1623–1635. MR Zbl

[Garrett and Hummel 2004] K. C. Garrett and K. Hummel, "A combinatorial proof of the sum of q-cubes", *Electron. J. Combin.* **11**:1 (2004), Research Paper 9, 6 pp. MR Zbl

[Pan 2015] H. Pan, "A Lucas-type congruence for q-Delannoy numbers", preprint, 2015. arXiv

forsterj@stolaf.edu   Department of Mathematics, Statistics and Computer Science,
                             St. Olaf College, Northfield, MN 55057, United States

garrettk@stolaf.edu   Department of Mathematics, Statistics and Computer Science,
                             St. Olaf College, Northfield, MN 55057, United States

jacobsel@stolaf.edu   St. Olaf College, Northfield, MN 55057, United States

acw8794@gmail.com   Department of Mathematics, Statistics and Computer Science,
                             St. Olaf College, Northfield, MN 55057, United States

Ulrich partitions for two-step flag varieties

Izzet Coskun and Luke Jaskowiak

(Communicated by Ravi Vakil)

Ulrich bundles play a central role in singularity theory, liaison theory and Boij–Söderberg theory. It was proved by the first author together with Costa, Huizenga, Miró-Roig and Woolf that Schur bundles on flag varieties of three or more steps are not Ulrich and conjectured a classification of Ulrich Schur bundles on two-step flag varieties. By the Borel–Weil–Bott theorem, the conjecture reduces to classifying integer sequences satisfying certain combinatorial properties. In this paper, we resolve the first instance of this conjecture and show that Schur bundles on $F(k, k + 3; n)$ are not Ulrich if $n > 6$ or $k > 2$.

1. Introduction

Let $j, k, l > 0$ be positive integers. Let

$$P = (a_1, \ldots, a_k \mid b_1, \ldots, b_j \mid c_1, \ldots, c_l)$$

be a strictly increasing sequence of integers divided into three nonempty subsequences $a_\bullet, b_\bullet, c_\bullet$. Let $P(t)$ denote the sequence

$$P(t) = (a_1 + t, \ldots, a_k + t \mid b_1, \ldots, b_j \mid c_1 - t, \ldots, c_l - t)$$

obtained by adding t to each of the entries in the sequence $a_\bullet$ and subtracting t from each of the entries in the subsequence $c_\bullet$. Set $N = kj + kl + jl$.

Definition 1.1. The partition P is called an *Ulrich partition* if the sequences $P(t)$ have exactly two equal entries for $1 \leq t \leq N$.

Note that $P(t)$ can have repeated entries for at most N values of t. We will refer to $P(t)$ as the time evolution of P at time t. Hence, Ulrich partitions are those for which there are a maximum number of collisions among the entries during their time evolution and these collisions all occur at consecutive times.

Two partitions P_1 and P_2 are *equivalent* if they differ by adding a constant to all the entries. If P_1 and P_2 are equivalent, then P_1 is Ulrich if and only if P_2 is. We always consider partitions up to equivalence. Our main theorem is the following.

Theorem 1.2. *If $P = (a_1, \ldots, a_k \mid b_1, b_2, b_3 \mid c_1, \ldots, c_l)$ is an Ulrich partition, then $k + l \leq 3$.*

Given a partition $P = (a_1, \ldots, a_k \mid b_1, \ldots, b_j \mid c_1, \ldots, c_l)$, we obtain a new partition P^s called the *symmetric partition* by multiplying all the entries by -1 and listing the entries in the reverse order:

$$P^s = (-c_l, \ldots, -c_1 \mid -b_j, \ldots, -b_1 \mid -a_k, \ldots, -a_1).$$

The partition P is Ulrich if and only if P^s is Ulrich. Similarly, there is a dual partition P^* obtained by

$$P^* = \big(c_1 - (N+1)t, \ldots, c_l - (N+1)t \mid b_1, \ldots, b_j \mid a_1 + t(N+1), \ldots, a_k + t(N+1)\big).$$

This is the partition $P(N + 1)$ reordered so that the entries are increasing. By running the time evolution backwards, it is clear that P is Ulrich if and only if P^* is Ulrich (see [Coskun et al. 2017, §3] for more details). We can also form $(P^s)^*$, which is Ulrich if and only if P is.

As a consequence of the proof, we obtain a complete classification of Ulrich partitions where the $b_\bullet$ subsequence has length 3. Up to equivalence and these symmetries, they are

$$(0 \mid 1, 2, 3 \mid 8), \quad (-8, 0 \mid 1, 2, 3 \mid 8), \quad (0 \mid 1, 2, 5 \mid 8), \quad (-1 \mid 1, 2, 6 \mid 7), \quad (0 \mid 1, 3, 6 \mid 8).$$

We now explain the significance of Ulrich partitions. Let $X \subset \mathbb{P}^m$ be an arithmetically Cohen–Macaulay projective variety of dimension d. A vector bundle $\mathcal{E}$ on X is called an *Ulrich bundle* if $H^i(X, \mathcal{E}(-i)) = 0$ for $i > 0$ and $H^j(X, \mathcal{E}(-j-1)) = 0$ for $j < d$ (see [Herzog et al. 1991; Brennan et al. 1987; Eisenbud et al. 2003]). These are the bundles whose Hilbert polynomials have d zeros at the first d negative integers. They play a central role in singularity theory, liaison theory and Boij–Söderberg theory. For example, if X admits an Ulrich bundle, then the cone of cohomology tables of X coincides with that of $\mathbb{P}^m$ [Eisenbud and Schreyer 2011]. Thus, classifying Ulrich bundles on projective varieties is an important problem in commutative algebra and algebraic geometry, as discussed by E. Coskun et al. [2013], I. Coskun et al. [2017], and Faenzi [2008], who also give further references. In particular, it is interesting to decide when representation theoretic bundles on flag varieties are Ulrich.

Let $0 < k_1 < k_2 < n$ be three positive integers. Set $k_0 = 0$ and $k_3 = n$. Let V be an n-dimensional vector space. The two-step partial flag variety $F(k_1, k_2; n)$ parameterizes partial flags $W_1 \subset W_2 \subset V$, where W_i has dimension k_i. The variety

$F(k_1, k_2; n)$ has a minimal embedding in projective space corresponding to the ample line bundle with class the sum of the two Schubert divisors. We will always consider $F(k_1, k_2; n)$ in this embedding and $\mathcal{O}(1)$ will refer to the hyperplane bundle in this embedding.

The variety $F(k_1, k_2; n)$ has a collection of tautological bundles

$$0 = T_0 \subset T_1 \subset T_2 \subset T_3 = \underline{V} = V \otimes \mathcal{O}_{F(k_1,k_2;n)},$$

where $\underline{V}$ is the trivial bundle of rank n and T_i, for $i = 1$ or 2, is the subbundle of $\underline{V}$ of rank k_i which associates to a point $[W_1 \subset W_2]$ the subspace W_i. Let $U_i = T_i/T_{i-1}$. Given $\lambda = (\lambda_1 \mid \lambda_2 \mid \lambda_3)$ a concatenation of partitions λ_i of length $k_i - k_{i-1}$, the Schur bundle E_λ is defined by

$$E_\lambda = \mathbb{S}^{\lambda_1} U_1^* \otimes \mathbb{S}^{\lambda_2} U_2^* \otimes \mathbb{S}^{\lambda_3} U_3^*,$$

where $\mathbb{S}^\lambda$ is the Schur functor of type λ.

Costa and Miró-Roig [2015] initiated the study of determining when Schur bundles are Ulrich. They showed every Grassmannian admits Ulrich Schur bundles and classified these bundles. Coskun et al. [2017] showed that Schur bundles on flag varieties with three or more steps are never Ulrich for their minimal embedding. They also constructed several infinite families of Ulrich Schur bundles on specific two-step flag varieties and showed that many two-step flag varieties do not admit Ulrich Schur bundles. They conjectured a complete classification of Ulrich Schur bundles on two-step flag varieties.

Conjecture 1.3 [Coskun et al. 2017, Conjecture 5.9]. *A two-step flag variety $F(k_1, k_2; n)$ does not admit an Ulrich Schur bundle with respect to $\mathcal{O}(1)$ if $k_2 \geq 3$ and $n - k_2 \geq 3$.*

The Borel–Weil–Bott theorem computes the cohomology of Schur bundles and allows one to determine whether a Schur bundle is Ulrich. There is a bijective correspondence between equivalence classes of Ulrich partitions of type $(n - k_2, k_2 - k_1, k_1)$ and Schur bundles E_λ on $F(k_1, k_2; n)$ which are Ulrich [Coskun et al. 2017, Proposition 3.5]. Hence, classifying Ulrich Schur bundles is equivalent to classifying Ulrich partitions. Consequently, as a corollary of Theorem 1.2, we resolve the first case of Section 1.

Theorem 1.4. *The flag variety $F(k, k+3; n)$ does not admit an Ulrich Schur bundle with respect to $\mathcal{O}(1)$ if $n > 6$ or $k > 2$.*

In particular, the only two step flag varieties of the form $F(k, k+3; n)$ that admit Ulrich Schur bundles are $F(1, 4; 5)$, $F(1, 4; 6)$ and $F(2, 5; 6)$. All the Ulrich Schur bundles on these varieties have been classified in [Coskun et al. 2017]. There has been work on classifying Ulrich Schur bundles on other homogeneous varieties using the same strategy (see [Fonarev 2016]).

2. The proof of the main theorem

Theorem 2.1. *There are no Ulrich partitions* $(a_1, \ldots, a_k \mid b_1, b_2, b_3 \mid c_1, \ldots, c_l)$ *with* $k + l > 3$.

We begin with the following simple observation, which is a special case of [Coskun et al. 2017, Lemma 4.3].

Lemma 2.2. *If* $P = (a_1, \ldots, a_l \mid b_1, \ldots, b_j \mid c_1, \ldots, c_k)$ *is an Ulrich partition, then all the entries in the sequences* $a_\bullet$ *and* $c_\bullet$ *are equal modulo 2.*

Proof. If P is Ulrich, the a_p and c_q entries of $P(t_{pq})$ must be equal at some time t_{pq}. From now on, we will express this by saying a_p and c_q collide at time $t = t_{pq}$. Hence $a_p + t_{pq} = c_q - t_{pq}$ or, equivalently, $c_q - a_p = 2t_{pq}$. Consequently, a_p and c_q are equal modulo 2. Since this holds for each $1 \le p \le l$ and $1 \le q \le k$, we conclude that all the entries in the sequences $a_\bullet$ and $c_\bullet$ have the same parity. Furthermore, their parities remain equal in $P(t)$ for all t. □

Let $P = (a_1, \ldots, a_k \mid b_1, b_2, b_3 \mid c_1, \ldots, c_l)$ be an Ulrich partition. Recall that we always assume $k, l > 0$. Up to symmetry and duality, there are three possibilities:

(1) The sequence b_1, b_2, b_3 may be consecutive.

(2) Only the entries b_1, b_2 may be consecutive.

(3) Finally, no two of the entries in $b_\bullet$ are consecutive.

We will analyze each of these cases separately.

The $b_\bullet$ sequence is consecutive. In this case, we will see that $k + l \le 3$ and up to symmetry and duality the two possible partitions are $(0 \mid 1, 2, 3 \mid 8)$ or $(-8, 0 \mid 1, 2, 3 \mid 8)$. In fact, we can analyze sequences where the $b_\bullet$ sequence is consecutive more generally.

Proposition 2.3. *Let P be an Ulrich partition of the form* $(a_1, \ldots, a_k \mid 1, 2, \ldots, r \mid c_1, \ldots, c_l)$, *where the $b_\bullet$ sequence consists of r consecutive integers. Assume that $r \ge 3$. Then $k + l \le 3$.*

Proof. Without loss of generality, we may assume that at $t = 1$, the collision is $a_k b_1$. Then for $1 \le t \le r$, the collision is $a_k b_t$. We claim that at $t = r + 1$, the collision must be $a_k c_1$. The collision must be either $a_{k-1} b_1$ or $a_k c_1$. If r is odd, then it cannot be $a_{k-1} b_1$ since otherwise a_{k-1} and a_k would have different parities. If r is even and the collision is $a_{k-1} b_1$, we obtain a contradiction as follows. Let t_0 be the time of the collision $a_k c_1$. Until that time all the collisions must be between an entry from $a_\bullet$ and an entry from $b_\bullet$. We conclude that $t_0 = ir + 1$ for some i. At time $t = t_0 + 1$, the collision cannot be $a_k c_2$. Otherwise, we would have $c_2 - c_1 = 2$ and the collisions $c_1 b_1$ and $c_2 b_3$ would occur at the same time. If $i > 1$, the collision at $t = t_0 + 1$ cannot be $b_r c_1$. Hence, at $t = t_0 + 1$, the collision must be $a_{k-i} b_1$. This

violates parity since a_k is even while a_{k-i} is odd. We conclude that at $t = r + 1$, the collision is $a_k c_1$.

Hence, for $t = r + 1 + i$ with $1 \leq i \leq r$, the collisions are $b_{r+1-i} c_1$. If the progression stops at time $t = 2r + 1$, we obtain the Ulrich partition $(0 \mid 1, 2, \ldots, r \mid 2r + 2)$. Else, at time $t = 2r + 2$, the collision must be $a_{k-1} c_1$. Otherwise, the collision would have to be $a_k c_2$. At time $t = 2r + 3$, since the collision could not be $a_k c_3$, the collision would have to be $a_{k-1} c_1$. Then at time $t = 3r + 3$, the values a_{k-1}, b_r and c_2 would collide simultaneously. This contradiction shows that the collision at $t = 2r + 2$ must be $a_{k-1} c_1$. Hence, for times $t = 2r + 2 + i$ with $1 \leq i \leq r$, the collisions must be $a_{k-1} b_i$. If the progression stops at $t = 3r + 2$, we obtain the Ulrich partition $(-2r - 2, 0 \mid 1, 2, \ldots, r \mid 2r + 2)$.

Otherwise, at time $t = 3r + 3$, the collision must either be $a_k c_2$ or $a_{k-2} c_1$. Then at time $t = 3r + 4$, the only possible collisions are $a_{k-2} c_1$ or $a_k c_2$, respectively, since the distance between consecutive entries in $a_\bullet$ or $c_\bullet$ has to be at least $r > 2$. If the order is $a_k c_2$ and $a_{k-2} c_1$, then at time $t = 3r + 4$ the entry c_2 is $3r + 2$ and a_{k-2} is $-r - 2$. The entries a_{k-2}, b_r and c_2 collide simultaneously at time $t = 5r + 5$. Hence, the order of collisions must be $a_{k-2} c_1$ at time $t = 3r + 3$ and $a_k c_2$ at time $3r + 4$. If $r \geq 5$, then at time $t = 3r + 5$, there cannot be any collisions. If $3 \leq r \leq 4$, the only possible collision at time $t = 3r + 5$ is $a_{k-3} c_1$. But then a_{k-3}, b_r and c_2 collide simultaneously at time $t = 5r + 8$. This is a contradiction. Hence, the time evolution must stop at time $t = 3r + 2$ and we conclude the proposition. $\qquad\square$

In particular, we conclude that up to equivalence and symmetries, the only Ulrich partitions where the $b_\bullet$ sequence consists of three or more consecutive integers are $(0 \mid 1, 2, \ldots, r \mid 2r + 2)$ and $(-2r - 2, 0 \mid 1, 2, \ldots, r \mid 2r + 2)$.

Exactly two of the $b_\bullet$ entries are consecutive. Up to symmetry and duality, we may assume that b_1 and b_2 are consecutive.

Lemma 2.4. *Assume that b_1 and b_2 are the only two consecutive entries in the $b_\bullet$ sequence and $P = (a_1, \ldots, a_k \mid b_1, b_2, b_3 \mid c_1, \ldots, c_l)$ is Ulrich. Then the $b_\bullet$ sequence up to equivalence and symmetry must be $1, 2, 5$ or $1, 2, 6$. In the first case, at time $t = 1$ the collision is $a_k b_1$. In the second case, at time $t = 1$ the collision is $b_3 c_1$.*

Proof. At time $t = 1$, the collision is either $a_k b_1$ or $b_3 c_1$. First, assume that at time $t = 1$ the collision is $b_3 c_1$. Since b_2 and b_3 are not consecutive, the collision at time $t = 2$ cannot be $c_1 b_2$. By parity, the collision cannot be $b_3 c_2$. Consequently, at time $t = 2$ the collision must be $a_k b_1$. Hence, at time $t = 3$, the collision is $a_k b_2$. If at time $t = 4$ the collision is $a_k c_1$, then the $b_\bullet$ sequence is $1, 2, 6$. Otherwise, the only possible collision is $a_{k-1} b_1$ since $a_k b_3$ or $b_2 c_1$ cannot occur before $a_k c_1$ and $b_3 c_2$ is excluded by parity. Moreover, $\mid b_3 - b_2 \mid \geq 8$ and $a_k - a_{k-1} = 2$.

The last collision at time $t = N$ is either $a_1 b_3$ or $b_1 c_l$. If it is $b_1 c_l$, then the collisions at time $t = N - 1$ and $t = N - 2$ must be $b_2 c_l$ and $a_l b_3$, respectively. Note

that at time $t = N - 2$, the collision cannot be $b_1 c_{l-1}$. Otherwise, $c_l - c_{l-1} = 2$ and c_l would collide with a_k at the same time as c_{l-1} collides with a_{k-1}. Then at time $t = N-3$, the collision cannot be $a_{k-1} b_3$ or $c_{l-1} b_1$ by parity. Since $b_3 - b_2 \geq 8$, the collision cannot be $a_1 c_l$. We conclude that at $t = N - 3$ there are no possible collisions. This is a contradiction.

If the last collision is $a_1 b_3$, then the two previous collisions must be $b_1 c_l$ and $b_2 c_l$ by parity. At time $t = N - 3$, the collision cannot be $b_1 c_{l-1}$ since $c_l - c_{l-1}$ cannot be 2. The collision cannot be $a_2 b_3$ by parity. It cannot be $a_1 c_l$ since $b_3 - b_2 \geq 8$. We obtain a contradiction. We conclude that if at $t = 1$ the collision is $b_3 c_1$, then at $t = 4$ the collision must be $a_k c_1$ and the $b_{\bullet}$ sequence is up to equivalence $1, 2, 6$.

Next assume that the collision at $t = 1$ is $a_k b_1$. Let $t = 2j + 1$ be the first odd time when the collision is not of the form $a_i b_1$. If $j = 1$, since the entries in $b_{\bullet}$ are not consecutive, at time $t = 3$ the collision must be $b_3 c_1$. Then at time $t = 4$, by parity, the only possible collision is $a_k c_1$. Therefore, the $b_{\bullet}$ sequence is $1, 2, 5$. If $j > 1$, then $a_k - a_{k-1} = 2$. The collision at time $t = 2j + 1$ must be $b_3 c_1$. Otherwise, the collision would have to be $a_k b_3$. Then at time $t = 2j + 2$, by parity the collision would have to be $a_k c_1$. Then the collisions $a_{k-1} b_3$ and $b_3 c_1$ would happen at the same time at $t = 2j + 3$. We conclude that at time $t = 2j + 1$ the collision is $b_3 c_1$. At time $t = 2j + 2$, by parity we cannot have a collision of the form $a_i b_1$ or $b_3 c_{l-1}$. We conclude that the collision must be $a_k c_1$. If $j > 1$, then at time $r = 2j + 2$ the collisions $a_{k-1} c_1$ and $a_k b_3$ occur at the same time leading to a contradiction. We conclude that $j = 1$ and the $b_{\bullet}$ sequence is $1, 2, 5$.   □

We thus obtain two standard Ulrich partitions of type $(1, 3, 1)$ given by $(0 \mid 1, 2, 5 \mid 8)$ and $(-1 \mid 1, 2, 6 \mid 7)$. To conclude the analysis in this case, we argue that these Ulrich partitions cannot be extended to longer Ulrich partitions.

Lemma 2.5. *The only Ulrich partition of the form*

$$(a_1, \ldots, a_{k-1}, a_k = 0 \mid b_1 = 1, b_2 = 2, b_3 = 5 \mid c_1 = 8, c_2, \ldots, c_l)$$

is $(0 \mid 1, 2, 5 \mid 8)$. *The only Ulrich partition of the form*

$$(a_1, \ldots, a_{k-1}, a_k = -1 \mid b_1 = 1, b_2 = 2, b_3 = 6 \mid c_1 = 7, c_2, \ldots, c_l)$$

is $(-1 \mid 1, 2, 6 \mid 7)$.

Proof. Suppose there exists an Ulrich partition of the form

$$(a_1, \ldots, a_{k-1}, 0 \mid 1, 2, 5 \mid 8, c_2, \ldots, c_l)$$

with k or l bigger than 1. Then the last collision at time $t = N$ must be either $a_1 b_3$ or $b_1 c_l$. If the collision is $a_1 b_3$, then by parity the collision at time $t = N - 1$ must be $b_1 c_l$. Then a_1 and c_l have different parities and can never collide. We obtain a contradiction. We conclude that at $t = N$ the collision must be $b_1 c_l$. Hence, at

time $t = N - 1$ the collision is $b_2 c_l$. If the collision at $t = N - 2$ is $a_1 b_3$, then the distance between a_1 and a_k (which is equal to $N - 7$) is equal to the distance between c_1 and c_l. Hence, these pairs collide simultaneously leading to a contradiction. We conclude that at time $t = N - 2$, the collision must be $b_1 c_{l-1}$. Hence the collisions at times $t = N - 3, N - 4$ must be $b_2 c_{l-1}$ and $b_3 c_l$, respectively. However, at time $t = N - 5$ there are no possible collisions. The collision cannot be $b_1 c_{l-2}$ by parity. There are no collisions between c_{l-1}, c_l and any entries in the $b_\bullet$ sequence. On the other hand, if a_1 collides with c_l, then at time $t = N - 4$ the $a_1 b_3$ collision coincides with the $b_2 c_{l-1}$ collision. This contradiction shows that $k = l = 1$.

Suppose there exists an Ulrich partition of the form

$$(a_1, \ldots, a_{k-1}, -1 \mid 1, 2, 6 \mid 7, c_2, \ldots, c_l)$$

with k or l bigger than 1. The argument is almost identical to the previous case. The last collision at time $t = N$ cannot be $a_1 b_3$. Otherwise, at time $t = N - 1$ the collision would have to be $b_1 c_l$ and the distance between a_1 and a_k would be equal to the distance between c_1 and c_l. We conclude that the collision at time $t = N$ is $b_1 c_l$. Hence, at time $t = N - 1$ the collision is $b_2 c_l$. At time $t = N - 2$, the collision cannot be $a_1 b_3$, otherwise at that time c_l would be at position 3 and would have different parity from a_1. We conclude that at time $t = N - 2$ the collision must be $b_1 c_{l-1}$. This determines the collisions at $t = N - 3, N - 4$ which must be $b_2 c_{l-1}$ and $b_3 c_l$. Then, as in the previous case, at time $t = N - 5$, there cannot be any collisions leading to a contradiction. This shows that $k = l = 1$. □

None of the $b_\bullet$ entries are consecutive.   In this case, we have the following lemma.

Lemma 2.6. *Let* $(a_1, \ldots, a_k \mid b_1, b_2, b_3 \mid c_1, \ldots, c_l)$ *be an Ulrich partition with* $k, l > 0$ *and such that no entries in the $b_\bullet$ sequence are consecutive. Then up to equivalence and symmetry the $b_\bullet$ sequence is* $1, 3, 6$.

Proof. Without loss of generality, we may assume that at $t = 1$ the collision is $a_k b_1$. By parity and the fact that $b_2 - b_1 > 1$, we conclude that at $t = 2$ the collision must be $b_3 c_1$. Similarly, by parity and the fact that $b_3 - b_2 > 1$, at time $t = 3$ the collision is either $a_k b_2$ or $a_{k-1} b_1$. If the collision is $a_k b_2$, then the collision at $t = 4$ has to be $a_k c_1$. By parity, it cannot be $a_{k-1} b_1$. It cannot be $b_3 c_2$, otherwise the collisions $b_1 c_1$ and $b_2 c_2$ would occur at the same time. We conclude that at time $t = 0$ the $b_\bullet$ sequence must be $1, 3, 6$ and $a_k = 0$ and $c_1 = 8$.

If the collision at time $t = 3$ is $a_{k-1} b_1$, then by parity the collision at $t = 4$ may only be one of $a_k b_2$, $b_2 c_1$ or $b_3 c_2$. It cannot be $b_2 c_1$, otherwise $a_k b_3$ and $a_{k-1} b_2$ would occur at the same time since both a_{k-1}, a_k and b_2, b_3 would be 2 apart. Similarly, it cannot be $b_3 c_2$, otherwise $a_k c_2$ and $a_{k-1} c_1$ would occur at the same time. We conclude that at $t = 4$, the collision is $a_k b_2$. At time $t = 5$, the collision cannot be $b_3 c_2$ by parity. Hence, it is either $a_{k-2} b_1$ or $a_k c_1$. It cannot

be $a_k c_1$, otherwise at time $t = 6$ all three a_{k-1}, b_2 and c_1 collide. Hence, at $t = 5$ the collision is $a_{k-2} b_1$. In this case, we have $b_3 - b_2 \geq 5$. Now consider the last two collisions at $t = N$ and $N - 1$. They are either $a_1 b_3$ at $t = N$ and $b_1 c_l$ at $t = N - 1$, or $b_1 c_l$ at $t = N$ and $a_1 b_3$ at $t = N - 1$. Notice that it cannot be the latter. Otherwise, the distance between a_1 and a_k would be equal to the distance between c_1 and c_l and the pair would collide simultaneously. We conclude that the collisions at $t = N$ and $N - 1$ must be $a_1 b_3$ and $b_1 c_l$, respectively. Then at time $t = N - 3$, the collision cannot be $a_2 b_3$ by parity. It cannot be $a_1 b_2$ or $b_2 c_l$ because of the distances between the entries in the $b_\bullet$ sequence. Finally, it cannot be $b_1 c_{l-1}$ since otherwise the distance between c_l and c_{l-1} would be 2 and they would collide with the pair a_k and a_{k-1} simultaneously. We conclude that this case is not possible. This concludes the proof of the lemma. $\qquad\square$

We thus get the standard Ulrich partition of type $(1, 3, 1)$ given by $(0 \,|\, 1, 3, 6 \,|\, 8)$. To conclude the analysis in this case, we argue that this Ulrich partition cannot be extended to longer Ulrich partitions.

Lemma 2.7. *The only Ulrich partition of the form*

$$(a_1, \ldots, a_{k-1}, a_k = 0 \,|\, b_1 = 1, b_2 = 3, b_3 = 6 \,|\, c_1 = 8, c_2, \ldots, c_l)$$

is $(0 \,|\, 1, 3, 6 \,|\, 8)$.

Proof. Suppose there were a longer Ulrich partition. Then the last two collisions at times $t = N$ and $t = N - 1$ must be $a_1 b_3$ and $b_1 c_l$, respectively. Otherwise, as in the previous cases, the distance between a_1 and a_k would equal the distance between c_1 and c_l. But then at time $t = N - 2$ there cannot be any collisions. The entries c_l and a_k do not collide with any entries in the $b_\bullet$ sequence or with each other by the distribution of the $b_\bullet$ sequence. The collision cannot be $b_1 c_{l-1}$ and it cannot be $a_{k-1} b_3$. Otherwise, the distance between a_k and a_{k-1} would be 2 and the collisions $a_k b_1$ and $a_{k-1} b_2$ would be at the same time. This contradiction concludes the proof. $\qquad\square$

Proof of Theorem 1.2. Let $P = (a_1, \ldots, a_k \,|\, b_1, b_2, b_3 \,|, c_1, \ldots, c_l)$ be an Ulrich partition. If the $b_\bullet$ sequence is consecutive, then by Proposition 2.3, up to symmetry, duality and equivalence, $P = (-8, 0 \,|\, 1, 2, 3 \,|\, 8)$ or $(0 \,|\, 1, 2, 3 \,|\, 8)$. If only two entries in the $b_\bullet$ sequence are consecutive, then by Lemmas 2.4 and 2.5, $P = (0 \,|\, 1, 2, 5 \,|\, 8)$ or $P = (-1 \,|\, 1, 2, 6 \,|\, 7)$. Finally, if none of the entries in the $b_\bullet$ sequence are consecutive, then by Lemmas 2.6 and 2.7, $P = (0 \,|\, 1, 3, 6 \,|\, 8)$. In all cases we have $k + l \leq 3$. $\qquad\square$

Acknowledgements

References

[Brennan et al. 1987] J. P. Brennan, J. Herzog, and B. Ulrich, "Maximally generated Cohen–Macaulay modules", *Math. Scand.* **61**:2 (1987), 181–203. MR Zbl

[Coskun et al. 2013] E. Coskun, R. S. Kulkarni, and Y. Mustopa, "The geometry of Ulrich bundles on del Pezzo surfaces", *J. Algebra* **375** (2013), 280–301. MR Zbl

[Coskun et al. 2017] I. Coskun, L. Costa, J. Huizenga, R. M. Miró-Roig, and M. Woolf, "Ulrich Schur bundles on flag varieties", *J. Algebra* **474**:1 (2017), 49–96.

[Costa and Miró-Roig 2015] L. Costa and R. M. Miró-Roig, "GL(V)-invariant Ulrich bundles on Grassmannians", *Math. Ann.* **361**:1 (2015), 443–457. MR Zbl

[Eisenbud and Schreyer 2011] D. Eisenbud and F.-O. Schreyer, "Boij–Söderberg theory", pp. 35–48 in *Combinatorial aspects of commutative algebra and algebraic geometry*, edited by G. Fløystad et al., Abel Symp. **6**, Springer, Berlin, 2011. MR Zbl

[Eisenbud et al. 2003] D. Eisenbud, F.-O. Schreyer, and J. Weyman, "Resultants and Chow forms via exterior syzygies", *J. Amer. Math. Soc.* **16**:3 (2003), 537–579. MR Zbl

[Faenzi 2008] D. Faenzi, "Rank 2 arithmetically Cohen–Macaulay bundles on a nonsingular cubic surface", *J. Algebra* **319**:1 (2008), 143–186. MR Zbl

[Fonarev 2016] A. Fonarev, "Irreducible Ulrich bundles on isotropic Grassmannians", preprint, 2016. arXiv

[Herzog et al. 1991] J. Herzog, B. Ulrich, and J. Backelin, "Linear maximal Cohen–Macaulay modules over strict complete intersections", *J. Pure Appl. Algebra* **71**:2–3 (1991), 187–202. MR Zbl

coskun@math.uic.edu   *Department of Mathematics, Statistics and CS, University of Illinois at Chicago, Chicago, IL 60607, United States*

ljasko2@uic.edu   *Department of Mathematics, Statistics and CS, University of Illinois at Chicago, Chicago, IL 60607, United States*

Guidelines for Authors

Submissions in all mathematical areas are encouraged. All manuscripts accepted for publication in *Involve* are considered publishable in quality journals in their respective fields, and include a minimum of one-third student authorship. Submissions should include substantial faculty input; faculty co-authorship is strongly encouraged. Authors may submit manuscripts in PDF format on-line at the Submission page at the Involve website.

Originality. Submission of a manuscript acknowledges that the manuscript is original and and is not, in whole or in part, published or under consideration for publication elsewhere. It is understood also that the manuscript will not be submitted elsewhere while under consideration for publication in this journal.

Language. Articles in *Involve* are usually in English, but articles written in other languages are welcome.

Required items. A brief abstract of about 150 words or less must be included. It should be self-contained and not make any reference to the bibliography. If the article is not in English, two versions of the abstract must be included, one in the language of the article and one in English. Also required are keywords and subject classifications for the article, and, for each author, postal address, affiliation (if appropriate), and email address.

Format. Authors are encouraged to use LATEX but submissions in other varieties of TEX, and exceptionally in other formats, are acceptable. Initial uploads should be in PDF format; after the refereeing process we will ask you to submit all source material.

References. Bibliographical references should be complete, including article titles and page ranges. All references in the bibliography should be cited in the text. The use of BibTEX is preferred but not required. Tags will be converted to the house format, however, for submission you may use the format of your choice. Links will be provided to all literature with known web locations and authors are encouraged to provide their own links in addition to those supplied in the editorial process.

Figures. Figures must be of publication quality. After acceptance, you will need to submit the original source files in vector graphics format for all diagrams in your manuscript: vector EPS or vector PDF files are the most useful.

Most drawing and graphing packages (Mathematica, Adobe Illustrator, MATLAB, etc.) allow the user to save files in one of these formats. Make sure that what you are saving is vector graphics and not a bitmap. If you need help, please write to graphics@msp.org with details about how your graphics were generated.

White space. Forced line breaks or page breaks should not be inserted in the document. There is no point in your trying to optimize line and page breaks in the original manuscript. The manuscript will be reformatted to use the journal's preferred fonts and layout.

Proofs. Page proofs will be made available to authors (or to the designated corresponding author) at a Web site in PDF format. Failure to acknowledge the receipt of proofs or to return corrections within the requested deadline may cause publication to be postponed.

involve